Self-Assembly of Boron-Based Supramolecular Structures

THÈSE N° 4184 (2008)

PRÉSENTÉE LE 26 SEPTEMBRE 2008
À LA FACULTE SCIENCES DE BASE
LABORATOIRE DE CHIMIE SUPRAMOLÉCULAIRE
PROGRAMME DOCTORAL EN CHIMIE ET GÉNIE CHIMIQUE

ÉCOLE POLYTECHNIQUE FÉDÉRALE DE LAUSANNE

POUR L'OBTENTION DU GRADE DE DOCTEUR ÈS SCIENCES

PAR

Nicolas CHRISTINAT

chimiste diplômé EPF
de nationalité suisse et originaire de Chabrey (VD)

acceptée sur proposition du jury:

Prof. J.-C. Bünzli, président du jury
Prof. K. Severin, directeur de thèse
Prof. E. Constable, rapporteur
Prof. P. J. Dyson, rapporteur
Dr J. Nitschke, rapporteur

ÉCOLE POLYTECHNIQUE
FÉDÉRALE DE LAUSANNE

Suisse
2008

Acknowledgements

I would like to thank…

Professor Kay Severin for giving me the opportunity to work on a fascinating research project and for keeping his door open for discussion at any time.

The members of the jury: Professors Jean-Claude Bünzli, Paul Dyson, Edwin Constable, and Jonathan Nitschke who have invested the time to read and evaluate my thesis work.

The work presented here would not have been possible without the help of Dr. Rosario Scopelliti and Dr. Euro Solari, who performed all X-ray crystallographic analyses. I also thank Dr. Anuji Abraham and Martial Rey for their help concerning NMR spectroscopy, Dr. Alain Razaname and Fransisco Sepulveda for the MS measurements, All the staff of the chemical store: Gladys Pasche, Anne-Lise Carrupt, Giovani Petrucci, and Jacques Gremaud, Patrick Favre for the IT service, and Anne Lene Odegaard and Cristina Zamanos-Epremian for the administrative support.

All my lab colleagues, past and present: Alexander, Andrey, Barnali, Burçak, Christian A., Christian S., Céline, Dalit, Davinia, Elvira, Emanuel, Estelle, Evgeny, Friederike, Isabelle, Joffrey, Justus, Katrin, Laurent, Mang, Marie-Line, Sebastian, Sébastien G., Sébastien R., Thomas, Vera, and Zaccharias. Thank you for your help and advices, as well as for the nice atmosphere in the lab.

All my friends who help me during the last four years, and in particular the "chemists" and "sat" friends: Adrian, Adrien, Anna, Annabelle, Carsten, Claudine, Céline, Chris, Filipo, Hans-Christoph, Ludivine, Marco, Nicolas, Ryan, Sebastiano, Steve, Tom. Thank you for sharing all the good and bad moments chemistry can provide.

My flatmate Mikael for his friendship and the fun we had together, but also for proof reading this manuscript.

Last but not least I also thank my family, and especially my parents and brother for their uncondiditional support and encouragements.

Abstract

This work describes the synthesis and characterization of boronic acid-based supramolecular structures. Macrocycles, dendritic structures, polymers, rotaxanes, and cages were assembled using four types of reversible reactions. The key point of the strategy is the parallel utilization of two –or more– of these reactions.

Initially, aryl and alkylboronic acids were condensed with dihydroxypyridine ligands to give tetrameric or pentameric macrocycles, in which four or five boronate esters are connected by dative B-N bonds. These macrocycles were then used as scaffolds for the assembly of more complex structures from the multicomponent reaction of formyl functionalized boronic acids, with dihydroxypyridine ligands and primary amines. Dendritic structures having a tetrameric or pentameric macrocyclic core and four, five, eight, or ten amine-derived groups in their periphery were obtained.

Three-component reactions were further used to prepare boronate ester polymers from aryl boronic acids, 1,2,4,5-tetrahydroxybenzene and either 1,2-di(4-pyridyl)ethylene or 4,4'-dipyridine. Crystallographic analyses show that the bis(dioxaborole) units are connected by dipyridyl linkers via dative B-N interactions. A computational study provides evidence that the polymers are strongly colored due to efficient intrastrand charge transfer excitations from the tetraoxobenzene to the dipyridyl linker. This latter property was used to assemble the first boron-based rotaxanes from 1,2-di(4-pyridyl)ethylene, catechol, 3,5-bis(trifluoromethyl)phenylboronic acid and 1,5-dinaphto-38-crown-10 or bis-*p*-phenylene-34-crown-10.

In the last part of this work, boronate ester condensations were combined with imine condensations to build organic macrocycles and cages. The former interaction was also used together with metal-ligand interactions to prepare rhenium-based macrocycles. Finally, a nanometer-sized macrocycle was obtained in one step from four chemically distinct building blocks via the simultaneous utilization of the three reversible reactions.

Keywords

IV

Résumé

Ce travail décrit la synthèse et la caractérisation de structures supramoléculaires construites à partir d'acides boroniques. Des macrocycles, structures dendritiques, polymères, rotaxanes et cages ont été assemblés en utilisant quatre types de réactions réversibles. Le point central de la stratégie est l'utilisation en parallèle de deux, ou plus, de ces réactions.

Dans un premier temps, des acides aryl- et alkylboroniques ont été condensés avec des ligands dihydroxypyridine pour obtenir des macrocycles tétramériques ou pentamériques, dans lesquels quatre ou cinq esters boroniques sont connectés par des liaisons datives B-N. Ces macrocycles ont ensuite été utilisés pour assembler des structures plus complexes à partir d'acides boroniques contenant un ou plusieurs groupe(s) formyle(s), de ligands dihydroxypyridine et d'amines primaires. Des structures dendritiques ayant un cœur macrocyclique tétramérique ou pentamérique, ainsi que quatre, cinq, huit ou dix groupes périphériques ont été obtenus.

Des réactions entre trois composants –acides arylboroniques, 1,2,4,5-tetrahydroxybenzène et 1,2-di(4-pyridyl)éthylène ou 4,4'-dipyridine– ont été utilisées pour préparer des polymères composés d'unités bis(dioxaborole). Des analyses cristallographiques ont montré que ces fragments étaient connectés par les ligands dipyridyle via des interactions datives B-N. Une étude computationelle a mis en évidence un transfert de charge entre les fragments tetraoxobenzène et dipyridyle. Cette dernière propriété a été utilisée pour assembler les premiers rotaxanes contenant du bore à partir de 1,2-di(4-pyridyl)éthylène, catéchol, d'acide 3,5-bis(trifluorométhyle)phénylboronique et de 1,5-dinaphto-38-crown-10 ou de bis-*p*-phenylene-34-crown-10.

Dans la dernière partie de ce travail, la formation d'esters boroniques a été combinée avec la formation d'imines pour la construction de macrocycles et de cages organiques. Ce même type de réaction a également été utilisé avec des interactions métal-ligand pour préparer des macrocycles de rhénium. Enfin, un macrocycle de taille nanométrique a été obtenu en une étape et à partir de quatre fragments chimiquement distincts en utilisant simultanément trois réactions réversibles.

Mots-clés

Acides boroniques – Auto-assemblage – Macrocycles – Imines – Réactions à composants multiples – Polymères – Rotaxanes – Cages

Table of Contents

Chapter 1

Introduction

2

1.1 Self-Assembly Reactions

Until recently, the synthesis of macrocycles and cage molecules was performed via the controlled sequential formation of covalent bonds. This methodology has the advantage that the resulting compounds are thermodynamically stable. However, a major drawback of this approach is that the synthesis becomes increasingly longer and more difficult as the scale of the target molecule increases. Theses difficulties are due to the impossibility to fix improperly connected bonds, which are kinetically inert. As a result, very low yields of the final target molecule are often obtained.[1]

To solve theses problems, various strategies have emerged. For instance, the use of a template molecule has proven to be efficient for the formation of cyclic molecules.[2,3] Another possibility is to use weaker interactions such as hydrogen-bonds or metal-ligand bonds. The intermediate products formed using these non-covalent interactions are kinetically labile. Typically, a fast equilibrium exists between the starting materials and all the potential products. This characteristic allows for an error correction mechanism to take place during the reaction and results in the formation of the thermodynamically most stable product. This process, known as self-correction, very often leads to the formation of a single product in high yield.[4,5] If no clear thermodynamic preference is expressed, several species are formed, which are in equilibrium with each other.[6,7] In other words, in this type of reactions, known as *self-assembly reactions*, components will assemble into the final desired structure through an exploration of alternative configurations.

In nature, self-assembly is very often based on hydrogen bonding, van der Waals interactions or weak electrostatic interactions.[8] For synthetic chemists, an alternative is to use metal-ligand interactions to build supramolecular structures.[9,10,11] This methodology offers many advantages. The first one is the large variety of metals and organic ligands that can be used. This allows for the synthesis of assemblies possessing various shapes, sizes, charges and functionalities. More important, metal-ligand bonds offer greater strength and directionality compared to the weaker interactions used in nature. This last point is of importance for the design of well defined architectures.

Another possibility to achieve self-assembly is to use reversible covalent interactions. For instance, reactions involving a carbonyl unit are of special interest because they can generally undergo a disconnection/reconnection cycle under mild conditions. In particular, the condensation between carbonyls and amines to form imines has proven to be highly interesting for the generation of fully organic supramolecular structures.[12]

This type of interaction is often used simultaneously with metal-ligand interactions in multicomponent self-assembly reactions.[13,14]

The condensation of boronic acids with diols is another type of reversible covalent interaction which can be implemented in self-assembly reactions. However, compared to metal-ligand interaction and imine condensation, boronate ester formation is rarely used in the context of supramolecular chemistry, and only a few structures incorporating the boronate ester motif have been reported so far.[15]

As the present research project describes the self-assembly of molecules incorporating boronic acids, imine, and metal fragments, the main characteristics of metal-ligand interaction, imine condensation, and boronate ester formation are briefly explained on the next pages. Some selected examples of supramolecular structures based on these interactions are also described.

1.2 Transition Metal-Based Self-Assembly

Over the last twenty years, interest in transition metal-based self-assembly has increased and research in this area has been extremely active, producing numerous two- and three-dimensional structures. Starting with simple polygons and polyhedra,[16,17] supramolecular chemists are now able to synthesize more complex structures such as grids,[18] helicates,[19] nanocapsules[20] and others.[21] As the shape of these assemblies is defined by the metal coordination geometry and the ligand binding site orientation, it is possible to design structures using simple geometrical considerations and strategies. During the course of the development of transition-metal-based self-assembly, three different strategies have emerged to build such architectures. These approaches are described in the next subparagraphs.

1.2.1 Directional Bonding Approach

This approach, also known as *molecular library model*, was pioneered by Verkade, who synthesized, as early as 1983, a molecular square from a metal carbonyl complex and a bridging diphosphine.[22] In 1990, Fujita reported the synthesis of the palladium-based square **A1**, using 4,4-bipyridyl as the ligand (Scheme 1.1).[23] The method was later rationalized by Stang.[9,10] Since then, numerous structures have been obtained using this strategy and the field has been reviewed by Stang,[16] Mirkin,[11] Fujita,[24] and others.[21]
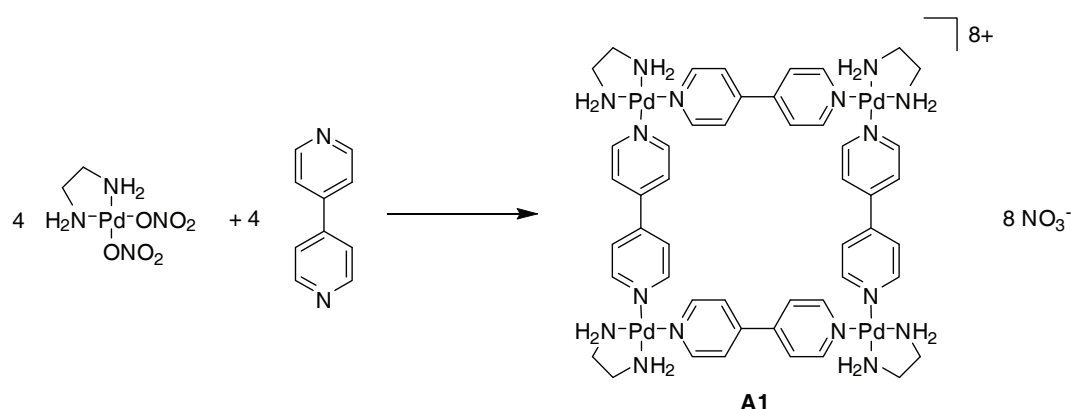
Scheme 1.1: Synthesis of a palladium-based molecular square.[23]

The directional bonding approach involves the reaction of metal centers with multibranched mondentate rigid ligands. Usually, the coordination on the metal ions is defined by the use of inert blocking ligands so that only sites having the desired geometry are available for coordination. The organic ligand can either be linear, having two binding sites with a 180° orientation relative to each other, or bent with other angles between the binding sites. Due to the high rigidity of the building blocks, the geometry of the final assembly is defined by their coordination angles, and careful geometrical considerations give access to a large collection of architectures, as illustrated in Figure 1.1.

However, things can be more complicated and the design principles described above can fail. Metal ions and bridging ligands can sometimes tolerate deviations from their ideal geometry and thus form complexes with unexpected shapes. Problems can also occur when no thermodynamic preference for a single complex is expressed. In this case, two or more species are in equilibrium with each other. This was nicely illustrated by Würthner[25] and Stang,[26] who obtained a triangle-square equilibrium of supramolecular assemblies based on Pd(II) and Pt(II) complexes, respectively.

Building Blocks	60°	90°	109.5°	120°	180°
60°				▱	△
90°		☐			☐
109.5°					⬠
120°	▱			⬡	⬡
180°	△	☐	⬠	⬡	

Figure 1.1: Accessible two-dimensional macrocycles using the directional bonding approach.[27]

If ditopic subunits are employed, only two-dimensional structures can be obtained. In order to build three-dimensional cages or polyhedra, at least one of the building blocks must have three binding sites. Here, the assembly can be either edge-directed or face-directed. The first case is an extension of the principle described above for 2D

structures, with all building blocks on the edges of the polyhedra and the faces left open. In the face-directed strategy, more enclosed cages can be formed using ligands covering the faces of the polyhedra.
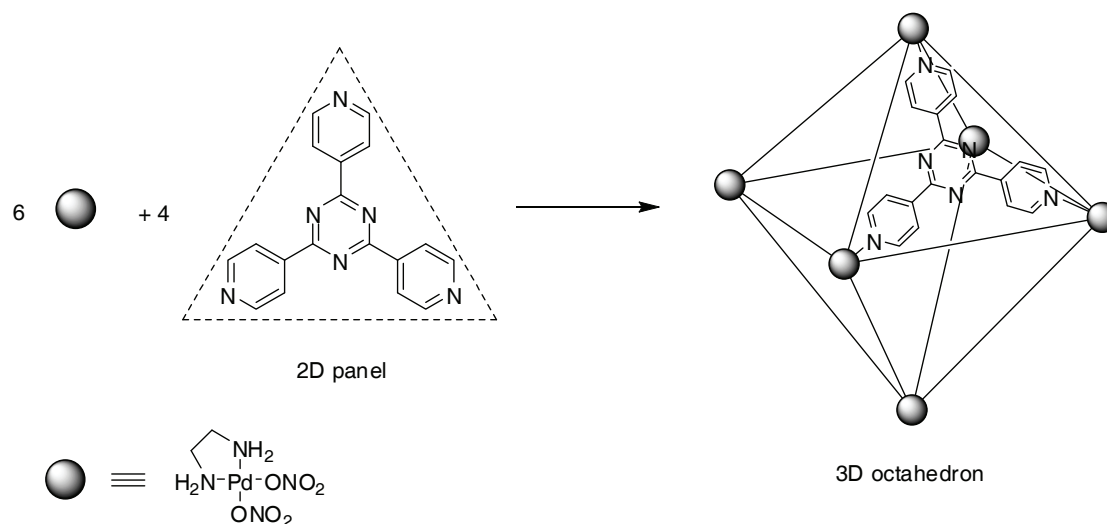
Scheme 1.2: Illustration of the edge-directed synthesis of 3D-architectures.[29]

This method, also referred to as *molecular paneling*, has been extensively used by Fujita, who reported many palladium based architectures,[28] for example, an octahedral cage formed with 2,4,6-tris(4-pyridyl)-1,3,5-triazine (Scheme 1.2).[29] Small molecules[30] as well as peptides[31] can be encapsulated in the hydrophobic cavity of the cage. It was also found that labile intermediates are stabilized[32] or reactions catalyzed[33] by the self-assembled cage.

1.2.2 Symmetry Interaction Approach

The symmetry interaction approach is another strategy for the construction of supramolecular architectures. The first complexes prepared by this strategy (**A2** and **A3** in Figure 1.2) were reported by Maverick.[34,35] It was later used by Saalfrank,[36,37] Lehn,[38,39,40] and Raymond[41,42] to assemble architectures containing transition- as well as main group metals. Unlike the directional bonding approach, this strategy uses multibranched chelating ligands and naked metals ions. As a result, neutral or negatively charged supramolecular clusters are obtained. Moreover, due to the chelation effect of the ligand higher binding constants are obtained than with monodentate ligands.

A2   **A3**
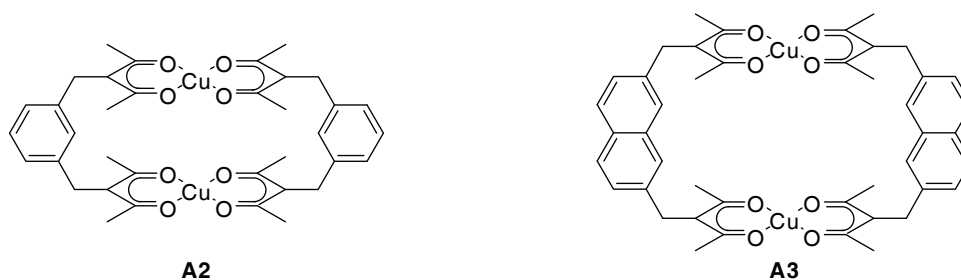
Figure 1.2: First complexes prepared using the symmetry interaction approach.[34,35]

As for the previous approach, the thermodynamic product of the reaction is the target in this strategy. But here, the shape is driven by the symmetry of the coordination sites of the metal center and its preferred coordination geometry. In addition, the orientation of the chelating ligands must be taken into account in order to obtain discrete structures rather than polymers or oligomers. Consequently, the design of a cluster using this strategy can be more difficult than with the two other approaches. In an effort to develop a rational synthetic approach to the construction of such ensembles, Raymond and Caulder have defined a few terms and geometric rules (Figure 1.3).[43,44]

The vector that represents the interactions between a ligand and metal is the *coordination vector*. The *chelate plane* is defined as the plane orthogonal to the major symmetry axis of the metal ion. All the chelating vectors of the chelating ligands lie in the chelate plane. Finally, the *approach angle* is the angle between the vector connecting the two coordinating atoms of a bidentate ligand projected down the (pseudo) 2-fold axis of the chelate group and the major symmetry axis of the metal complex.

(a)   (b)   (c)
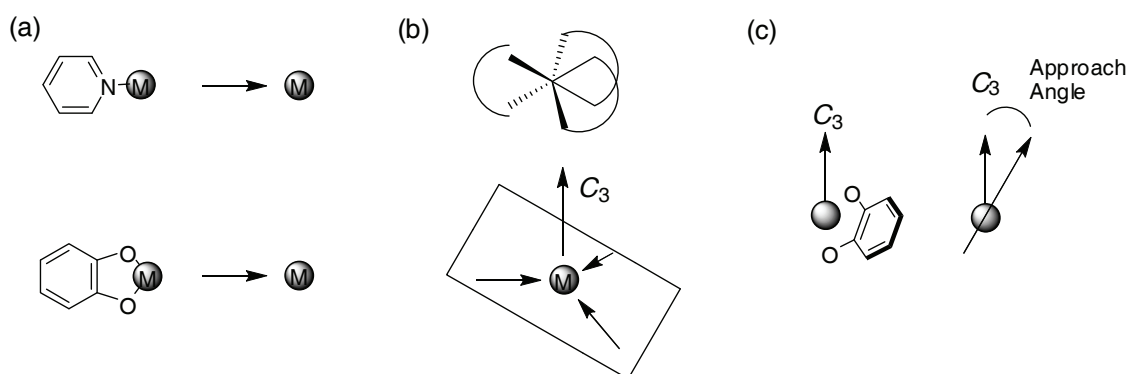
Figure 1.3: Definitions used in the symmetry interaction approach: (a) the coordination vector, (b) the chelate plane, and (c) the approach angle.[43,44]

In principle, by using these symmetry considerations, it is possible to form clusters having any symmetry. The symmetry elements corresponding to the point group of the final assembly are given by the metal and ligand. In other words, to form a M_2L_3 triple helicate having a D_3 symmetry, the building blocks must have a C_2 and a C_3 axis. If the two axes are perpendicular and the two coordination planes are parallel, it is possible to design a triple helicate using a metal having a pseudo-octahedral coordination geometry and a ligand with a C_2 symmetry axis. The orientation of the symmetry elements is a crucial factor. If the axes have an angle of 54.7° between each other, an adamantoid cluster is formed instead of a triple-stranded helicate (Figure 1.4).
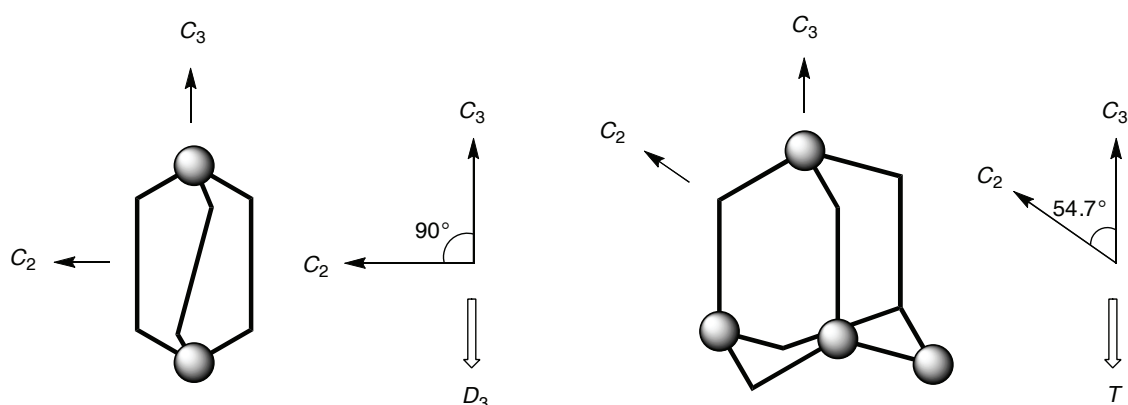
Figure 1.4: Two clusters having the same symmetry elements but with different orientations.

A particularly interesting class of complexes obtained by the symmetry interaction approach was investigated by Raymond and co-workers. A M_4L_6 tetrahedral complex is formed when metal ions (Ga^{3+}, Al^{3+}, In^{3+} or Fe^{3+}) are mixed with ligand **A4** and a base (Scheme 1.3). The corners of the assembly are occupied by the metal ions and the ligands are located on the edges, creating a negatively charged container molecule (overall charge: -12) that is soluble in water and polar solvents but possessing a hydrophobic cavity. The complex is able to encapsulate a large variety of monocationic species, such as ammonium and phosphonium ions or Cp_2Co^+ and Cp_2Fe^+ in its cavity
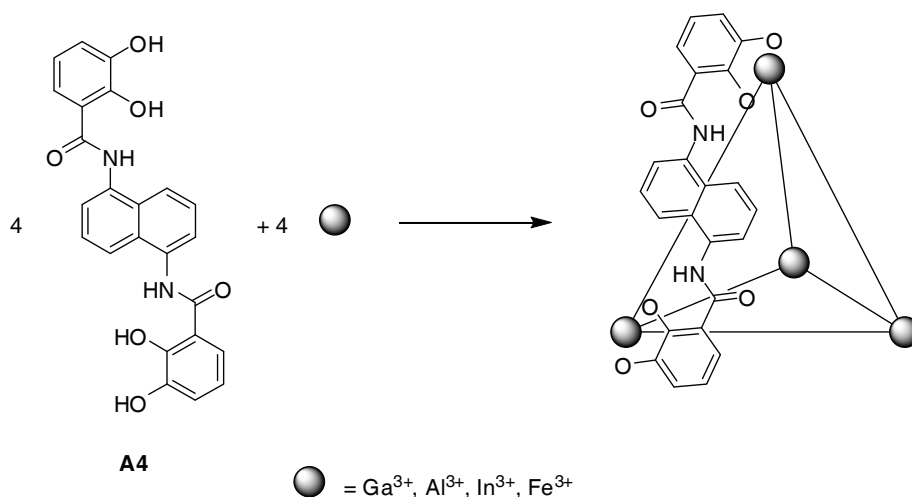
Scheme 1.3: Raymond's M_4L_4 tetrahedral cluster.[42]

The host-guest chemistry of the gallium complex has been extensively studied. It allows for encapsulating reactive species, such as $[Cp^*(PMe_3)Ir(C_2H_4)]^+$, a complex able to activate the C-H bonds of aldehydes.[45] Due to encapsulation, unusual selectivities are observed. Also remarkable is the fact that the cage can act as supramolecular catalyst for the aza-Cope rearrangement of ammonium cations.[46] The vessel has also been found to promote orthoformate hydrolysis[47] and to catalyze deprotection of acetals[48] in basic medium.

1.2.3 Weak-Link Approach

This strategy was first demonstrated by Mirkin,[49,50] who has also later reviewed the field.[51] The weak-link approach is different from the first two strategies. The idea here is that the final assembly still possesses a free coordination site on the metal center. To achieve this goal, flexible, hemilabile ligands are used. In general, they are chelate ligands but with two donor atoms having different affinities towards the metal ion. When a hemilabile ligand is mixed with a metal ion, an intermediate condensed (closed) structure is formed, where all donor atoms are coordinated to the metal. In a second step, the open form of the macrocycle is obtained by selective cleavage of the weakest metal-ligand bond by addition of a better ligand, the so called *ancillary ligand* (Scheme 1.4).
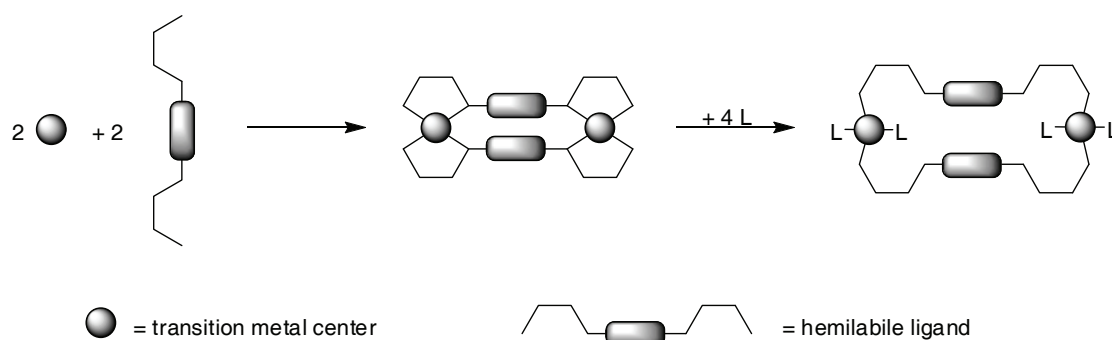
Scheme 1.4: Principle of the weak-link approach.

This strategy offers the possibility to use flexible ligands to form discrete complexes without the typical competition problems of oligomerization and polymerization that can arise when using such ligands. It also leaves an open coordination site on the metal center, which can be used either for host-guest chemistry or to create a larger assembly.

A major drawback of this method is that the condensed intermediate is the kinetic product of the reaction, with the 1:1 metal:ligand complex being the thermodynamic product. This can result in thermal instability of the structures formed with this approach. However, it seems that the energy barrier between the monomer and the dimer is too high to allow for a fast degradation of the condensed intermediate.

Nice applications of this strategy were given again by Mirkin and co-workers, who formed molecular cylinders, in two steps, starting from the dinuclear Rh(I) compound **A5**. In a first step, the complex is opened using CO or acetonitrile as an ancillary ligand. Subsequent addition of 4,4'-biphenyldicarbonitrile or 4,4'-biphenyldiisocyanide respectively leads to the formation of cylinder **A6** (Scheme 1.5).[50]
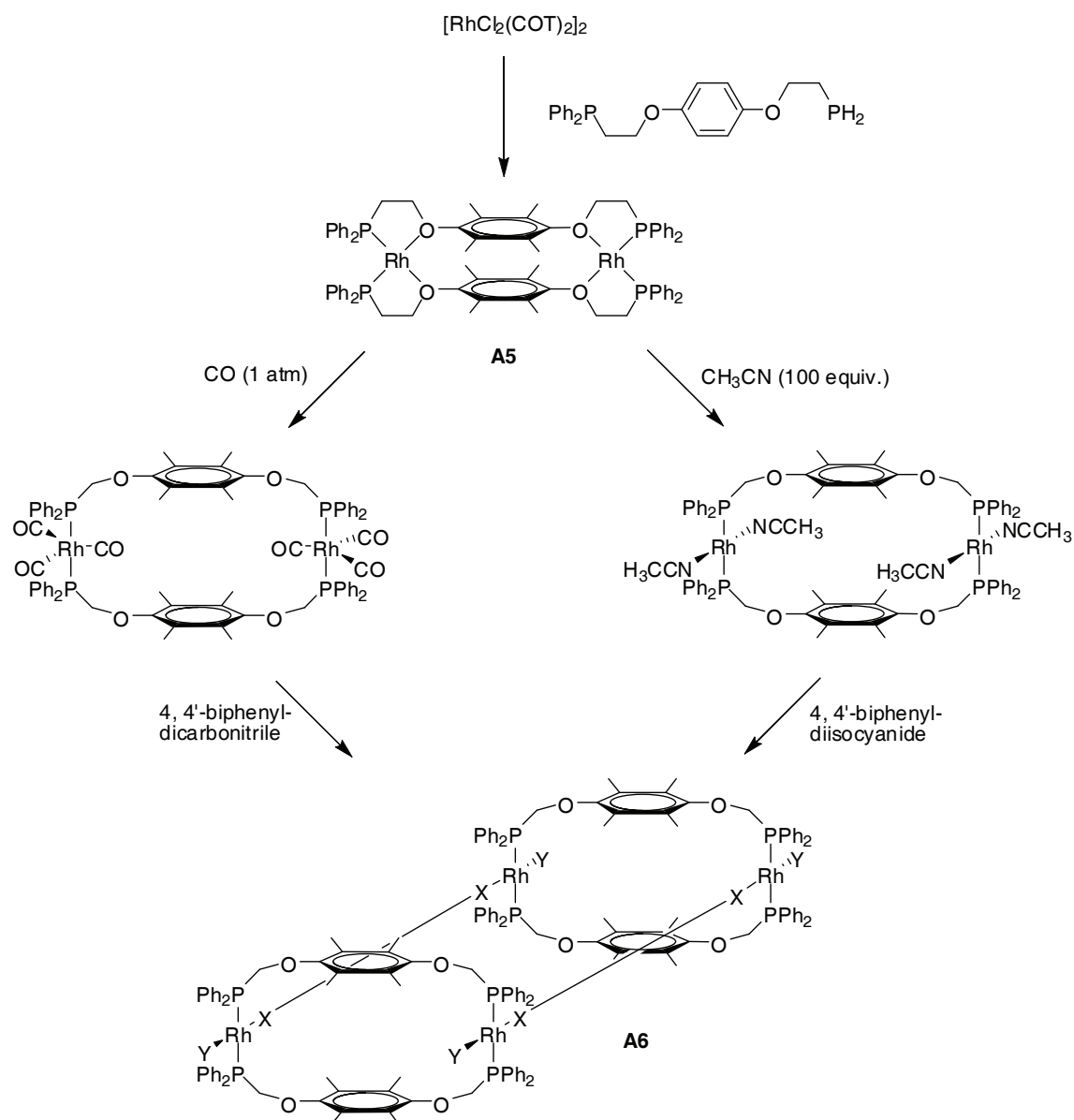
Scheme 1.5: Formation of a molecular cylinder using the weak-link approach.[50]

Salen-type complex of Cr(III), Co(III) or Zn(II) incorporated into the ligand backbone were found to be allosteric catalysts for various reactions such as ring opening of epoxides,[52] acyl transfer reactions[53] and phosphate diesters transesterification.[54]

These three synthetic strategies have been tested with many different metals ions. Among the most popular are Pd(II),[24] Pt(II),[55] Re(I),[56] Ru(II), and Cu(II)[57,58] but other transition metals have successfully been used as well. Examples of structures incorporating Ag(I),[59] Au(I),[60] Zn(II),[61] Fe(II),[62] Ir(III), Rh(III),[63] and Cd(II)[64] are found in the literature. Main group[65] and *f*-block elements[66,67] have also been investigated.

For the organic part of the assembly, namely the bridging ligand, N-heterocycles such as pyridine and pyrazine have been used extensively.[68] To ensure rigidity, benzene, ethylene and ethyne spacers are common.[69] Metals can also be coordinated by the oxygen atoms of a catechol,[70] acetate,[71] ether or ketone. Phosphorous, sulfur and carbon can also be used as donor atoms.[72]

In spite of the large number of metal-based structures already obtained, there is still plenty of room for new architectures incorporating unusual metal fragments and newly design ligands. It is thus reasonable to assume that transition metal-based self-assembly will remain an interesting topic for the next years.

1.3 Imine-Based Constructions

1.3.1 General Considerations

The condensation of primary amines with carbonyl compounds was discovered by Schiff in 1864.[73] Almost 150 years later, this acid catalyzed reaction is still the most common way to form imines (or Schiff bases) and other C=N compounds (also referred to as azomethine linkage in the case of a CH=N fragment). The mechanism of the reaction is well known, and as all steps are reversible, the Schiff base is formed under thermodynamic control. The only by-product of the reaction is water. To obtain high yields, water can be removed from the reaction mixture by azeotropic distillation or using molecular sieves. In addition to the formation/hydrolysis mechanism (path a in Scheme 1.6), imine compounds can be involved in two other reversible reactions: transimination (b) and imine metathesis (c). Unlike the first reaction, the last two do not require the mediation of a third constituent (i.e. water) and breaking of the C=N linkage.
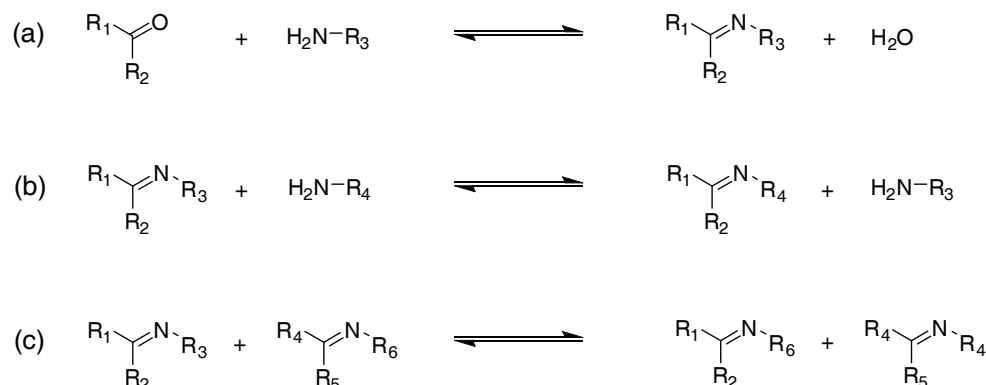
Scheme 1.6: Reversible reactions involving imines.

Because of its reversible character, the imine bond has been extensively used in dynamic combinatorial chemistry (DCC) to generate dynamic combinatorial libraries (DCL). The stability of the condensation product is greatly influenced by the substitution and electronic characteristics of the reagents and in particular of the carbonyl fragment. For example, aromatic aldehydes give the most stable products as reactions involving aryl ketones require complete elimination of water. Imines are thermodynamically unstable in presence of water, which can considerably complicate the analysis of DCLs. The hydrolysis rate of imines is increased by electron-withdrawing substituents and decreased by electron-donating ones. To avoid this problem, water free conditions

are often used in imine based dynamic combinatorial chemistry. Another important property of imines is that they can easily be reduced to the corresponding amine by common reducing agents such as sodium borohydride or sodium cyanoborohydride. This allows for making shape persistent molecules or, when applied to a DCL, to "freeze" the library, in order to ease the analysis for example. Similarly, it was demonstrated that Ugi four-component reaction can be used to freeze imine exchange.[74]

As mentioned before, dynamic equilibria and thermodynamic control are two characteristics of central importance in a self-assembly reaction. As these two properties can be found in imine chemistry, a large number of structures are assembled via the formation of imine bonds. Due to the presence of a nitrogen donor atom, imines can easily coordinate to metal ions. For this reason, they are often used together with metal-ligand interactions to construct supramolecular architectures. In the next two sections, a few examples of such structures are discussed.

1.3.2 Metal-Free Assemblies

Macrocycles are among the simplest assemblies that can be formed by imine condensations. They can be synthesized by mixing a dicarbonyl compound with a diamine in a 1:1 ratio. However, this reaction is not as simple as it looks like, and very often, mixtures of cyclic and linear products are obtained. The reaction begins with the formation of a [1+1] condensation product **I** (Scheme 1.7), that can further react with the diamine or dicarbonyl to give the [2+1] product **II** and the [1+2] product **III**, respectively. Finally, reproducing the same reaction gives either the closed [2+2] macrocycle **IV** or the linear oligomer **V**. The latter can further react to give either larger macrocycles or higher linear oligomers. Another possibility to obtain macrocycle **IV** is to condensate two molecules of **I**.[12]
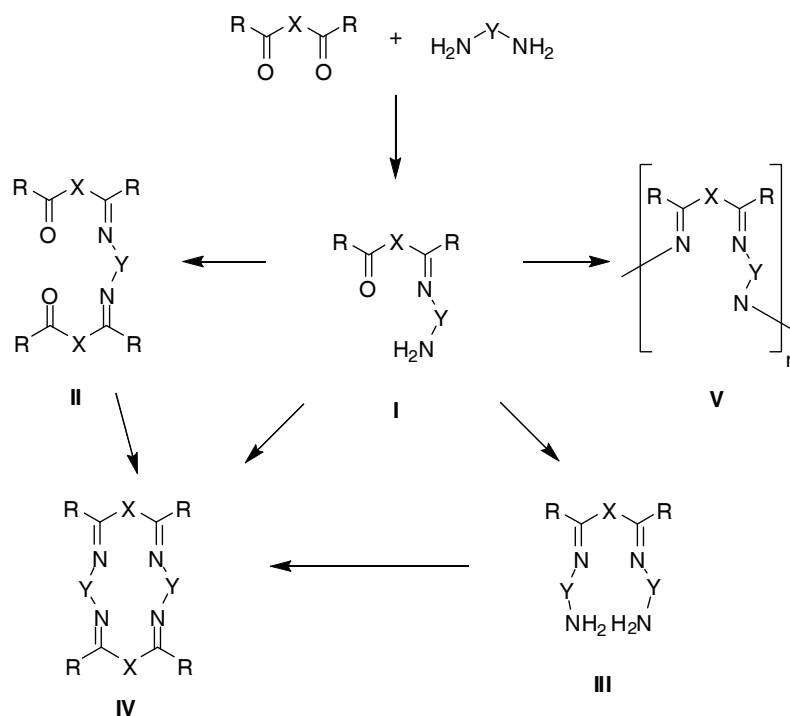
Scheme 1.7: Condensation of a diamine with a dicarbonyl compound.[12]

The main difficulty in the synthesis of polyimine macrocycles is to obtain a pure product. Very often, mixtures of macrocycles (e.g. [2+2], [3+3], [4+4] condensation products) are obtained, together with insoluble oligomers and polymers. Numerous factors can influence the product ratio. Reactions conditions (solvent, ratio, and concentration of reactants) were found to influence the formation of condensation products. The sterical and geometrical characteristics of the building-blocks are also important, in particular the nature of the diamine. Flexible, aliphatic diamines are more nucleophilic than aromatic ones and are thus more reactive in Schiff base condensations. A drawback of this flexibility is that these amines tend to give oligomeric products. To favor the formation of cyclic products over oligomers, high dilution techniques or metal templates are used. On the opposite, more rigid, aromatic diamines are more prone to give well-defined macrocycles. However, a major disadvantage of this type of reagent is their lower nucleophilicity compared to aliphatic diamines. This is especially true for the second condensation of conjugated diamines (i.e. phenylenediamine). In this case, an acidic catalyst is often required to form the macrocycle in good yield.

During the last years, rigid aliphatic diamines have emerged as valuable directing elements to form polyimine macrocycles. These building blocks combine the good reactivity of aliphatic diamines with the rigidity of aromatic diamines. In this context, *trans*-1,2-diaminocyclohexane has been extensively used, in particular with 1,4-

benzene-dicarbonyl compounds. Because the diamine posses a 60° dihedral angle between the NH_2 groups and the dicarbonyl compound a 180° dihedral angle between the CHO groups, triangular [3+3] condensation products are obtained (Scheme 1.8).[75] Other dicarbonyl compounds have also been successfully tested, resulting in [2+2] and [3+3] condensation products.[76,77]
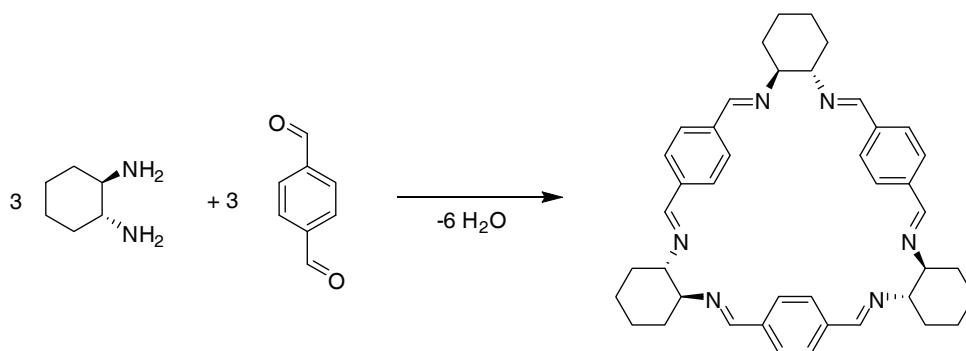
Scheme 1.8: Synthesis of a triangular macrocycle.[75]

The same methodology can be applied to the synthesis of polycyclic compounds. Replacing the diamine by a trisamine leads to the formation of macrobicycles ([3+2 condensation products]), that can be classified as cryptands.[78] Tris(2-aminoethyl)amine (tren) is often used with various rigid dialdehydes (Scheme 1.9).

A = O, NH
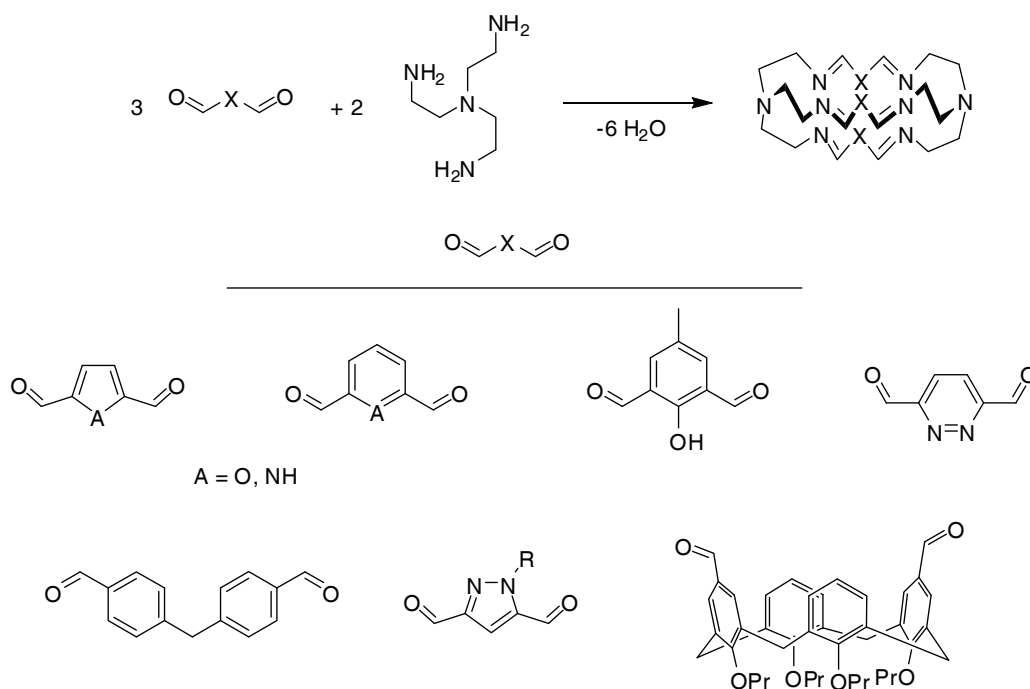
Scheme 1.9: Formation of macrobicycles by imine condensation.[12]

The synthesis is typically performed in an alcoholic solvent under high dilution conditions (10^{-2} M) and the products are obtained in reasonable to good yields (40-65%). As Lehn's cryptands, these imino-macrobicycles can bind various metal cations in their cavity. After reduction of the imines bonds, anions can be bound in the cavity. Following the same trend, polycyclic compounds were formed using a tris-aldehyde and a diamine[79] or a dialdehyde and a tetraamine.[80] The chemistry of imine macrocycles and polymacrocycles has been reviewed several times, in particular by Vigato and Tamburini, who wrote comprehensive reviews.[13,14]

Schiff base condensation was also used to assemble large capsules from more sophisticated fragments. Cram showed that hemicarcerand **A8** can be synthesized by connecting two formyl-functionalized cavitands **A7** via four 1,3-diaminobenzene linkers (Scheme 1.10).[81] Hemicarceplexes can then be prepared with a large variety of guests, such as ferrocene. Latter, Stoddart and co-workers studied diamine exchange on **A8.**[82] They also showed that ferrocene can be released from the hemicarceplexe according to a new path involving imine exchange. In this mechanism, one diamine bridge is opened by imine hydrolysis, allowing the guest to escape. Re-condensation then restores the starting hemicarcerand. The half-life of escape of ferrocene can be dramatically decreased by addition of trifluoroacetic acid, a catalyst for imine exchange, or of an excess of 1,3-diaminobenzene, which stabilizes the open intermediate.
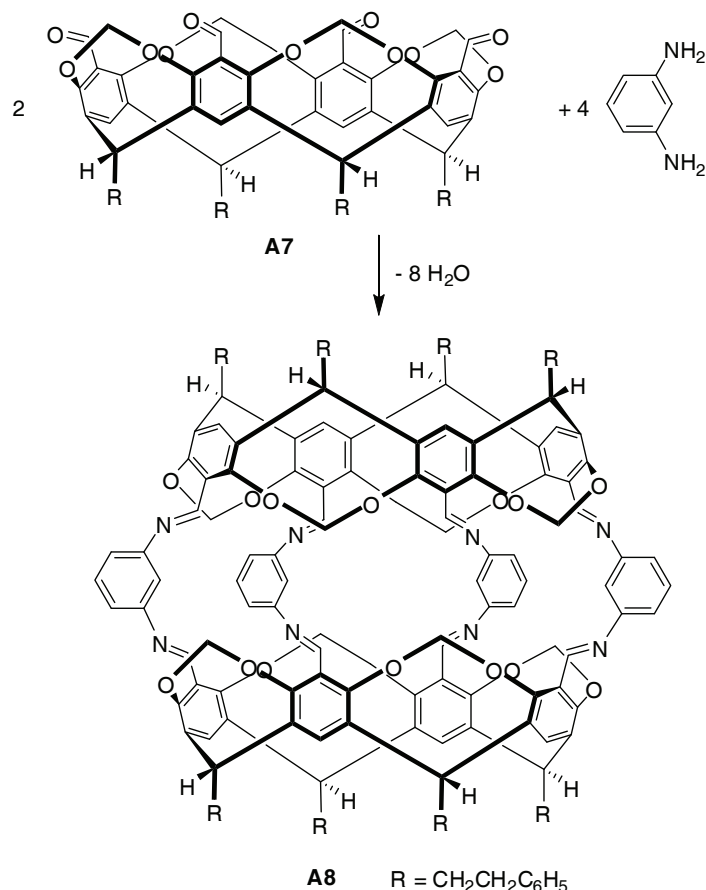
Scheme 1.10: Hemicarcerand synthesis by imine condensations.[81]

Recently, Warmuth reported the formation of even larger container compounds, by condensation of **A7** with alkyl-diamines in CHCl$_3$ and in presence of trifluoroacetic acid. When 1,3-diaminopropane or 1,4-diaminobutane were used, dimeric capsules were obtained. When the shorter ethylene-1,2-diamine was used, a bigger, hexameric capsule was obtained (Scheme 1.11).[83] The same reaction performed in THF instead of chloroform led to the formation of a tetrameric capsule and the reaction in dichloromethane to an octameric one.[84] This large solvent effect can't be explained by the presence of solvent molecules in the cavity. Most likely, specific interactions with the host surface are involved. In a recent publication, the same group also described the formation of a rhombicuboctahedral capsule from a tetraformyl cavitand and 1,3,5-tris(*p*-aminophenyl)benzene.[85]

A7   R = CH$_2$(CH$_2$)$_3$CH$_3$

+ H$_2$N(CH$_2$)$_3$NH$_2$
CDCl$_3$, CF$_3$COOH

+ H$_2$N(CH$_2$)$_2$NH$_2$
CDCl$_3$, CF$_3$COOH
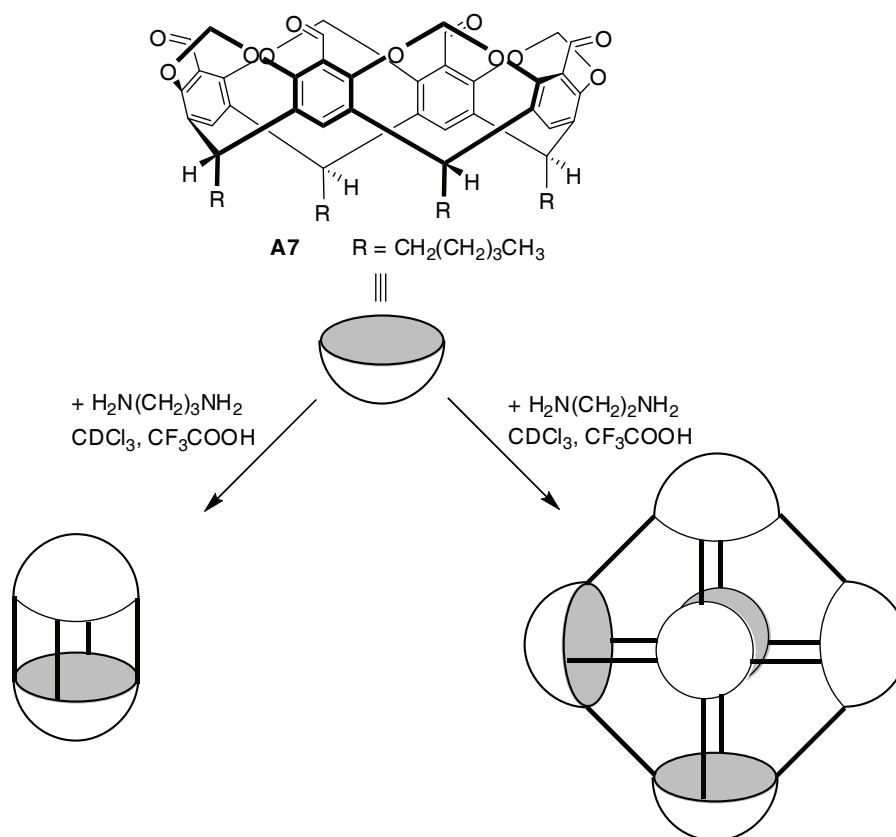
Scheme 1.11: Capsules formed from cavitand **A7** and two different diamines.[83]

Imine condensations were also used to create interlocked structures, such as rotaxanes. Stoddart first illustrated this principle with the synthesis of the [2]-rotaxane **A11** by clipping imino-crown ether **A9** on ammonium dumbbell **A10** (Scheme 1.12).[86] During the synthesis, a library of cyclic and linear oligomers (containing 50% of [24]-crown-8 **A9**) was first prepared by mixing 2,6-diformylpyridine and tetraethylene glycol bis(2-aminophenyl)ether in acetonitrile. The dumbbell was then added, producing [2]-rotaxane **A11**, in equilibrium with other compounds. Here, the ammonium center served as a template for the formation of **A9** but also stabilizes the resulting structure through hydrogen bonding. Interestingly, reduction of the imine bond was faster on the rotaxane than on the free macrocycle, thus driving the equilibrium toward the formation of the rotaxane.
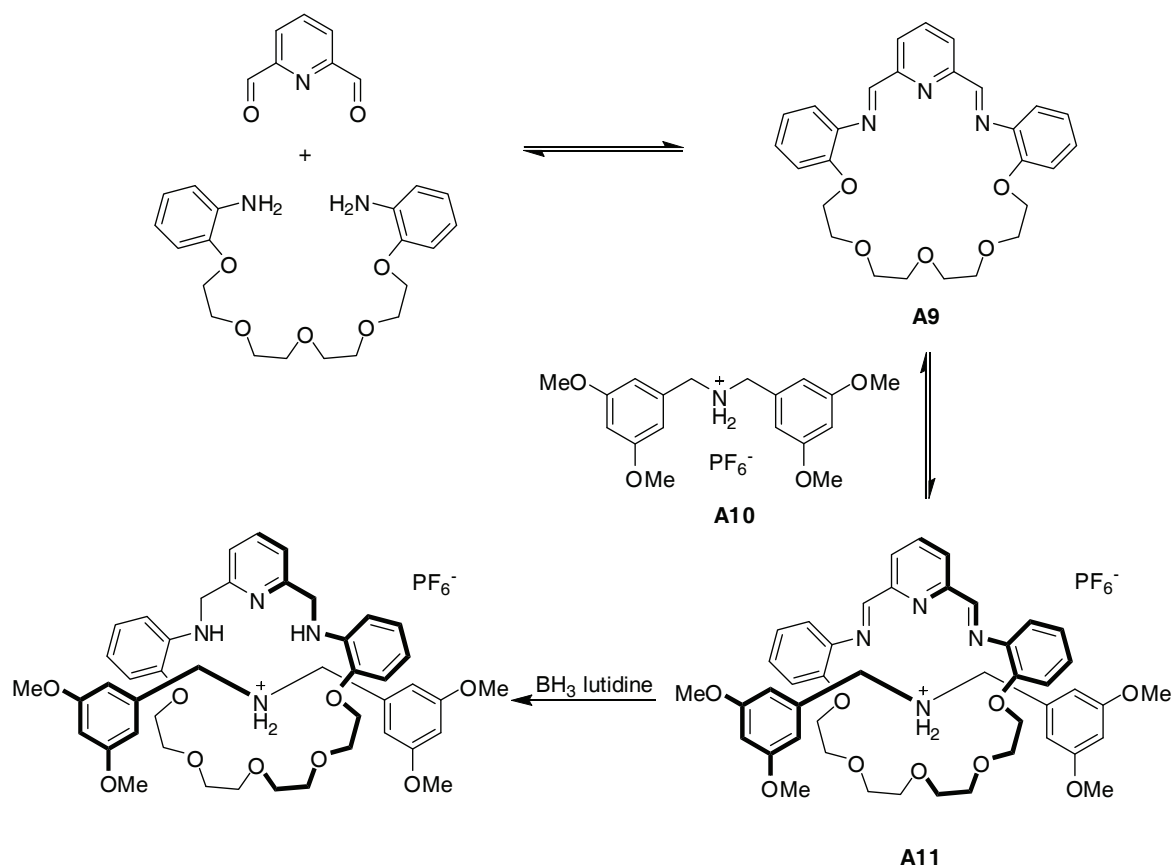
Scheme 1.12: Stoddart's self-assembled rotaxane.[86]

After this first example, the Stoddart group prepared more complex interlocked structures such as [3]- and [4]-rotaxanes, cyclic rotaxanes[87] and suitanes.[88]

1.3.3 Metal-Templated Synthesis

The last example of § 1.3.2 shows that using a template molecule can greatly improve the synthesis of imine-based cyclic structures. In particular, transition metal ions have proven to be good templating agents. Imine (or amine) fragments can bind to the metal and then acquire a well defined spatial orientation. Chelating ligands can be formed through further condensation between fragments, finally resulting in the formation of a closed cyclic ligand, which can be also stabilized by the metal ion. This mechanism allows for the amplification of one particular macrocycle out of a DCL of imine condensation products. The first demonstration of this concept was provided by Busch in the 1960s with the self-condensation of o-aminobenzaldehyde to give a tetrameric

macrocycle around a Ni(II) or Cu(II) ion.[89] The size and shape of the amplified macrocycle depends on the coordination geometry and the size of the metal template. For instance, it was shown that different macrocycles can be selectively amplified from the same mixture of imine fragments, depending on the metal used.[90]

Nitschke and co-workers used this kind of template synthesis to create complex structures. In an approach named *subcomponent self-assembly*, they used metal-ligand interactions and imine condensations simultaneously to form various copper(I) complexes, such as macrocycles, helicates, grids, and even a catenane.[91] Most of these structures were prepared in water, and interestingly, a mutual stabilization between imines and Cu(I) was observed.[92] Complexes architectures can be predicted by analyzing the rigidity, geometry and length of the subcomponents used, as shown by the selection between macrocycle **A12** and catenane **A13** (Scheme 1.13).[93]
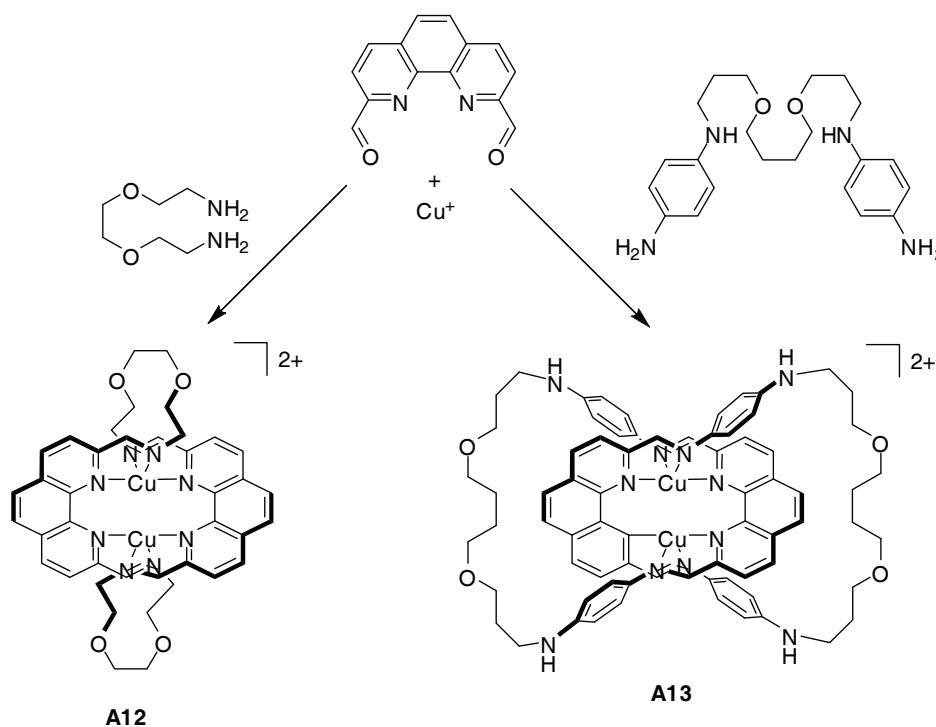
Scheme 1.13: Reaction of 1,10-phenanthroline-2,9-dicarbaldehyde and copper(I) with two different diamines.[93]

The possibility to transform one structure into another was also studied. This substitution chemistry operates both at the covalent and coordinative level. Steric encumbrance, chelate effects, pK_a differences and nucleophilicity drive these transformations.

Other research groups also used metal templated imine condensation to form various architectures.[94,95] The most impressive success of this approach is probably the assembly of molecular Borromean rings by Stoddart's group.[96] This highly symbolic motif, formed by three interlocked rings, had long been targeted by synthetic chemists and various strategies have been tested.[97] The key to success finally proved to be the simultaneous condensation of two types of organic fragments (an exo-bidentate and an endo-tridentate ligand) with zinc acetate. A [2+2] imine condensation allows for the formation of a macrocycle and three of these rings are linked together by six Zn(II) ions (Scheme 1.14).
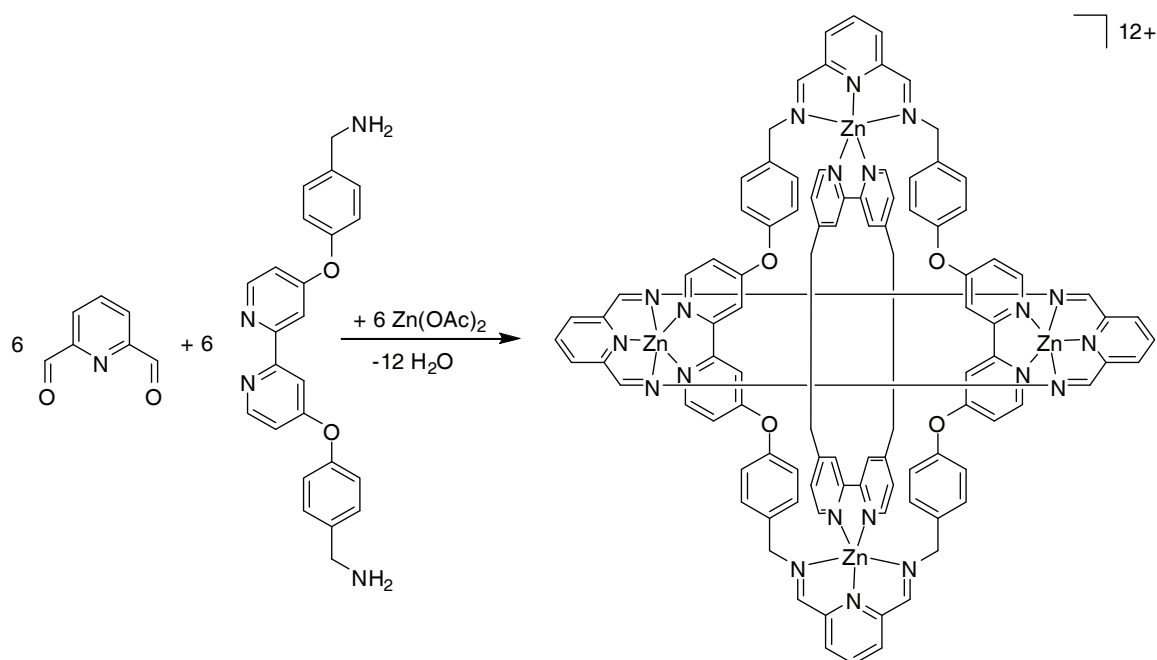
Scheme 1.14: Self-assembly of Borromean rings.[96]

The final structure is assembled in high yield (95%) from 18 components, and 12 covalent imine bonds as well as 30 coordinative bonds are formed during the reaction. It was later shown that copper(II) can also be used as a template to the formation of Borromean rings and that a 1:1 mixture of Zn(II) and Cu(II) led to the formation of a Solomom link.[98]

1.4 Boron-Based Supramolecular Architectures

1.4.1 Boronic Acids

Boronic acids are trivalent boron containing compounds, the boron atom being surrounded by two hydroxyl group and one alkyl or aryl fragment.[99] These reagents, first prepared by Frankland,[100] became very popular when Suzuki and Miyaura discovered their use in metal catalyzed cross-coupling reactions with halides.[101,102] In addition to their interesting reactivity, boronic acids compounds are non-toxic, stable and easy to handle. Their preparation is also relatively simple, from Grignard reagents and trialkyl borate.[103] These reasons make boronic acids a particularly interesting class of synthetic intermediates.

While cross-coupling reactions involve breaking of the B-C bond and elimination of the boron containing fragment, other reactions can preserve the boronic acid scaffold. Theses reactions, described below, can be classified in three categories and affect either the B-O bond or the free coordination site of the boron center.

1.4.1.1 Acid-Base Interactions

Structurally, boronic acids posses a trivalent boron atom which is sp^2 hybridized, with a vacant p orbital orthogonal to the plane of three substituents. Due to this deficient valence, boronic acids are mild Lewis acids and can react with bases. Boronic acids are not Brønsted acids, despite the presence of two hydroxyl groups, and they are in equilibrium in water with their anionic tetrahedral species (Scheme 1.15).[104]
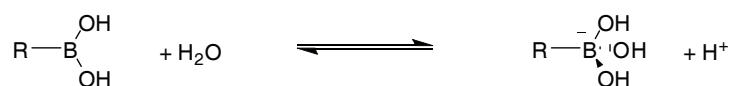
Scheme 1.15: Acid-base equilibrium of boronic acids in water.

The pK_a value of boronic acids depends on the electronic and steric nature of their substituent. Alkyl boronic acids are less acidic than aryl ones: Phenyl boronic acid has a pKa of 8.7[105] and methyl boronic acid has a pK_a of 10.4.[106] One of the most acidic boronic acid known is 3-pyridyl boronic acid, with a pK_a value of 4.0.[107] It has also been

observed that different isomers can have different pK_a values and that bulky substituents proximal to the boryl group decrease the acidity.

Boron compounds can form acid-base adducts with amines, and in this case a coordinative (or dative) B-N bond is formed. The bond strength depends on the substitution on both fragments: Electron deficient boronic acids and electron rich amines form more stable complexes. Since the discovery of the BMe_3-NH_3 adduct, numerous related compounds have been prepared. In order to obtain quantitative information, the B-N bond was studied in term of bond length, bond energy and tetrahedral character (THC). Bond length values ranging from 1.57 Å for the covalently bonded cubic boron nitride[108] to 2.91 Å (sum of the van de Waals radii of boron and nitrogen)[109] were observed. Brown also observed very different values for the gas phase dissociation enthalpies of amine boranes, going from 52 to 152 KJ mol^{-1}.[110] The tetrahedral character, calculated from the bond angles at the boron atom, allows for the evaluation of the geometry of boron adducts.[111] It can be calculated using the following equation:

$$ \text{THC [\%]} = \left[1 - \frac{\sum_{n=1\text{-}6} \left| 109.5 - \theta_n \right|^\circ}{90^\circ} \right] \times 100 $$

Where θ_n are the six angles around the boron atom. Höpfl examined a serie of 144 structures having a B-N bond.[112] He found a correlation between bond length and tetrahedral character and identified factors which weaken the B-N bond, such as ring strain and steric encumbrance.

The nature of the B-N interaction in an o-(N,N-dialkylaminomethyl)arylboronate system has been studied by Anslyn and co-workers.[113,114] In solution, they observed the formation of an intramolecular B-N bond in chloroform and insertion of solvent in methanol. Similarly, the presence of the dative bond in the solid state depends on the crystallization solvent. NMR titrations also revealed that B-N bond formation is promoted by coordination of electron-withdrawing substrates (diols).

1.4.1.2 Boroxine Formation

As mentioned above, boronic acids are stable compounds, in particular towards atmospheric oxidation. However, they can easily loose water, to form anhydrides, and in particular the cyclic trimeric boroxine. Boronic acids very often co-exist with their

anhydrides in both solid state and solution. The equilibrium between acid and anhydride is greatly influenced by the substitution on the organic fragment. A recent NMR study of differently 4-substituted phenyl boronic acids shows that boroxine formation is reversible at room temperature (in $CDCl_3$) and that electron donating groups help support boroxines formation.[115] Calculated equilibrium constants were found to be rather small. Usually, dehydration reactions can be driven to completion by careful removal of water from the reaction mixture.
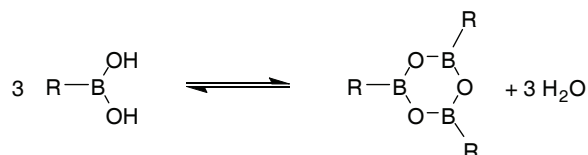
Scheme 1.16: The boronic acid- boroxine equilibrium.

Boroxines, with their planar B_3O_3 ring, are isoelectronic to benzene, and may possess a partial aromatic character.[116] Similar to boronic acids, they interact with bases, but donor molecules can only coordinate to one boron atom of the B_3O_3 ring.[117] Coordination of another equivalent of base is strongly disfavored, presumably because of steric strain.[118] However, boroxines having two four-coordinated boron atoms have been reported, but in this case the B-N interaction is intramolecular.[114] Coordination of a N-donor ligand is a fluxional process, according to NMR experiments.[119]

1.4.1.3 Boronate Esters Formation

Boronic acids easily react with diols to form boronate esters, with loss of water.[120] Here again, products and reactants are in equilibrium with each other, and ester formation can be favored by elimination of either water or product from the reaction mixture. With 1,2-diols, five-membered cyclic esters are formed and six-membered rings are formed with 1,3-diols. Boronate esters can be prepared from a large variety of diols and boronic acids, and over the years, trends about their stability toward hydrolysis have been observed: Six-membered esters were found to be more stable than five-membered rings.[121] Substitution on the diol fragment also helps stabilizing the ester. Aromatic diols form less stable esters than aliphatic ones. Diethanolamines forms very stable boronic esters. The presence of an internal B-N bond prevents coordination of a water molecule on boron, and thus formation of a key intermediate in the hydrolysis reaction.

Boronate esters can be involved in transesterification reactions with free diols. In this case, similar reactivity trends were observed.[122] It was also observed that boronic acids undergo similar condensation reactions with fragments where one or both of the hydroxyl groups have been replaced by primary or secondary amines or carboxylic acids.

Since its discovery in the 1950's, boronate ester formation has been extensively used in carbohydrate chemistry, for protection and sensing purposes.[123] Numerous studies about the highly complex boronic acid-diol equilibrium in aqueous media have been conducted. Two very important trends can be pointed out (summarized in Scheme 1.17): Ester formation is favored by a high pH (K_E' > K_E) and free boronic acids have lower Lewis acidity than their complexes with 1,2-diols (pK_a > pK_a').
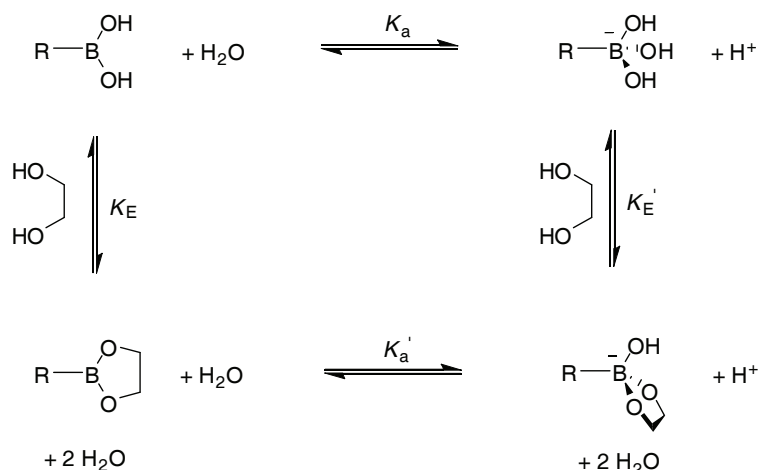
Scheme 1.17: Acid-base and esterification equilibria involving boronic acids.

1.4.1.4 Potential in Supramolecular Chemistry

During the last years, supramolecular chemists began to be interested in boronic acids, because they saw similarities with transition metals. Being Lewis acids, they are able to form bonds with donor atoms such as oxygen, nitrogen, sulfur or phosphorus. Another possible reaction of boronic acids is the condensation with diols, such as catechol, a class of ligands commonly use in supramolecular chemistry. Moreover, these reactions are reversible, although bond energies are typically high. This characteristic ensures the formation of the thermodynamically most stable product, through the "error correction" mechanism. Thus, boronic acids are potentialy good reactants for self-assembly reactions.

Boronic acids are also highly directional elements, and their geometry can either be trigonal planar, for the Lewis acidic boronic acid/ester, or tetrahedral, for the acid-base adduct. This characteristic facilitates the incorporation of this building block in supramolecular assemblies.

However, compared to its transition-metal analogue, boron-based supramolecular chemistry is still largely underexploited, and only a few structures have been reported so far. These structures are described in the next pages, and are classified according to the type of assembly.

1.4.2 Macrocycles and Cages

First examples in the field of boron-based self-assembly were reported by the group of Farfàn and Höpfl. In 1997, they presented the synthesis of the tetrameric macrocycle **A14** from phenyl boronic acid and 2,6-pyridinedimethanol (scheme 1.18a).[124] Interestingly, this ligand was shown to be a tridentate chelating ligand with metal ions, but with the smaller boron, only one chelate ring can be form. The pending methanol arm is thus forced to condense with another fragment, initiating macrocyclization. The same group latter reported that monochelation can be achieved using **A15**, a ligand with longer, more flexible arms (Scheme 1.18b).[125]
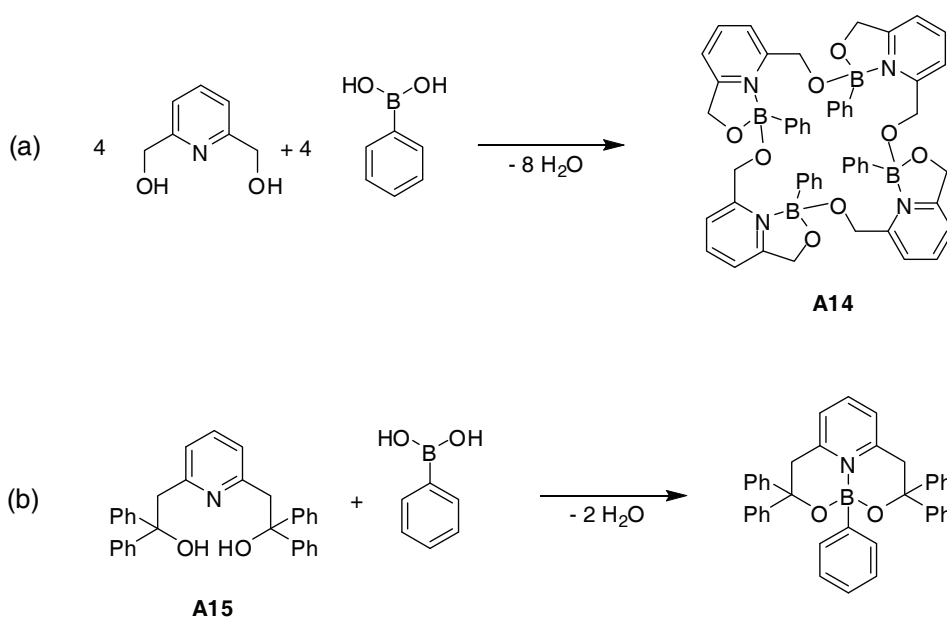
Scheme 1.18: Condensation of phenyl boronic acid with tridentate amino dialcohols ligands.[124,125]

The same researchers also investigated the condensation of boronic acids with other tridentate amino dialcohols ligands obtained from salicylaldehyde and aliphatic[126] or aromatic aminoalcohols.[127] The goal here was to obtain dimeric macrocycles that can be seen as analogues to cyclophanes (Scheme 1.19a). In their study, Farfàn and Höpfl observed that, although dimers can be synthesized, electronic effects, as well as steric and transannular strains greatly influence the geometry of the assembly. Indeed, they also observed the formation of monomeric species (b), as well as polymeric ones (c), or incomplete condensation products (d).
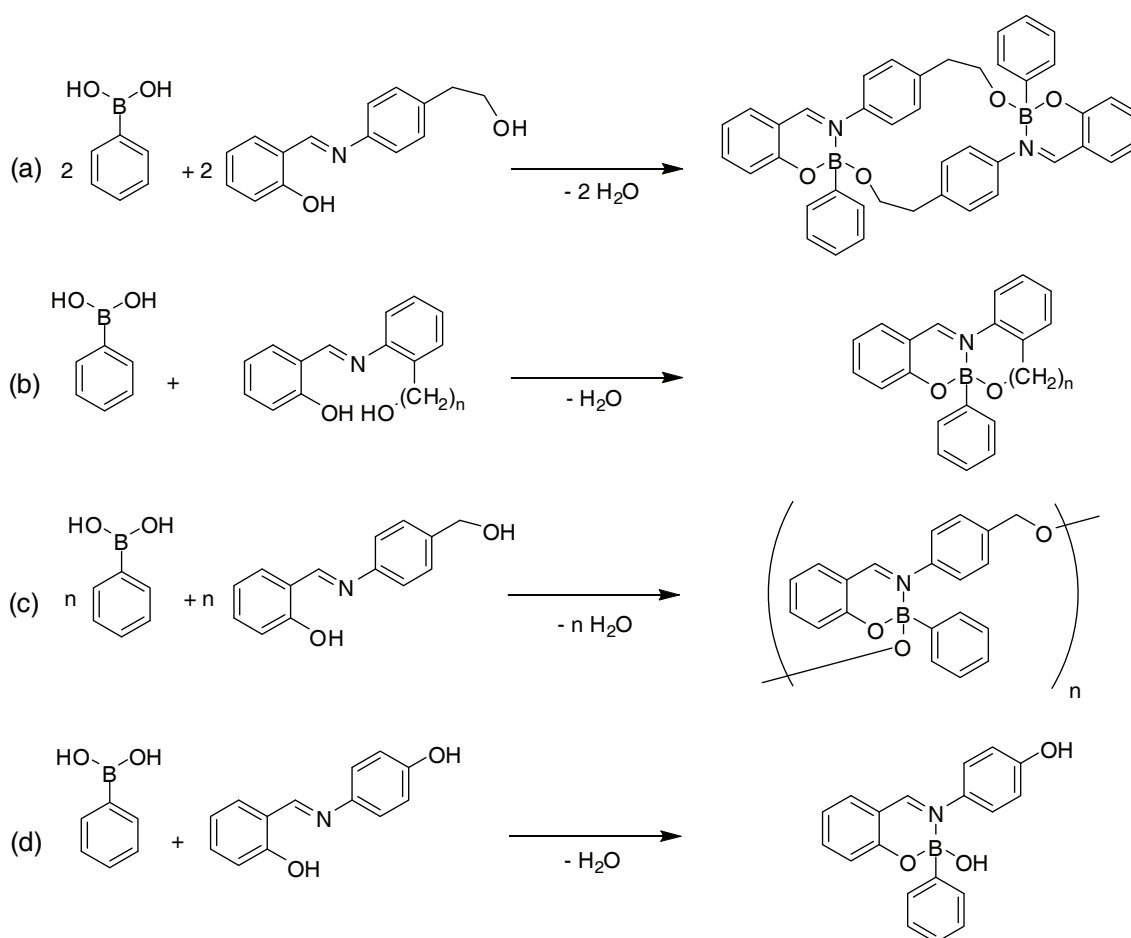
Scheme 1.19: Possible products of the condensation reaction between phenyl boronic acid and different tridentate ligands.[126,127]

The salicylaldehyde fragment has also been used in condensation reactions with 3-aminophenyl boronic acid to form a tetrameric macrocycle.[128] In this reaction, an imine is first formed, followed by condensation of four units to produce a macrocycle. Finally, the unreacted hydroxyl groups condense with a molecule of solvent (i.e. an alcohol) to

produce the final structure. This tetrameric macrocycle seems to be somehow an exception, because only trimers were observed when different carbonyl compounds such as 2-hydroxyacetophenone, 2-hydroxybenzophenone and substituted salicylaldehyde were used (Scheme 1.20a). X-ray analyses have shown that these macrocycles have a calix[3]arene-like conformation and that solvent molecules are located in their cavity.[129,130] Recently, a polymacrocyclic compound has been obtained using the same strategy with bridged bis(salicylaldehyde) ligand **A16** (Scheme 1.20b).[131]
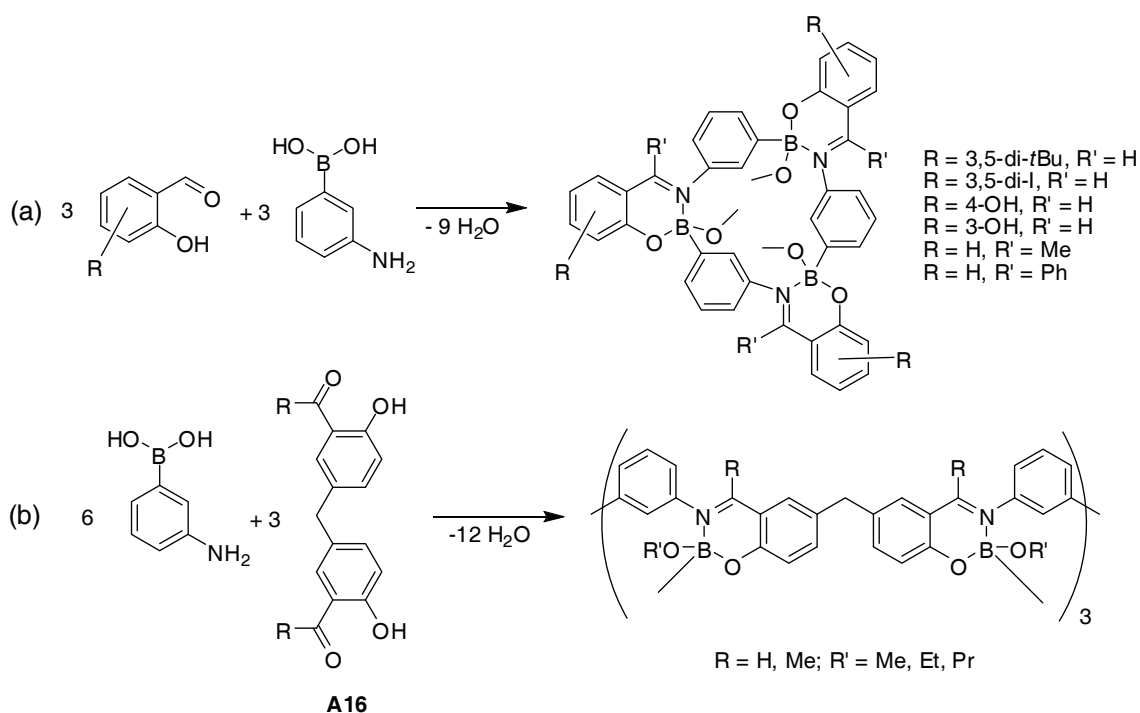
Scheme 1.20: Formation of boron containing calix[3]arenas.[129 -131]

The Shinkai group used boronic acid-diol condensation together with metal-ligand interaction to build supramolecular structures.[132] They condensed 3-pyridyl boronic acid dimethyl ester with a porphyrin functionalized with two catechol units. Depending on the metal coordinated in the porphyrin ring, different structures were obtained. With zinc, a dimeric complex was formed; with magnesium, a polymer was produced. This can be explained by the different coordination numbers of both metals (five vs. six).

Dreos and co-workers used a very similar approach to build dinuclear boxes with cobaloximes and 3- or 4-pyridylboronic acids, but condensed the boronic acid with the two oxygen atoms of the oxime functional groups of the macrocyclic ligand.[133,134] The

same group latter prepared a trimeric complex using 3-aminophenyl boronic acid together with cobaloxime and a polymeric one from 3-aminophenyl boronic acid and rhodoxime.[135]

Recently, different research group have presented new boron-based supramolecular structures. Aldridge and co-workers prepared dimeric macrocycle **A17** from 1,1'-ferrocenediboronic acid and pentaerythritol (scheme 1.21).[136] When using (1*R*,2*S*,5*R*,6*S*)-tetrahydroxycyclooctane as bridging ligand, only oligomers were formed. MALDI-mass spectrometry allowed for the detection of oligomers containing up to seventeen identical units.
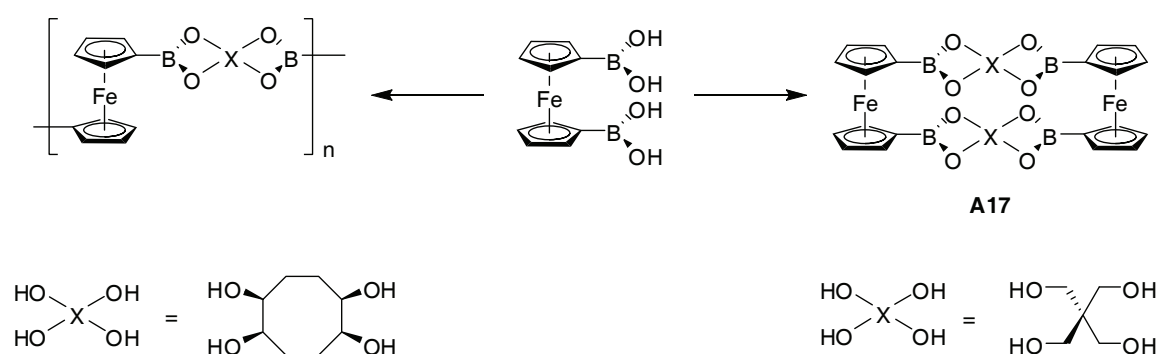
Scheme 1.21: Aggregation of 1,1'-ferrocenediboronic acid with two different tetraols.[136]

Iwasawa studied dynamic self-assembly between racemic tetraol **A18** and 1,4-benzenediboronic acid.[137] It was observed that macrocycles were only formed in presence of an appropriate template. When the two building blocks were mixed in pure methanol, an insoluble polymeric material was obtained, but when using an aromatic solvent together with methanol, formation of macrocycles was favored. With toluene, a [2+2] condensation product was obtained, and X-ray analyses showed the presence of a toluene molecule in the cavity, suggesting that π - π interactions between toluene and the phenyl ring of the boronic acid may be responsible for the formation of the closed structure. When benzene was employed instead of toluene, the [3+3] macrocycle was obtained, with two benzene molecules included in the cavity. Both types of macrocycles can be interconverted in presence of the appropriate guest and methanol. Naphtalene and triphenylene were found to be appropriate templates for the [2+2] and the [3+3] macrocycle, respectively.
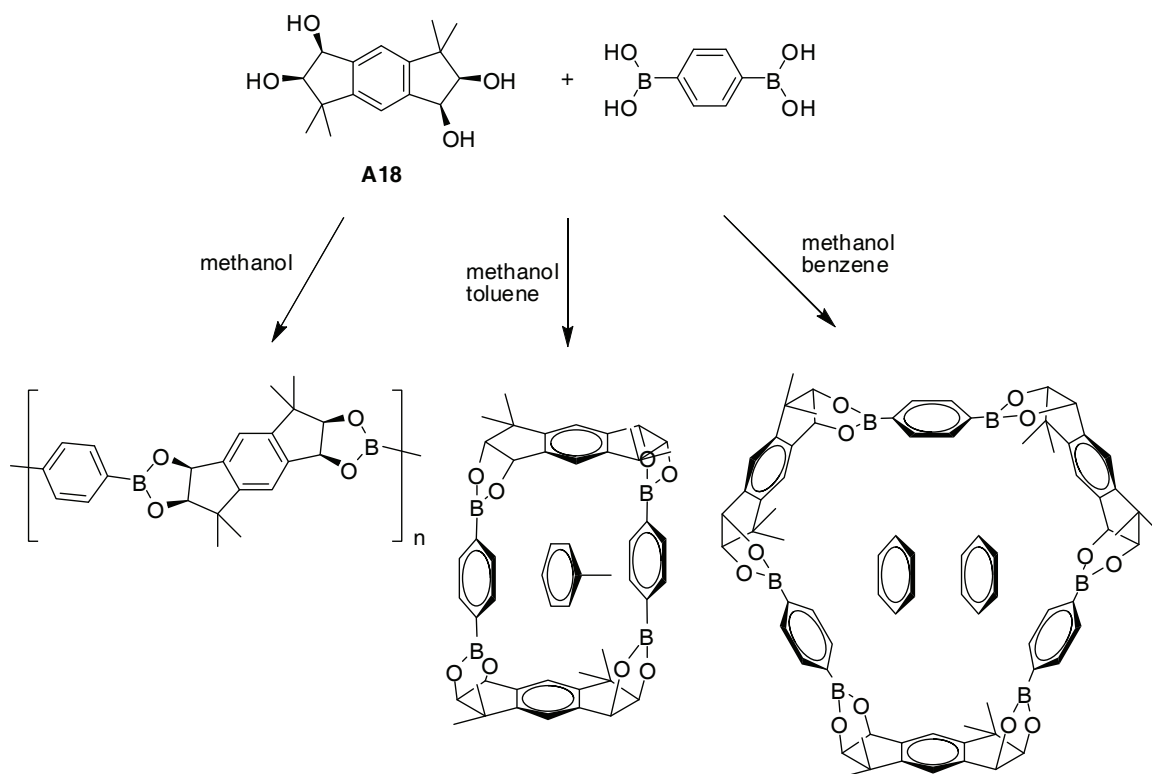
Scheme 1.22: Templated synthesis of boronate macrocycles.[137]

Kubo and co-workers reported the formation of an heterodimeric capsule from triboronic acid **A19** and calix[3]arene derivative **A20** driven by ion pair recognition (Scheme 1.23).[138] The two fragments only interact with each other (forming a boronate ester) if Et_4NAcO is present in solution. One molecule of Et_4N^+ is encapsulated in the cavity and acts as a template. The anion AcO^- probably promotes boronate ester formation by coordination on boron and is then rapidly replaced by a methoxy group (solvolysis and methoxy insertion). Capsule formation is also pH dependent: Lowering the pH leads to the disassembly of the capsule and subsequent addition of a base allows for its reassembly.
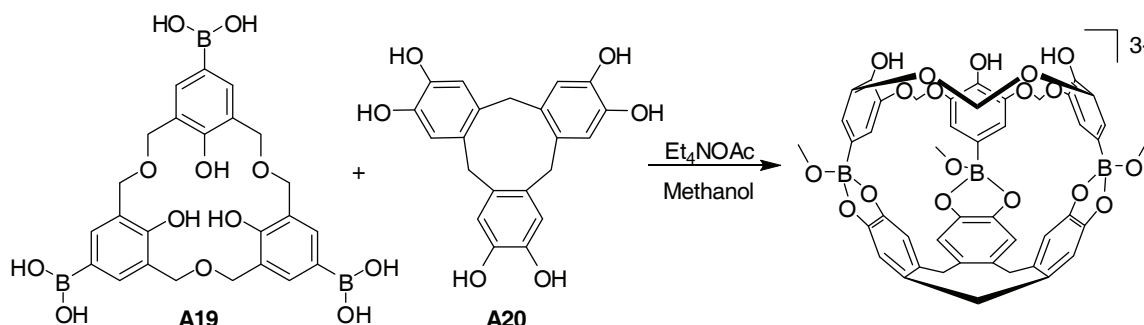
Scheme 1.23: Ion pair driven capsule formation.[138]

Very recently, Nitschke studied the iminoboronate ester motif in subcomponent self-assembly.[139] 2-Formylphenyl boronic acid was reacted with various amines and diols, producing boronate esters having a B-N intramolecular bond, as previously reported by James.[140,141] Factors influencing the reactions, such as electron density, delocalization capability, and solubility of the subcomponents, were identified and subsequently macrocycle **A21** and cage **A22** were prepared (Scheme 1.24).

A21

A22
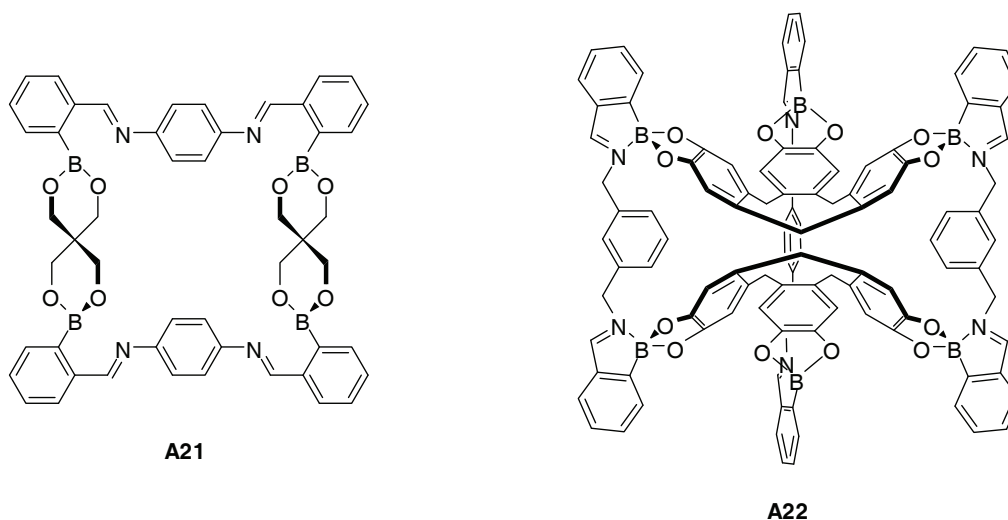
Scheme 1.24: Structures obtained by subcomponent self-assembly.[139]

1.4.3 Polymers, Covalent Organic Frameworks

Mikami and Shinkai were the first to investigate the field of boronic acid based polymers. They studied the reaction of diboronic acid **A23** with saccharides[142] and chiral tetraol **A24** and **A25**.[143] 4,4'-Substitution on the biphenyl was used in order to avoid formation of a 1:1 adduct with the polyol fragment and the amine groups were used to stabilize the boronate ester by formation of intramolecular N-B bonds. After analyses by CD spectroscopy, these polymers were suspected to have a helical structure similar to DNA. Shimizu and coworkers also used boronate ester formation to connect diboronic acid **A26** and glucosamides **A27**, **A28** and **A29**.[144]
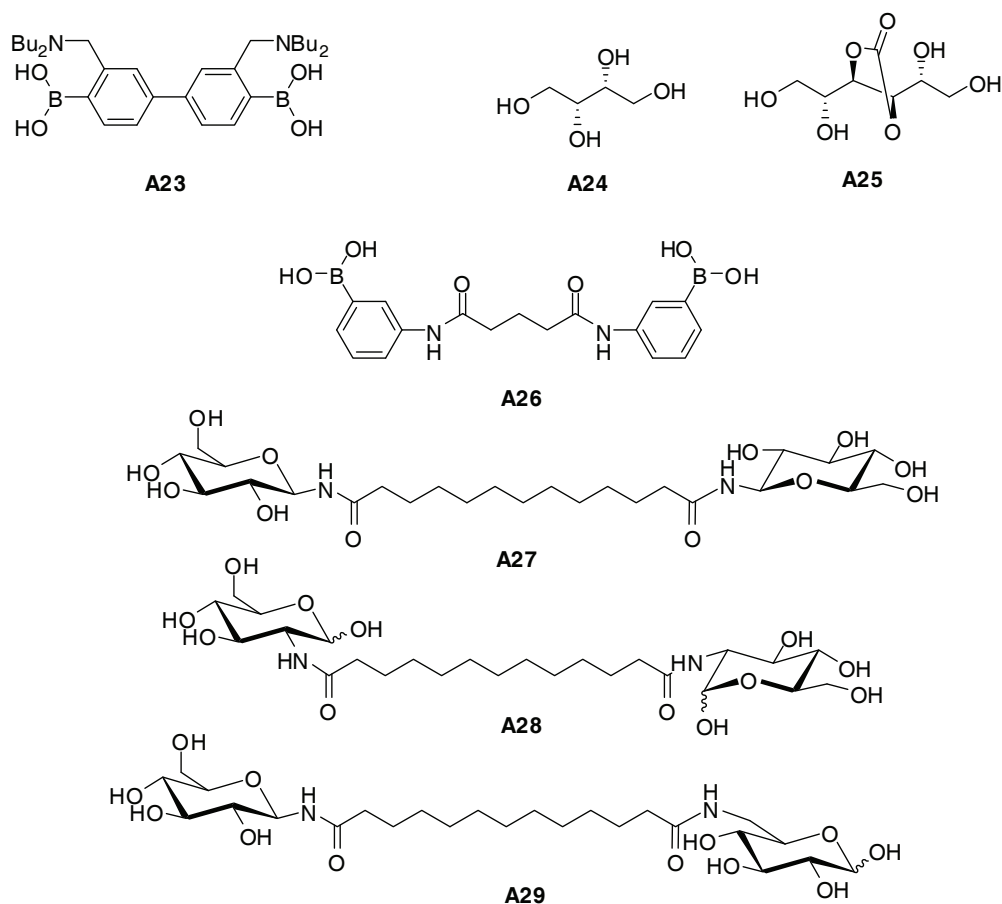
Scheme 1.24: Building blocks for the synthesis of helical polymers.

In 2005, Lavigne reported the synthesis of a dynamic polymer, in which the subunits are covalently linked.[145] To do so, pentaerythritol and 9,9-dihexylfluorene-2,7-diboronic acid were reacted with each other to form a six-membered boronate ester (named dioxaborolane). As both building blocks are ditopic, a linear chain was grown by repeating the same condensation reaction. Gel permeation chromatography (GPC) revealed a molecular weight of 28000, indicating that the chain is composed of 58 repeated units. The interest of this system is that the polymer can be subject to hydrolytic degradation and then self-repaired, by storage under reduced pressure. The process can be repeated several times, but it was observed that the length of the chains decreases.
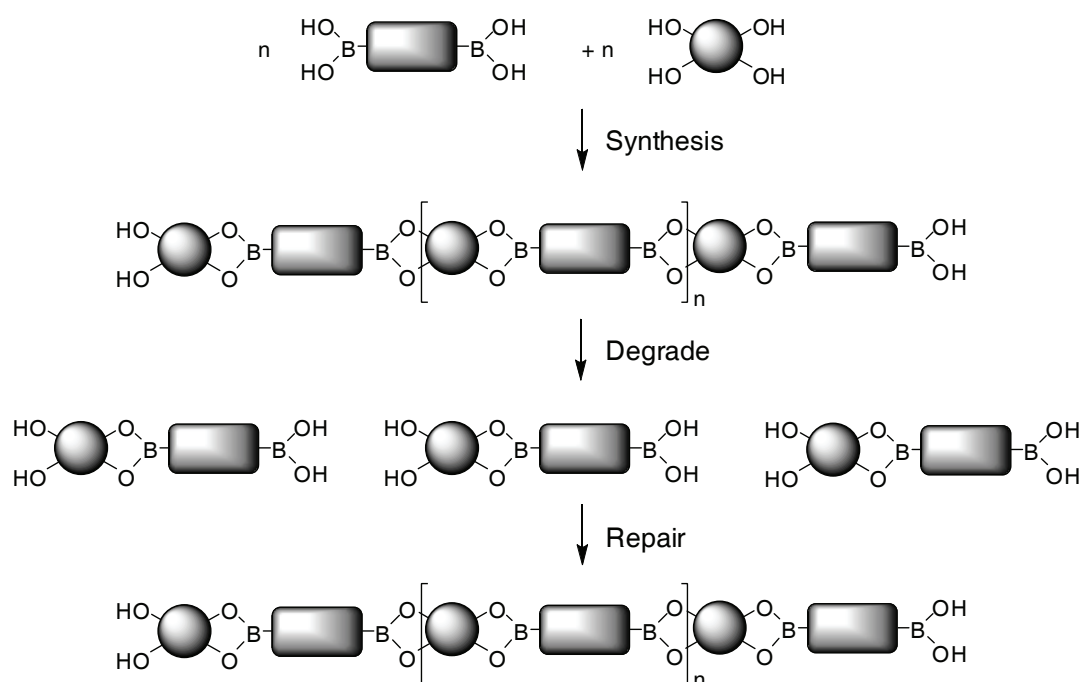
Scheme 1.25: Principle of the boronic acid based self-repairing polymers.

The same group, later slightly modified the system by using 1,2,4,5-tetrahydroxybenzene instead of pentaerythritol.[146] As a result, an extended conjugation along the polymer chain was obtained, and an emission of blue light was observed upon excitation. Using the same strategy, a polymer based on 1,4-phenyldiboronic acid was also prepared.[147] Ding and co-workers studied the optical properties of a cross-linked polymer formed by self-condensation of monomers having two boronic acids functional groups separated by oligofluorenes or carbazole linkers.[148]

Covalent organic frameworks (COFs), a particular class of polymeric materials, have been studied by Yaghi's group. COFs are crystalline, extended organic structures. They are porous, have high surface area and are considered as promising materials for gas storage. In a first publication, Yaghi reported the preparation of 2D networks from 1,4-phenyldiboronic acid.[149] Two types of condensation were performed with this building block: either a self-condensation (boroxine formation) or a condensation with 2,3,6,7,10,11-hexahydroxytriphenylene. Both products display high thermal stability, high porosity (pore size going from 7 to 27 Å), high surface area (711 and 1590 m^2 g^{-1} respectively) and a structure derived from graphite. A similar network, with an inverted connectivity was also reported by Lavigne[150] and later again by Yaghi, who created networks with larger pores by using extended di- and triboronic acids.[151] Three

dimensional COFs were also prepared by using fragments bearing four boronic acid functional groups.[152]
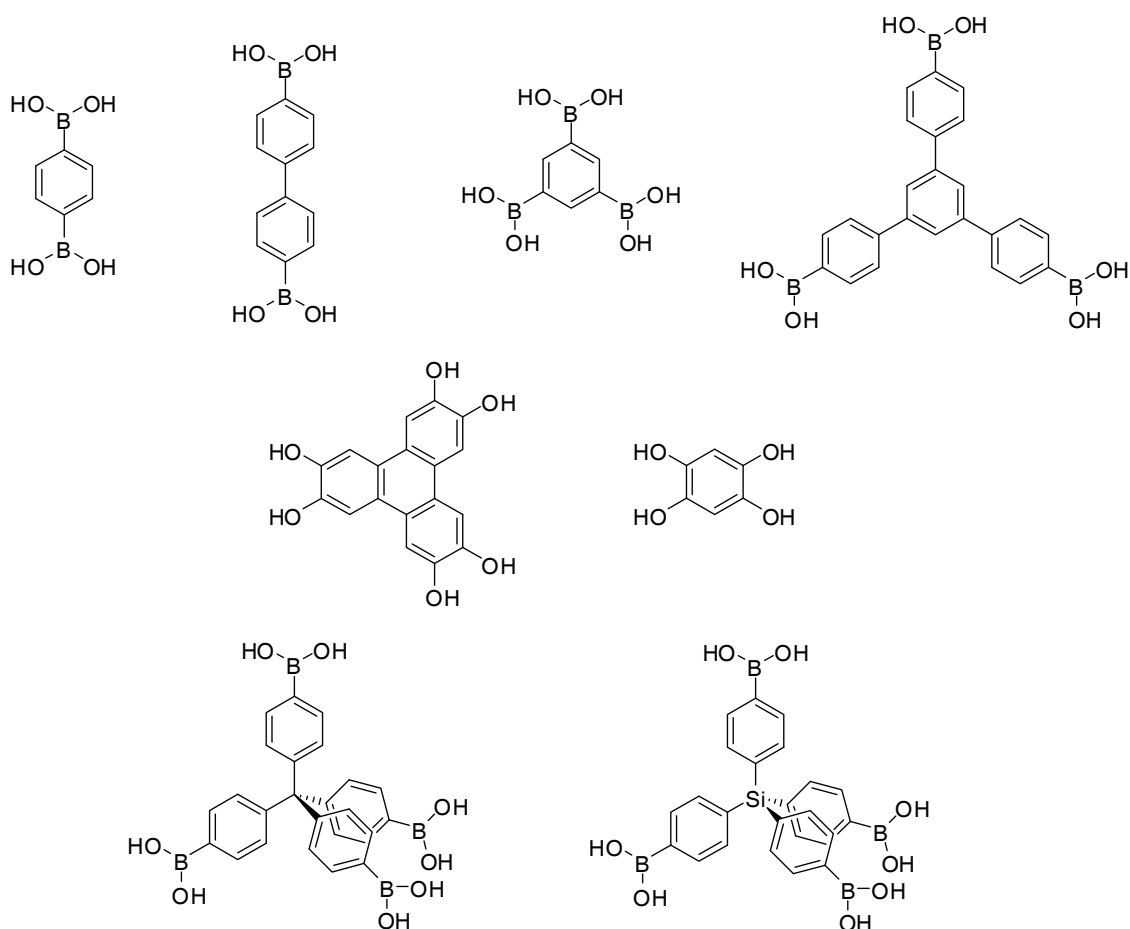
Scheme 1.26: Fragments used in the preparation of covalent organic frameworks.

1.4.4 Hydrogen-bonded Structures

Similar to carboxylic acids, boronic acids are able to form cyclic hydrogen-bonded dimers in the solid state (Figure 1.5). Wüst and co-workers used tetraboronic acids with a rigid tetraphenylmethyl or tetraphenylsilyl framework to build diamondoid networks through hydrogen bonding.[153] In the crystal, they observed a five-fold interpenetration of the networks. Each network is also connected to four neighbors via H-bonding. Despite this interpenetration, there is sufficient space for guest inclusion and guest exchange without cristallinity loss.
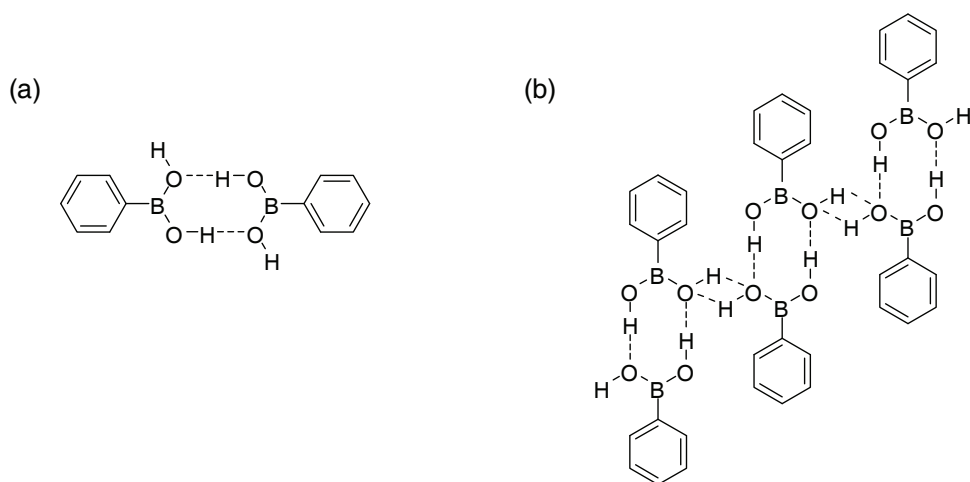
Figure 1.5: (a) Hydrogen bonded dimer of phenyl boronic acid; (b) extended network.

Recently, phenyl boronic acid and 4-methoxyphenyl boronic acid were found to co-crystallize with 4,4'-dipyridyl and 1,2-bis(4-pyridyl)ethylene. In the solid state, both types of building blocks are held together by H-bonds between the $B(OH)_2$ groups and the nitrogen atoms, forming one dimensional networks.[154]

1.4.5 Other Boron-Based Architectures

All architectures described above incorporate a boronic acid fragment in their structure. This dominance of boronic acids in the field is probably due to their well-established chemistry, ease of handling and the availability of a large variety of derivatives. However, some alternative boron-containing fragments were also used to build interesting architectures.

Similar to boronic acids, boranes are Lewis acids that can form adduct with N-donor ligands. Using this property, Siebert and co-workers prepared imidazolylborane macrocycles such as **A30** (Figure 1.6) from chloroborane or dimethylbromoborane and 1-trimethylsilylimidazole. A mixture of tetrameric and pentameric cycles as well as higher oligomers was obtained, and the two main products could be separated by chromatography.[155] Variation of the substitution on the imidazole ring indicated that the preferred ring size is tetrameric. However, with small substituents, pentameric macrocycles could be obtained.[156]

Diethyl(3-pyridyl)borane was found to self-assemble into a tetrameric macrocycle **A31** both in the solid state and in solution.[157] A recent study also demonstrated that the

geometry of the assembly is influenced by the substitution on boron, and that exchange reactions can be performed.[158] Similarly, the isomeric diethyl(2-pyridyl)borane self-condensates into dimers.[159]

One dimensional polymers such as **A32** were prepared by condensation of a bidentate Lewis base having a fragment with two boronate moieties. This concept was used by Wagner and co-workers to form linear chains via reaction of 1,1'-ferrocenyldiborane and 4,4'-dipyridyl derivatives[160] or pyrazine.[161] They observed that charge-transfer complexes were formed and that the polymer is in equilibrium with its constituents. The electrochemistry of the poly-ferrrocenes chains was also studied. Using a related approach, ferrocene containing macrocycles were prepared.[162]

A30

A31

A32
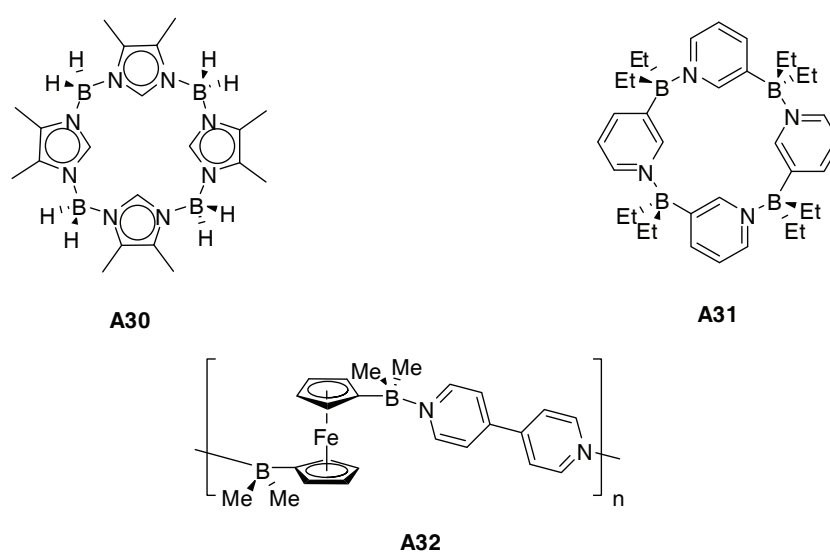
Figure 1.6: Examples of supramolecular borane structures.[155,157,160]

Trimethylborate is an alternative boron source. Its condensation with a spiro-tetraol, in presence of a base, produced molecular square **A33** (Figure 1.7).[163] In the solid state, the tetraanionic squares are stacked on top of each other and glued together by cations to form infinite columns.

Double helicate **A34** was prepared by reaction of *ortho*-linked hexaphenols with sodium borohydride.[164] In this helicate structure, the two strands are held together by two spiroborates formed with the terminal biphenol. An octacoordinated sodium cation is also found at the center of the complex.

Condensation between a catechol functionalized dipyrrin ligand and trichloroborane produced a mixture of trimeric (**A35**), tetrameric and pentameric macrocycles.[165] Separation of the different oligomers can be performed by chromatography and then

GPC. Because it possesses a cavity covered with oxygen atoms, the trimeric specie shows interactions with large alkali-metal ions such as K^+, Rb^+ and Cs^+.

Boron macrocycles incorporating actinide ions were reported by Eisen (**A36**).[166] In this reaction between an organoactinide and an excess of catecholborate, the metal acts as a template for the formation of a 15-membered, hexaoxo, trianionic ligand, formed by three catecholborate units linked by catechol bridges.

A33

A35

A34 ⬤ Sodium

A36
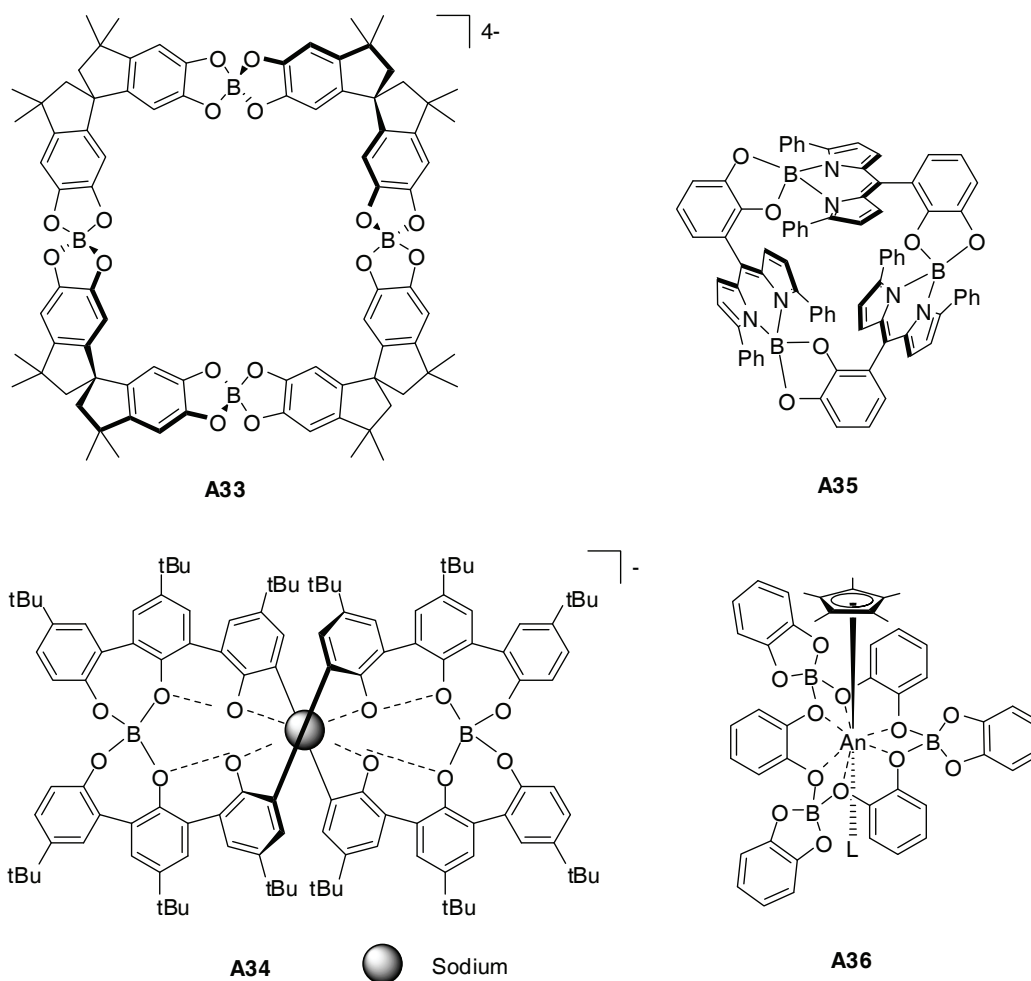
Figure 1.7: Examples of boron containing supramolecular assemblies.[163 -166]

1.5 Aims of This Work

The aim of this work is to further investigate the potential of boronic acids as building blocks in supramolecular chemistry. In particular, the possibility to build complex structures in a single step will be tested. To do so, reactions involving the boron center (boronate ester formation, coordination of a N-donor ligand) as well as other reversible reactions such as metal-ligand coordination and imine condensation will be used in parallel.

First, reactions of various aryl- and alkyl- boronic acids with N,O,O'-tridentate ligands will be investigated. Formation of macrocyclic species can be expected, as this class of ligand was successfully used in self-assembly reactions with transition metals, producing metallamacrocycles. Subsequently, the possibility to use these macrocycles as scaffold for the formation of dendritic structures will be investigated. Our strategy to build such structures involves the simultaneous condensation of three different types of building blocks.

This concept of multicomponent self-assembly will also be applied to the synthesis of complex structures such as polymers, rotaxanes, macrocycles, and cages. All these compounds will be prepared by simultaneous condensation of a boronic acid with several different molecular building blocks.

Chapter 2

Synthesis of Boronate Macrocycles

2.1 Introduction

In this chapter, reactions between aryl- or alkyl- boronic acids and N,O,O'-tridentate ligands are described. 2,3-Dihydroxypyridine and 3,4-dihydroxypyridine were chosen as ligands because they were successfully used in the formation of transition metal macrocycles. With these two ligands, tetrameric and pentameric boronate macrocyclic structures were obtained and comprehensively characterized both in solution and in the solid state.

2.1.1 Metallamacrocycles with Dihydroxypyridine Ligands

Ligands in which two catechol or pyridine units are connected by a rigid linker were extensively used as building blocks in transition metal-based supramolecular chemistry. Dihydroxypyridine ligands (sometimes also called hydroxy-pyridone, according to their tautomeric structure) are N,O,O'-tridentate chelating ligands, which combine characteristics of both fragments. They were successfully used in self-assembly reactions with various transition metals, forming macrocyclic structures. In particular, Severin and co-workers prepared trimeric macrocycles from 2,3-dihydroxypyridine and half-sandwich complexes of ruthenium(II), rhodium(III), and iridium(III) (Scheme 2.1).[63,167] The synthesis is easy (both building blocks are simply mixed in presence of a base), efficient, and versatile, with possible variations of the arene ligand and of the metal ion. The later property allowing for fine-tuning of the solubility and redox properties of the assemblies.
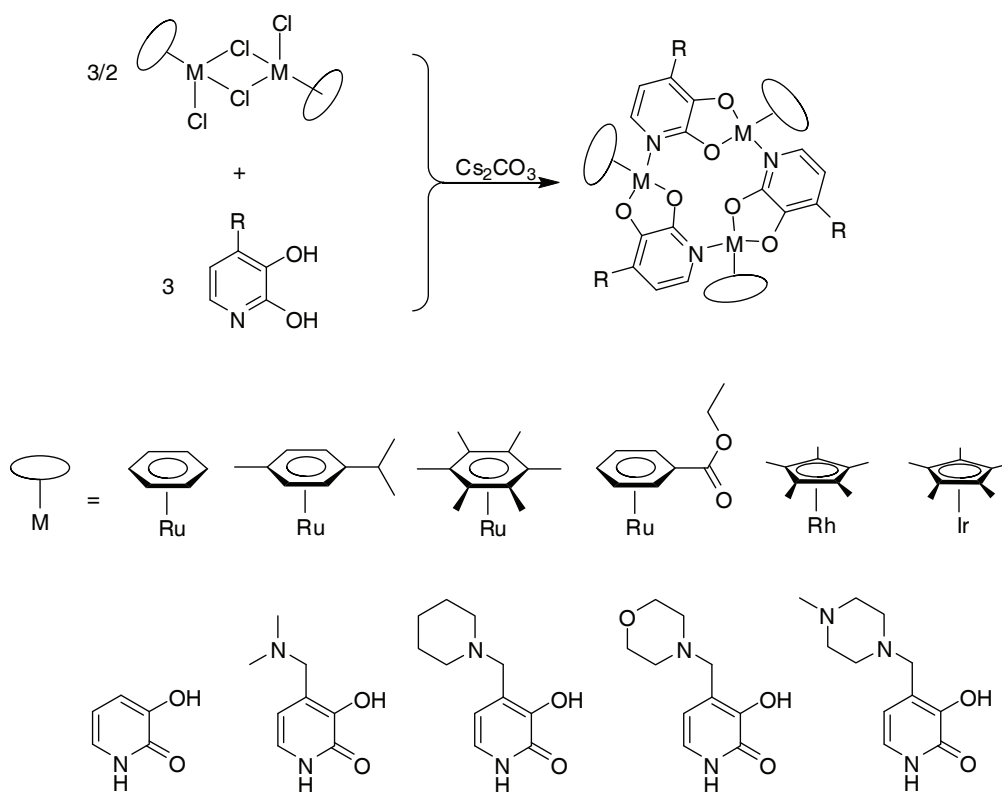
Scheme 2.1: Formation of trimeric macrocycles from 2,3-dihydroxypyridine ligands and half-sandwich complexes.[167,172]

These trimeric macrocycles can be seen as metal containing analogues of 12-crown-3 and are often referred to as metallacrowns complexes.[168] Similar to crown ethers, they are able to encapsulate small alkali ions. In particular, these 12-metallacrown-3 complexes show high affinities and selectivities for lithium and sodium ions.[169,170] Selective complexation of lithium in water can even be achieved using a piperidine derivative of the ligand.[171,172]

Another interesting property of this class of macrocycles is their dynamic nature. Because they possess a labile metal-nitrogen bond, they can be involved in scrambling experiments and exchange monomeric fragments with each other. A dynamic combinatorial library (DCL) can be generated by mixing macrocycles having different metal-arene fragments.[173] The relative stability of each member of the DCL is usually dictated by the size of the π-ligand, but Li^+ can be used as a target and influence the composition of the library.[174]

More complex supramolecular structures were also created using bridged N,O,O'-tridentate ligands. For instance, two trimeric macrocycles can be connected by ligands bearing two 2,3-dihydroxypyridine units, forming extended triple helicates,[175] which showed affinities for phosphate and acetate anions in water.[176] Surprisingly, related

cylindrical structures were obtained from the reaction of (arene)Ru(II) complexes with a tripodal ligand.[177]

Using tridentate ligands with different geometries and substituents, macrocycles with various sizes and aggregation numbers were obtained.[178] In particular, 3,4-dihydroxy-2-methyl-pyridine in combination with [(cymene)RuCl$_2$]$_2$ or [(Cp*)RhCl$_2$]$_2$ also forms trimers. Due to a different geometry, these complexes are unable to encapsulate alkali metal ions.[179] Other transition metals such as palladium(II)[180] and rhenium(I)[181] were also reacted with related tridentate ligands to form macrocycles of various sizes and geometries (Figure 2.1).
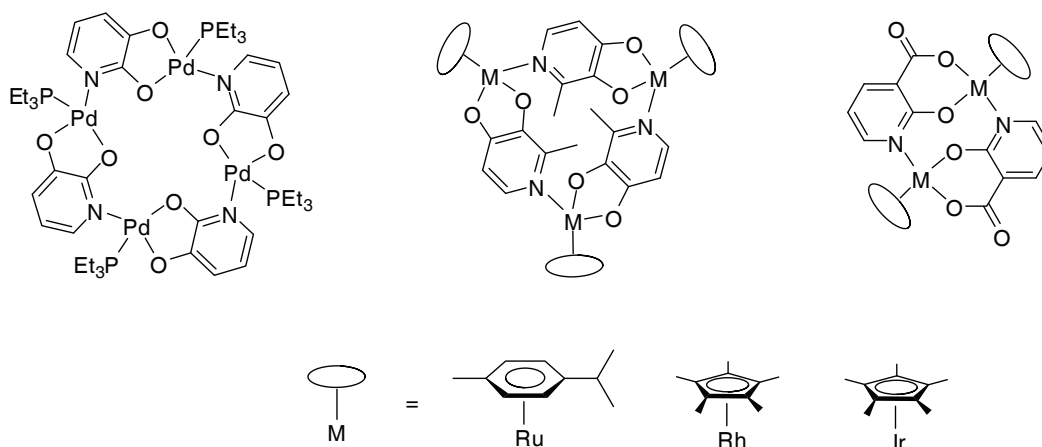
Figure 2.1: Selected examples of macrocycles formed by reaction of N,O,O'-tridentate ligands with transition metals.[178-180]

2.1.2 Boronic Acids as Building Blocks

Similar to transition metals, boronic acids were expected to be good reaction partners for dihydroxypyridine ligands. It was assumed that they form five-membered boronate esters when reacted with these ligands. Then, interaction of a Lewis-acidic boron center and with the N-donor atom can promote the self-assembly of monomeric units into boron-based macrocycles. As the geometry of the boron containing fragments and half-sandwich complexes is similar (tetrahedral), macrocycles which are structurally similar to metallamacrocycles should be obtained.

In order to favor the spontaneous self-assembly of the monomers, reactions can be performed in apolar non-donor solvents such as chloroform, benzene or toluene.

Another advantage of such solvents is that they allow for the azeotropic elimination of the by-product water from the reaction mixture.

Because a large number of different boronic acids are commercially available, various macrocycles can be formed. A fine tuning of the solubility and dynamic nature of the final assemblies can be expected. Formation of compounds having different geometries and shapes can be achieved by using tridentate ligand with various geometries.

2.2 Results and Discussion

2.2.1 Boron Macrocycles with 2,3-Dihydroxypyridine

Initially, the reaction between the simplest building blocks, namely phenyl boronic acid and 2,3-dihydroxypyridine, was investigated. The reagents were suspended in dry benzene, which was found to be the best solvent among those tested ($CHCl_3$, toluene, THF). The suspension was refluxed for 15 hours using a Dean-Stark trap and then filtered to eliminate insoluble material (presumably unreacted compounds). Upon cooling, the product precipitated from the reaction mixture. After filtration and washing with pentane, pure macrocycle **1** was obtained in good yield (51%). The reaction is believed to occur as depicted in Scheme 2.2, with first formation of the boronate ester, followed by self-assembly of the monomeric units into macrocycle **1**.

	Aryl	R_2
1	C_6H_5	H
2	C_6H_5	$CH_2(NC_4H_8O)$
3	$2,3,6\text{-}C_6H_2F_3$	H
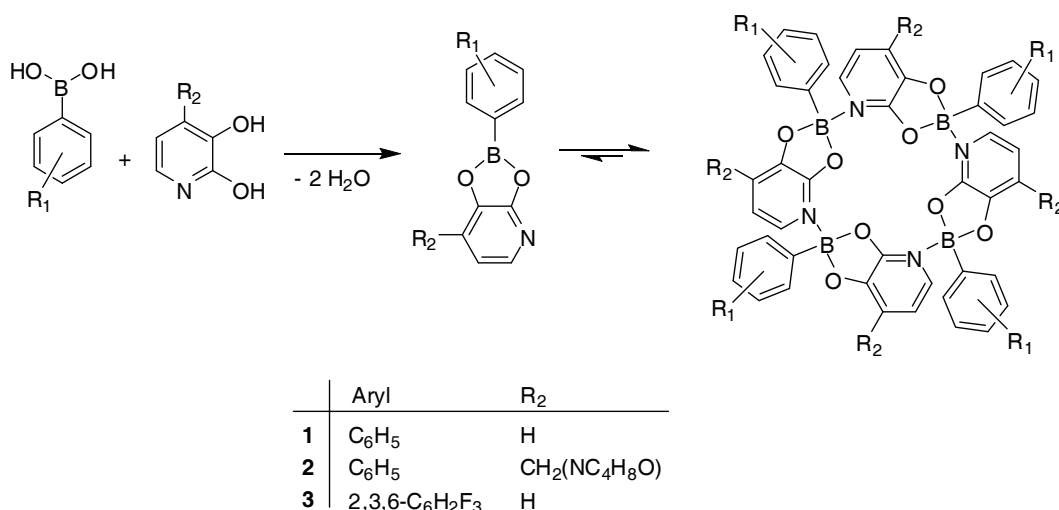
Scheme 2.2: Synthesis of the tetrameric macrocycles **1-3**.

^{1}H and ^{13}C NMR analyses of **1** showed the formation of a very symmetric complex because only one set of signals was found for the phenyl group as well as for the pyridine ligand. The ^{11}B NMR spectrum displays only one broad pick at 11.5 ppm. The upfield shift compared to typical ^{11}B signals of trigonal planar boronate esters at ~30 ppm is characteristic of a boron atom with a tetrahedral geometry.[182] According to these analyses, a macrocyclic complex was formed, but since NMR spectroscopy is not suited to determine the aggregation number n of the macrocycle, a single crystal X-ray analysis was performed. In the solid state, macrocycle **1** was found to be a

tetrameric assembly, with a perfect S_4 symmetry (Figure 2.2). The four boron centers represent stereogenic centers and have alternate configuration (RSRS). As expected, the boron atom has a tetrahedral geometry and the five-membered boronate esters as well as the coordinative N-B bonds are formed. Compound **1** can be seen as a molecular square with the planes of two adjacent dihydroxypyridine ligands nearly orthogonal to each other.
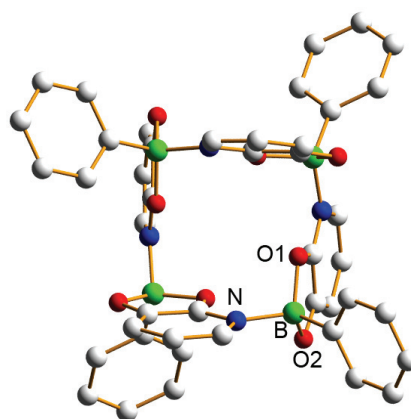
Figure 2.2: Structure of macrocycle **1** in the crystal. Hydrogen atoms and solvent molecules have been omitted for clarity.

It is interesting to note that macrocycle **1** differs from what was previously observed when the same ligand was reacted with half-sandwich complexes of Ru(II), Rh(III), and Ir(III). Although these metal fragments display the same (pseudo)tetrahedral geometry than four-coordinated boron atoms, they exclusively form trimeric assemblies with 2,3-dihydroxypyridine.[63,167-177] In term of overall structure, **1** is more related to the tetrameric macrocycle formed by reaction of 2,3-dihydroxypyridine with the square-planar palladium complex [(Et$_3$P)PdCl$_2$]$_2$.[180]

The possibility of using substituted boronic acids or ligands in the self-assembly reaction was investigated. The same reaction was performed using either 2,3-dihydroxy-4-morpholino-methyl-pyridine or 2,3,6-trifluorophenyl boronic acid as building blocks and complexes **2** and **3** were obtained. These two compounds are structurally very similar to **1**, as evidenced by NMR and X-ray analyses (Figure 2.3). The crystallographic S_4 is not present any more in **2** and **3**, and B-O and B-N bonds are slightly shorter than in **1**. Accordingly, the macrocycle is slightly contracted (shorter B···B distance). Relevant bond distances for the three complexes are summarized in Table 2.1.
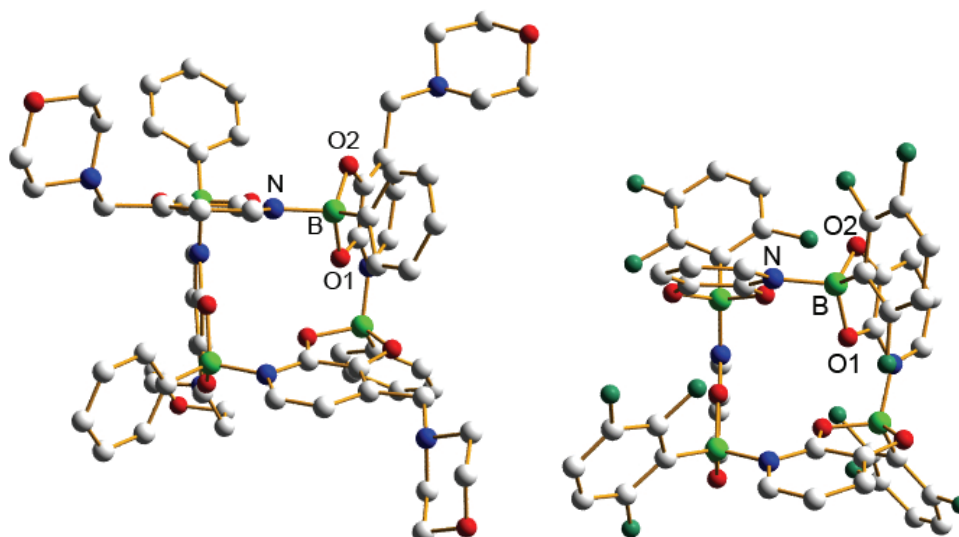
Figure 2.3: Structure of macrocycles **2** (left) and **3** (right) in the crystal. Hydrogen atoms and solvent molecules have been omitted for clarity.

Table 2.1: Selected bond distances (Å) and THC (%) for compounds **1**-**3**.

	B-N	B-O1	B-O2	B···B'[a]	THC
1	1.601(2)	1.529(2)	1.496(2)	5.624(2)	78.5
2[b]	1.587(6)	1.524(5)	1.481(5)	5.318(7)	82.4
3[b]	1.58(1)	1.506(9)	1.487(9)	5.31(1)	78.7

[a] The distance between the boron atoms opposite to each other is given

[b] Averaged values are given

Using the six angles around the boron atom, the tetrahedral character (THC) was calculated for the three complexes (see § 1.4.1.1 for the formula). It was found to be on average 80%. This high value correlates well with the short N-B bond distances. It is important to note that the average B-N bond length (1.59 Å) is among the shortest reported for dative B-N bonds[112] and is shorter than the B-N bond of the adduct between 4-picoline and phenylcatecholborane (1.651(3) or 1.654(4) Å) or methylcatecholborane (1.660(2) or 1.6444(19) Å).[183]

In the ^{1}H NMR spectrum of **2**, the presence of two doublets for the diastereotopic methylene protons of the ligand reflects the presence of the boron stereogenic centers. ^{1}H NMR spectroscopy was also used to test the kinetic stability of the tetrameric assemblies through a scrambling experiment: Equimolar amounts of **1** and **2** were mixed in CDCl$_3$ and spectra were recorded after 0.5, 1, 5 and 24 hours. In all cases, spectra which are superposition of the spectra of pure **1** and **2** were obtained. No

peaks corresponding to new species could be detected, indicating that complexes are unable to exchange fragments with each other, at least at room temperature.

Attempts to characterize the macrocycles by electrospray or MALDI mass spectrometry failed. Only peaks corresponding to fragments of the tetramers were detected. Apparently, the B-N bond is too weak to survive the ionization process. Another hypothesis is that one or more of the aryl substituents is lost during ionization as it was reported for dimeric macrocycles.[184] Complexes with different substituents on both fragments were prepared but due to the impossibility to analyze them either by MS or X-ray diffraction, a complete characterization could not be performed. However, it is likely that their overall geometry is similar to compounds **1**-**3**.

2.2.2 Boron Macrocycles with 3,4-Dihydroxypyridine

After the promising results obtained with 2,3-dihydroxypyridine, reactions with the isomeric 3,4-dihydroxypyridine were investigated. This ligand can be synthesized in five steps from Kojic acid[185,186] and is expected to form macrocycles having a different geometry than those obtained with 2,3-dihydroxypyridine.[179] The reactions were performed similarly to tetramer syntheses (i.e. reflux in benzene in presence of a Dean-Stark trap followed by hot filtration) with four different aryl- and alkyl-boronic acids (Scheme 2.3). In all cases, NMR experiments on the crude reaction mixture showed formation of condensation products in over 80% yield. Pure products could be precipitated in variable yields (20-86%) from the reaction mixture after reduction of the volume of solvent and/or addition of pentane.

	R
4	$4\text{-}CH_3C_6H_4$
5	$4\text{-}(H_3C)CC_6H_4$
6	$3\text{-}C_6H_4F$
7	n-butyl
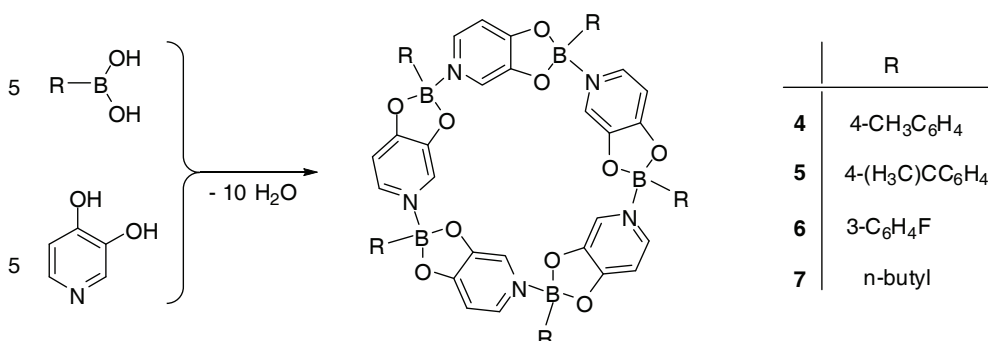
Scheme 2.3: Formation of the pentameric macrocycles **4**-**7**.

Again, NMR measurements showed formation of highly symmetric compounds, with the presence of only one set of signals on the spectra. The presence of the B-N dative bond was confirmed by the broad peak at ~ 10 ppm in the ^{11}B NMR spectra. Single crystal X-ray analyses of compounds **4**, **6**, and **7** gave decisive information about the nature of the assembly. The condensation of alkyl- or aryl boronic acids with 3,4-dihydroxypyridine produced pentameric macrocycles (Figures 2.4 and 2.5). The use of differently substituted boronic acids did not affect the self-assembly process. It is thus assumed that the structure of **5** is similar. The conformation of the five stereogenic boron centers is the same (either SSSSS or RRRRR). In fact, the two enantiomers of a complex are found in the same crystal, forming closely packed dimers with intercalating boronate side chains, as illustrated in Figure 2.6.
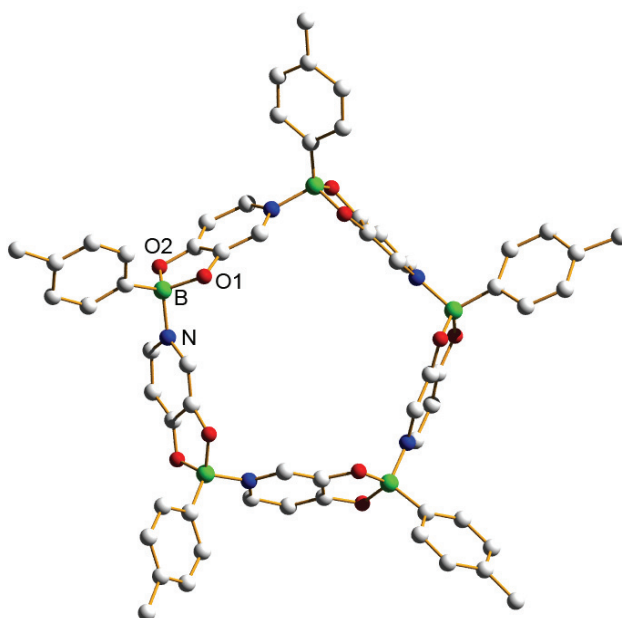
Figure 2.4: Solid state structure of the macrocycle **4**. Hydrogen atoms and solvent molecules have been omitted for clarity.
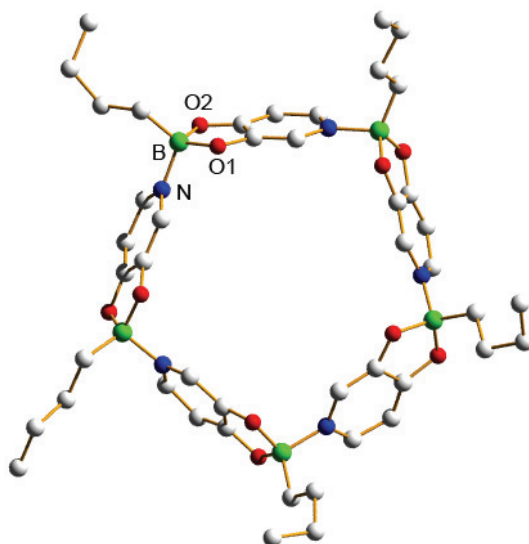
Figure 2.5: Solid state structure of macrocycles **7**. Only one of the two independent macrocycles found in the crystal of **7** is shown. Hydrogen atoms and solvent molecules have been omitted for clarity.

Similar to what was found for the tetrameric assemblies, the B-N bond in the complexes **4**, **6**, and **7** is short, as shown by the average bond length of 1.60 Å. The size of the cavity (B···B' ~ 9.8 Å) is almost double compared to the tetrameric assemblies. Other bond lengths are also similar to what was observed in compounds **1**-**3**. These values are summarized in Table 2.2.

Table 2.2: Selected average bond distances (Å) and THC (%) for the compounds **4**, **6**, and **7**.

	B-N	B-O1	B-O2	B···B'[a]	THC
4	1.600(13)	1.509(33)	1.520(17)	9.846	72.4
6	1.606(13)	1.497(7)	1.502(15)	9.819	73.3
7	1.608(11)	1.510(8)	1.523(10)	9.879	74.2

[a] The mean distance between two non-consecutive boron atoms is given
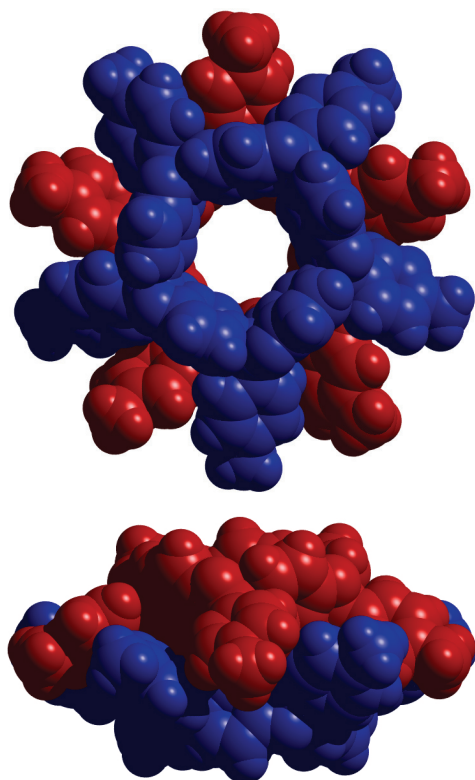
Figure 2.6: Space-filling representation of the two enantiomers (RRRRR in blue and SSSSS in red) of macrocycle **4** in the crystal (top and side view). A dimer with intercalating side chains is observed.

Scrambling experiments with complexes **5** and **6** showed that the macrocycles are stable in solution. No peaks corresponding to mixed complexes could be detected on the NMR spectrum 15 minutes after mixing. A self-sorting behavior of the macrocycles can be excluded because mixed species were obtained when the synthesis was performed using equimolar amounts of 4-*tert*-butylphenyl boronic acid and 3-fluorophenyl boronic acid. This behavior is in accordance with what was observed for the tetrameric assemblies and may be explained by the strong B-N interactions within these compounds.

NMR investigations on compounds **4-7** revealed a very interesting feature. When NMR spectra were recorded in C_6D_6 instead of $CDCl_3$ strong differences for the chemical shifts of the protons of the bridging pyridine ligands were observed (Figure 2.7).
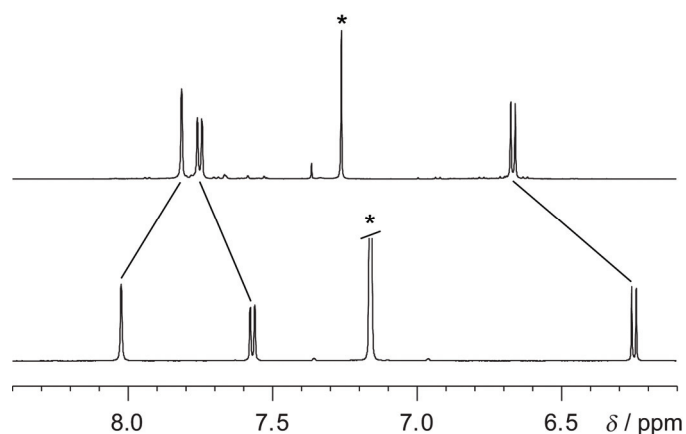
Figure 2.7: Part of the ^{1}H NMR spectrum of macrocycle **7** in CDCl$_3$ (top) and C$_6$D$_6$ (bottom). The signals of the solvent molecules are indicated with an asterisk.

These differences can be attributed to ring current effects of the benzene molecule located in the macrocycles cavity. This hypothesis is supported by the presence of a benzene molecule in the cavities of crystalline **6** (Figure 2.8) and **7** (only one of the two crystallographically distinct macrocycles). NMR titration experiments were performed in order to get information about the binding of the guest molecule. Binding was found to be weak, as addition of ten equivalents of C$_6$D$_6$ to a CDCl$_3$ solution of **6** only resulted in minor changes of the chemical shifts. Displacements of the peaks were only observed with significantly higher benzene concentrations.
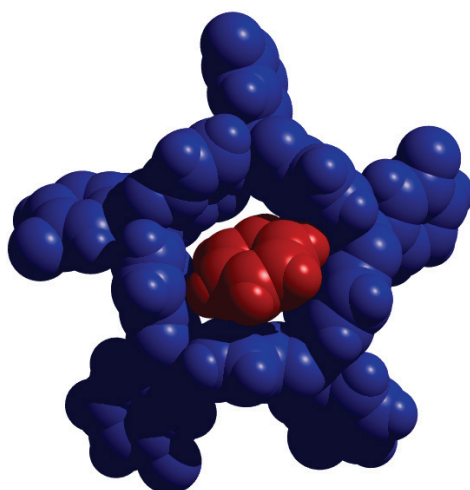
Figure 2.8: Space-filling representation of the molecular structure of macrocycle **6** and the co-crystallized benzene molecule found within its cavity.

2.2.3 Use of Other Ligands

3,4-Dihydroxy-2-methyl-pyridine was also tested in condensation reactions with boronic acids. Unlike 3,4-dihydroxypyridine, this ligand did not lead to the formation of macrocyclic species. According to preliminary NMR and X-ray diffraction experiments, only monomers were formed. Apparently, the methyl substituent is bulky enough to prevent formation of the B-N bonds and consequently macrocyclization.

Other tridentate ligands were also tested in self-assembly reactions with boronic acids. For instance, the condensation between 2-hydroxynicotinic acid and phenyl boronic acid produced a trimeric macrocycle, according to a X-ray crystallographic analysis. Unfortunately, the experiment was difficult to reproduce, presumably because of the instability of the assembly. Attempts to solve this problem by using differently substituted building blocks or ligands with a similar geometry were unsuccessful. 2,3-Dihydroxyquinoline and 4-imidazolecarboxylic acid are two other ligands. which are known to form macrocycles with (arene)Ru(II) and Cp*Rh(III) complexes.[178] They were tested with various boronic acids but in all cases, no indication of the formation of condensation products was detected.

2.3 Conclusions

In summary, the reaction between various aryl- and alkyl-boronic acids and dihydroxypyridine ligands was investigated. When 2,3-dihydroxypyridine was used, four-membered macrocycles were obtained. The isomeric 3,4-dihydroxypyridine led to the formation of pentameric macrocycles. In this reaction, a boronic acid first condenses with the two adjacent hydroxyl groups of the ligand to form a boronate ester. The monomeric units then self-assemble into a macrocycle via formation of intermolecular dative B-N bonds. This synthetic strategy is different from what has been previously reported for the construction of boron containing macrocycles, where the macrocyclization was performed via formation of a covalent B-O bond.[124]

It is also interesting to note that when condensed with organometallic half-sandwich complexes of Ru(II), Rh(III), and Ir(III), 2,3-dihydroxypyridine and 3,4-dihydroxypyridine exclusively form trimeric macrocycles. Apparently, the smaller boron atom, with its more rigidly fixed geometry is able to switch the assembly process from n = 3 to n = 4 and 5 respectively. Another difference between boron- and metallamacrocycles is their kinetic stability. As the latest are labile and can exchange fragments with each other, their boron analogues are kinetically inert. This can be explained by the difficulty to break the strong intermolecular B-N bond, which is one of the shortest reported so far.

Chapter 3

Multicomponent Assembly of Boron-Based Dendrimers

3.1 Introduction

In this chapter, the preparation of boron-based dendritic structures is described. To form these complexes, the tetrameric and pentameric macrocycles described in chapter 2 were used as scaffolds. Amino- and formyl-functionalized macrocycles were prepared and then decorated with formyl- or amine-based dendrons, respectively. The dendritic structures were obtained in a one-pot multicomponent reaction between a dihydroxypyridine ligand, a functionalized boronic acid and amines or aldehydes. Similarly, the possibility to form boroxine-based dendritic structures was investigated.

3.1.1 Dendrimers

Dendrimers are globular, monodisperse macromolecules, which are built around a central focal point, or core, from which bonds emerge radially with a regular branching pattern.[187] The latter property allows distinguishing dendrimers from hyperbranched polymers, which usually display an irregular branching pattern. Not all regularly branched molecules are dendrimers. To be classified as a dendrimer, a globular molecule must have a low viscosity in solution. This property can only be reached if the molecule possesses a certain critical size.

Over the years, different synthetic methodologies have been developed for the preparation of dendrimers. One usually distinguishes two approaches: The divergent synthesis (from the core of the molecule to its periphery) and the convergent synthesis (from the periphery to the core). In 1990, Hawker and Fréchet described a stepwise convergent synthesis of dendritic macromolecules.[188] They formed polyether molecules in a repetitive two-step process. The reaction starts with the condensation of 3,5-dihydroxybenzylalcohol with benzyl bromide to give the first generation benzyl alcohol ([G1]-OH), which is subsequently converted to the benzyl bromide ([G1]-Br) and further reacted with another molecule of 3,5-dihydroxybenzylalcohol to form the second generation benzyl alcohol ([G2]-OH). Repetition of these two steps leads to the formation of higher generation dendrimers (up to the sixth generation). Due to their well-established preparation and easy modification, the so-called Fréchet-type dendrons have often been used in dendrimers chemistry.[189]

3.1.1 Self-Assembled Dendrimers

Although most of the dendrimers reported to-date have been prepared using classical organic synthetic methods, examples of structures built on non-covalent interactions can be found in the literature.[190,191] An example of such self-assembled dendritic structure was presented by Zimmermann and co-workers.[192] They prepared Fréchet-type dendrons which were functionalized at their focal point with a rigid unit bearing four carboxylic acids. These dendrons have the potential to self-assemble into a hexameric dendrimer by formation of H-bonds between carboxylic acid functional groups (Figure 3.1).
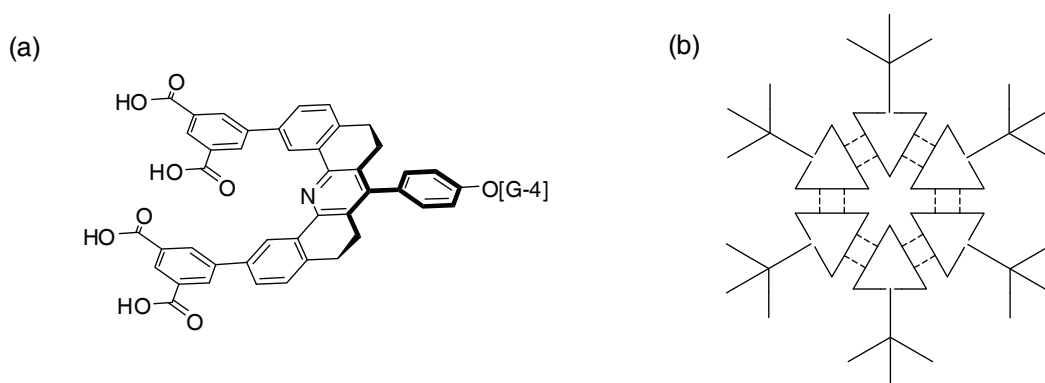
Figure 3.1: Zimmermann's self-assembled dendrimer: (a) the tetra-carboxylic acid monomeric unit and (b) schematic representation of the hexameric assembly.[192]

In theory, two modes of assembly exist for this system: either a discrete hexameric "rosette" or a linear infinite polymer. The mode of assembly is dictated by the dendritic generation. If small dendrons are used, linear aggregates are formed but at higher dendritic generation, the discrete hexameric assembly is exclusively obtained.

Recently, Hirsch and co-workers presented a hydrogen-bond-mediated synthesis of dendrimers by self-assembly of three building blocks.[193] In their strategy, no dendritic subunits are used, but rather a tritopic core unit, branching elements, and end caps. All these elements can be connected to each other via H-bonds. Variation of the ratio of the three units allows for the preparation of dendrimers of different generations. To the best of our knowledge, this system is the only example of multicomponent self-assembly of dendritic structures.

Most of the self-assembled dendrimers reported to-date were constructed using metal-ligand interactions. Transition metals have been used as branching centers, cores,

connecting units, or termination groups.[194] Dendrimers have also been assembled using electrostatic interactions, for instance, between a cationic metal core and anionic carboxylate dendrons.[195]

Stang and his group chose a slightly different approach to build metallodendrimers. Instead of assembling their structures around a naked metal ion, they created cavity core dendrimers which were formed by a metal-based polygon core decorated with dendrons.[196,197] The synthesis involved the reaction of a di-platinium acceptor unit with a dendritic, ditopic donor ligand. The shape of the assembly is dictated by the geometry of the building blocks, following the rules of the directional bonding approach. With this strategy, they obtained rhomboidal and hexagonal metallodendrimers, decorated with a maximum of six dendrons (Scheme 3.1).
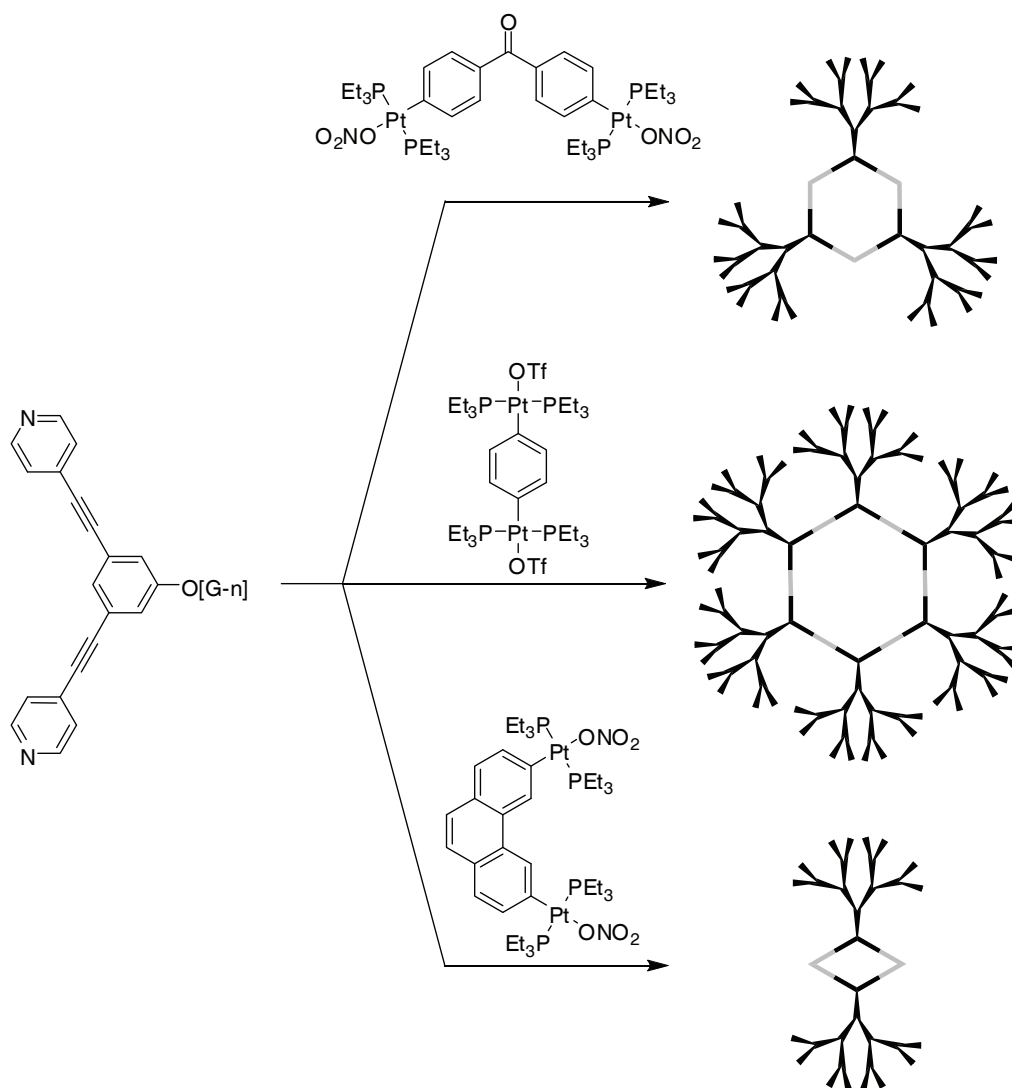
Scheme 3.1: Metallodendrimers reported by Stang and co-workers.[196,197]

A clear advantage of the self-assembly strategy is that it allows for the simultaneous and easy assembly of several dendrons into a dendritic structure. However, a major drawback of this approach is the huge synthetic work to be performed prior to the self-assembly reaction. In addition to unavoidable dendrons synthesis, the self-assembling building blocks have to be functionalized and connected to dendrons. This ligand modification often requires tricky and time-consuming multi-step reactions that make the whole process less attractive.

On the following pages, the multicomponent self-assembly of dendritic structures is presented. Our strategy is to use tetrameric and pentameric macrocycles described in chapter 2 as well as boroxines as scaffolds for the synthesis of dendritic structures. In our approach, formation of the macrocyclic core and connection with small dendrons are performed simultaneously. To do so, three reversible and independent reactions are used in parallel: boronate ester formation, addition of N-donor ligands to boronate esters, and imine condensations.

3.2 Results and Discussion

3.2.1 Boron-Based Dendritic Structures

Prior to the formation of dendritic structures, the possibility to form functionalized pentameric macrocycles similar to **4-7** (see § 2.2.2) was investigated. 3,4-dihydroxypyridine was reacted with 3-formylphenyl boronic acid and 3-aminophenyl boronic acid, under standard reaction conditions, producing complexes **8** and **9** in good yield (51 and 56% respectively) (Scheme 3.2).
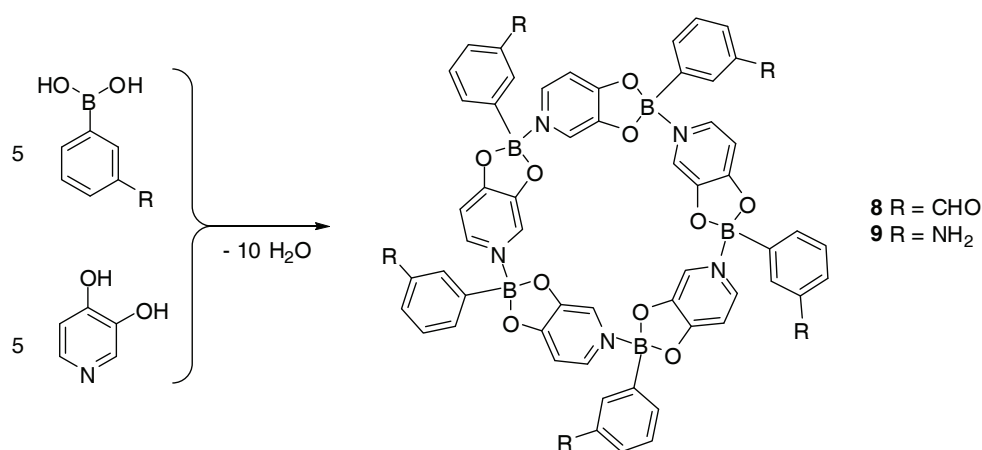
Scheme 3.2: Formation of functionalized macrocycles **8** and **9**.

^{1}H NMR spectra of **8** and **9** were similar to those of complexes **4-7**, with the presence of signals characteristic for the functional groups, indicating that neither the formyl nor the amino groups interfered with the assembly process. The ^{11}B NMR spectra display the expected signal for a tetrahedral geometry at the boron center, indicating formation of the B-N bond. Attempts to grow single-crystals of compounds **8** and **9** were unsuccessful, but based on NMR investigations one can reasonably assume that their structure is similar to those of complexes **4**, **5**, and **7**. One should also point out that the presence of five functional groups at the periphery of the macrocycles reduces the solubility of **8** and **9** in apolar solvents.

Having established that the presence of formyl or amino functional groups did not influence complex formation, the possibility to perform imine condensation in parallel to macrocyclization was tested. In a first set of experiments, 3-formylphenyl boronic acid,

3,4-dihydroxypyridine and primary amines such as aniline and cyclohexylamine were condensed (Scheme 3.3).
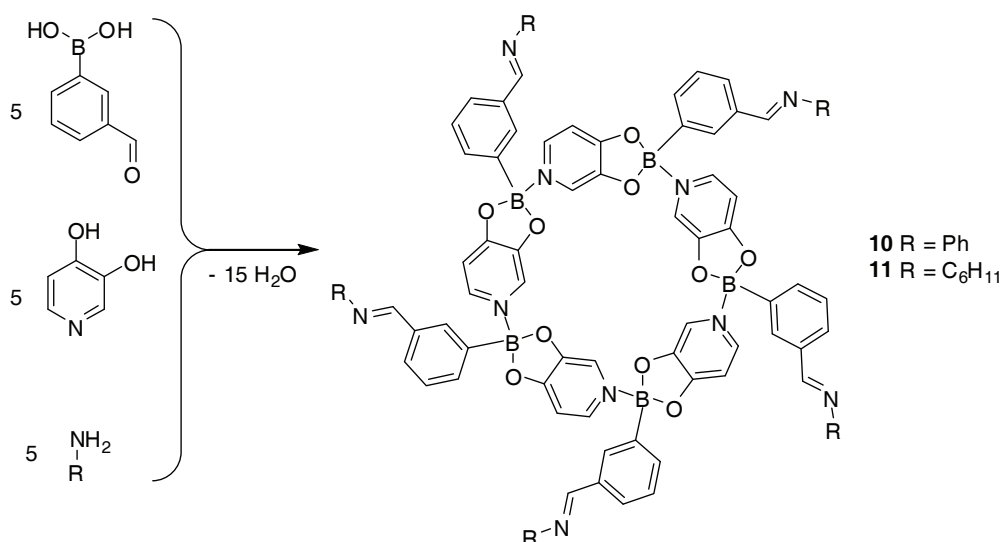
Scheme 3.3: Three-component reaction of 3-formylphenyl boronic acid, 3,4-dihydroxypyridine and an amine to form complexes **10** and **11**.

Again, the ^{1}H NMR spectra of **10** and **11** were in agreement with the formation of a pentameric macrocycle with five imine-based side-chains: signals for the protons of the bridging ligand and the boronic acid were present and unshifted compared to those of compounds **4**-**9**. In addition, the aldehyde signal at 9.99 ppm had disappeared and a new one corresponding to the CH=NR proton had appeared at 8.42 (**10**) and 8.29 (**11**) ppm. In order to get confirmation of the structure and connectivity of these compounds, single-crystals of **10** were grown and analyzed by X-ray diffraction. The structure of the complex in the crystal is depicted in Figure 3.2.
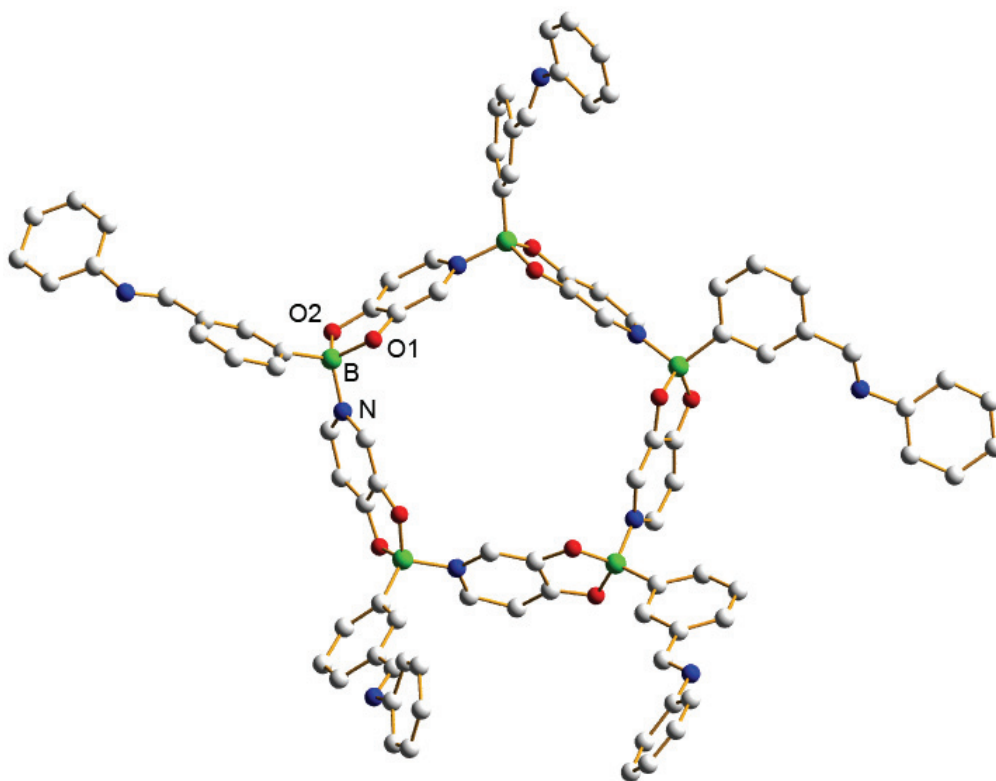
Figure 3.2: Structure of macrocycle **10** in the crystal. Hydrogen atoms and solvent molecules have been omitted for clarity.

The macrocyclic core of **10** is structurally very similar to what was previously observed for **4**, **5**, and **7**. The macrocycle is formed by five identical boronate ester subunits connected via B-N bonds. At its periphery, five benzylideaniline side chains are dandling out, forming a star shape complex. The diameter of the complex (maximum H-to-H distance) is 30 Å. All imine bonds have a trans geometry and no interactions between boron and the imine nitrogen could be detected. Bond angles and distances are similar to what was observed for complexes **4**, **6**, and **7**. Selected values are shown in Table 3.1.

Table 3.1: Selected bond distances (Å) and THC (%) for complex **10**.

	B-N	B-O1	B-O2	B⋯B'[a]	THC
10	1.579(17)	1.513(10)	1.523(10)	9.9584	76.9

[a] The mean distance between two non-consecutive boron atoms is given

It is possible to reverse the connectivities and condensate 3-aminophenyl boronic acid, 3,4-dihydroxypyridine and an aldehyde. This was demonstrated by the synthesis of

complex **12** (Scheme 3.4). As compound **10**, it has five benzylidenaniline side chains but the macrocycle is attached to the aniline side.
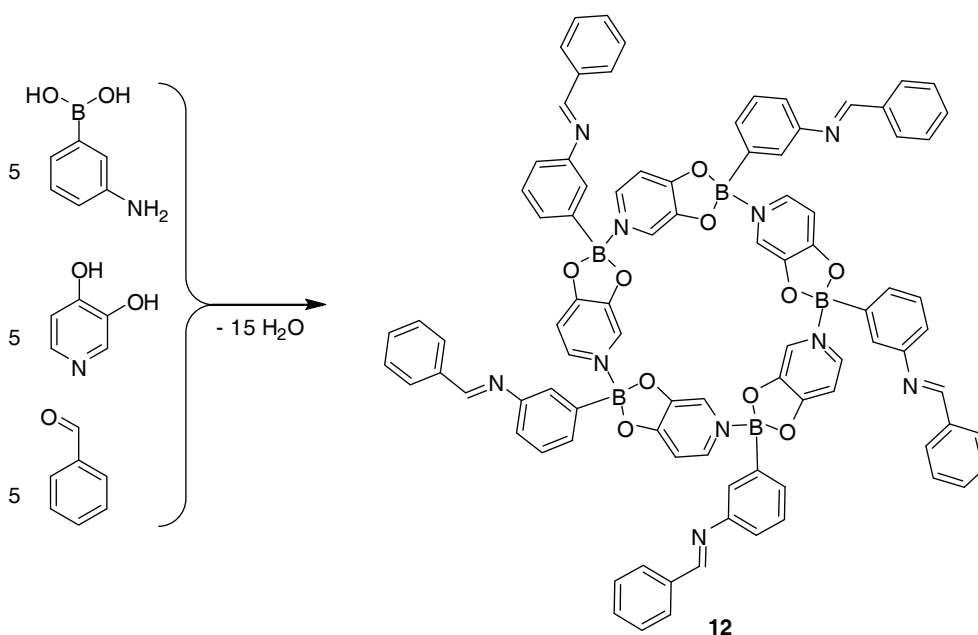
Scheme 3.4: Three-component reaction of 3-aminophenyl boronic acid, 3,4-dihydroxypyridine and benzaldehyde to form complex **12**.

The successful formation of complexes **10**-**12** proves that it is possible to perform imine condensation in parallel to the assembly of boronate macrocycles. So, it suggests that by using small dendrons instead of simple amines (or aldehydes), dendritic structures can be assembled in a single step. In order to increase the number of side chains at the periphery of the macrocycle, 3,5-diformylphenyl boronic acid was used instead of 3-formylphenyl boronic acid. Reactions with 3,4-dihydroxypyridine (and a primary amine) should lead to the formation of dendrimers with ten amine-derived groups at the periphery. If 2,3-dihydroxypyridine is used as a bridging ligand, dendritic structures with a tetrameric core and eight side chains can be obtained. This strategy was tested with several aniline and benzylamine derivatives, including the small dendron 3,5-(benzyloxy)benzylamine (Scheme 3.5).[198]

	Type	R
13	**A**	Bn
14	**A**	p-C$_6$H$_4$Br
15	**B**	Ph
16	**B**	p-C$_6$H$_4$Br
17	**B**	CH$_2$-3,5-C$_6$H$_3$(OBn)$_2$
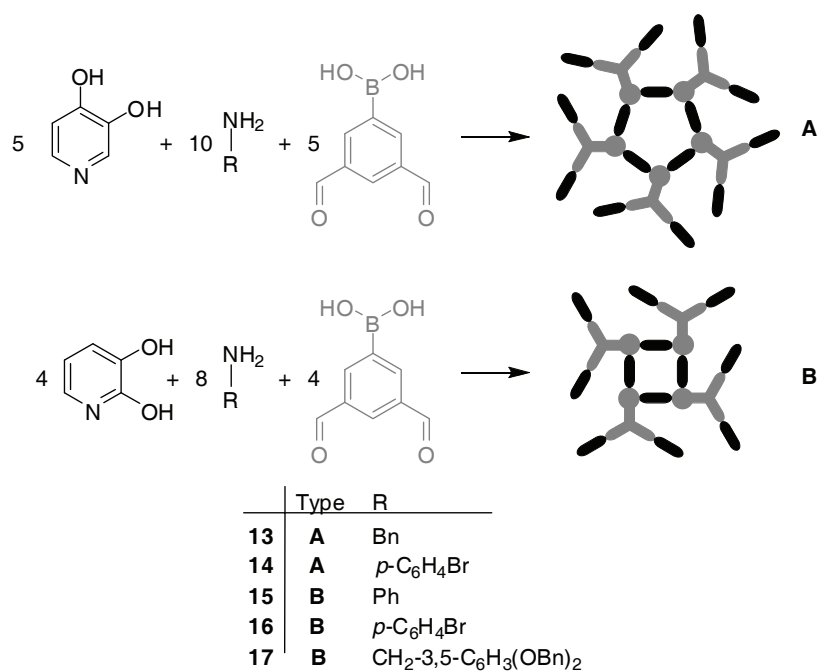
Scheme 3.5: Three-component assembly of dendritic structures **13**-**17**.

In all cases, the expected condensation products **13**-**17** were formed, as shown by NMR analyses. The five structures were isolated in ~50% yields and in good purity. The crude yield was around 80% for pentamers **13** and **14** and almost quantitative for tetrameric assemblies **15**-**17**. The purity of the compounds was determined by NMR spectroscopy and elemental analyses. Attempts to characterize the complexes by X-ray diffraction or mass spectrometry were not successful. The spectrum of compound **17** is shown in Figure 3.3. The complete condensation of the peripherical aldehydes is evidenced by the absence of the aldehyde peak at 10 ppm and the single signal observes for the imine protons. Successful macrocyclization is confirmed by the presence of the three signals for the bridging ligand.

17
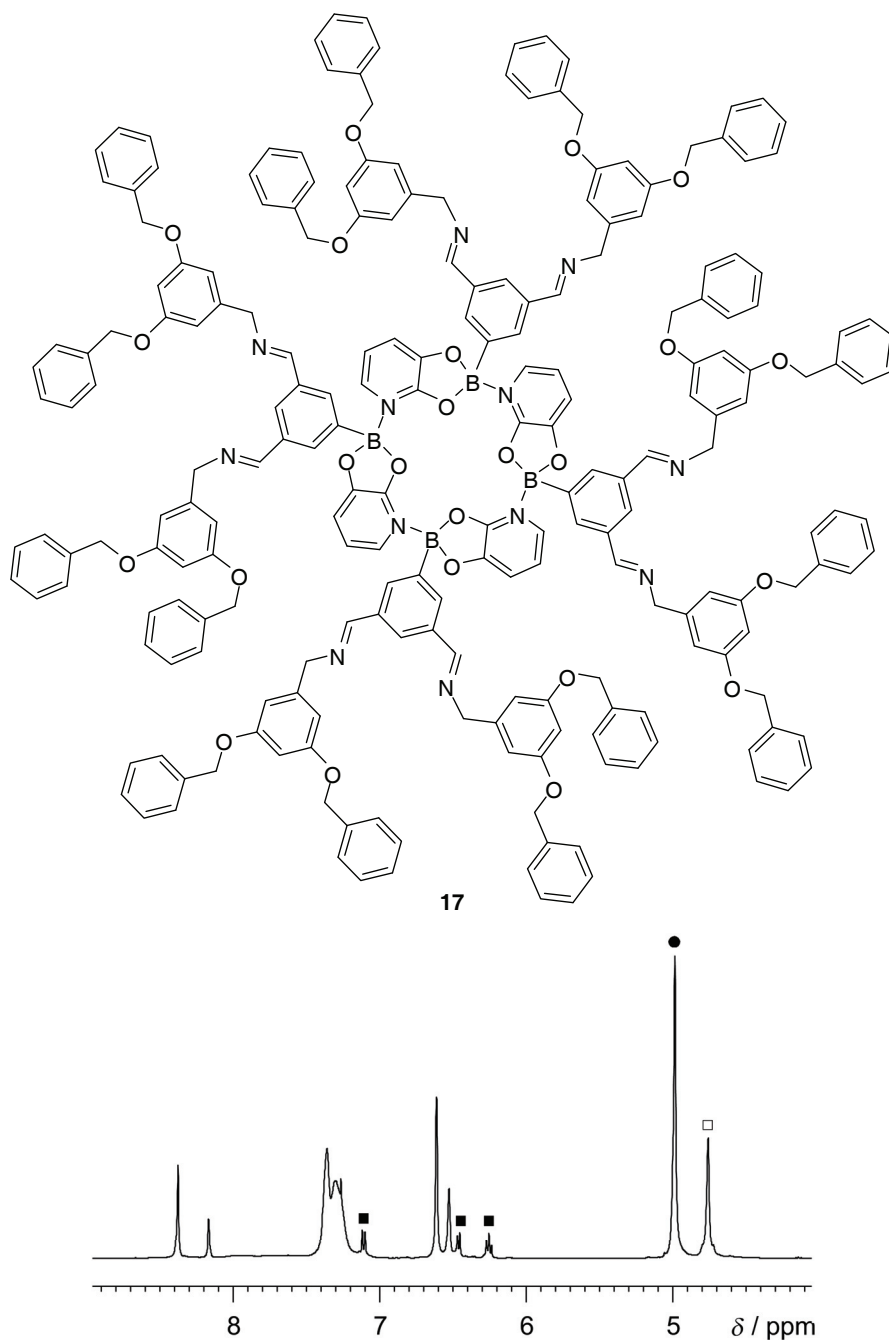
Figure 3.3: ^{1}H NMR spectrum of dendrimer **17** in CDCl$_3$. Signals of the bridging pyridine ligands are denoted with the symbol ■ and signals of the methylene groups are labeled with the symbol □ (NCH$_2$) and ● (OCH$_2$).

The possibility to perform imine exchange (transimination) at the periphery of dendritic structures was tested. Compound **16** was chosen for this experiment because it was built using the electron-poor 4-bromoaniline. It was reported that this fragment can be displaced by addition of an electron-rich aniline.[199] When eight equivalents of 4-methoxyaniline were added to a CDCl$_3$ solution of **16**, a fast exchange reaction took

place, with an equilibrium strongly in favor of the incorporation of the electron-rich aniline (Figure 3.4). Addition of an excess of 4-methoxyaniline (up to 24 equivalents) did not allow to completely displace 4-bromoaniline. Instead, a slight degradation of the complex was observed. Using more basic amines such as benzylamine in the exchange reaction with **16** also led to a degradation of the macrocyclic complex. Indeed, NMR analyses revealed that benzylamine is able to disrupt the N-B bond of **16** and coordinates to the boron center.
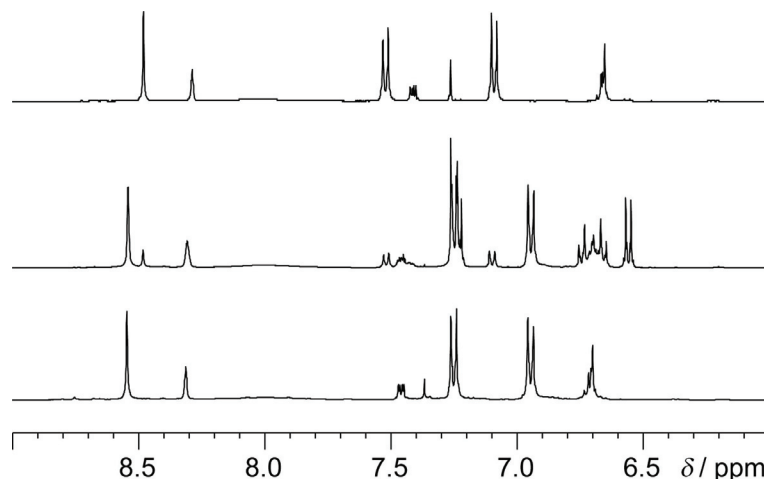
Figure 3.4: Part of the ^{1}H NMR (CDCl$_3$) spectrum of a) the *p*-bromoaniline-based assembly **16**; b) a mixture of **16** and eight equivalents of *p*-methoxyaniline after equilibration; c) the pure *p*-methoxyaniline-based assembly.

3.2.2 Boroxine-Based Dendritic Structures

Following the successful preparation of dendritic structures based on boronate macrocycles, the possibility to use boroxine rings as scaffolds for the formation of dendritic structures was investigated. The strategy to assemble such structures is similar to the synthesis of dendrimers described in § 3.2.1, but a 1,2-bis(4-pyridyl)ethylene linker was used instead of a dihydroxypyridine bridging ligand, together with 3,5-diformylphenyl boronic acid, and an amine. As before, three reversible reactions were performed simultaneously to assemble the targeted structure: 1) The amine reacts with an aldehyde group of the boronic acid fragment to form an imine. 2) Three boronic acid molecules condense to form a boroxine six-membered

ring. 3) Two boroxine rings are bridged by the 1,2-bi(4-pyridyl)ethylene ligand, through formation of two B-N dative bonds.

First, a non dendritic model compound was prepared by refluxing a toluene solution of 1,2-bi(4-pyridyl)ethylene and 3,5-bis(trifluoromethlyl)phenyl boronic acid (Scheme 3.6).
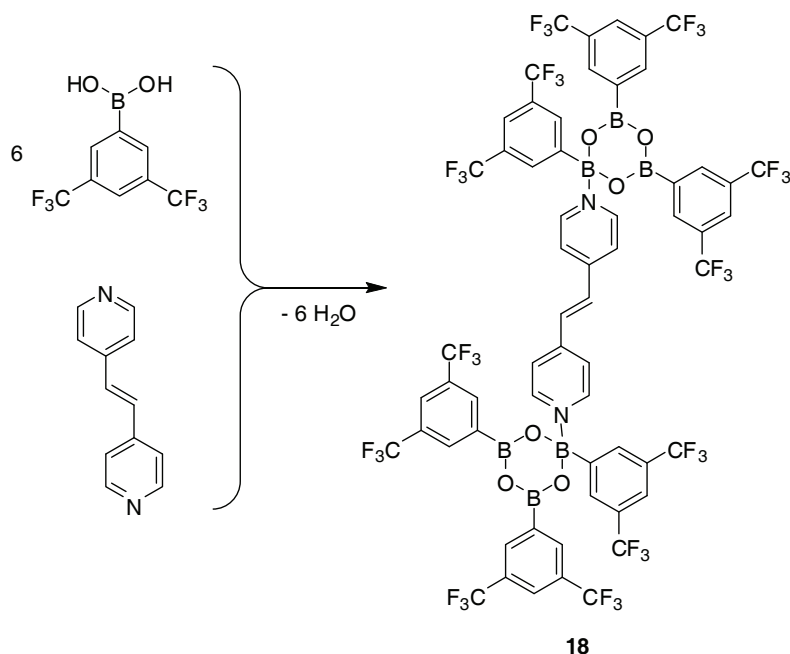
Scheme 3.6: Synthesis of diboroxine complex **18**.

Complex **18** was isolated in good yield and displayed very low solubility in apolar solvents such as benzene, toluene, and chloroform. For this reason, the analysis of complex **18** in solution by NMR spectroscopy was difficult. It was possible, however, to perform a single crystal X-ray analysis and consequently to obtain structural information about **18** (Figure 3.5). As expected, the two six-membered boroxine rings are formed and connected by one 1,2-bis(4-pyridyl)ethylene ligand. Two different geometries can be distinguished for the boron atoms: B(1) has a tetrahedral geometry and B(2) and B(3) are trigonal planar. The two boroxine rings are almost planar, with the tetrahedral boron atoms slightly out of the plane. All ring angles are about 120°, except the O-B(1)-O angle which is closer to the 109.5° value expected for a tetrahedral geometry (114.2°). The two different coordination geometries of boron atoms lead to huge differences in B-O bond lengths (Table 3.1), the B-O bonds of the tetrahedral boron center being considerably longer (1.455 vs. 1.367 Å). A similar effect is observed for the B-C bond but to a smaller extend (1.601 vs. 1.561 Å). The B-N bond of **18** is longer than what was observed for macrocycles **1**-**17** but of similar length than other adducts between boronate esters and dipyridyl ligands (see chapter 5). The lower

tetrahedral character (THC) of **18** can probably be explained by the relatively weak B-N interaction but also by the unfavorable geometry around B(1) (tetrahedral boron center incorporated in a boroxine ring). Overall, the molecule has a crystallographic C_2 symmetry about an axis passing through the center of the ethylenic double bond.
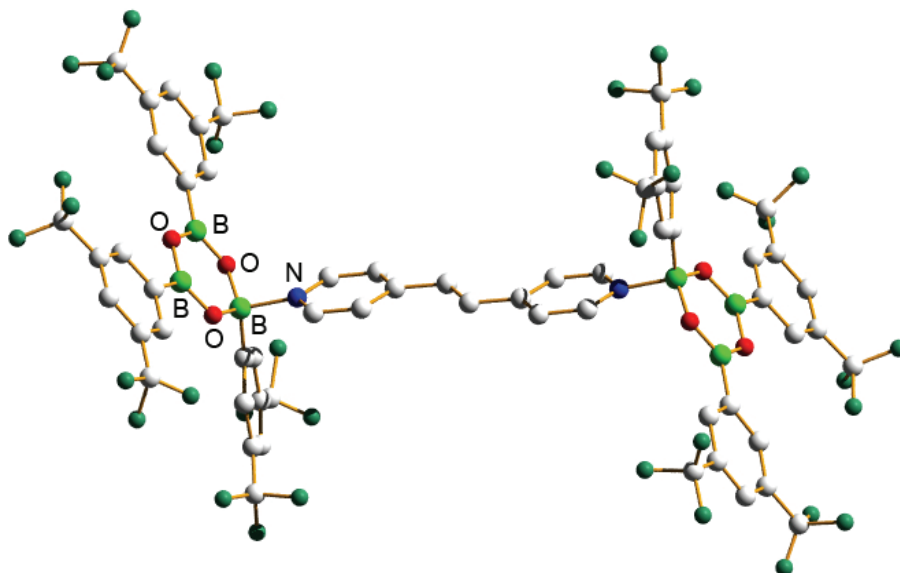
Figure 3.5: Structure of complex **18** in the crystal.

Table 3.1: Selected average bond distances (Å) and THC (%) for complex **18**.

	B1-N	THC	B1-O[a]	B2-O[a]	B3-O[a]
18	1.6565(37)	68.3	1.455	1.366	1.368

[a] Average values are given

Having established the overall geometry of complex **18**, a three-component reaction was performed between 1,2-bi(4-pyridyl)ethylene, 3,5-diformylphenyl boronic acid, and benzylamine (Scheme 3.7).
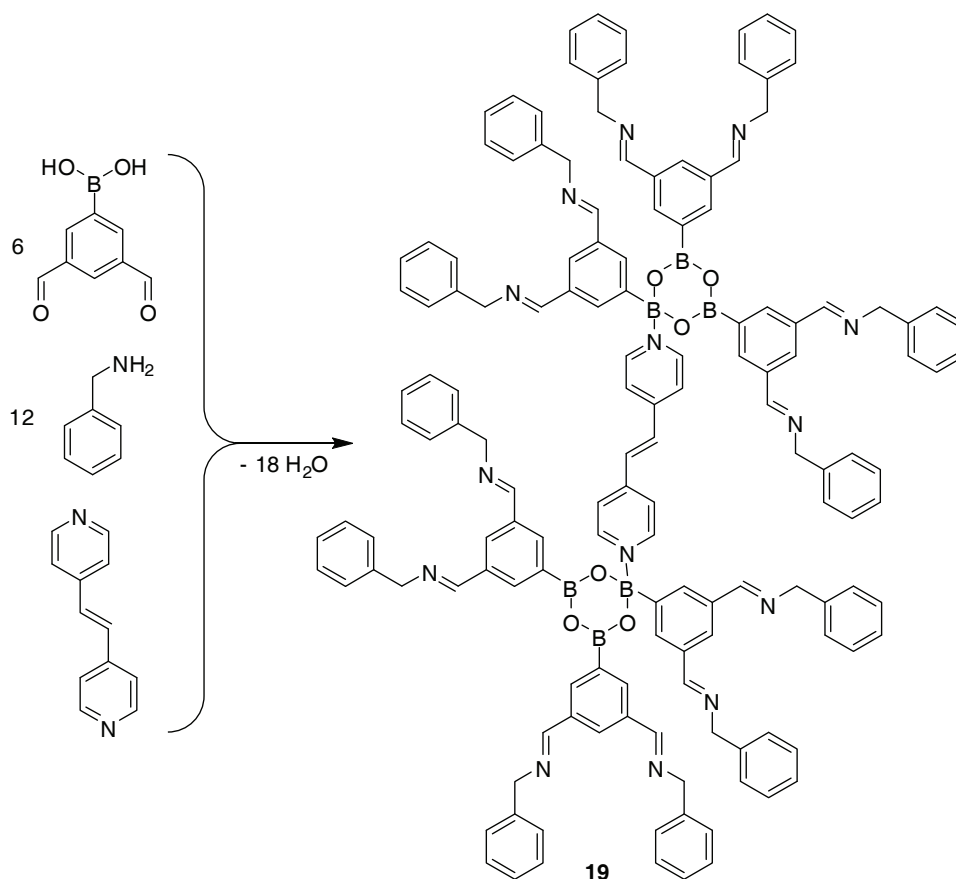
Scheme 3.7: Synthesis of boroxine-based dendritic structure **19**.

In this reaction, the dendritic structure **19,** bearing twelve benzyl groups at its periphery, is obtained in 55% yield. Unlike complex **18**, **19** is highly soluble in apolar organic solvents, and NMR investigations were possible. ^{1}H NMR indicated that the expected condensation reactions had occurred, as signals for the boroxine part as well as for the 1,2-bi(4-pyridyl)ethylene fragment were found on the spectrum. Only one set of signals was found for the boroxine side chains, meaning that a fast equilibrium between three- and four-coordinated boron centers exists. In other words, the N-donor ligand is not attached to a single boron center but is rather able to switch rapidly from a boron atom to another. This type of fluxional behavior was already reported for a $B_3O_3Ph_3$(7-azaindole) complex.[119] In this case, ^{1}H NMR studies showed that the 7-azaindole ligand is involved in an intermolecular migration, meaning that it dissociate from a boron atom and then reattach to another one. The absence of an aldehydes peak at ~10 ppm is characteristic of a complete imine condensation and of the good purity of **19**. The ^{11}B NMR spectrum of **19** displays a single peak at $\delta = 26.0$ ppm. This intermediate chemical shift value indicates a fast equilibrium between trigonal planar

boron centers and tetrahedral ones. It thus corroborates the observation made with ^{1}H NMR.

The reaction leading to compound **19** was repeated with the small dendron 3,5-(benzyloxy)benzylamine as an amine containing fragment. First NMR investigations indicate that a complex similar to **19** was formed, but unfortunately, it was so far not possible to isolate it in its pure form. Work is currently in progress to resolve this problem.

3.3 Conclusions

In this chapter, a new strategy for the self-assembly of dendritic structures is presented. The boron-based macrocycles described in chapter 2, were used as scaffolds for the formation of larger, more complex architectures by decoration of their periphery with small dendrons. Importantly, the core of the structure and the dendritic periphery were assembled simultaneously. To do so, three reversible and largely independent reactions were used in parallel: Condensation of aldehydes with primary amines, addition of N-donor ligands to boronate ester, and condensation of boronic acids with aromatic diols. By using dihydroxypyridine ligands together with mono- or di-formyl functionalized boronic acids and primary amines, tetrameric macrocycles with four or eight dendrons at the periphery as well as pentameric structures decorated with five or ten dendrons were prepared. An intrinsic advantage of the method is its flexibility, as either the core or the periphery of the structure can be varied independently. The core of the dendritic structure was found to be kinetically inert but substitution reactions could be performed at its periphery. The latter property could be of interest for a post-modification of the structure.

To further test the potential of this multicomponent synthetic strategy, the possibility to form boroxine-based dendritic architectures was investigated. Again, a three-component synthesis between 3,5-diformylphenyl boronic acid, 1,2-bis(4-pyridyl)ethylene, and benzylamine was performed. In this synthesis, a structure with two bridged boroxine rings decorated with twelve benzyl units was obtained.

Chapter 4

Synthesis of Boronate Polymers

4.1 Introduction

This chapter describes the formation of boronate ester polymers by three-component reactions. Aryl boronic acids were reacted with 1,2,4,5-tetrahydroxybenzene and a dibyridyl linker to produce one-dimensional polymeric chains. X-ray crystallographic analyses revealed that the polymers are assembled via formation of dative B-N interactions as well as covalent B-O bonds.

4.1.1 Boron Containing Polymers

The extension of the concepts of supramolecular chemistry[4,5] from discrete species to polymers leads to the definition of a new class of material called supramolecular polymers. These structures are assembled using non covalent interactions and are dynamic by nature, allowing for error correction during the growth process.[200] As for discrete species, the supramolecular chemistry of polymers is largely dominated by transition metal coordination chemistry and H-bonding chemistry.[201,202] During the last years however, a few research groups investigated the possibility of using other types of interactions to build constitutional dynamic polymers. For instance, aldehyde-amine condensation was used to produce dynamic, polymeric systems ("dynamers").[203,204]

Similarly, the labile, yet, covalent boron-oxygen bond was used to create polymers with a boronate ester backbone. The groups of Shinkai[142,143] and Shimizu[144] were the first to report the assembly of polymers by condensation of diboronic acids with sugar derivatives. Recently, Lavigne and co-workers showed that poly(dioxaborolane)s[145] and poly(dioxaborole)s[146,147] can be obtained by the condensation of diboronic acids with pentaerythritol or 1,2,4,5-tetrahydroxybenzene. Simultaneously, Yaghi and his group reported the formation of covalent organic frameworks (COFs) by condensation of di- or tri-boronic acids and 2,3,6,7,10,11-hexahydroxytriphenylene.[149,151,152]

Alternatively, boron containing polymers can be assembled by formation of B-N bonds. This concept was first demonstrated by Wagner and co-workers, who reported the polymerization of 1,1'-ferrocenyldiborane with 4,4'dipyridyl derivatives[160] or pyrazine.[161] Using a similar reaction, the Jäkle group prepared linear polymers from di(thienyl)borane functionalized polystyrene building blocks and 4,4'-dipyridyl.[205,206]

More details about these boron-based polymeric structures can be found in § 1.4.3 and § 1.4.5.

On the next pages, an approach allowing for the assembly of boron containing polymers combining these two strategies is described. Boronic acid-diol condensation and donor acceptor interaction were used in parallel to generate novel polymer architectures by three-component reactions.

4.2 Results and Discussion

To evaluate the possibility to generate boronate polymers with ditopic N-donor ligands, a mixture of 1,2-bis(4-pyridyl)ethylene, two equivalents of 4-ethylphenylboronic acid, and two equivalents of 1,2,4,5-tetrahydroxybenzene was refluxed in benzene using a Dean-Stark trap. After hot filtration, a clear and slightly yellow solution was obtained, from which, upon cooling, a dark-purple solid (**20**) precipitated in good yield (81%) (Scheme 4.1). When 4-ethylphenylboronic acid was replaced by 4-*tert*-butylphenyl boronic acid, a similar behavior was observed and a dark precipitate (**21**) formed.

At room temperature, compounds **20** and **21** displayed very low solubility in common coordinating and non coordinating organic solvents such as benzene, chloroform, acetonitrile, and tetrahydrofuran. **20** and **21** could only be dissolved in hot chloroform and dissolution was associated with a strong color change: pale yellow solutions were obtained from the dark-purple suspensions. Upon cooling down to room temperature, the dark solid precipitated again, indicating that the color change is a reversible process.
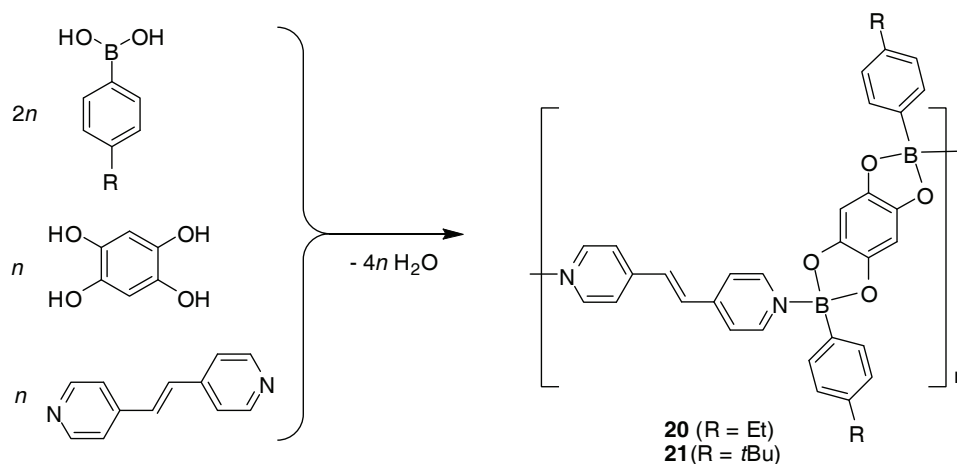
Scheme 4.1: Synthesis of polymers **20** and **21**.

A CDCl$_3$ solution of polymer **20** was analyzed by ^{1}H NMR spectroscopy and its spectrum was nearly a superposition of those of 1,2-bis(4-pyridyl)ethylene and bis(dioxaborole) **22** ($\Delta\delta < 0.1$ ppm). The latter complex was formed by condensation of 4-ethylphenylboronic acid and 1,2,4,5-tetrahydroxybenzene (Figure 4.1) following a reported procedure.[207] **20** was also analyzed by ^{11}B NMR giving a single signal at $\delta = 28.8$ ppm. This chemical shift value is close to what was obtained for **22** ($\delta = 34.6$ ppm) but very different from the expected value for a tetracoordinated boron atom ($\delta \sim 10$

ppm).[182] This data suggested that the chloroform solution of **20** contained mainly dissociated 1,2-bis(4-pyridyl)ethylene and bis(dioxaborole) **22**. The small difference in chemical shifts can be explained by the existence of a fast equilibrium between the dissociated fragments and a minor amount of B-N adducts. A similar thermal dissociation of a polymer into its constituents was reported by Wagner and co-workers for their borylated ferrocene polymers.[160,161]

Scheme 4.2: Equilibrium (in CHCl₃) between polymer **20** and its constituents **22** and 1,2-bis(4-pyridyl)ethylene (left) and the color change observed upon heating (right).

Because of the reversible formation of polymer **20**, single crystals of sufficient quality for an X-ray diffraction analysis could be grown from a CHCl₃/pentane solution. The crystallographic analysis confirmed the polymeric structure and revealed the formation of a zig-zag chain of diboronate esters bridged by 1,2-bis(4-pyridyl)ethylene linkers (Figure 4.1)
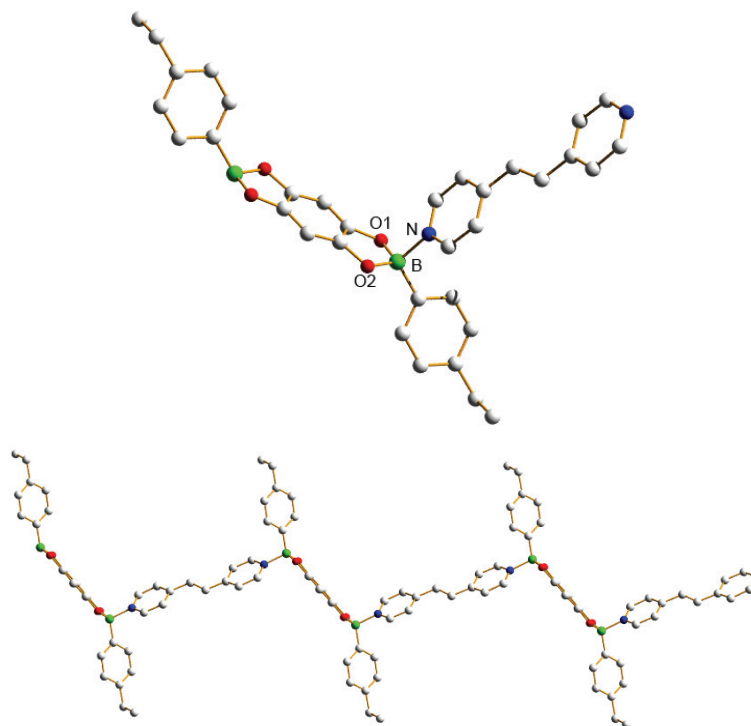
Figure 4.1: Structure of polymer **20** in the crystal. View of the repeating unit (top) and of the polymeric chain (bottom). Only one of the two independent subunits is shown. Solvents molecules and hydrogen atoms have been omitted for clarity.

Two independent polymeric chains were found in the crystal. With an average length of 1.677 Å, the B-N bond in **20** is long compared to what was observed for adducts between boronate ester and sp^2–nitrogen donors ligands.[112] This is also longer than what was observed for tetrameric and pentameric macrocycles **1-10** described in chapters 2 and 3. Accordingly, the calculated tetrahedral character is relatively low (THC$_{av}$ = 72.5%). These observations corroborate the results of the NMR spectroscopic experiments and suggest that the B-N bond in **20** is weak. With an average value of 1.479 Å, the B-O bonds are longer than what was observed for trigonal planar boronate esters similar to **22** (B-O 1.388-1.395 Å)[207] but shorter than those of complexes **1-10**. This shows that the length of the B-O bond depends on the strength of the B-N bond (i.e. a strongly bounded B-N adduct possess a longer B-O bonds).

In order to test the flexibility of the strategy, the same reaction that led to the formation of polymer **20** was repeated with different building blocks. 1,2,4,5-Tetrahydroxybenzene was reacted with 4,4'-dipyridyl and either 3,5-dimethylphenyl boronic acid (**23**) or 3,5-bis(trifluoromethyl)phenyl boronic acid (**24**), respectively

(Scheme 4.3). In both cases, a dark-purple polymer was obtained as the reaction product. Again, heating a $CHCl_3$ suspension of **23** or **24** led to a color change attributed to the disruption of the polymer chain into its constituents.
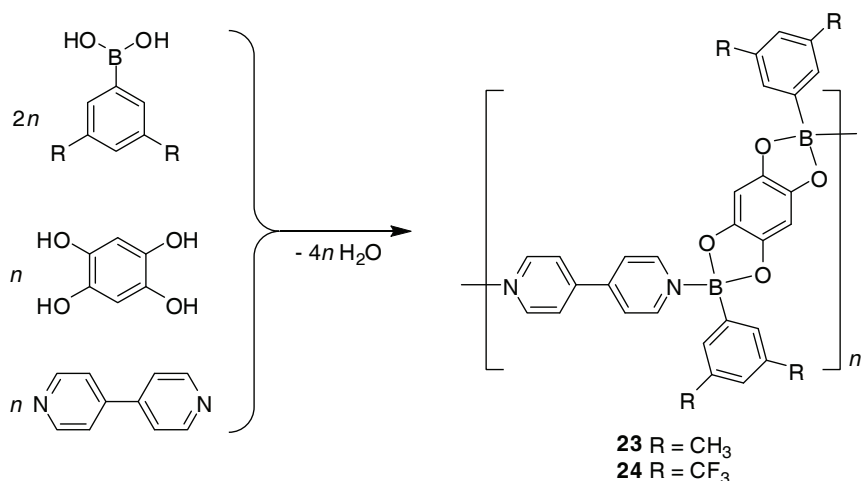
Scheme 4.3: Synthesis of polymers **23** and **24**.

The molecular structure of **23** and **24** is very similar to what was observed for compound **20**. The bis(dioxaborole) subunits are connected by 4,4'-dipyridyl ligands, forming a zig-zag chain (Figure 4.2). The bond lengths of **23** and **24** are very similar to those of **20** (Table 4.1). Correlating with the long B-N bonds, rather low tetrahedral character values were obtained for both compounds (69.5% for **23** and 70.0% for **24**).

Table 4.1: Selected (average) bond distances (Å) and THC (%) for polymers **20**, **23**, and **24**.

|	B-N	B-O[a]	THC
20	1.677	1.479	72.5
23	1.702(5)	1.475	69.5
24	1.6782(59)	1.471	70.0
[a] Average values are given			
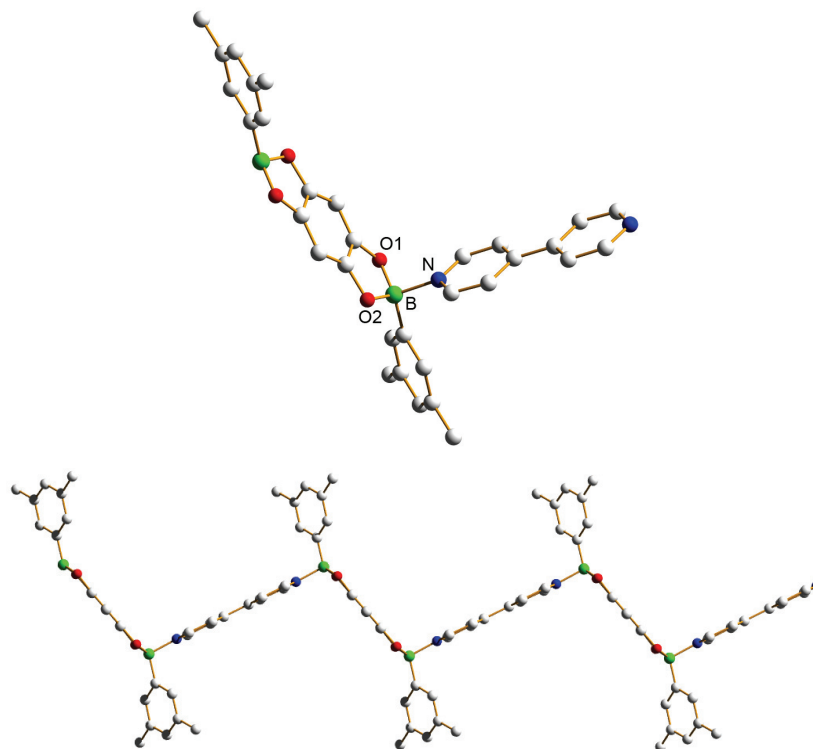
Figure 4.2: Structure of polymer **23** in the crystal. View of the repeating unit (top) and of the polymeric chain (bottom). Hydrogen atoms have been omitted for clarity.

Polymers **20**, **21**, and **23** were analyzed by solid-state ^{11}B NMR. With peaks around 10 ppm, their spectra were in agreement with the depicted structures (Figure 4.3 a, b, and d). Unlike these three compounds, the product of the reaction between methyl boronic acid, 4,4'-dipyridyl, and 1,2,4,5-tetrahydroxybenzene (**25**) showed a different behavior. **25** was also a dark-purple poorly soluble material, but its ^{11}B NMR spectra showed two peaks at ca. 9 and 32 ppm (Figure 4.3 c)). As the former peak is characteristic for a four-coordinated boron center, the second one is related to a trigonal planar boron atom. We therefore propose that compound **25** is the monoadduct [MeB($C_6H_2O_4$)BMe(bipy)] with one trigonal and one tetragonal boron center. Apparently, the methyl boronic ester is not sufficiently Lewis acidic to promote extended polymerization.

Similarly, the reaction of 2,4,6-trifluorophenyl boronic acid with pentaerythritol and 4,4'-dipyridyl did not allow for the formation of a polymeric chain. ^{1}H and ^{11}B NMR revealed that the dioxaborolane units were formed, but no coordination of the N-donor ligand to the boron center was observed. A likely explanation is that using a more electron donating aliphatic tetraol fragment instead of the aromatic 1,2,4,5-tetrahydroxybenzene decreases the Lewis acidity of the boronic ester and prevents coordination of the 4,4'-dipyridyl linker.
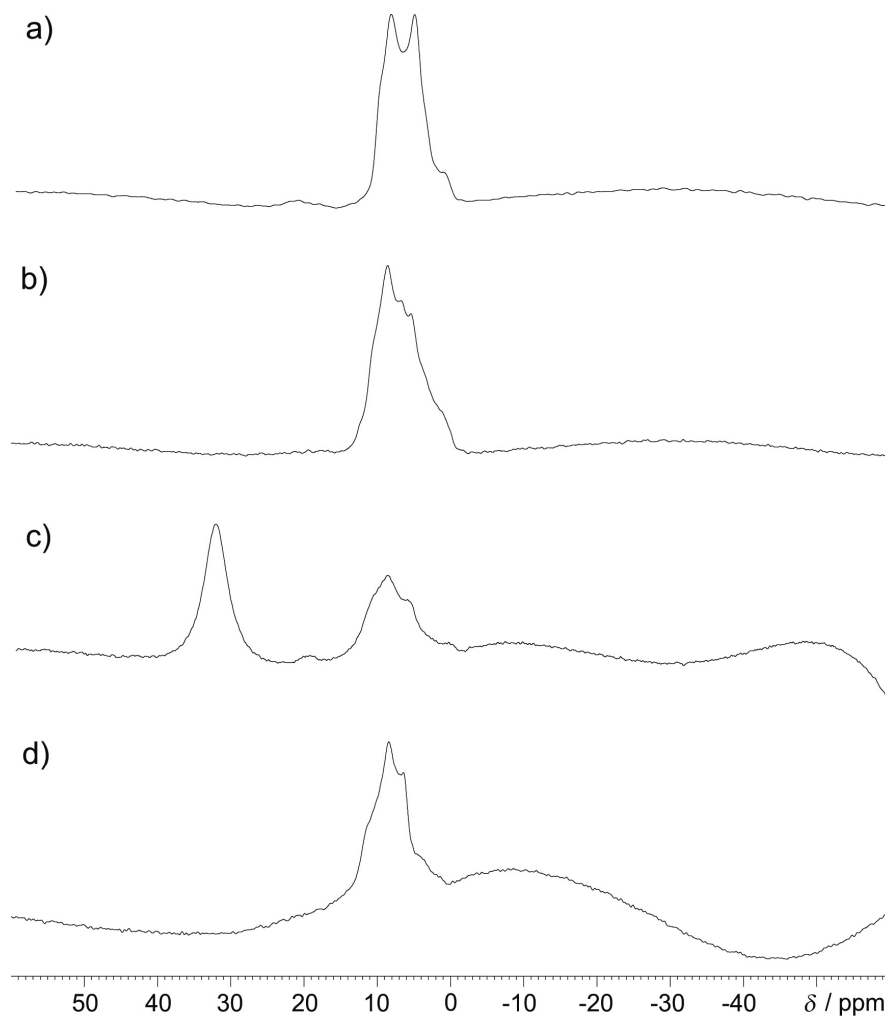
Figure 4.3: Solid-state ^{11}B NMR spectra of polymers **20** (a), **21** (b), **23** (d), and adduct **25** (c).

A striking feature of polymers **20**, **21**, **23**, and **24** is their very dark-purple color. Because this color disappears upon dissolution in chloroform, it must be the fully assembled polymer, which gives rise to the strong absorption. To understand this phenomenon, single-point second order approximate coupled-cluster (CC2)[208] calculations of the electronic excitation on model systems were performed (theoretical studies were carried by Dr. Michele Cascella and Prof. Ursula Röthlisberger). The building blocks 1,2-bis(4-pyridyl)ethylene and 4,5-dihydroxyphenyl-4-ethylphenylborole showed the first absorption peak in the near-UV region (4.2 and 3.8 eV respectively), which is consistent with the finding that the solution containing the non-assembled monomers is nearly colorless. In contrast, the assembled acid-base complex showed a transition in the yellow-green region (2.2 eV), which is in agreement with the observed purple coloration of its crystals.
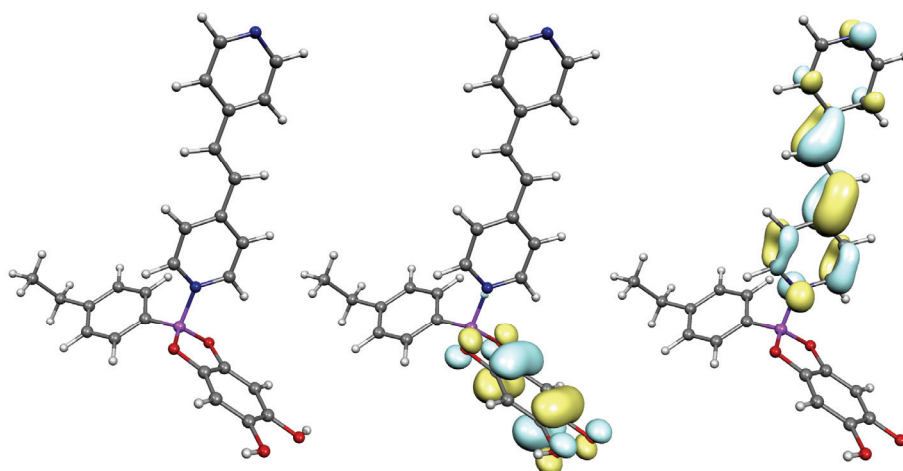
Figure 4.4: Left: theoretical cluster-model of the polymeric acid-base bair. Center-right: HOMO-LUMO orbitals responsible for the charge-transfer optical transition in the yellow-green region.

Decomposition of the optical excitation in the visible region onto a molecular orbital basis shows that it has an almost pure HOMO-LUMO π-π* character (88%). This transition corresponds to an intrastrand charge-transfer excitation from the hydroxyl-phenyl ring of the dioxaborol moiety to the 1,2-bis(4-pyridyl)ethylene ring (Figure 4.4).[160,161,209,210] Charge-transfer transitions internal to the dioxaborole strand, specifically between the hydroxyl-phenyl and the ethyl-phenyl rings, are not strongly affected by the presence of the pyridyl base; therefore, they do not contribute to the absorption in the visible region, and they remain confined in the UV region of the spectrum. Furthermore, it should be noted that there is no orbital contribution of boron and thus no extended conjugation as observed for polymers containing tricoordinate boron.[146]

4.3 Conclusions

In summary, the synthesis and characterization of new one-dimensional boron containing polymers was described. The compounds were prepared by condensation of aryl boronic acids with 1,2,4,5-tetrahydroxybenzene and 4,4'-dipyridyl or 1,2-bis(4-pyridyl)ethylene respectively. The polymer backbone is composed of bis(dioxaborole) moieties bridged by bipyridyl linkers. Because the polymer chain is assembled via weak B-N interactions, its formation is reversible. The latter property allowed for the growth of single crystals and subsequently for structural investigations. Due to the formation of B-N bonds, the dipyridyl fragment of the polymer becomes electron-deficient and is involved in intrastrand charge-transfer excitation from the hydroxyl-phenyl ring of the dioxaborol moiety, as evidenced by theoretical investigations. Another interesting property of the system is its flexibility. Various aryl boronic acids and dipyridyl linkers were successfully used in the self-assembly reaction. In contrast, the less acidic methyl boronic acid is unable to promote extended polymerization.

Chapter 5

Boron-Based Rotaxanes

5.1 Introduction

Following the work on polymers presented in chapter 4, related dimeric boronate ester compounds were prepared via three-component reactions. Their complex formation with various crown ethers was then studied. With dibenzo-30-crown-10, a clip-like host-guest complex was obtained, whereas with bis-*p*-phenylene-34-crown-10 and 1,5-dinaphto-38-crown-10, rotaxanes were isolated. These two complexes represent the first examples of boron containing rotaxanes.

5.1.1 Interlocked Structures

Interlocked molecules such as rotaxanes and catenanes are challenging and appealing synthetic targets for chemists. The early syntheses of such compounds relied on the statistical association of two components, which resulted in low yields and time-consuming work-up.[211] During the last 25 years, however, more efficient synthetic procedures have been developed.[212,213] Because interlocked molecules consist of two or more components held together mechanically rather than covalently, a precise control over the spatial orientation of the different fragments is needed in order to increase the synthetic efficiency. Modern strategies often use weak interactions[213] (H-bonds, metal-ligand interactions, π-π stacking, hydrophobic interactions) or templates[214,215] (transition metals, anions) in order to create a precursor of the final assembly. The next step usually involves irreversible formation of a covalent bond to transform the precursor into the desired complex, while retaining its geometry.

[2]Rotaxanes, for instance, can be prepared by two different strategies: stoppering, or clipping (Scheme 5.1). The stoppering route involves preparation of a [2]pseudorotaxane precursor and subsequent end-capping of the linear component (b). Similarly, [2]catenanes can be obtained by macrocyclization of the linear component (a). In the clipping synthesis, [2]rotaxanes are prepared by cyclization of an acyclic precursor around a linear template (c).
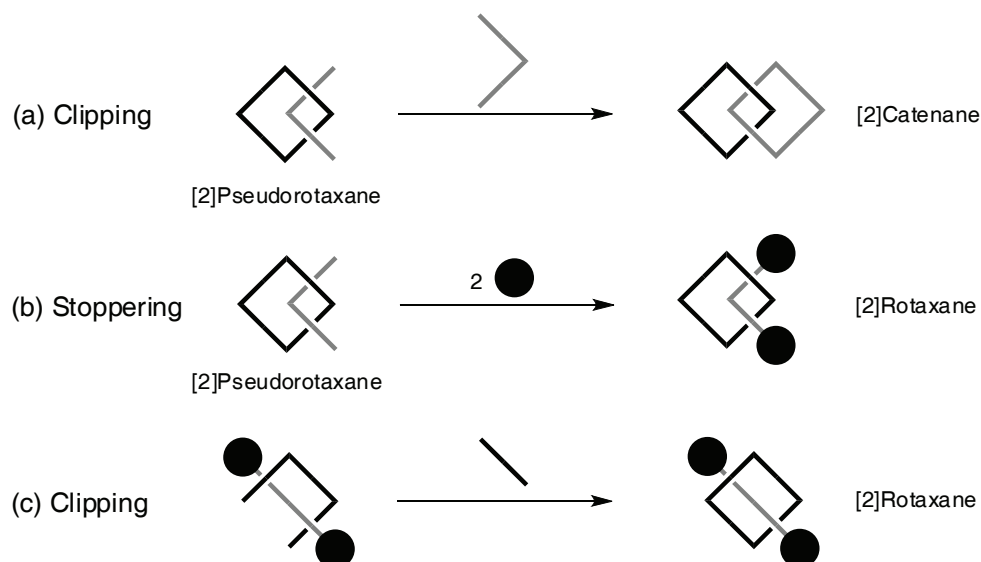
Scheme 5.1: Schematic representation of the possible synthetic routes to [2]rotaxanes and [2]catenanes.

A major drawback of the strategies a-c is that the final bond-forming reaction is performed under kinetic control, resulting in the irreversible formation of undesired side-products (non-interlocked products). Consequently, low yields are obtained. As already mentioned, a possible solution to this problem is to perform the last step under thermodynamic control, using either reversible covalent or non-covalent interactions.

5.1.2 Synthesis of Rotaxanes under Thermodynamic Control

In contrast to a kinetically controlled synthesis, the thermodynamically controlled approach allows for a re-equilibration of the side-products to form the more stable desired structure in good yield. It also allows for the formation of interlocked structures from their preformed components ("magic ring" or "magic dumbbell" trick).

Over the last years, several research groups have been studying the formation of interlocked molecules under thermodynamic control. Very often, the simplest compounds of the family, namely [2]rotaxanes or [2]catenanes were targeted, but the formation of more complex structures has also been reported.

As already described in § 1.3.2, the Stoddart group prepared [2]rotaxanes under thermodynamic control using imine condensations. This reversible interaction was coupled with the well-known binding of dialkyl-ammonium ions to [24]crown-8 to build

[2]rotaxanes either by stoppering[216] or by clipping.[86,217] The scope of this strategy was later increased with the preparation of more complex interlocked structures. [87,88,218,219] Other reversible covalent bonds were also combine with the ammonium ion templated synthesis of rotaxanes. For instance, Takata and co-workers assembled [2]- and [3]rotaxanes using a stoppering strategy together with reversible thiol-disulfide exchange (Scheme 5.2).[220] A clipping strategy and the more rarely used olefin metathesis were applied by Grubbs et al. for the preparation of [2]rotaxanes.[221] In this case the metathesis reaction was mediated by a ruthenium carbene catalyst, which ensured reversibility.
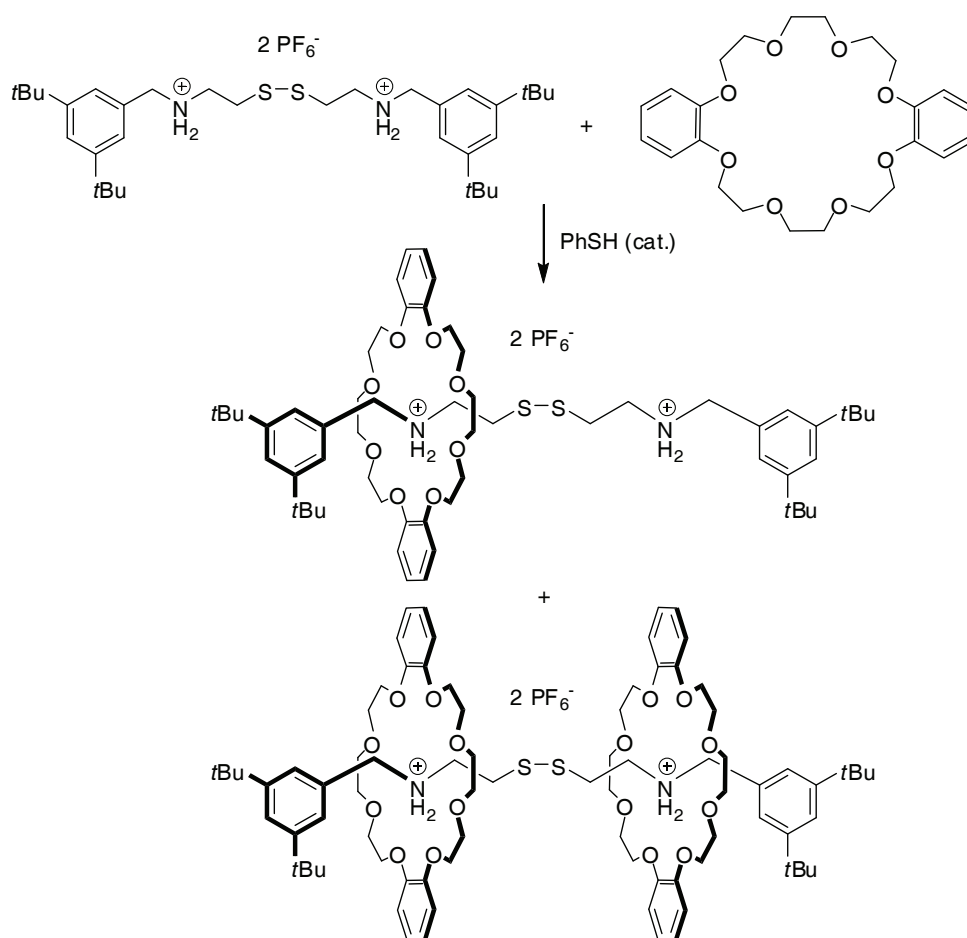
Scheme 5.2: Synthesis of disulfide-based [2]- and [3]rotaxanes.[220]

As for the preparation of macrocyclic and cage molecules (§ 1.2), non-covalent metal-ligand interactions were used for the formation of rotaxanes. Various strategies were successfully employed. For instance, the stoppering approach was used by Anderson,[222] and Sanders. The latter used metal containing porphyrin stoppers to trap a 1,5-dinaphto-38-crown-10 ring on a naphtodiimide-based dumbbell.[223] The clipping

strategy was tested by Jeong,[224] and Hunter, who clipped a Zn- porphyrin dimeric macrocycle on a complementary axle.[225] As an extension to these studies on simple, discrete systems, Kim[226,227,228] and Loeb[229,230] independently reported the formation of coordination polyrotaxanes and metal-organic rotaxane frameworks.

On the next pages, the preparation of boron-based rotaxanes is presented. The basis for this project is the finding that bis(dioxaborole)s can be polymerized by addition of 4,4'-dipyridyl or 1,2-bis(4-pyridyl)ethylene (chapter 4). An interesting feature of these polymers is that upon coordination to two bis(dioxaborole)s units, the dipyridyl linkers become electron-deficient. As a result, the polymers are purple colored, due to an efficient intrastrand charge-transfer between the electron-rich bis(dioxaborole) moieties and the dipyridyl units. The dipyridyl moieties can be seen as partially charged analogues of the herbicide paraquat. This dicationic fragment has been extensively used in the synthesis of interlocked structures,[231,232] since discovering its host-guest complex behavior with various dibenzo-crown ethers.[233,234,235] Our strategy was to synthesize monomeric electron-deficient dipyridyl complexes and to study their host-guest chemistry with dibenzo-crown ethers, in order to produce rotaxanes.

5.2 Results and Discussion

Initially, the formation of dimeric boronate esters was studied. These compounds were synthesized via one-pot reactions of a boronic acid with catechol and a dipyridyl linker (either 4,4'-dipyridyl or 1,2-bis(4-pyridyl)ethylene). Subsequently, the formation of host-guest complexes between the dimeric axle and various crown ethers was investigated.

5.2.1 Formation of Dimeric Boronate Esters

In order to test the possibility to form complexes having two boronate esters bridged by a dipyridyl ligand, boronate ester **26** was prepared (Scheme 5.3). The reaction is very simple: both reagents were refluxed in toluene, with azeotropic elimination of water. The crude product was then purified by sublimation under vacuum. In this purification process, single crystals of sufficient quality for an X-ray diffraction analysis were formed. The structure of boronate ester **26** was thus clearly established (Scheme 5.3, bottom).
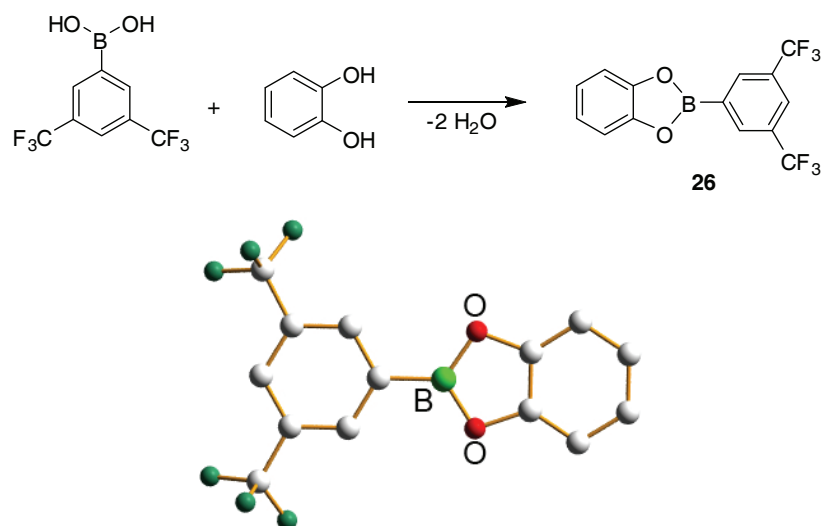
Scheme 5.3: Preparation of boronate ester **26** (top) and its structure in the crystal (bottom). Hydrogen atoms have been omitted for clarity.

Stoichiometric amounts of either 4,4'-dipyridyl or 1,2-bis(4-pyridyl)ethylene were then added to a CDCl$_3$ solution of **26**. The addition immediately led to the appearance of a yellow-orange color. Since a color change was also observed upon assembly of the

polymeric chains described in chapter 4, this phenomenon can again be attributed to a charge-transfer between the two dioxaboroles and the bipyridyl linker. It is thus a good indication that the N-donor ligand coordinates to the boron centers.

To simplify the synthesis and to obtain more material for further analyses, a one-pot reaction between 3,5-bis(trifluoromethyl)phenyl boronic acid, catechol and either 4,4'-dipyridyl or 1,2-bis(4-pyridyl)ethylene was performed. This procedure led to the formation of the adducts **27** and **28**, respectively (Scheme 5.4).
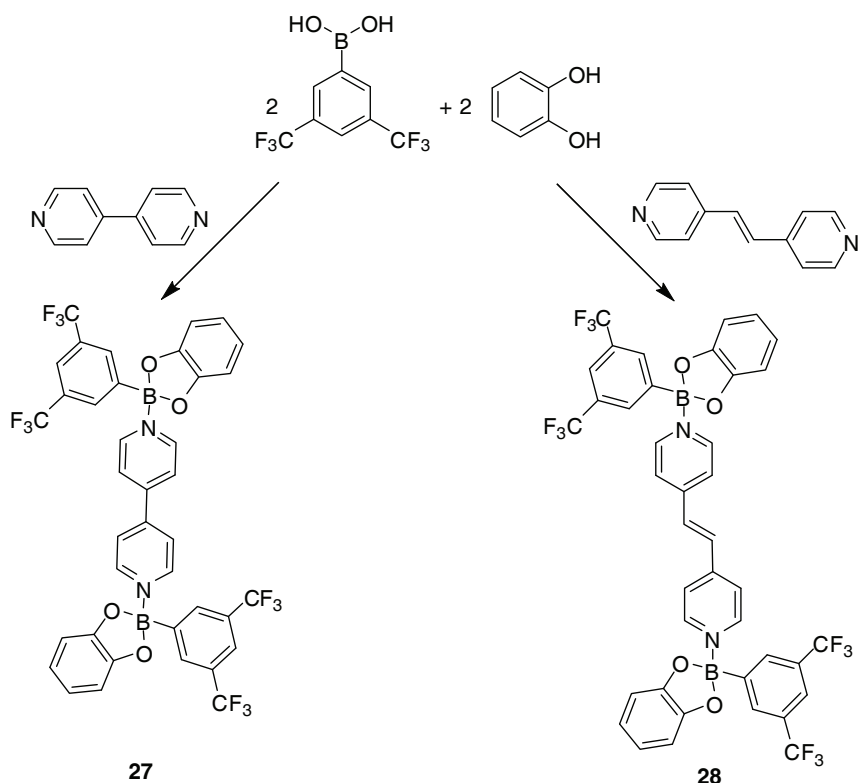
Scheme 5.4: Synthesis of **27** and **28**.

^{1}H NMR analyses indicate the formation of 2:1 adducts between **26** and the dipyridyl ligands. Formation of the B-N bonds is indicated by a shielding of the peaks corresponding to the boronate ester and a deshielding of the dipyridyl signals compared to the uncoordinated fragments. The ^{11}B NMR spectra of **27** and **28** display a single signal at δ = 20.3 and 15.6 ppm respectively. Both signals are shifted upfield compared to the signal obtained for the trigonal planar boron center of **26** (δ = 31.9 ppm), corroborating the ^{1}H NMR analyses and the formation of B-N bonds. However, the observed upfield shift is not as large as expected, in particular for compound **27**. ^{11}B NMR chemical shift values in the range 10-15 ppm were previously observed for macrocycles **1-17** (see chapters 2 and 3) which are complexes with strong B-N bonds.

An explanation for the higher values obtained for **27** and **28** is that the B-N adducts are in fast equilibrium with their dissociated components. This phenomenon results in intermediate chemical shift values.

Compounds **27** and **28** were also analyzed by X-ray crystallography. For both adducts, single crystals were obtained, but only for **28** was their quality sufficient for a proper analysis. The structure of **28** is composed of a dipyridyl linker coordinated to two boronate esters (Figure 5.1). The molecule has a crystallographic C_2 symmetry about an axis passing through the center of the ethylenic double bond. The X-ray analysis is in line with the NMR data and confirms the suspected geometry of the boron centers, as well as the 2:1 stoichiometry of the adduct of **26** with 1,2-bis(4-pyridyl)ethylene.
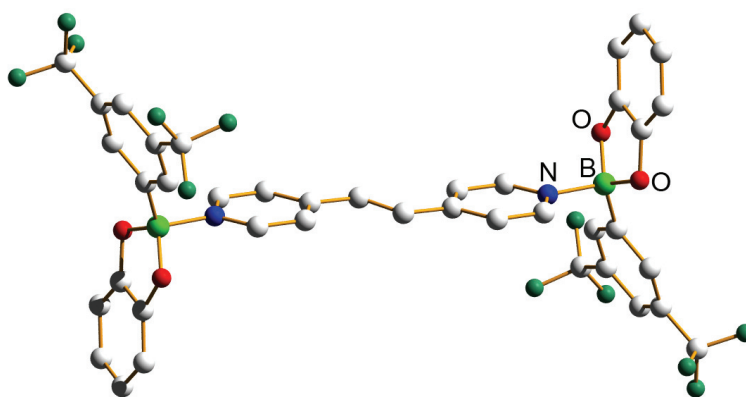
Figure 5.1: Structure of complex **28** in the crystal. Hydrogen atoms and solvent molecules have been omitted for clarity.

The B-N and B-O bond distances found for compound **28** are within the expected range (Table 5.1).[112,183] Coordination of a N-donor ligand to the boron center considerably elongates the B-O bonds, as shown by the ~0.08 Å difference in bond length between **26** and **28**. Compared to the polymers **20**, **23**, and **24** (see chapter 4), the B-N bond in **28** is slightly shorter, and accordingly, the tetrahedral character (THC) is higher. These differences can probably be explained by the use of a more Lewis acidic boronic acid together with a more electron rich dipyridyl linker. Compared to macrocyclic complexes described in chapter 2, the B-O bonds in **28** are shorter, as the B-N bond is longer. The latter observation is in line with the higher ^{11}B NMR chemical shift value obtained for **28**. Finally, the THC value calculated for **28** is within the expected range.

Table 5.1: Selected bond distances (Å) and THC (%) for compounds **26** and **28**.

	B-O1	B-O2	B-N	THC
26	1.3820(24)	1.3820(24)	-	-
28	1.4581(18)	1.4704(19)	1.6526(19)	75.3

In order to obtain more information about the stability of the aggregates **27** and **28** in solution, NMR titration experiments were performed: A 10 mM solution of boronate ester **26** in CDCl$_3$ was titrated with various amounts of either 4,4'-dipyridyl or 1,2-bis(4-pyridyl)ethylene. The addition of increasing amounts of dipyridyl linker resulted in gradual changes in the ^{1}H NMR spectra indicating that the formation of pyridyl adducts is fast on the NMR time scale. Fitting of the titration isotherm to a 2:1 binding model gave the two binding constants.[236] For the titration of **26** with 4,4'-dipyridyl, a first binding constant of $K_1 = 1.2 \ (\pm \ 0.9) \ 10^4 \ M^{-1}$ and a second binding constant of $K_2 = 1.8 \ (\pm \ 0.2) \ 10^2 \ M^{-1}$ were calculated. The same experiment with 1,2-bis(4-pyridyl)ethylene allowed to obtain slightly higher binding constants of $K_1 = 1.3 \ (\pm \ 0.9) \ 10^4 \ M^{-1}$ and $K_2 = 3.2 \ (\pm \ 0.5) \ 10^2 \ M^{-1}$ (typical figures for the NMR titration can be found in the experimental part). A likely explanation for the small differences observed in the binding constants of the two linkers is that the presence of an ethylenic double bond in 1,2-bis(4-pyridyl)ethylene makes it more electron rich than 4,4'-dipyridyl, and consequently coordinates more easily to boron centers. According to the obtained binding constants for the step-wise formation of **27** and **28**, it can reasonably be assumed that in both cases, the major species in solution is the mono-adduct.
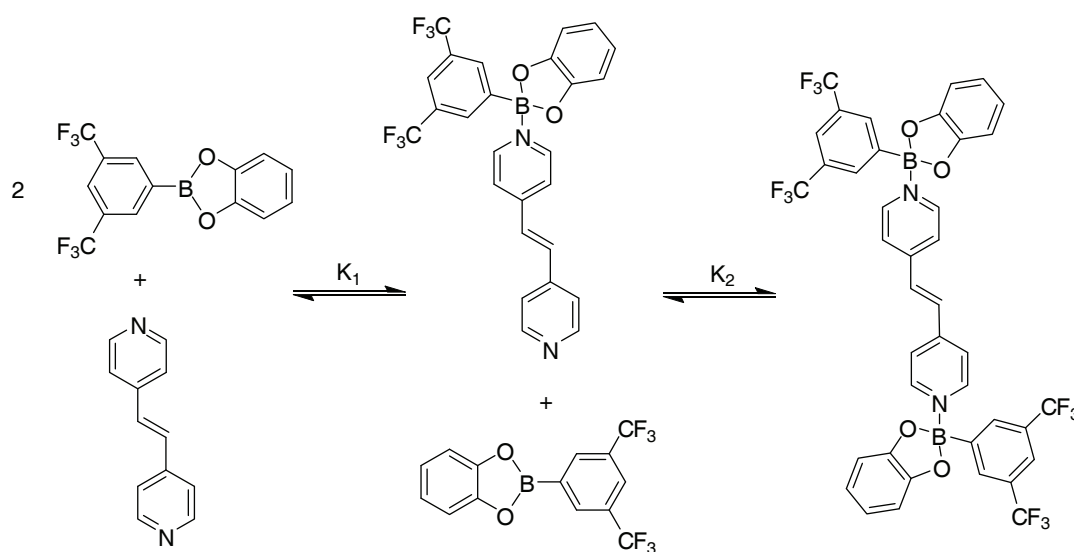
Scheme 5.5: Step-wise formation of adduct **28**.

Similar condensation reactions were performed with more acidic boronic acids such as 2,3,6-trifluorophenyl boronic acid and pentafluorophenyl boronic acid and the electron poor diol 4,5-dichlorocatechol. The objective was to prepare complexes having stronger B-N bonds and consequently more electron deficient dipyridyl linkers. The latter property was believed to favor the formation of rotaxanes with crown ethers. With these building blocks, complexes similar to **27** and **28** (same stoichiometry and geometry) can indeed be formed, according to preliminary analyses. Unfortunately, the presence of many halogen atoms on the boronate ester greatly decreases their solubility and consequently prevented further studies.

5.2.2 Complexes with Crown Ethers

After these first experiments on the formation of dimeric boronate esters, compounds **27** and **28** were chosen to serve as dumbbells for the preparation of rotaxanes with crown ethers. As **27** and **28** can easily be formed in a one-pot reaction, the same procedure was applied to the formation of the corresponding rotaxanes. In a first experiment, 3,5-bis(trifluoromethyl)phenyl boronic acid, catechol, 1,2-bis(4-pyridyl)ethylene, and 1,5-dinaphto-38-crown-10 were dissolved in a 2:2:1:1 ratio in toluene and heated to reflux using a Dean-Stark trap (Scheme 5.6).
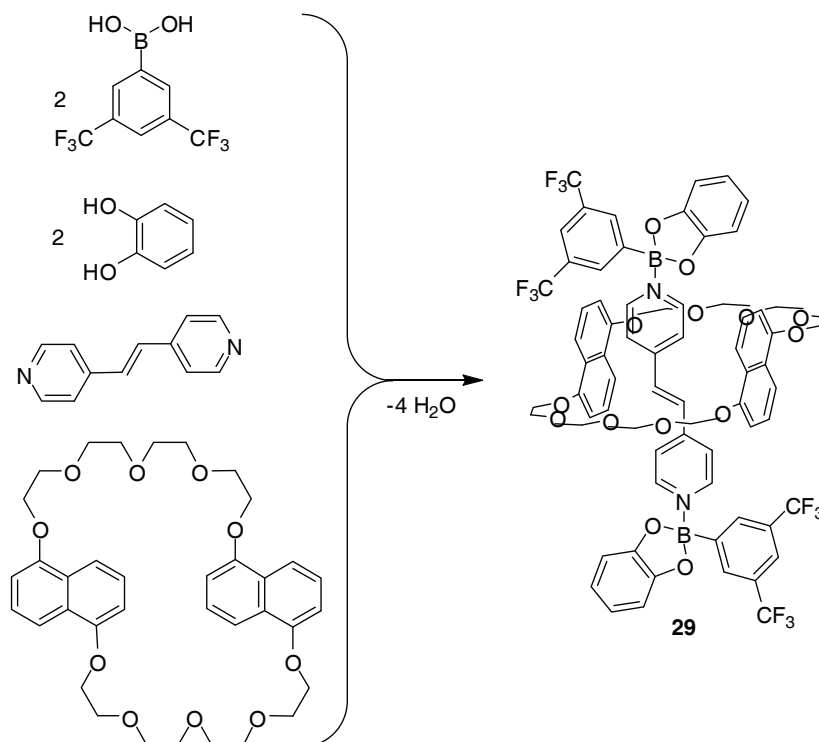
Scheme 5.6: One-pot synthesis of rotaxane **29**.

As shown above, dumbbell **28** can be prepared under these conditions, by condensation of the boronic acid with the catechol and subsequent coordination of 1,2-bis(4-pyridyl)ethylene via dative B-N bonds. Since the B-N bond formation is reversible, it is believed that the crown ether can slip on the electron deficient axle to form rotaxane **29**. Spectroscopic and crystallographic analyses showed that this strategy was successful. After one hour of reflux and removal of most of the solvent, a yellow precipitate was isolated in good yield (67%). NMR investigations showed that the isolated precipitate contained both axle and crown ether in the expected ratio. Compared to the spectrum of the free axle **28**, the spectrum of **29** displayed slightly up-field shifted signals (~ 0.1 ppm) for the 1,2-bis(4-pyridyl)ethylene and no significant shifts for the boronate ester signals (Figure 5.2).
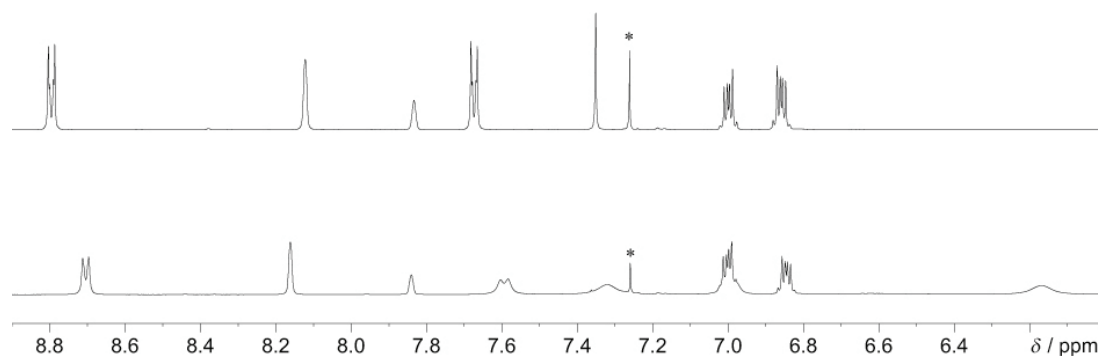
Figure 5.2: Part of the ^{1}H NMR spectrum of complexes **28** (top) and **29** (bottom). Both spectra were recorded at a 10 mM concentration. The signal of the solvent molecule is denoted with an asterisk.

Unlike the axle part, signals of the crown ether part of **29** are considerably broader than those of the free 1,5-dinaphto-38-crown-10. Moreover, shifts of up to 0.3 ppm are observed, indicating the presence of interactions between the axle and the crown ether. In addition, a 1 ppm up-field shift is observed in the ^{11}B NMR spectrum of **29**, indicating that the presence of the crown ether influences the strength of the B-N bond. Clear evidence for the formation of rotaxane **29** was obtained by X-ray crystallography (Figure 5.3). The structure of **29** is comprised of a dipyridyl axle, two boronate ester stoppers, and the crown ether, which wrapped around the axle.
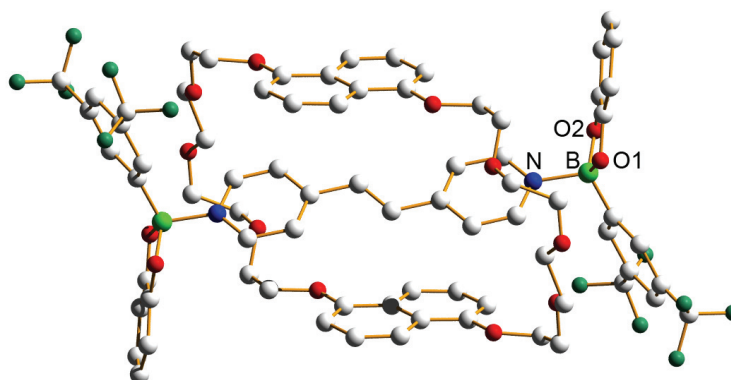
Figure 5.3: Structure of rotaxane **29** in the crystal. Hydrogen atoms and solvent molecules have been omitted for clarity.

The molecule has a crystallographic C_2 symmetry about an axis passing through the center of the ethylenic double bond and the dioxonaphtalene rings. The 1,2-bis(4-pyridyl)ethylene linker is sandwiched between the two coplanar dioxonaphtalene groups of the crown ether, which are 7.71 Å apart from each other. The plane defined

by the pyridyl groups of the axle are slightly twisted with respect to the plane defined by the dioxohaphtalene rings (twist angle: 29.9°). In addition to π-stacking interactions, there are C-H⋯O hydrogen bonds between the α-CH groups of the pyridyl rings and an O-atom of the crown ether. The lengths of the B-O and B-N bonds together with the tetrahedral character are summarized in Table 5.2. All bond lengths are within the expected range.[112] Compared to compound **28**, the B-N bond of **29** is slightly shorter. This is in correlation with the small difference observed for the ^{11}B NMR chemical shift values of these two compounds. Surprisingly, the tetrahedral character is lower for **29** than for **28**.

Table 5.2: Selected bond distances (Å) and THC (%) for compounds **29-31**.

	B-O	B-N	THC
29	1.455(14)	1.641(14)	73.6
	1.489(13)		
30	1.46[a]	1.64[a]	76.0
32	1.47[a]	1.636(5)	78.0
		1.662(5)	

[a]Averaged values are given

In order to test the flexibility of the approach, a similar four-component reaction was performed, but bis-*p*-phenylene-34-crown-10 was used instead of 1,5-dinaphto-38-crown-10. Under the same reaction conditions, a yellow precipitate was again isolated in good yield (63%). As for compound **29**, NMR analyses revealed the presence of all four building blocks and evidence for the formation of rotaxane (**30**) came from an X-ray diffraction analysis. The overall structure of **30** is similar to that of **29**, as shown in Figure 5.4.
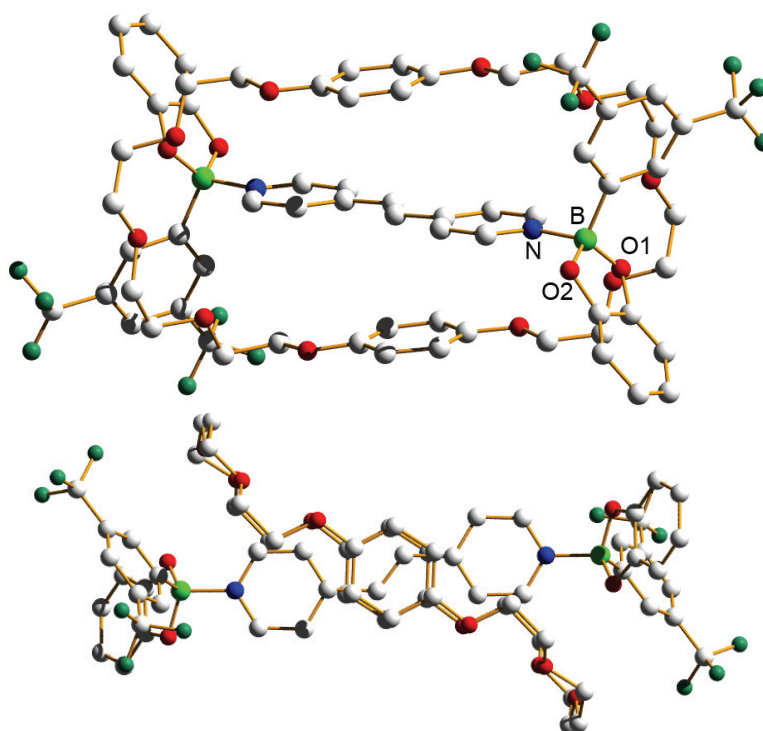
Figure 5.4: Structure of rotaxane **30** in the crystal. Top: view from the side; bottom: view along the C_2 symmetry axis. Only one of the two crystallographically independent rotaxanes is shown. Hydrogen atoms and solvent molecules have been omitted for clarity.

Again, the crown ether wraps around the 1,2-bis(4-pyridyl)ethylene axle, which is connected to two boronate esters via dative B-N bonds. The unit cell contains two halves of independent rotaxanes with a C_2 symmetry, which display comparable bond lengths. Contrary to what has been observed for rotaxane **29**, the planes defined by the phenylene rings are nearly coplanar with that defined by the 1,2-bis(4-pyridyl)ethylene axle. Consequently, the aromatic rings of the crown ether in **30** are closer to each other (7.00 and 7.06 Å). The phenylene rings are aligned with the ethylenic double bond of the axle (Figure 5.4 bottom). Several C-H···O contacts between the α-CH groups of the pyridyl rings and O-atoms of the crown ether are observed.

The multicomponent reaction of 1,2-bis(4-pyridyl)ethylene, catechol, and 3,5-bis(trifluoromethyl)phenyl boronic acid with a third type of crown ether, dibenzo-30-crown-10 also resulted in the formation of a yellow precipitate (**31**). An NMR spectroscopic analysis of the precipitate revealed the presence of signals derived from all four building blocks. Unfortunately, single crystals for a crystallographic analysis could not be obtained. In order to obtain more structural information about host-guest complexes with this type of crown ether, a slight modification was introduced: 4,4'-

dipyridyl was used instead of 1,2-bis(4-pyridyl)ethylene. The multicomponent reaction of catechol, 3,5-bis(trifluoromethyl)phenyl boronic acid, and dibenzo-30-crown-10 with this closely related linker led to the formation of compound **32** in 60% yield. Single crystals could be obtained from a cold toluene solution of **32**, revealing that the crown ether binds to the 4,4'-dipyridyl axle in a clip-like fashion (instead of wrapping around it as required for a rotaxane) (Figure 5.5). This type of host-guest complex is not surprising as *o*-phenylene-based crown ethers such as dibenzo-30-crown-10 have a known tendency to bind cationic guests in a clip-like fashion.[237,238,239]
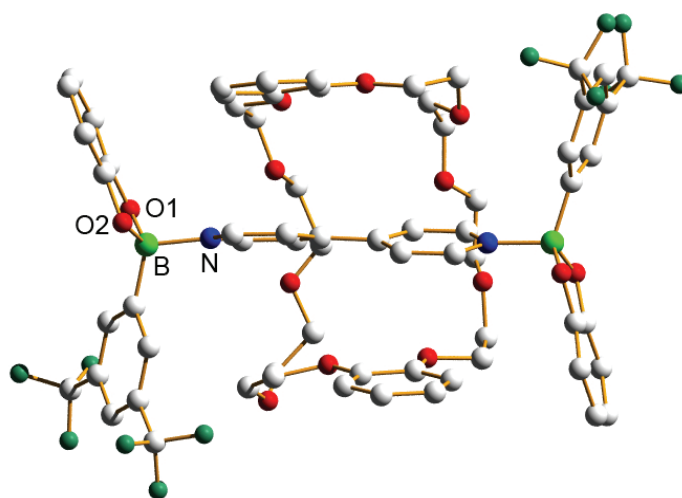

Figure 5.5: Structure of complex **32** in the crystal. Hydrogen atoms and solvent molecules have been omitted for clarity.

As previously observed for rotaxanes **29** and **30**, the phenylene rings of the crown ether of **32** show π-π interactions with the pyridyl rings of the axle. In addition, there are numerous weak hydrogen bonds between the pyridyl H-atoms and the O-atoms of the crown ether. The lengths of the B-N and the B-O bonds are similar to what was observed for **29** and **30** (Table 5.2).

5.3 Conclusions

This chapter describes the synthesis of boron-based rotaxanes. To prepare these structures, four-component self-assembly reactions between an aryl boronic acid, catechol, a dipyridyl linker, and a crown ether were used. In these one-pot reactions, the boronic acid and the catechol first condense to form a boronate ester. Then, the dipyridyl linker coordinates to the Lewis-acidic boronate ester, becoming electron deficient. The lowering of the electron density on the linker increases its affinity for electron rich crown ethers and drives the formation of host-guest or interlocked complexes. The boronate esters not only act as Lewis acids, but also as stoppers, mechanically trapping the crown ether once coordinated to the dipyridyl axle. An important feature of these boron-based rotaxanes is their dynamic B-N bonds. NMR titrations showed that the formation of the dipyridyl adduct is fast on the NMR time scale and allowed for the calculation of the two binding constants ($K_1 \sim 10^4$ M^{-1} and $K_2 \sim 10^2$ M^{-1}). According to these values, rotaxane formation can be rationalized by assuming that the crown ether slips on the mono adduct followed by reversible addition of the second boronate ester stopper. A disadvantage for future applications is that the highly labile B-N bond cannot be easily fixed by changing the solvent or the temperature. However, the dynamic nature of the B-N bond can be advantageous for construction of boron-based polyrotaxanes.

Chapter 6

Multicomponent Assembly of Boronic Acid-Based Macrocycles and Cages

6.1 Introduction

This chapter describes the synthesis of macrocyclic and cage-like molecules by multicomponent self-assembly. The structures were formed by simultaneous condensation of three or four different types of building blocks, using independent reactions in parallel (one pot syntheses).

6.1.1 Multicomponent Assembly

Multicomponent assembly, which can be defined as the assembly of several chemically distinct building blocks, is relatively common in nature. For instance, the 30S subunit of bacterial ribosome is obtained by assembly of ribosomal RNA with 21 unique proteins.[240] Synthetic supramolecular chemistry aims to use the principles of biomolecular self-assembly to construct artificial structures. However, despite the tremendous research activity in the field of supramolecular chemistry, the formation of structures from three or more distinct building blocks is still not very well developed. The major challenge of multicomponent self-assembly is to correctly "program" the system or, in other words, to introduce sufficient information in the building blocks so that only one well-defined product is obtained. For instance, the one-step preparation of molecular rectangles from a metal ion and two bridging ligands of different length is only possible under certain conditions, which take advantage of steric constrains.[241] More generally, sterically demanding ligands were often used to favor the formation of mixed-ligand aggregates over homoaggregates.[242] This concept was successfully used in the preparation of cages,[243,244] grids,[245] ladders,[246,247] cylinders,[248,249] and others.[250,251,252]

Another possibility to achieve multicomponent self-assembly is to simultaneously use different type of interactions. For example, reversible imine bond formation has often been used together with metal-ligand interaction to form complex assemblies such as grids,[253,254] helicates,[255,256] catenanes,[94] Borromean rings,[96] and others.[91,95] The strategy usually involves formation of a covalent imine bond in the coordination sphere of the metal, with formation of a M-N bond with the imine nitrogen. The metal ion can be considered as a template for imine condensation, and helps to stabilize the covalent bond (the inverse may also be true). A more detailed discussion about selected structures obtained via this methodology can be found in paragraph 1.3.3.

6.1.2 Boron-Based Systems

Recently, an analogous concept using a boronic acid instead of a metal ion was developed by the groups of James and Nitschke. They employed two types of reversible interactions: the condensation of boronic acids with diols and imine formation (Scheme 6.1 bottom).
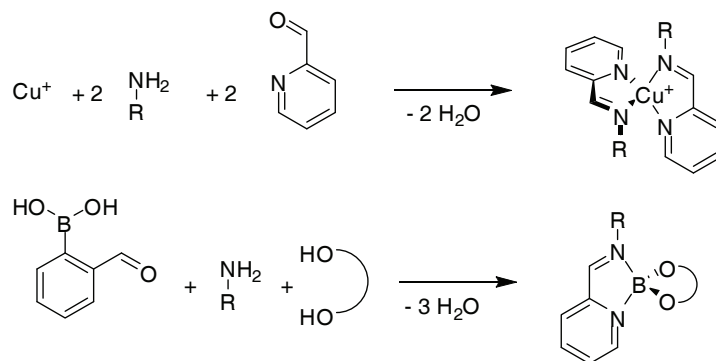
Scheme 6.1: Cu(I) templated imine formation (top) and the related iminoboronate ester motif (bottom).[139]

James et al. used this type of system to measure the enantiomeric purity of either primary amines[140] or diols[141] by ^{1}H NMR. Their protocol simply requires to mix 2-formylphenyl boronic acid, an enantiopure diol (or primary amine), and the amine (or diol) in CDCl$_3$ in presence of molecular sieve. Nitschke and co-workers studied a related system where 2-formylphenyl boronic acid was reacted with various diols and primary amines.[139] The use of diamines together with bis- or tris-diols allowed for the building of a macrocycle and a cage via three-component self-assembly (see § 1.4.2).

To the best of our knowledge, boronate ester formation as never been used together with metal-ligand interaction to create supramolecular architectures. A few structures, however, incorporate a spiroborate motif and metal ions. Albrecht and co-workers reported the hierarchical assembly of double stranded helicates from trimethyl borate, carbonyl substituted catechols and lithium carbonate (Figure 6.1 left).[257] Formation of the helical structure is believed to occur in two steps. In a first recognition event, mononuclear catechol complexes are formed and subsequently, the lithium cations bind to the carbonyl functional groups, bridging two mononuclear moieties.[258] Gudat and co-workers used a stepwise strategy to form silver containing macrocycles.[259] In their approach, a diphosphine complex was first prepared by reaction of boric acid with a catechol phosphine in presence of a base. A silver salt was subsequently added to

the boron containing ligand, producing monomeric or dimeric macrocycles, depending on the geometry of the catechol phosphine (Figure 6.1, center and right).

R = OMe, OEt, H
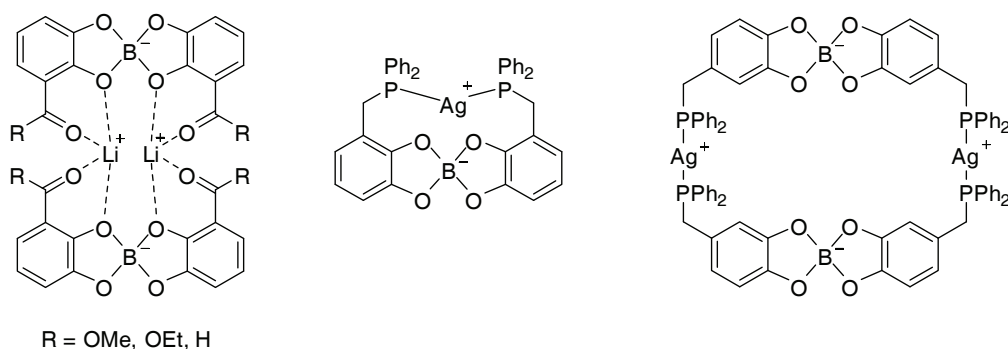
Figure 6.1: Examples of boron and metal containing complexes.[257,259]

In this manuscript, several boron containing multicomponent assemblies have already been described. They were built using two types of interaction involving the boron center: boronate esters formation and Lewis acid-base interactions with N-donor ligands. In the case of the dendritic structures described in chapter 3, imine condensations were used in parallel with these two interactions. In this case, the Lewis acidic boron only interacts with the pyridine ligand and not with the nitrogen atom of the imine bond. This property allowed for the construction of well-defined structures in good yield.

6.2 Results and Discussion

Based on the promising results described in the previous chapters, the potential of multicomponent assembly to form boron-based structures was further investigated. First, the possibility to create macrocycles and cages via the parallel utilization of imine condensation and boronate ester formation was tested. The synthesis of these fully organic macrocyclic and cage-like molecules is described in the next paragraph. Subsequently, metal-ligand interaction and boronate ester formation were used to prepare rhenium macrocycles. Finally, the three types of interaction were combined, allowing for the formation of large cyclic structures in a single step from four different types of building blocks.

6.2.1 Organic Macrocycles and Cages

In a first set of experiments, 3-formylphenyl boronic acid was reacted with pentaerythritol and 1,4-diaminobenzene. These three building blocks were selected in order to avoid undesired interactions, for example between boron centers and the N-atom of the imine bonds. The meta isomer of formylpenyl boronic acid was chosen because no intramolecular B-N bonds can be formed, contrary to what was reported by James[140,141] and Nitschke[139] for the isomeric 2-formylphenyl boronic acid. In order to avoid possible intermolecular B-N interactions, the electron rich tetraol linker pentaerythritol and the electron poor 1,4-diaminobenzene were selected. The reaction was performed with stoechiometric amounts of each reagent in a 2:1 toluene/THF mixture. Toluene allowed removing the by-product water by azeotropic distillation. THF was added to help solubilize the pentaerythritol, which possesses a very limited solubility in apolar organic solvents. After a 7 hours reflux, and complete removal of the THF, the reaction mixture was filtered to eliminate insoluble side products, which most likely consist of polymeric condensation products. Pure macrocycle **33** was then isolated in 44% yield, by precipitation followed by recristallization from CHCl$_3$/hexane (Scheme 6.2).
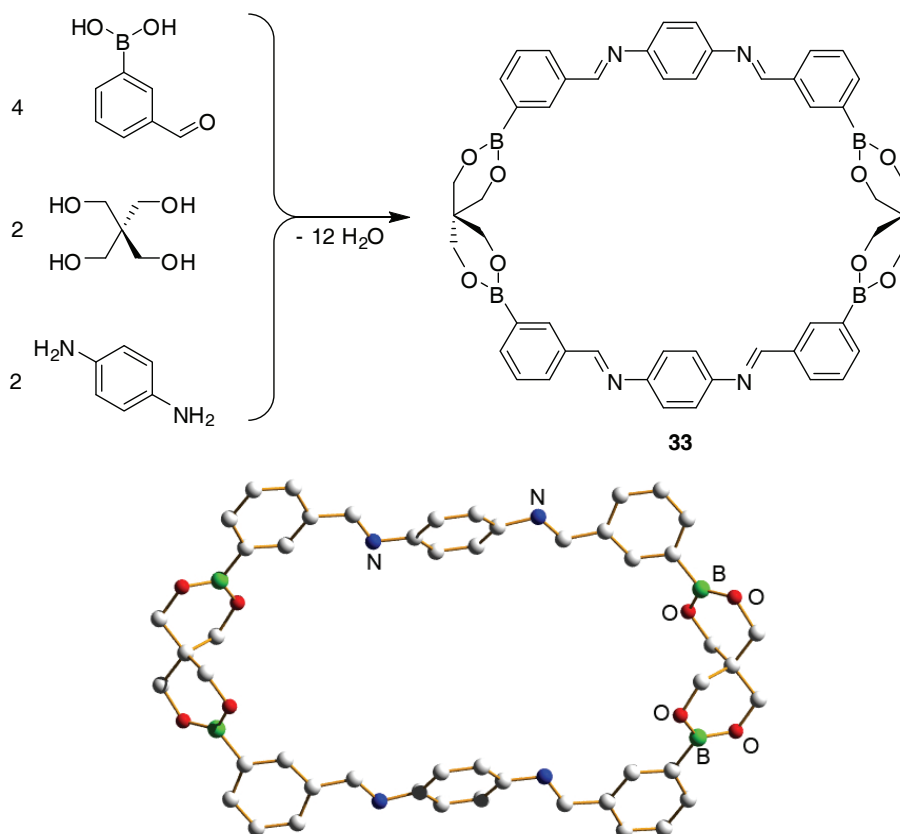
Scheme 6.2: Formation of macrocycle **33** (top) in a [4+2+2] condensation reaction and its structure in the crystal (bottom). Hydrogen atoms and solvent molecules have been omitted for clarity.

Compound **33** was comprehensively characterized by NMR spectroscopy, elemental analysis, and single crystal X-ray crystallography. The high symmetry of the macrocycle is reflected by the presence of only one set of signal in the ^{1}H NMR spectrum for each of the different building blocks. In particular, the methylene proton of the boronate ester gave rise to a simple singlet, indicating that the macrocycle possesses sufficient conformational flexibility to render them equivalent. X-ray diffraction analyses showed that macrocycle **33** is formed by condensation of four 3-formylphenyl boronic acid molecules with two pentaerythritol fragments and two 1,4-diaminobenzene linkers ([4+2+2] condensation reaction). The molecule has C_2 symmetry and all the imine bonds have the preferred *trans* geometry. The diameter of the 42-membered macrocycle is 17.2 Å (maximum B···B distance). With an average bond length of 1.365 Å, the B-O bonds of **33** are similar to what was reported by Aldridge et al. for their ferrocene containing macrocycle.[136] The "bite angle" for the bridging pentaerythritol (B···C(spiro)···B angle) is 132.3° and the BO$_2$ planes are significantly twisted (torsion angle 50.3°). Macrocycle **33** is the thermodynamically most

stable product of the reaction, as no peaks corresponding to new species could be detected in its ^{1}H NMR spectrum after 24h.

The analysis of macrocycle **33** showed that the pentaerythritol fragment possesses a certain flexibility, which favors formation of small rings over larger ones. To test whether larger macrocycles can be obtain from this type of multicomponent reactions, a more rigid tetraol linker, *all-exo*-bicyclo[2.2.1]heptane-2,3,5,6-tetraol,[260] was reacted with stoichiometric amounts of 3-formylphenyl boronic acid and 1,4-diaminobenzene (Scheme 6.3). Following a procedure similar to that described above, macrocycle **34** was obtained in moderate yield (28%).
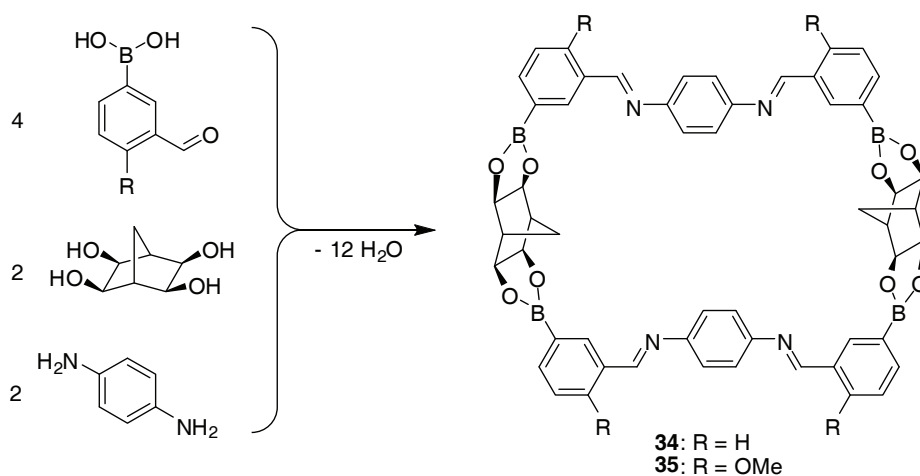
Scheme 6.3: Formation of macrocycles **34** and **35** in a [4+2+2] condensation reaction.

All NMR data were in agreement with the formation of a symmetric, macrocyclic condensation product. Unfortunately, no single crystal suitable for an X-ray diffraction analysis could be grown, so that no structural information could be obtained. Mass spectrometry also failed to provide additional evidence. The reaction was therefore repeated with 3-formyl-4-methoxyphenyl boronic acid instead of 3-formylphenyl boronic acid, and compound **35** was obtained in 24% yield. Fortunately, single crystals of the latter compound could be grown, and an X-ray diffraction analysis was performed. Despite the low quality of the crystals, the connectivity and overall geometry of the macrocycle were clearly established. According to these analyses, macrocycle **35** is a [4+2+2] condensation product (Figure 6.2). The molecule has crystallographic C_2 symmetry, with the *all-exo*-bicyclo[2.2.1]heptane-2,3,5,6-tetraol fragment bridging two boronate esters with an angle of ~120° (angle between BO_2 planes).

Figure 6.2: Structure of macrocycle **35** in the crystal. Hydrogen atoms and solvent molecules have been omitted for clarity.

As no larger macrocycles could be obtained from more rigid fragments, the geometry of the building blocks was changed, and 4-formylphenyl boronic acid was used instead of 3-formylphenyl boronic acid. As before, the reaction with 1,4-diaminobenzene and either pentaerythritol or *all-exo*-bicyclo[2.2.1]heptane-2,3,5,6-tetraol gave a mixture of complete and incomplete condensation products, but here, the isolation of a single macrocyclic product was not accomplished.

Other diamines, such as the meta and para isomers of xylylenediamine, were also screened in the macrocyclization reaction. These building blocks are expected to be more reactive toward aldehydes, and consequently to increase the yield of condensation products. However, the flexibility of that type of diamines can be a major disadvantage for the formation of a single well-defined product. The experiments were performed with *all-exo*-bicyclo[2.2.1]heptane-2,3,5,6-tetraol, which was reacted either with 3-formylphenyl boronic acid and p-xylylenediamine or with 4-formylphenyl boronic acid and m-xylylenediamine and macrocycles **36** and **37** were obtained respectively (Scheme 6.4).
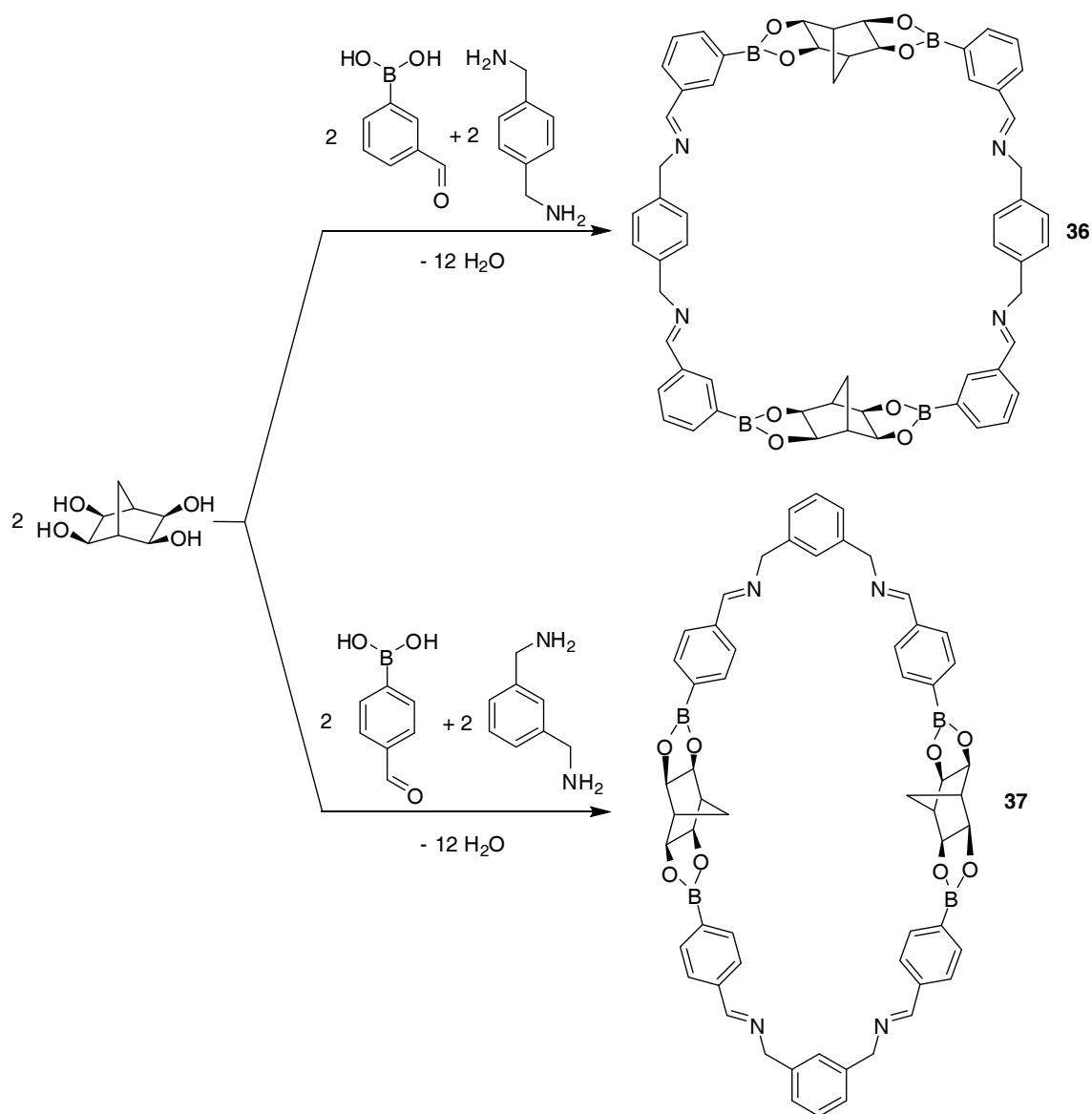
Scheme 6.4: Formation of macrocycles **36** and **37** in [4+2+2] condensation reactions.

As for compounds **33**-**35**, macrocycles **36** and **37** were prepared by refluxing stoechiometric amounts of the three building blocks in THF/toluene (1:2). During the reactions, large amounts of insoluble materials were produced (presumably polymeric or oligomeric condensation products), so that **36** could only be isolated by crystallization and **37** in very low yield (12%). The two macrocycles were analyzed by ^{1}H NMR spectroscopy, which indicated the formation of symmetric, macrocyclic condensation products. MALDI mass spectrometry analyses were performed in order to obtain information about the size of the assemblies. In both cases, molecular peaks corresponding to the [4+2+2] condensation products were identified.

Single crystals of macrocycles **36** and **37** were grown, and X-ray crystallographic analyses confirmed that both are [4+2+2] condensation products with crystallographic C_2 symmetry (Figures 6.3 and 6.4 respectively). Their shape, however, is slightly different: **37** is an oval, cyclic molecule, having a long 21.4 Å axle (diamine-diamine distance) and a shorter 8.0 Å one (distance between the bridging C-atoms of the tetraol). In **36**, these distances are 14.4 and 12.0 Å respectively, indicating a bowl-shaped molecule. The average B-O bond lengths (1.383 Å for **36** and 1.372 Å for **37**) are within the expected range for trigonal planar boronate esters.[136] The angles between BO_2 planes are slightly different (124.8° for **36** and 131.3° for **37**), indicating that the tetraol fragment possesses some flexibility.
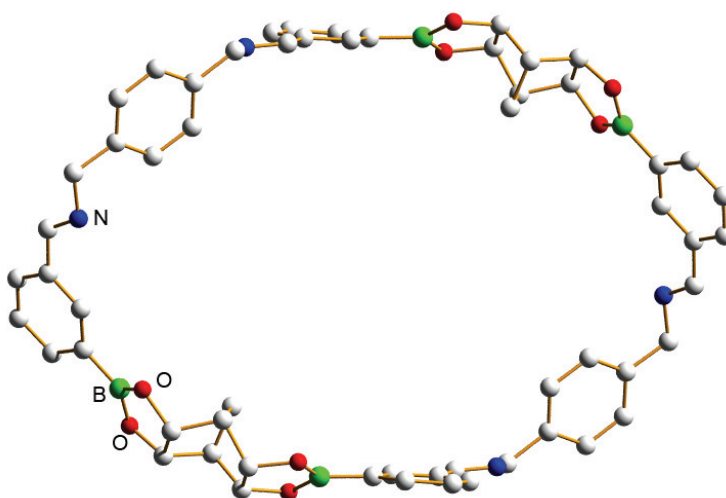
Figure 6.3: Structure of macrocycle **36** in the crystal. Hydrogen atoms and solvent molecules have been omitted for clarity.
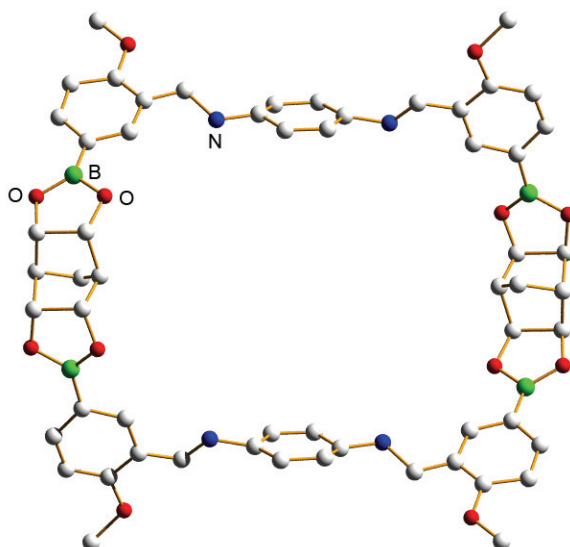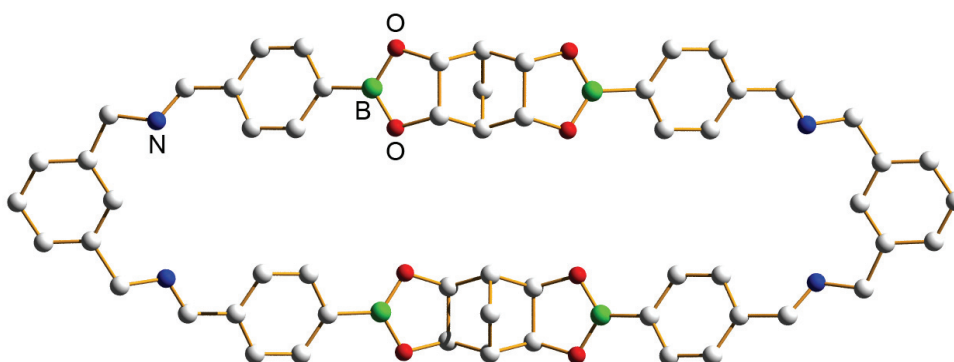


Figure 6.4: Structure of macrocycle **37** in the crystal. Hydrogen atoms and solvent molecules have been omitted for clarity.

Contrary to compounds **33-35**, which were synthesized from 1,4-benzenediamine, macrocycle **37** is thermodynamically unstable. The ^{1}H NMR analysis of a CDCl$_3$ solution of pure **37** left at room temperature for twelve hours revealed the formation of a new macrocycle, as shown by the appearance of a new set of signals in the spectrum. Investigations are currently in progress to identify this new species and to study the equilibrium with its precursor. Very preliminary results seem to indicate that the new observed macrocycle is a [6+3+3] condensation product and that several hours are required to reach the equilibrium. In the near future, the thermodynamic behavior of **36** will also be investigated.

As the parallel utilization of boronate ester formation and imine condensation proved to be a successful methodology for the preparation large organic macrocycles, we subsequently investigated its potential for the generation of cage-like structures. Toward this goal, the diamine fragment was replaced by tris(2-aminoethyl)amine (tren), which was reacted with pentaerythritol and 3-formylphenyl boronic acid. Unfortunately the reaction resulted in a product of very low solubility, which prevented further characterization. When 4-formylphenyl boronic acid was used, however, a product (**38**) that displayed higher solubility in chloroform was isolated (Scheme 6.5).
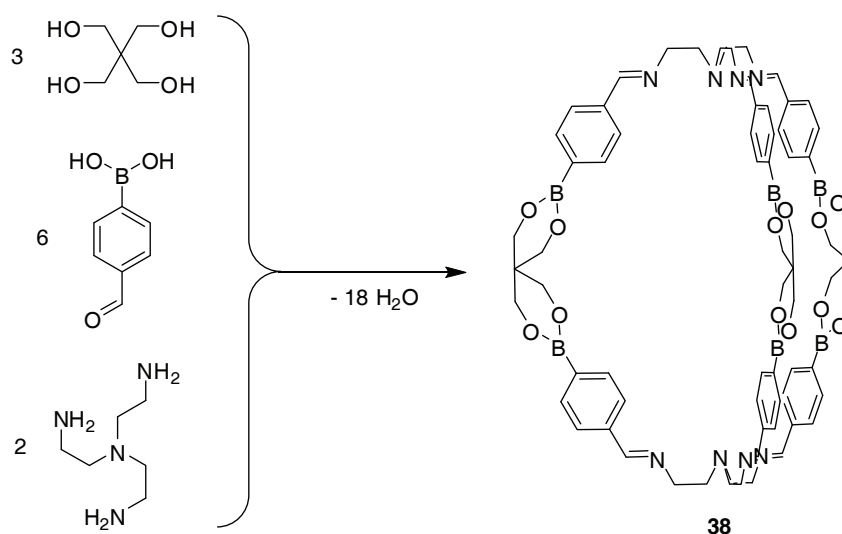
Scheme 6.5: Formation of cage **38** in a [6+3+2] condensation reaction.

According to ^{1}H NMR analyses, the condensation reactions were complete and compound **38** is highly symmetrical. Confirmation of the desired cage structure came from ESI mass spectrometry and single crystal X-ray crystallography. The quality of the results of the latter was very low, but the connectivity and the overall geometry were clearly established (Figure 6.5). The macrobicycle **38** was formed by condensation of

six boronic acid molecules, three pentaerythritol molecules, and two triamine molecules ([6+3+2] condensation), and isolated in a remarkable high 82% yield, given that the formation of 18 covalent bonds is required for its assembly. The cage, which can be classified as a cryptand,[78] has the form of an ellipsoid with a length of 20.5 Å (maximum N···N distance). The three boronate ester chains wrap around each other in a slightly helical fashion. Related tren-based cryptands have been prepared by [3+2] condensation reaction with simple dialdehydes (§ 1.3.2),[74,261,262,263,264,265] but the reported structures are significantly smaller than **38** (d(N···N) ≈ 10 Å).[263] Similar to other tren-based cryptands, cage **38** can act as a dinucleating ligand for copper(I). When two equivalents of [Cu(CH$_3$CN)$_4$(PF$_6$)] in acetonitrile were added to a chloroform solution of **38**, the quantitative formation of cryptate [Cu$_2$(**38**)(PF$_6$)$_2$] was observed, as evidenced by ^{1}H NMR spectroscopy and ESI mass spectrometry. Most likely, the Cu$^+$ ions are bound to the N atoms of the cage, as it was observed for smaller tren-based cryptands.[264,266,267]
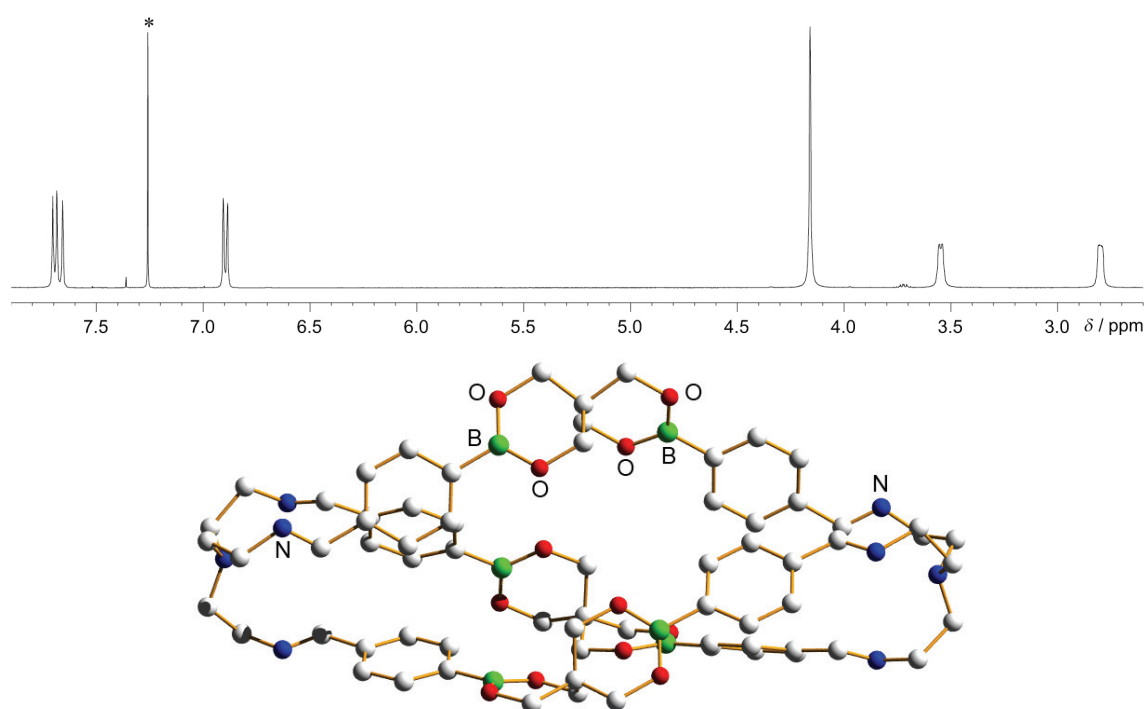
Figure 6.5: Part of the ^{1}H NMR (CDCl$_3$) spectrum of cage **38** (top) and its structure in the crystal (bottom). Hydrogen atoms and solvent molecules have been omitted for clarity.

As already mentioned, the isolation and characterization of a cage using 3-formylphenyl boronic acid (or a derivative) was not successful. Other building blocks variations were also introduced, in order to test the scope of the reaction. The

replacement of pentaerythritol by *all-exo*-bicyclo[2.2.1]heptane-2,3,5,6-tetraol resulted in the formation of insoluble material. It was possible, however, to use 1,3,5-trisaminomethyl-2,4,6-triethylbenzene[268] as a triamine in the [6+3+2] condensation reaction. Cage **39** was obtained in good yield (53%), using the procedure established for the preparation of **38**. The product was comprehensively characterized by NMR spectroscopy, elemental analysis, ESI mass spectrometry, and X-ray crystallography. All data are in agreement with a cage structure similar to that of **38**. The solid state structure of **39** is shown in Figure 6.6.

Figure 6.6: Structure of cage **39** in the crystal. Hydrogen atoms and solvent molecules have been omitted for clarity.

Cage **39** contains two 1,3,5-trisaminomethyl-2,4,6-triethylbenzene fragments connected by three boronate ester linkers. The distance between the two aromatic rings is about 18.7 Å, which is similar to what was found for the N···N distance of cage **38**. Due to a larger C(spiro)···C(spiro) distance (13.3 Å vs. 8.3 Å), the internal volume of cage **39** is higher than that of **38**. Other structural parameters such as the average B-O bond length (1.365 Å), the B···C(spiro)···B angle (136.9°), and the torsion angles between BO_2 planes (56.7°) are similar to what was observed for others pentaerythritol-based macrocycles.[136]

6.2.2 Metal-Based Macrocycles

In addition to the synthesis of fully organic macrocycles, transition metal-based assemblies were prepared. In a first experiment, pentaerythritol was reacted with 4-pyridine boronic acid and [ReBr(CO)$_5$] (Scheme 6.6). The last building block was chosen because it is known to be a versatile starting material for the formation of [ReBr(CO)$_3$(N-donor ligand)$_2$] complexes.[269] Again, the reaction was performed in a THF/toluene 1:2 mixture, in order to help solubilize the pentaerythritol and to favor the formation of the ReBr(CO)$_3$(N-donor ligand)$_2$] complex.[270] After elimination of most of the solvent, a yellow solid (**40**) precipitated from the reaction mixture. Pure compound **40** was isolated in high yield (80%) and analyzed by NMR spectroscopy, which revealed the formation of a highly symmetric complex, with the presence on the spectrum of only one set of signals for all building blocks. As for the organic macrocyclic and macrobicyclic compounds **33**, **38**, and **39**, a singlet was observed for the methylene protons of the boronate ester, indicating that **40** possess a certain conformational flexibility. The infrared spectrum of **40** was characteristic of a Re(CO)$_3$ complex with strong bands in the carbonyl region at υ_{CO} = 2021, 1918, and 1885 cm^{-1}. The analysis of the metal complex by mass spectrometry was not successful, but fortunately, X-ray quality single crystals could be grown from a 1,2-dichloroethane/pentane solution of **40**, allowing to establish the macrocyclic nature of the assembly (Figure 6.7).

Scheme 6.6: Formation of macrocycle **40** in a [4+2+2] condensation reaction.
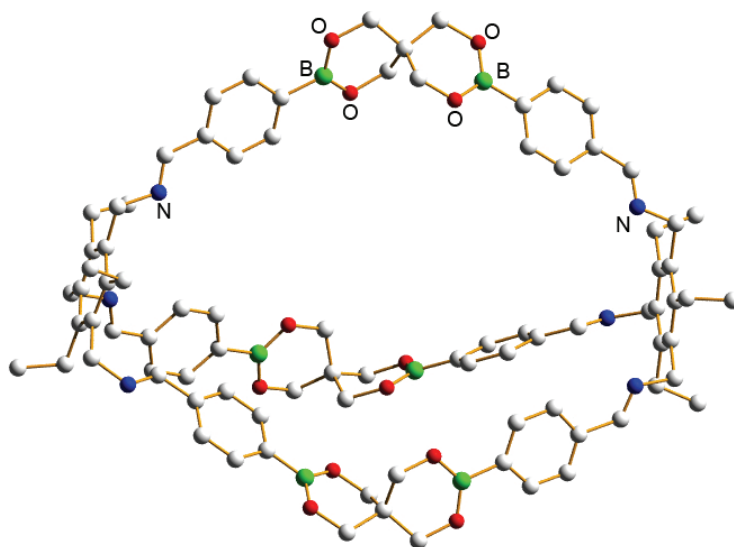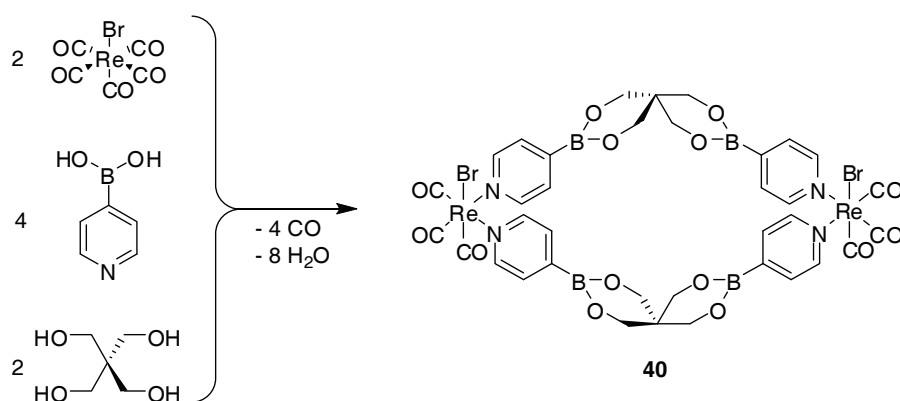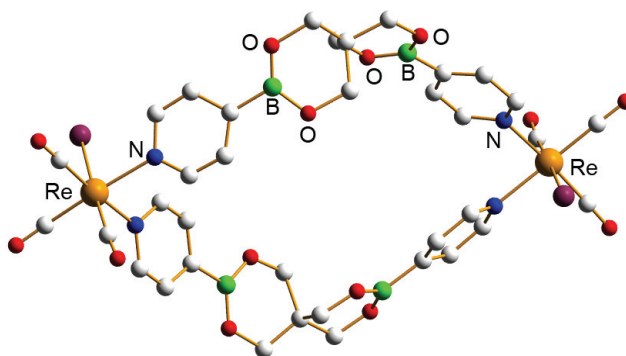
Figure 6.7: Structure of macrocycle **40** in the crystal. Hydrogen atoms and solvent molecules have been omitted for clarity.

Macrocycle **40** contains two {ReBr(CO)$_3$} fragments bridged by two organic ligands, each of which is the condensation product of two 4-pyridine boronic acid molecules with one pentaerythritol molecule. The bromide and the carbonyl *trans* to the bromide are statistically disordered in a ratio of 75:25. Macrocycle **40** has a ring size of 32 atoms and a diameter of 15.1 Å (Re···Re distance). With an average bond length of 1.355 Å, the B-O bonds of **40** are within the expected range for macrocycles containing sp^2 hybridized boron centers.[136] Similar to dimeric macrocycle **33**, the BO$_2$ planes are significantly twisted (torsion angles 55.1° and 61.1°). The "bite angles" for the organic ligand (B···C(spiro)···B angle) are 131.7° and 132.3°. The Re-N bonds (Re-N$_{av}$ 2.204 Å) are also of comparable length than what was reported for molecular squares[271] and rectangles[272] having ReX(CO)$_3$ (X = Cl, Br) as corners. It is interesting to point out that most of the reported supramolecular structures obtained by condensation of [ReBr(CO)$_5$] with ditopic N-donor ligands are molecular squares.[269] In the case of macrocycle **40**, the organic ligand, and in particular the pentaerythritol fragment is too bend and too flexible to form bigger macrocycles than dimers.

Attempts to prepare macrocycles having more rigid organic ligand, by replacement of pentaerythritol by *all-exo*-bicyclo[2.2.1]heptane-2,3,5,6-tetraol, were unfortunately unsuccessful. Reaction of 3-pyridine boronic acid with pentaerythritol and [ReBr(CO)$_5$], however, is possible. Following the procedure established for macrocycle **40**, compound **41** was obtained in good yield (71 %), and then comprehensively characterized. All NMR data were in agreement with a macrocyclic structure. The ^{1}H NMR spectrum displays three signals (one singlet and two doublets) for the methylene protons of the boronate ester. This observation indicates that the CH$_2$ protons are not equivalent, presumably because macrocycle **41** possesses a certain ring strain. A single crystal X-ray analysis was performed and in the solid state, compound **41** was found to be a [4+2+2] condensation product (Figure 6.8). Macrocycle **41** is smaller than

40 (Re···Re distance 13.6 Å vs. 15.1 Å), but other structural parameters such as the average B-O (1.363 Å) and Re-N (2.226 Å) bond lengths, are similar to those of **40**. The B···C(spiro)···B angle (137.0°) and the torsion angle of the BO_2 planes (57.3°) are also within the expected range.[136] The bromide and the carbonyl *trans* to the bromide are statistically disordered in a ratio of 87:13.
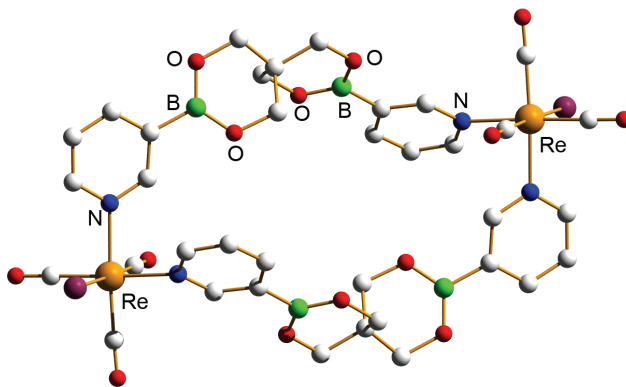
Figure 6.8: Structure of macrocycle **41** in the crystal. Hydrogen atoms and solvent molecules have been omitted for clarity.

Macrocycles **40** and **41** show that boronate ester formation and metal-ligand interaction can be used in parallel for the one-pot synthesis of large assemblies. To test the scope of the synthetic approach, we investigated whether it is possible to combine these two types of reversible interactions, with a third one, namely imine condensation.
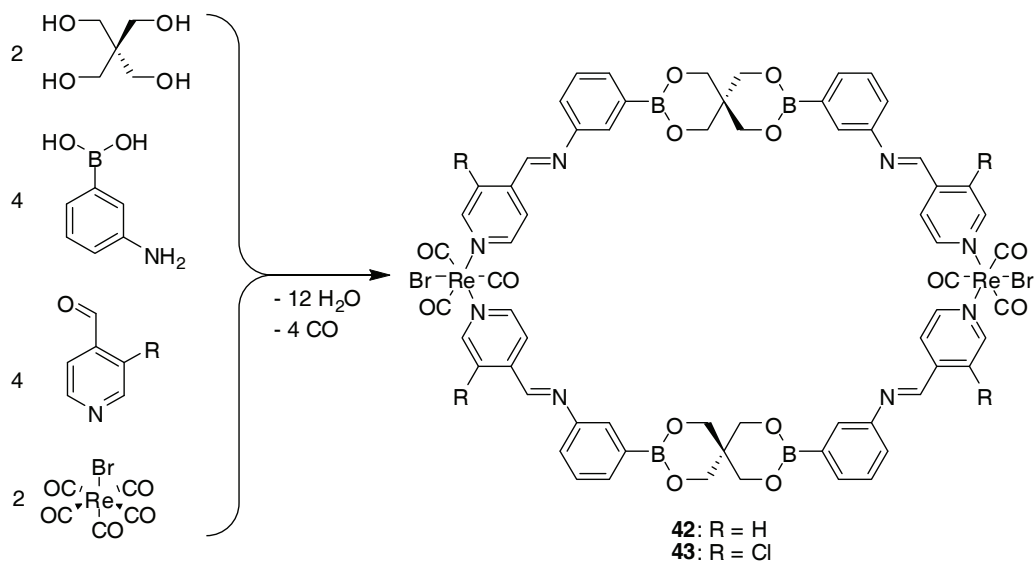
Scheme 6.7: Formation of macrocycles **42** and **43** in [4+4+2+2] condensation reactions.

[ReBr(CO)$_5$] was thus reacted with 4-formylpyridine, 3-aminophenyl boronic acid, and pentaerythritol (Scheme 6.7). Refluxing a THF/toluene solution of the building blocks resulted in the formation of a yellow solid (**42**). The analytical data (IR, ^{1}H, ^{13}C and ^{11}B NMR spectroscopy) of this complex were in agreement with the desired macrocyclic structure. Unfortunately, attempts to obtain additional structural information by mass spectrometry or crystallography were unsuccessful. The same reaction was therefore repeated with 3-chloro-4-formylpyridine instead of 4-formylpyridine, and compound **43** was obtained in 58% yield. Fortunately, the introduction of the chloro substituents allowed to obtain single crystals of sufficient quality to perform a crystallographic analysis. The result confirmed that a metallamacrocyclic structure had formed (Figure 6.8).
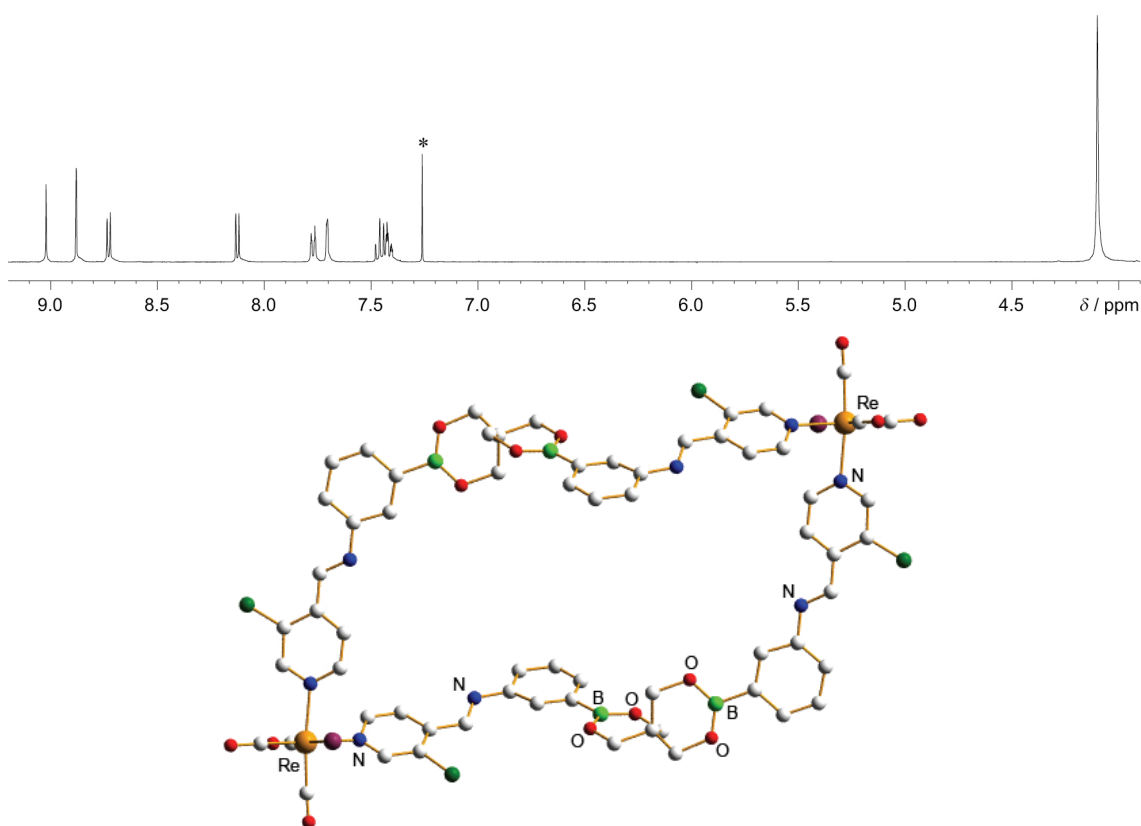
Figure 6.8: Part of the ^{1}H NMR (CDCl$_3$) spectrum of macrocycle **43** (top) and its structure in the crystal (bottom). The asymmetric unit contains two independent macrocycles, only one of which is shown. Hydrogen atoms and solvent molecules have been omitted for clarity.

Two independent but structurally very similar complexes are present in the crystal (half of each complex in the asymmetric unit). The molecules have a C_2 symmetry, and display bond lengths (B-O$_{av}$ 1.366 Å and Re-N$_{av}$ 2.247 Å) and angles (B···C(spiro)···B

angle 138.7° and torsion angle 64.0°) comparable to those of **40** and **41**. The bromide and the carbonyl *trans* to the bromide are statistically disordered in a ratio of 7:3. The two [ReBr(CO)$_3$] fragments are connected by two bridging ligands, each of which is the condensation product of two boronic acid molecules, two 3-chloro-4-formylpyridine molecules, and one pentaerythritol molecules. The one-pot synthesis of complex **43** thus requires the formation of 12 covalent and 4 metal-ligand bonds. With a ring size of 52 atoms and a diameter of approximately 24 Å (Re⋯Re distance), **43** is by far the largest boron-based macrocycle described to date.

As for the previous syntheses, the flexibility of the four-component assembly was tested. An inversion of the connectivity of the imine bond was first tested. In this synthesis, pentaerythritol and [ReBr(CO)$_5$] were condensed with 3-formylphenyl boronic acid and 4-aminopyridine, following a standard procedure. NMR investigations on the reaction mixture showed that the boronic acid condensed with the tetraol, and the N-donor ligand with the rhenium complex. However, peaks corresponding to the amine and formyl functional groups were found in the spectrum, indicating that imine bond was problematic. The absence of imine condensation is probably due to the nature of the amine fragment, which, once coordinated to a metal, is too electron deficient to be involved in condensation reactions. To resolve this problem, a methylene spacer was introduced between the pyridine ring and the amine functional group. In other words, 4-(aminomethyl)pyridine was used instead of 4-aminopyridine, together with pentaerythritol, 3-formylphenyl boronic acid, and [ReBr(CO)$_5$] (Scheme 6.8).
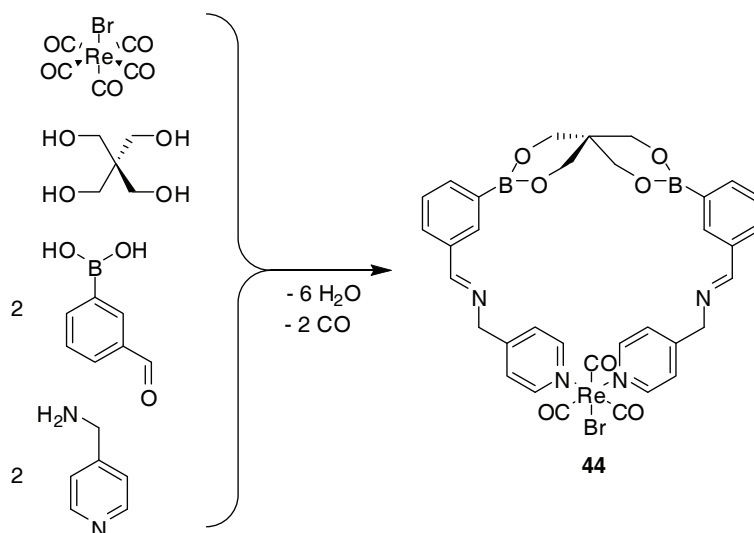
Scheme 6.8: Formation of complex **44** in a [2+2+1+1] condensation reaction.

The reaction was performed under standard conditions and a white solid (**44**) was isolated in good yield (67%). NMR and IR analyses again indicated the formation of a very symmetric, macrocyclic complex. The nature of the assembly was unambiguously revealed by an X-ray crystallographic analysis. The result confirmed the formation of a metal containing cyclic structure, but here the organic ligand is flexible enough to wrap around a single metal center (Figure 6.9).
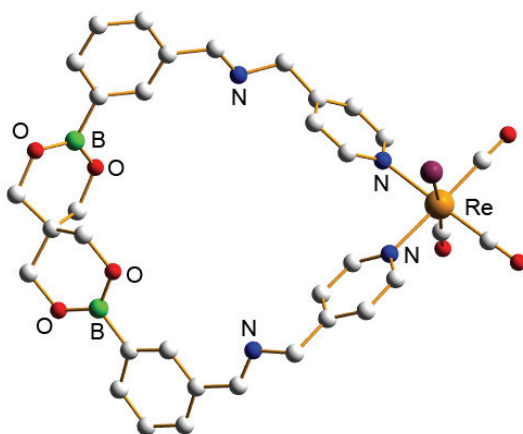
Figure 6.9: Structure of complex **44** in the crystal. Hydrogen atoms and solvent molecules have been omitted for clarity.

Macrocycle **44** has a ring size of 28 atoms and a diameter (c(spiro)···Re distance) of 11.8 Å. Its bond lengths (B-O_{av} 1.365 Å and Re-N_{av} 2.224 Å) and angles (B···C(spiro)···B angle 134.9° and torsion angle 55.2°) are similar to what was observed for other macrocycles described in this chapter. This observation indicates the absence of significant ring strain in **44**. In order to prepare larger macrocycles, 4-formylphenyl boronic acid was used instead of 3-formylphenyl boronic acid, but after a standard reaction, it was not possible to isolate a single product out of the reaction mixture. Indeed, the presence of large aldehydes peaks in the ^{1}H NMR spectrum indicated that the reaction mixture contained mostly incomplete condensation products.

Other metal complexes were also tested in three-or four-component reactions similar to those performed with [ReBr(CO)$_5$]. For instance, the molybdenum complexes [Mo(CO)$_6$] and [(1,3,5-C$_6$H$_3$(CH$_3$)$_3$)Mo(CO)$_3$], which are known to be versatile starting material for the formation of [Mo(CO)$_3$(N-donor ligand)$_3$] complexes,[273,274] were used in attempts to prepare analogues of compounds **40**-**43**. Unfortunately, condensation reactions with either 4-pyridine boronic acid and pentaerythritol, or 4-formylpyridine, 3-aminophenyl boronic acid, and pentaerythritol only resulted in the formation of insoluble complexes.

Half-sandwich complexes of ruthenium and rhodium, such as [(p-Pr^{i}C$_6$H$_4$Me)RuCl$_2$]$_2$ and [(C$_5$Me$_5$)RhCl$_2$]$_2$ were reacted with 4-formylpyridine, 3-aminophenyl boronic acid, and pentaerythritol (Scheme 6.9).
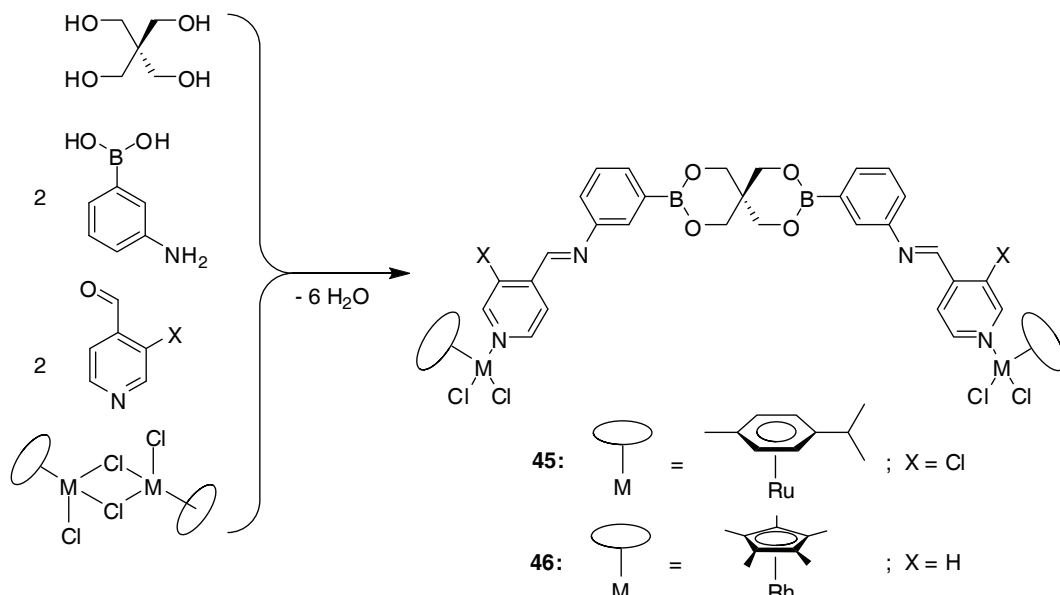
Scheme 6.9: Preparation of complexes **45** and **46**.

The NMR spectra of the resulting complexes (**45** and **46**) showed that the three expected condensation reactions had occurred, as signals corresponding to the four building blocks were found. Unfortunately, no mass spectrometry or X-ray crystallographic data could be collected, so the structures of compounds **45** and **46** remain hypothetical. Nevertheless, it can be reasonably assumed that both complexes possess the rod-like structures shown in Scheme 6.9. Subsequently, the preparation of macrocyclic structures from **45** and **46** was investigated. To do so, the complexes were reacted with Ag(O$_3$SCF$_3$) in dichloromethane, in order to abstract a chlorine ligand from the metal center and to create chloro-bridged, tetranuclear complexes. Unfortunately, these reactions did not allow for the isolation of the desired compounds. Instead, a complex mixture of degradation products was obtained. Apparently, the organic ligand didn't resist the addition of the silver salt.

6.3 Conclusions

In summary, the multicomponent synthesis of macrocyclic and cage-like molecules has been described. The targeted structures were assembled by using simultaneously two or more reversible and largely independent interactions. First, boronate ester formation and imine condensation were used in parallel. Organic macrocycles were prepared via one-pot condensations of a tetraol with a formyl-functionalized boronic acid and a diamine. When a trisamine was used instead of the diamine, large cryptand-type cages were obtained.

Subsequently, boronate ester formation was coupled with metal-ligand interaction to build small dimeric rhenium-based macrocycles. Finally, the three types of interaction were used in parallel, resulting in the formation of nanometer-sized structures, such as a 2.4 nm large macrocycle.

A major advantage of the multicomponent synthesis is its great flexibility. In theory, all building blocks involved in the reaction can be modified, and a large variety of assemblies can be obtained. In practice, some limitations appeared, such as solubility of the products, orthogonality of the reactions, and reactivity of the building blocks. Another drawback of the methodology is the difficulty to predict the shape and the geometry of the final assembly. This is a direct consequence of the utilization of many building blocks, that all have a certain degree of freedom and flexibility. It is likely, however, that many interesting structures can be prepared using this strategy. Because the condensation reactions are reversible, multicomponent synthesis can also be of interest in the context of dynamic combinatorial chemistry.[6,7]

Chapter 7

General Conclusions

This thesis describes the synthesis and characterization of boronic acid-based supramolecular structures. The reported structures were assembled using four reversible reactions involving either the boron center (Scheme 7.1 a and b) or the aryl substituent (c and d) of a boronic acid fragment. In particular, the possibility to use simultaneously two or more of these reactions was investigated. This strategy allowed for the one-pot synthesis of large and complex structures from very simple building blocks, in a multicomponent assembly process.
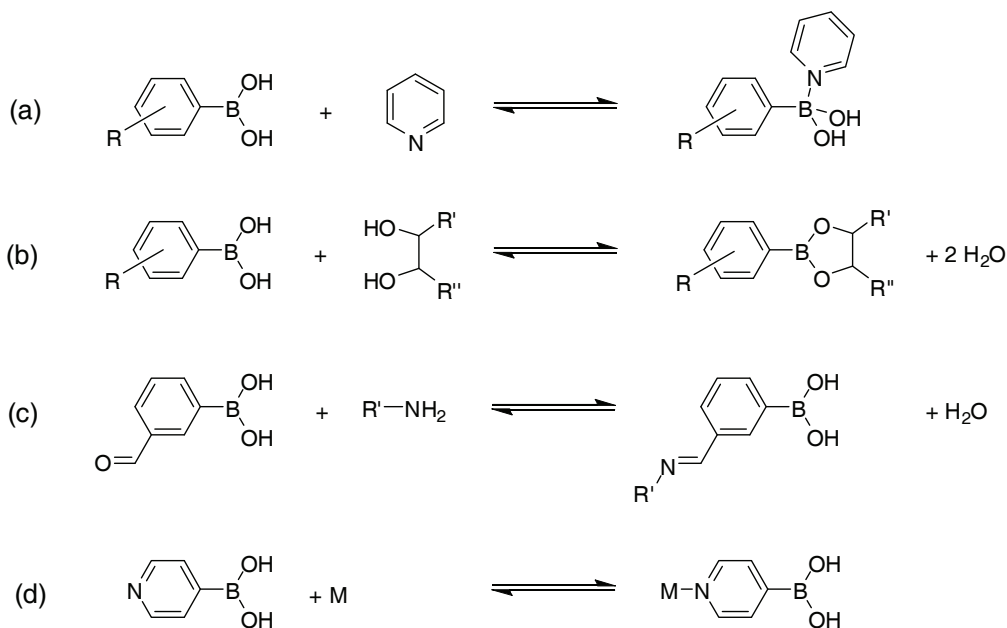
Scheme 7.1: Reversible interactions involving boronic acids for the construction of the supramolecular assemblies: addition of a N-donor ligand (a), boronate ester formation (b), imine condensation (c), and metal-ligand interaction (d).

Initially, simple, non-functionalized aryl- and alky-boronic were condensed with dihydroxypyridine ligands. These ligands were chosen because they are known to form trimeric macrocycles with $[(arene)RuCl_2]_2$ and $[(Cp^*)MCl_2]_2$ complexes (M = Ir, Rh).[167,172] With boronic acids, however, complexes having different geometries were obtained. The condensation reactions of 2,3-dihydroxypyridine with boronic acids exclusively produced tetrameric assemblies,[275] whereas pentameric macrocycles were obtained with 3,4-dihydroxypyridine.[276] These results confirm that, similar to transition metals, boronic acids can be condensed with organic ligands to construct supramolecular assemblies.

Macrocycles were assembled using two types of reversible reactions: boronate ester formation and addition of N-donor ligands to boronate esters. When a third type of reversible interaction, namely imine condensation, was added, dendritic structures having tetrameric or pentameric macrocycles as scaffolds were obtained.[276] The synthetic strategy is straightforward, as the three building blocks (a dihydroxypyridine ligand, an amino- or formyl-functionalized boronic acid and an aldehyde/amine) are simply mixed together. This methodology allows for the fast and efficient preparation of dendritic structures. Similarly, boroxine-based dendritic structures were prepared from the condensation reaction of a formyl-functionalized boronic acid with a primary amine and a dipyridyl linker.

Boronate ester formation and addition of N-donor ligands to boronate esters were further used to assemble polymeric chains from aryl boronic acids, 1,2,4,5-tetrahydroxybenzene and either 4,4'-dipyridyl or 1,2-bis(4-pyridyl)ethylene.[277] Crystallographic analyses showed that the bis(dioxaborole) units are connected by dipyridyl linkers throught dative B-N interactions, and that the polymer strands have a zig-zag geometry. An interesting property of the polymers is their strong color, which is due to an efficient intrastrand charge-transfer excitation from the electron-rich tetraoxobenzene to the electron deficient dipyridyl linker, as evidenced by a computational study.

The latter property was used as a basis for the synthesis of rotaxanes by the four-component self-assembly reaction of 3,5-bis(trifluoromethyl)phenyl boronic acid, catechol, 1,2-bis(4-pyridyl)ethylene, and either 1,5-dinaphtho-38-crown-10 or bis-*p*-phenylene-34-crown-10.[278] In these rotaxanes, two boronate esters are connected by a dipyridyl linker, via B-N bonds. Due to coordination, the linker becomes electron deficient and thus possesses an increased affinity for electron-rich crown ethers. The boronate esters also act as stoppers and their interaction with the dipyridyl linker is reversible, allowing the crown-ether to slip on the axle.

In the last part of this work, we investigated whether boronate ester formation can be use simultaneously with imine condensations or metal-ligand interactions to construct large macrocyclic structures.[279] This strategy allowed for the assembly of organic mono- and bicyclic complexes from a tetraol, a formyl-functionalized boronic acid, and a di- or tri-amine. The cage-liked complexes, in particular, were formed in high yield and showed promising host-guest chemistry. Following a similar procedure, rhenium-based macrocycles were formed using pyridine boronic acids. Finally, a combination of the two approaches allowed obtaining assemblies from four chemically distinct building blocks. For instance, a large dinuclear complex was prepared from [ReBr(CO)$_5$], 4-formylpyridine, 3-aminophenyl boronic acid, and pentaerythritol. To create this

structure, twelve fragments were simultaneously assembled via the formation of twelve covalent as well as four coordination bonds.

Overall, the results described in this work showed that boronic acids can be very attractive building blocks for the construction of supramolecular assemblies. As during the last years an increasing number of supramolecular structures incorporating boronic acids have been reported,[15,280] one can reasonably assume that the field will continue to attract interest in the next years, and that several new and interesting boron-based structures will be reported.

Evidence was also given that multicomponent reactions can be used for the construction of large assemblies from very simple building blocks. The key point of the strategy is the parallel utilization of reversible and largely independent reactions. In this regard, the use of boronic acids appears to be ideally suited, as they can be involved in many different condensation reactions.

Because it uses several very simple building blocks that can be easily varied, the multicomponent approach should allow for the construction of structurally very diverse assemblies. This latter point is potentially very interesting for the preparation of "tailor made" structures, for host-guest applications for instance. The modular nature and the fact that the reactions are reversible can also be of interest in the context of dynamic combinatorial chemistry.

Chapter 8

Experimental Part

8.1 General and Instrumentation

General: All reactions were carried out under an atmosphere of dry dinitrogen using standard Schlenk techniques unless specified otherwise. Most of the synthesized compounds are not very air and water sensitive and can be handled in air for a few hours without significant decomposition. Solvents (anytical grade purity) were degassed and stored under a dinitrogen atmosphere and were used without further purification. Benzene, chloroform, dichloromethane, diethyl ether, hexane, and tetrahydrofuran were dried and degassed by chromatography (Innovative Technology purification system) if not specified otherwise.

NMR Spectroscopy: The ^{1}H, ^{11}B, and ^{13}C NMR spectra were recorded on a Bruker Advance DPX 400 MHz spectrometer using the residual protonated solvents[281] (^{1}H, ^{13}C) as internal standards or $BF_3 \bullet OEt_2$ (^{11}B) as an external standard. ^{19}F NMR spectra were recorded on a Bruker Advance 200 spectrometer using $CFCl_3$ as an external standard. The solid-state ^{11}B NMR spectra were recorded on a Bruker DRX 400 spectrometer with a 7.0 widebore magnet by utilizing a 3-mm CPMAS probehead. A solution of boric acid in H_2O was used as an external standard ($\delta = 19.3$ ppm). All spectra were recorded at room temperature.

Elemental Analysis: Elemental analyses were performed on a EA 1100 CHN Instrument. It should be mentioned that the elemental analyses of boronic acid derivatives may be complicated by the formation of incombustible boron carbide residues during analyses, which may lead to strong deviations for the carbon value.[123]

Mass Spectrometry: MS spectra were measured on a Q-Tof Ultima Micromass mass spectrometer equipped with a Z-spray type ESI source and on a Axima-CFR+, MALDI-TOF spectrometer.

IR Spectroscopy: IR spectra were recorded on a Perkin Elmer Spectrum One Golden Gate FT/IR spectrometer.

X-Ray Crystallography: Diffraction data were collected at different temperatures using $Mo_{K\alpha}$ radiation on a 4-circle kappa gognometer equipped with an Oxford Diffraction KM4 Sapphire CCD detector, a marresearch mar345 IPDS detector, or a Bruker APEX II CCD detector. Cell refinement and data reduction was performed with CrysAlisRED

1.7.1. All structures were refined using the full-matrix least-squares on F^2 with all non-H atoms anisotropically defined. The hydrogen atoms were placed in calculated positions using the "riding model". Structure refinement and geometrical calculations were carried out with SHELXL-97.[282,283] All graphic representations were generated with Diamond 3.1e from the corresponding cif files. Details of the crystals, data collection, and structure refinement are listed in Tables 9.1-9.13.

Chemicals: The starting compounds 2,3-dihydroxy-4-morpholino-methyl-pyridine,[284] 3,4-dihydroxypyridine,[185,186] 3,4-dihydroxy-2-methyl-pyridine,[186] 3,5-(benzyloxy)benzylamine,[198] 1,2,4,5-tetrahydroxybenzene,[285] 1,5-dinaphto-38-crown-10,[286] bis-*p*-phenylene-34-crown-10,[232] *all-exo*-bicyclo[2.2.1]heptane-2,3,5,6-tetraol,[260] [Cu(CH$_3$CN)$_4$(PF$_6$)],[287] trisaminomethyl-2,4,6-triethylbenzene,[268] [ReBr(CO)$_5$],[288] [(*p*-Pr^{i}C$_6$H$_4$Me)RuCl$_2$]$_2$,[289] and [(C$_5$Me$_5$)RhCl$_2$]$_2$[290] were synthesized according to literature procedures.

2,3,6-frifluorophenyl boronic acid, 2,3-dihydroxypyridine, cyclohexylamine, benzaldehyde, benzylamine, 3,5-bis(trifluoromethyl)phenyl boronic acid, 1,2-bis(4-pyridyl)ethylene, 4,4'-dipyridyl, catechol, pentaerythritol, 4-formylpyridine, and 4-aminopyridine were purchased from Fluka. Phenyl boronic acid, 4-*tert*-butylphenyl boronic acid, methyl boronic acid, 3-formyl-4-methoxyphenyl boronic acid, and 3-pyridine boronic acid were purchased from Alfa Aesar. 2-Hydroxynicotinic acid, 4-methylphenyl boronic acid, and 3-fluorophenyl boronic acid were purchased from Lancaster. *n*-Butyl boronic acid, 3-formylphenyl boronic acid, aniline, 3-aminophenyl boronic acid monohydrate, 4-bromoaniline, 4-ethylphenyl boronic acid, 3,5-dimethylphenyl boronic acid, and 4-formylphenyl boronic acid were purchased from Acros. 4-Imidazolecarboxylic acid, 2,3-dihydroxyquinoline, 3,5-diformylphenyl boronic acid, pentafluorophenyl boronic acid, 4,5-dichlorocatechol, 1,4-diaminobenzene, *m*-xylylenediamine, tris(2-aminoethyl)amine, 4-pyridine boronic acid, 3-chloro-4-formyl-pyridine, and 4-(aminomethyl)pyridine were purchased from Aldrich. *p*-Xylylenediamine was purchased from Merck

8.2 Synthesis

General procedure for the synthesis of compounds 1-3: A suspension of the respective aryl boronic acid (0.7 – 1.8 mmol) and 2,3-dihydroxypyridine (0.7 – 1.8 mmol) in freshly distilled benzene (40 – 60 mL) was heated under reflux using a Dean-Stark trap. After 2 – 15 h, the mixture was filtered hot and the filtrate was allowed to cool to ambient temperature. Reduction of the volume and/or addition of pentane cause the precipitation of a white powder, which was isolated, washed with pentane and dried under vacuum. **1** precipitated directly from the reaction mixture and was purified analogously to the other complexes. Crystals were obtained by slow diffusion of pentane into a solution of the respective complex in CH_2Cl_2 (**1**) or benzene (**2**, **3**).

[(C₆H₅)B(C₅H₃NO₂)]₄ (1):
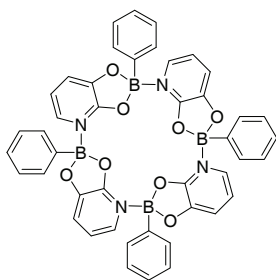
Yield: 51%. ^{1}H NMR (400 MHz, CDCl₃): δ = 6.61 (t, [3]J = 7 Hz, 4 H, pyridine), 6.67 (d, [3]J = 6 Hz, 4 H, pyridine), 6.99 (d, [3]J = 7 Hz, 4 H, pyridine), 7.05 – 7.35 (m, 20 H, phenyl); ^{13}C NMR (400 MHz, CDCl₃): δ = 114.17, 115.78, 127.69, 128.09, 128.12, 132.04, 151.26, 163.83; ^{11}B NMR (400 MHz, CDCl₃): δ = 11.5; Elemental anal. (%) calc. for $C_{44}H_{32}B_4N_4O_8$: C 67.07, H 4.09, N 7.11. Found: C 67.32, H 4.18, N 6.86.

[(C₆H₅)B(C₅H₃NO₂CH₂(C₄H₈NO)]₄ (2):
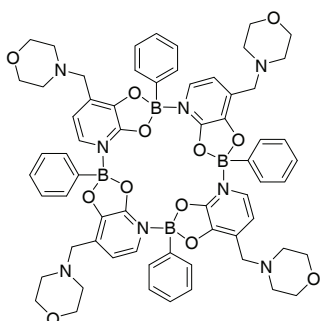
Yield: 84%. ^{1}H NMR (400 MHz, CDCl₃): δ 2.36-2.55 (m, 16H, morpholine N(CH₂)₂), 3.42 (d, [3]J = 15 Hz, 4 H, NCH₂),), 3.60 (d, [3]J = 15 Hz, 4 H, NCH₂), 3.63-3.75 (m, 16H, morpholine O(CH₂)₂), 6.68 (d, [3]J = 6 Hz, 4 H, pyridine), 6.84 (d, [3]J = 6 Hz, 4 H, pyridine), 7.08-7.36 (m, 16H, phenyl). ^{13}C NMR (101 MHz, CDCl₃): δ 53.79, 55.32, 67.12, 114.86, 127.66, 127.87, 128.03, 131.85, 149.13, 162.87. ^{11}B NMR (128 MHz, CDCl₃): δ 13.1. Elemental anal. calcd (%) for $C_{64}H_{68}B_4N_8O_{12}$: C 64.90 H 5.79 N 9.46. Found: C: 60.58 H 6.13 N 7.83.

[(2,3,6-C$_6$H$_2$F$_3$)B(C$_5$H$_3$NO$_2$)]$_4$ (3):
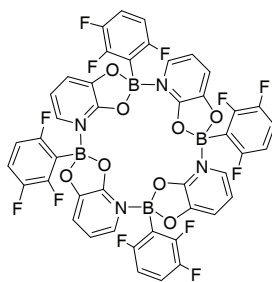
Yield: 84%. ^{1}H NMR (400 MHz, CDCl$_3$): δ 6.55 (b, 4 H, pyridine), 6.62 – 6.82 (m, 4 H, pyridine), 6.87 (d, ^3J = 6 Hz, 4 H, pyridine), 6.98-7.19 (m, 8 H, phenyl). ^{13}C NMR: no data. ^{11}B NMR (128 MHz, CDCl$_3$): δ 10.6. Elemental anal. calcd (%) for C$_{44}$H$_{20}$B$_4$F$_{12}$N$_4$O$_8$: C 52.64 H 2.01 N 5.58. Found: C: 50.26 H 2.39 N 5.18.

General procedure for the synthesis of compounds 4-9: A suspension of the respective aryl or alkyl boronic acid (0.5 – 1.0 mmol) and 3,4-dihydroxypyridine (0.5 – 1.0 mmol) in freshly distilled benzene (**4** – **8**) or chloroform (**9**) (50 – 60 mL) was heated under reflux using a Dean-Stark trap. After 4 – 7 h, the mixture was filtered hot and the filtrate was allowed to cool to ambient temperature. Reduction of the volume and/or addition of pentane cause the precipitation of a white powder, which was isolated, washed with pentane and dried under vacuum. **5** precipitated directly from the reaction mixture and was purified analogously to the other complexes. Crystals were obtained by slow diffusion of pentane into a solution of the respective complex in chloroform (**4**) or benzene (**6**, **7**).

[(*p*-Tol)B(C$_5$H$_3$NO$_2$)]$_5$ (4):
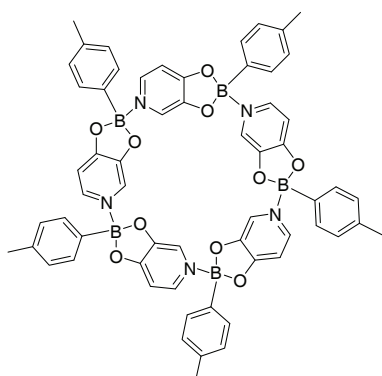
Yield: 66%. ^{1}H NMR (400 MHz, CDCl$_3$): δ 2.30 (s, 15H, CH$_3$), 6.82 (d, ^3J = 6 Hz, 5 H, pyridine), 7.07 – 7.16 (m, 10 H, phenyl), 7.26 (d, ^3J = 8 Hz, 10 H, phenyl), 7.99 (d, ^3J = 6 Hz, 5 H, pyridine), 8.04 (s, 5 H, pyridine). ^{1}H NMR (400 MHz, C$_6$D$_6$): δ 2.19 (s, 15H, CH$_3$), 6.19 (d, ^3J = 6 Hz, 5 H, pyridine), 7.10-7.26 (m, 10 H, phenyl), 7.58 (d, ^3J = 7 Hz, 10 H, phenyl), 7.71 (d, ^3J = 6 Hz, 5 H, pyridine), 8.11 (s, 5 H, pyridine). ^{13}C NMR (101 MHz, CDCl$_3$): δ 21.48, 106.61, 123.10, 128.73, 131.18, 137.43, 137.97, 152.11, 164.65. ^{11}B NMR (128 MHz, CDCl$_3$): δ 12.7 ($h_{1/2}$ = 700 Hz). Elemental anal. calcd (%) for C$_{60}$H$_{50}$B$_5$N$_5$O$_{10}$: C 68.30 H 4.78 N 6.64. Found: C: 66.98 H 5.01 N 6.38.

[(*p*-C$_6$H$_4$-*i*-Bu)B(C$_5$H$_3$NO$_2$)]$_5$ (5):
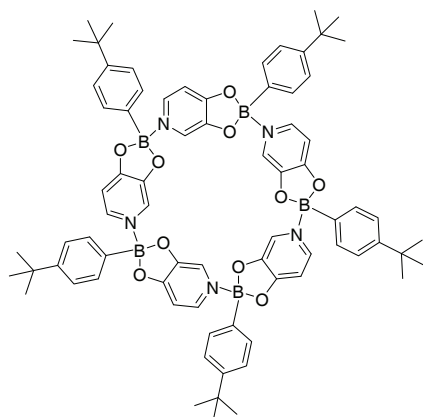
Yield: 86%. ^{1}H NMR (400 MHz, CDCl$_3$): δ 1.28 (s, 45H, C(CH$_3$)$_3$), 6.82 (d, ^3J = 6 Hz, 5 H, pyridine), 7.24 – 7.39 (m, 20 H, phenyl), 8.00 (d, ^3J = 6 Hz, 5 H, pyridine), 8.05 (s, 5 H, pyridine). ^{13}C NMR (101 MHz, CDCl$_3$): δ 31.45, 106.56, 123.18, 124.91, 128.50, 131.01, 137.48, 151.14, 152.11, 164.89. ^{11}B NMR (128 MHz, CDCl$_3$): δ 13.0 ($h_{1/2}$ = 780 Hz). Elemental anal. calcd (%) for C$_{75}$H$_{80}$B$_5$N$_5$O$_{10}$: C: 71.18 H 6.33 N 5.44. Found: C: 72.05 H 6.35 N 5.46.

[(*m*-C$_6$H$_4$F)B(C$_5$H$_3$NO$_2$)]$_5$ (6):
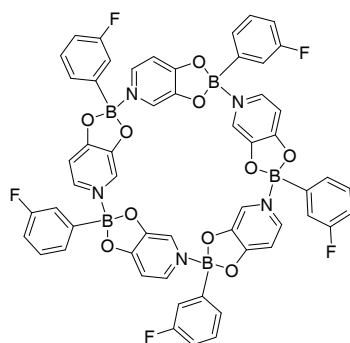
Yield: 31%. ^{1}H NMR (400 MHz, CDCl$_3$) : δ = 6.87 [d, ^3J = 6 Hz, 5 H, H^5 pyridone], 6.90-6.99 [m, 5 H, phenyl], 7.05-7.16 [m, 10 H, phenyl], 7.20-7.30 [m, 5 H, phenyl], 8.00 [d, ^3J = 6 Hz, 5 H, H^6 pyridone], 8.06 [s, 5 H, H^2 pyridone]; ^{1}H NMR (400 MHz, C$_6$D$_6$) : δ = 6.12 [d, ^3J = 6 Hz, 5 H, H^5 pyridone], 6.85-6.93 [m, 5 H, phenyl], 7.04-7.11 [m, 5 H, phenyl], 7.24-7.31 [m, 5 H, phenyl], 7.39-7.48 [m, 5 H, phenyl], 7.57 [d, ^3J = 6 Hz, 5 H, H^6 pyridone], 7.98 [s, 5 H, H^2 pyridone]; ^{13}C NMR (101 MHz, CDCl$_3$) : δ = 106.96, 115.17 [d, $^2J_{CF}$ = 21 Hz], 117.58 [d, $^2J_{CF}$ = 19 Hz], 123.06, 126.54 [d, $^4J_{CF}$ = 3 Hz], 129.80 [d, $^3J_{CF}$ = 7 Hz], 137.58, 152.03, 162.96 [d, $^1J_{CF}$ = 246 Hz], 164.64; ^{11}B NMR (128 MHz, CDCl$_3$) : δ = 12.3; ^{19}F NMR (188 MHz, C$_6$D$_6$) : δ = -113.64. Elemental anal. calcd (%) for C$_{55}$H$_{45}$B$_5$F$_5$N$_5$O$_{10}$•0.5 C$_6$H$_6$: C 62.53 H 3.44 N 6.29. Found: C 61.06 H 3.73 N 5.88.

[(*n*-Bu)B(C$_5$H$_3$NO$_2$)]$_5$ (7):
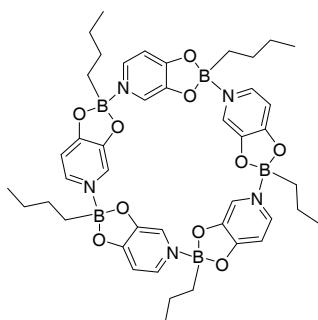
Yield: 20%. ^{1}H NMR (400 MHz, CDCl$_3$): δ 0.62-0.71 (m, 10 H, n-butyl), 0.79-0.90 (m, 15 H, n-butyl), 1.05 – 1.19 (m, 10 H, n-butyl), 1.21 – 1.34 (m, 10 H, n-butyl), 6.67 (d, ^3J = 6 Hz, 5 H, pyridine), 7.75 (d, ^3J = 6 Hz, 5 H, pyridine), 7.81 (s, 5 H, pyridine). ^{1}H NMR (400 MHz, C$_6$D$_6$): δ 0.83 – 1.02 (m, 25 H, n-butyl), 1.45 – 1.61 (m, 20 H, n-butyl), 6.25 (d, ^3J = 6 Hz, 5 H, pyridine), 7.57 (d, ^3J = 6 Hz, 5 H, pyridine), 8.02 (s, 5 H, pyridine). ^{13}C NMR (101 MHz, C$_6$D$_6$): δ 14.37, 26.32, 27.28, 106.04, 122.82, 136.59, 152.58, 164.88. ^{11}B NMR (128 MHz, C$_6$D$_6$): δ 15.5 ($h_{1/2}$ = 770 Hz). Elemental anal. calcd (%) for C$_{45}$H$_{60}$B$_5$N$_5$O$_{10}$•C$_5$H$_{12}$: C 62.74 H 7.58 N 7.32. Found: C 61.89 H 7.84 N 7.91.

[(*m*-C$_6$H$_4$CHO)B(C$_5$H$_3$NO$_2$)]$_5$ (8):
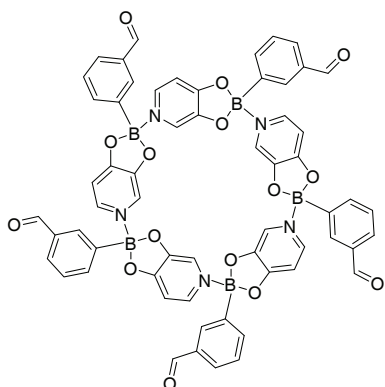
Yield: 51%. ^{1}H NMR (400 MHz, CDCl$_3$): δ 6.91 (d, ^3J = 6 Hz, 5 H, pyridine), 7.46 (t, ^3J = 8 Hz, 5 H, phenyl), 7.66 (d, ^3J = 7 Hz, 5 H, phenyl), 7.78 (d, ^3J = 8 Hz, 5 H, phenyl), 7.96 (s, 5 H, phenyl), 8.06 (d, ^3J = 6 Hz, 5 H, pyridine), 8.10 (s, 5 H, pyridine), 9.99 (s, 5H, CHO). ^{13}C NMR (101 MHz, CDCl$_3$): δ 107.19, 123.04, 128.71, 130.04, 132.38, 135.94, 137.29, 137.67, 152.11, 164.71, 193.13. ^{11}B NMR (128 MHz, CDCl$_3$): δ 13.0 ($h_{1/2}$ = 820 Hz). Elemental anal. calcd (%) for C$_{60}$H$_{40}$B$_5$N$_5$O$_{15}$•0.5C$_6$H$_6$: C 65.00 H 3.72 N 6.02. Found: C 64.38 H 3.94 N 5.59.

[(*m*-C$_6$H$_4$NH$_2$)B(C$_5$H$_3$NO$_2$)]$_5$ (9):
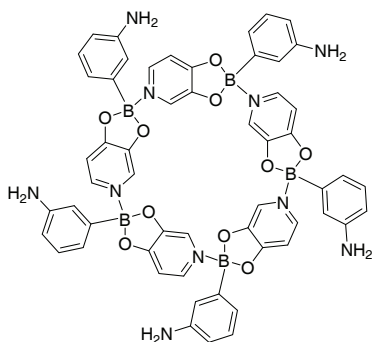
Yield: 56%. ^{1}H NMR (400 MHz, CDCl$_3$): δ 3.57 (b, 10 H, NH$_2$), 6.61 (d, ^3J = 8 Hz, 5 H, phenyl), 6.71 (s, 5 H, phenyl), 6.76 (d, ^3J = 7 Hz, 5 H, phenyl), 6.82 (d, ^3J = 6 Hz, 5 H, pyridine), 7.09 (t, ^3J = 7 Hz, 5 H, phenyl), 7.98 (d, ^3J = 6 Hz, 5 H, pyridine), 8.04 (s, 5 H, pyridine). ^{13}C NMR (101 MHz, CDCl$_3$): δ 106.63, 115.26, 117.88, 121.44, 123.11, 129.04, 137.47, 146.00, 151.95, 164.61. ^{11}B NMR (128 MHz, CDCl$_3$): δ 13.0 ($h_{1/2}$ = 680 Hz). Elemental anal. calcd (%) for C$_{55}$H$_{45}$B$_5$N$_{10}$O$_{10}$•1.5 CHCl$_3$•1.5 C$_5$H$_{12}$: C 57.05 H 4.83 N 10.40. Found: C 56.25 H 5.05 N 9.99.

[(*m*-C$_6$H$_4$CH=NPh)B(C$_5$H$_3$NO$_2$)]$_5$ (10):
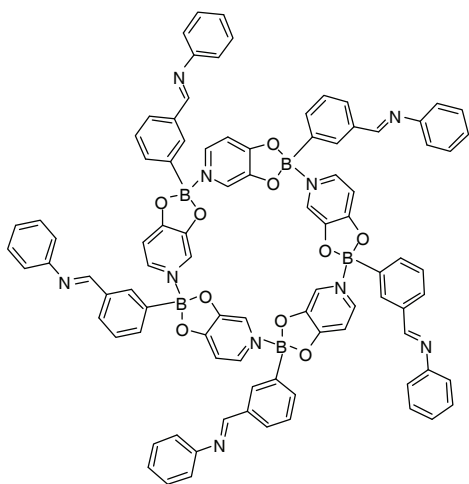
A suspension of 3-formylphenylboronic acid (150 mg, 1.0 mmol), 3,4-dihydroxypyridine (111 mg, 1.0 mmol) and aniline (112 mg, 1.2 mmol) in distilled benzene (60 mL) was heated under reflux using a Dean-Stark trap. After 6 h, the suspension was filtered hot. The volume of the filtrate was reduced to 10 mL and pentane (20 mL) was added, which resulted in the precipitation of a white solid. The precipitate was filtered, washed with pentane and dried under vacuum. Yield: 120 mg, 40%. ^{1}H NMR (400 MHz, CDCl$_3$): δ 6.90 (d, ^3J = 6 Hz, 5 H, pyridine), 7.14 – 7.22 (m, 15 H, phenyl), 7.31 – 7.43 (m, 15 H, phenyl), 7.51 (d, ^3J = 7 Hz, 5 H, phenyl), 7.83 (d, ^3J = 8 Hz, 5 H, phenyl), 7.96 (s, 5 H, phenyl), 8.07 (d, ^3J = 6 Hz, 5 H, pyridine), 8.13 (s, 5 H, pyridine), 8.42 (s, 5H, imine). ^{13}C NMR (101 MHz, CDCl$_3$): δ 107.03, 121.02, 123.16, 125.87, 128.51, 128.77, 129.22, 131.79, 134.29, 135.69, 137.62, 152.14, 152.46, 161.27, 164.71. ^{11}B NMR (128 MHz, CDCl$_3$): δ 13.2 ($h_{1/2}$ = 1060 Hz). Elemental anal. calcd (%) for C$_{90}$H$_{65}$B$_5$N$_{10}$O$_{10}$: C 72.04 H 4.37 N 9.33. Found: C 68.29 H 4.67 N 8.88. Crystals were obtained by slow diffusion of pentane into a solution of **10** in chloroform.

[(*m*-C₆H₄CH=NCy)B(C₅H₃NO₂)]₅ (11):
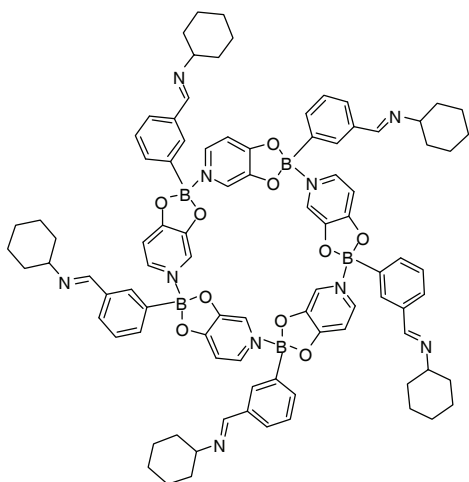
A suspension of 3-formylphenylboronic acid (150 mg, 1.0 mmol), 3,4-dihydroxypyridine (111 mg, 1.0 mmol) and cyclohexylamine (119 mg, 1.2 mmol) in distilled benzene (60 mL) was heated under reflux using a Dean-Stark trap. After 6 h, the suspension was filtered hot. The volume of the filtrate was reduced to half and pentane (30 mL) was added, which resulted in the precipitation of a white solid. The precipitate was filtered, washed with pentane and dried under vacuum. Yield: 77 mg, 25%. ^{1}H NMR (400 MHz, CDCl₃): δ 1.15 – 1.42 (m, 20 H, cyclohexyl), 1.48 – 1.88 (m, 30 H, cyclohexyl), 3.10 – 3.21 (m, 5 H, cyclohexyl), 6.86 (d, ^3J = 6 Hz, 5 H, pyridine), 7.32 (t, ^3J = 8 Hz, 5 H, phenyl), 7.41 (d, ^3J = 7 Hz, 5 H, phenyl), 7.64 – 7.73 (m, 10 H, phenyl), 8.01 (d, ^3J = 6 Hz, 5 H, pyridine), 8.07 (s, 5 H, pyridine), 8.29 (s, 5H, imine). ^{13}C NMR (101 MHz, CDCl₃): δ 25.03, 25.78, 34.49, 70.24, 106.88, 123.12, 127.76, 128.27, 131.30, 133.25, 136,08, 137.57, 152.08, 159.51, 164.66. ^{11}B NMR (128 MHz, CDCl₃): δ 13.9 ($h_{1/2}$ = 1000 Hz). Elemental anal. calcd (%) for C₉₀H₉₅B₅N₁₀O₁₀: C 70.61 H 6.26 N 9.15. Found: C 68.30 H 6.52 N 8.65.
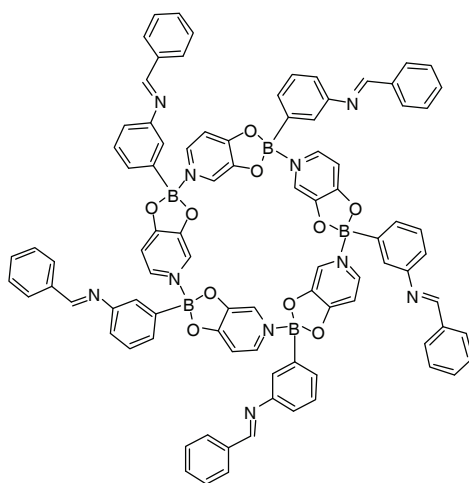
[(*m*-C₆H₄N=CHPh)B(C₅H₃NO₂)]₅ (12):

A suspension of 3-aminophenylboronic acid monohydrate (155 mg, 1.0 mmol), 3,4-dihydroxypyridine (111 mg, 1.0 mmol) and benzaldehyde (127 mg, 1.2 mmol) in distilled benzene (60 mL) was heated under reflux using a Dean-Stark trap. After 6 h, the suspension was filtered hot. Upon cooling, a white solid precipitated. The precipitate was filtered, washed with pentane and dried under vacuum. Yield: 167 mg, 56%. ^{1}H NMR (400 MHz, CDCl₃): δ 6.86 (d, ^3J = 6 Hz, 5 H, pyridine), 7.10 (d, ^3J = 8 Hz, 5 H, phenyl), 7.22 – 7.28 (m, 5 H, phenyl), 7.32 (t, ^3J = 8 Hz, 5 H, phenyl), 7.39 – 7.47 (m, 15 H, benzyl), 7.83 – 7.91 (m, 10 H,

benzyl), 8.04 (d, ^3J = 6 Hz, 5 H, pyridine), 8.10 (s, 5 H, pyridine), 8.43 (s, 5H, imine). ^{13}C NMR (101 MHz, CDCl$_3$): δ 106.82, 120.44, 123.16, 123.82, 123.99, 128.48, 128.81, 128.91, 131.30, 136.47, 137.57, 151.72, 152.09, 160.32, 164.67. ^{11}B NMR (128 MHz, CDCl$_3$): δ 11.6 ($h_{1/2}$ = 1170 Hz). Elemental anal. calcd (%) for C$_{90}$H$_{65}$B$_5$N$_{10}$O$_{10}$•C$_6$H$_6$: C 73.04 H 4.53 N 8.87. Found: C 72.06 H 4.68 N 8.59.

{[C$_6$H$_3$(CH=NBn)$_2$]B(C$_5$H$_3$NO$_2$)}$_5$ (13):
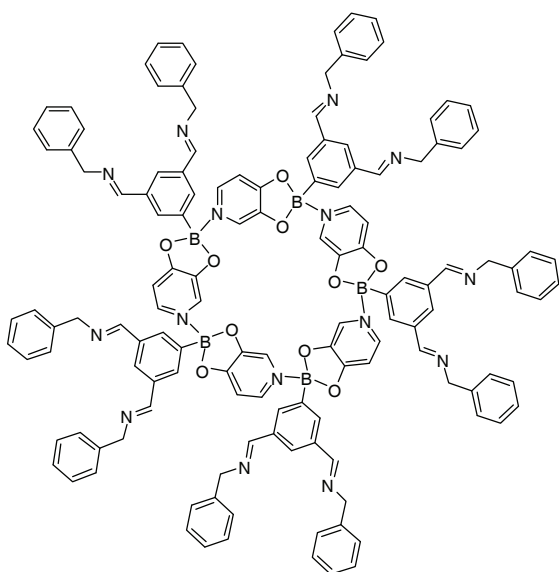
A suspension of 3,5-diformylphenylboronic acid (89 mg, 0.5 mmol), 3,4-dihydroxypyridine (56 mg, 0.5 mmol) and benzylamine (108 mg, 1.0 mmol) in distilled benzene (80 mL) was stirred at room temperature for 2 h. The suspension was then heated under reflux using a Dean-Stark trap. After 6 h, the solution was allowed to cool. The volume of the filtrate was reduced to 20 mL and pentane (20 mL) was added, which resulted in the precipitation of a white solid. The precipitate was filtered, washed with pentane and dried under vacuum. Yield: 115 mg, 53%. ^{1}H NMR (400 MHz, CDCl$_3$): δ 4.80 (s, 20 H, benzyl), 6.85 (d, ^3J = 6 Hz, 5 H, pyridine), 7.21 – 7.38 (m, 50 H, phenyl), 7.92 (s, 10 H, phenyl), 8.02 (d, ^3J = 6 Hz, 5 H, pyridine), 8.08 (s, 5 H, pyridine or phenyl), 8.10 (s, 5 H, pyridine or phenyl), 8.39 (s, 10 H, imine). ^{13}C NMR (101 MHz, CDCl$_3$): δ 65.22, 107.11, 123.07, 127.14, 128.24, 128.61, 133.28, 133.41, 136.11, 137.63, 139.19, 152.04, 162.27, 164.63. ^{11}B NMR (128 MHz, CDCl$_3$): δ 11.2 ($h_{1/2}$ = 1050 Hz). Elemental anal. calcd (%) for C$_{90}$H$_{95}$B$_5$N$_{10}$O$_{10}$: C 75.19 H 5.14 N 9.74. Found: C 73.66 H 5.19 N 9.35.

{[C$_6$H$_3$(CH=NC$_6$H$_4$Br)$_2$]B(C$_5$H$_3$NO$_2$)}$_5$ (14):
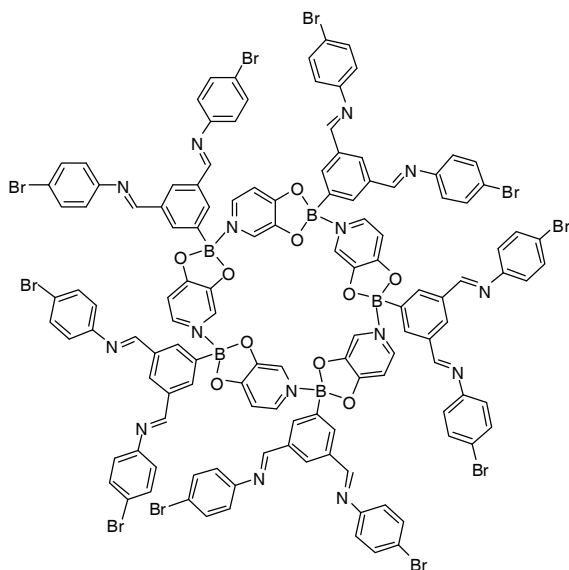
A suspension of 3,5-diformylphenylboronic acid (89 mg, 0.5 mmol), 3,4-dihydroxypyridine (56 mg, 0.5 mmol) and 4-bromoaniline (189 mg, 1.1 mmol) in distilled benzene (60 mL) was heated under reflux using a Dean-Stark trap. After 6 h, the suspension was filtered hot. The volume of the filtrate was reduced to 10 mL and pentane (10 mL) was added, which resulted in the precipitation of a white solid. The precipitate was filtered, washed with pentane and dried under vacuum. Yield: 169 mg, 60%. ^{1}H NMR (400 MHz, CDCl$_3$): δ 6.45 (d, ^3J = 6 Hz, 5 H, pyridine), 6.68 (d, ^3J = 8 Hz, 20 H, phenyl), 7.36 (d, ^3J = 8 Hz, 20 H, phenyl), 7.60 (s, 5 H, phenyl), 7.72 (s, 10 H, phenyl), 7.82 (s, 5H, pyridine), 8.02 (d, ^3J = 6 Hz, 5 H, pyridine), 9.06 (s, 5H, imine). ^{13}C NMR (101 MHz, CDCl$_3$): δ 107.35, 119.47, 122.74, 123.61, 129.04, 132.17, 133.75, 135.44, 137.60, 141.78, 150.70, 151.91, 159.77, 164.29. ^{11}B NMR (128 MHz, CDCl$_3$): δ 10.1 ($h_{1/2}$ = 1000 Hz). Elemental anal. calcd (%) for C$_{125}$H$_{80}$B$_5$Br$_{10}$N$_{15}$O$_{10}$•0.5 C$_6$H$_6$: C 54.05 H 2.94 N 7.39. Found: C 53.54 H 3.14 N 6.95.

{[C$_6$H$_3$(CH=NPh)$_2$]B(C$_5$H$_3$NO$_2$)}$_4$ (15):
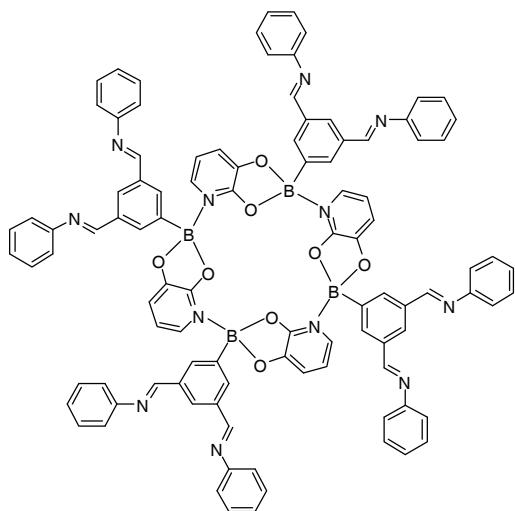
A suspension of 3,5-diformylphenylboronic acid (178 mg, 1.0 mmol), 2,3-dihydroxypyridine (111 mg, 1.0 mmol) and aniline (224 mg, 2.4 mmol) in distilled benzene (80 mL) was heated under reflux using a Dean-Stark trap. After 6 h, the suspension was filtered hot. The volume of the filtrate was reduced to 10 mL, which resulted in the precipitation of a white solid. The precipitate was filtered, washed with

pentane and dried under vacuum. Yield: 224 mg, 56%. ^{1}H NMR (400 MHz, CDCl$_3$): δ 6.65 – 6.77 (m, 8 H, pyridine), 7.18 – 7.29 (m, 24 H, phenyl), 7.34 – 7.45 (m, 16 H, phenyl), 7.47 – 7.52 (m, 4 H, pyridine), 8.04 (b, 8 H, phenyl), 8.32 (s, 4 H, phenyl), 8.52 (s, 4H, imine). ^{13}C NMR (101 MHz, CDCl$_3$): δ 115.68, 118.14, 120.85, 126.18, 127.93, 128.49, 129.45, 130.06, 136.45, 142,00, 150.88, 152.25, 160.38, 163.28. ^{11}B NMR (128 MHz, CDCl$_3$): δ 13.6 ($h_{1/2}$ = 960 Hz). Elemental anal. calcd (%) for C$_{100}$H$_{72}$B$_4$N$_{12}$O$_8$: C 74.46 H 4.50 N 10.42. Found: C 71.97 H 4.54 N 10.07.

{[C$_6$H$_3$(CH=NC$_6$H$_4$Br)$_2$]B(C$_5$H$_3$NO$_2$)}$_4$ (16):

A suspension of 3,5-diformylphenylboronic acid (71 mg, 0.40 mmol), 2,3-dihydroxypyridine (44 mg, 0.40 mmol) and 4-bromoaniline (165 mg, 0.96 mmol) in distilled benzene (60 mL) was heated under reflux using a Dean-Stark trap. After 6 h, the suspension was filtered hot. The volume of the filtrate was reduced to 20 mL and pentane (15 mL) was added, which resulted in the precipitation of a white solid. The precipitate was filtered, washed with pentane and dried under vacuum. Yield: 158 mg, 71%. ^{1}H NMR (400 MHz, CDCl$_3$): δ 6.60 – 6.72 (m, 8 H, pyridine), 7.09 (d, ^3J = 9 Hz, 16 H, phenyl), 7.31 – 7.43 (m, 4 H, pyridine), 7.52 (d, ^3J = 8 Hz, 16 H, phenyl), 8.03 (b, 8 H, phenyl), 8.28 (s, 4 H, phenyl), 8.48 (s, 4H, imine). ^{13}C NMR (101 MHz, CDCl$_3$): δ 115.60, 116.86, 118.00, 119.73, 122.51, 127.88, 130.42, 132.16, 132.56, 136.25, 142.04, 150.86, 160.58, 163.26. ^{11}B NMR (128 MHz, CDCl$_3$): δ 12.3 ($h_{1/2}$ = 850 Hz). Elemental anal. calcd (%) for C$_{100}$H$_{64}$B$_4$Br$_8$N$_{12}$O$_8$: C 53.52 H 2.87 N 7.49. Found: C 53.54 H 2.98 N 7.47.

{[C₆H₃(CH=NCH₂C₆H₃(OBn)₂)₂]B(C₅H₃NO₂)}₄ (17):
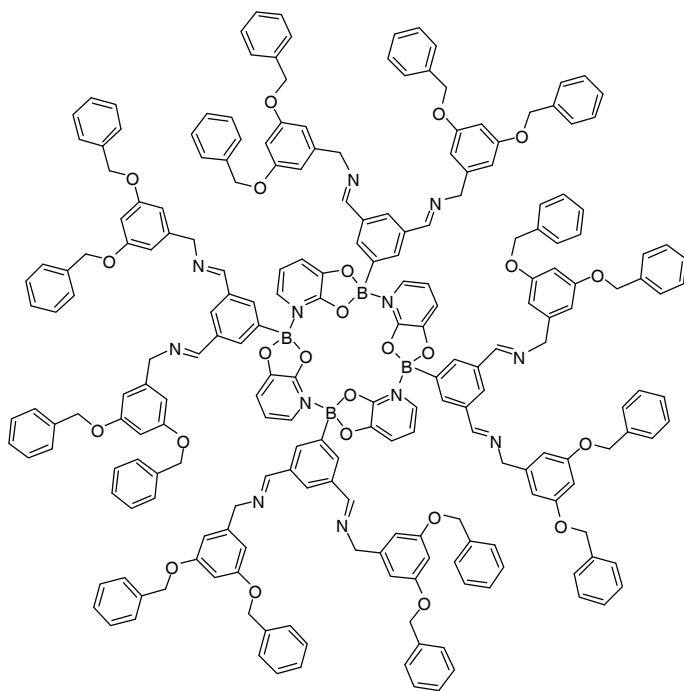
A suspension of 3,5-diformylphenylboronic acid (36 mg, 0.2 mmol), 2,3-dihydroxypyridine (22 mg, 0.2 mmol) and 3,5-bis(benzyloxy)benzylamine (128 mg, 0.4 mmol) in distilled benzene (80 mL) was stirred at room temperature for 2 h. The suspension was then heated under reflux using a Dean-Stark trap. After 6 h, the solution was allowed to cool. The volume of the filtrate was reduced to 10 mL and pentane (15 mL) was added, which resulted in the precipitation of a slightly brown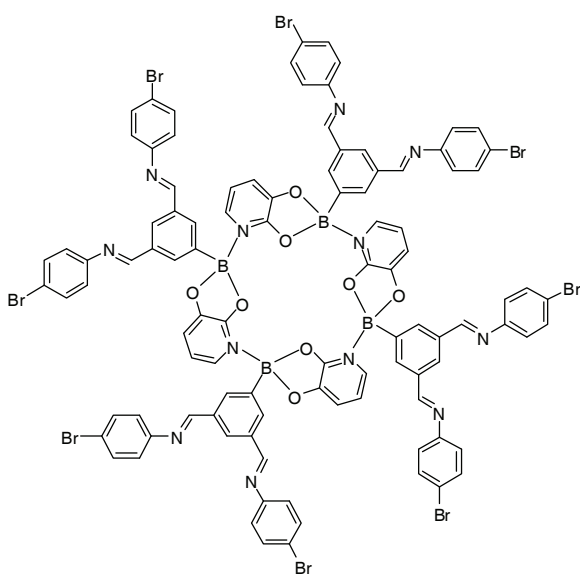 solid. The precipitate was filtered, washed with pentane and dried under vacuum. Yield: 86 mg, 46%. ^{1}H NMR (400 MHz, CDCl₃): δ 4.76 (s, 16 H, benzyl), 4.99 (s, 32 H, benzyl), 6.25 (t, ^3J = 7 Hz, 4 H, pyridine), 6.46 (d, ^3J = 7 Hz, 4 H, pyridine), 6.52 (s, 8 H, phenyl), 6.61 (s, 16 H, phenyl), 7.11 (d, ^3J = 7 Hz, 4 H, pyridine), 7.16-7.47 (m, 80 H, phenyl), 7.96 (b, 8 H, phenyl), 8.16 (s, 4 H, phenyl), 8.37 (s, 8 H, imine). ^{13}C NMR (101 MHz, CDCl₃): δ 65.39, 70.14, 100.81, 107.62, 115.40, 118.04, 127.65, 128.06, 128.64, 136.06, 136.92, 141.53, 150.50, 160.20, 162.16, 162.97. ^{11}B NMR (128 MHz, C₆D₆): δ 10.4 ($h_{1/2}$ = 1320 Hz). Elemental anal. calcd (%) for C₂₂₀H₁₈₄B₄N₁₂O₂₄: C 77.19 H 5.42 N 4.91. Found: C 75.95 H 5.18 N 4.86.

Diboroxine 18:
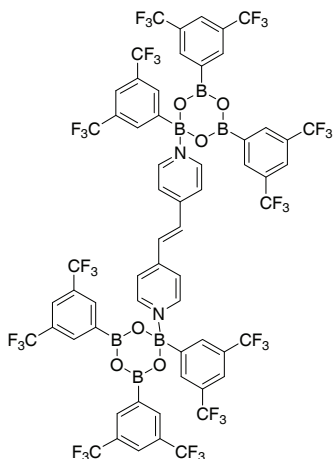
A suspension of 3,5-bis(trifluoromethyl)benzeneboronic acid (154.8 mg, 0.6 mmol) and 1,2-bis(4-pyridyl)ethylene (18.2 mg, 0.1 mmol) in toluene (75 mL) was heated under reflux using a Dean-Stark trap. After 1h, 60 mL of solvent was distilled. Upon cooling of the colourless solution, a white solid precipitated. This precipitate was filtered, washed with pentane and dried under vacuum. Yield: 140.9 mg, 83%. Elemental anal. calcd. for $C_{60}H_{28}B_6F_{36}N_2O_6 \cdot 0.75C_7H_8$ C 46.35 H 2.03 N 1.66. Found: C 46.58 H 1.82 N 1.64. Crystals were obtained by slow evaporation of a solution of **18** in toluene.

Diboroxine 19:
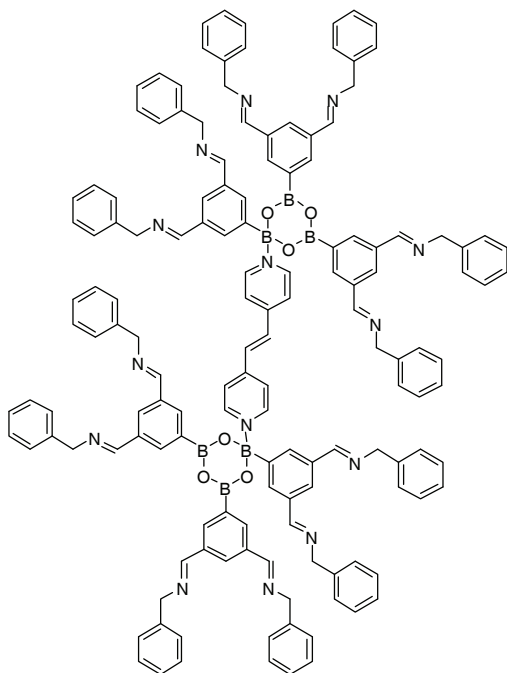
A suspension of 3,5-diformylphenylboronic acid (21.3 mg, 0.12 mmol), 1,2-di(4-pyridyl)ethylene (3.6 mg, 0.02 mmol) and benzylamine (25.7 mg, 0.24 mmol) in distilled benzene (60 mL) was then heated under reflux using a Dean-Stark trap. After 2 h, 55 mL of solvent was distilled the solution was allowed to cool to room temperature. Hexane (5 mL) was added, which resulted in the precipitation of a white solid. The precipitate was filtered, washed with pentane and dried under vacuum. Yield: 24.2 mg, 55%. ^{1}H NMR (400 MHz, CDCl$_3$): δ 4.82 (s, 24 H, benzyl), 7.16-7.35 (m, 62 H, phenyl+ethylene), 7.50 (d, ^3J = 5Hz, 4 H, pyridyl), 8.27 (s, 6 H, phenyl), 8.43 (s, 12 H, imine or phenyl), 8.47 (s, 12 H, imine or phenyl), 8.84 (d, ^3J = 5Hz, 4 H, pyridyl). ^{13}C NMR (101 MHz, CDCl$_3$): δ 65.10, 122.46, 127.19, 128.25, 128.43, 128.65, 129.02, 131.67, 135.77, 136.43, 139.21, 147.13, 162.56. ^{11}B NMR (128 MHz, CDCl$_3$): δ 26.0. Elemental anal. calcd (%) for $C_{144}H_{124}B_6N_{14}O_6$: C 78.21 H 5.65 N 8.87. Found: C 74.73 H 5.67 N 8.24.

Polymer 20:
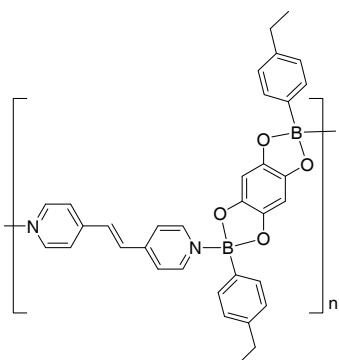
A suspension of 4-ethylphenylboronic acid (135 mg, 0.90 mmol), 1,2,4,5-tetrahydroxybenzene (64 mg, 0.45 mmol) and 1,2-di(4-pyridyl)ethylene (82 mg, 0.45 mmol) in distilled benzene (90 mL) was heated under reflux using a Dean Stark trap. After 8 h, the suspension was filtered hot and the filtrate was allowed to cool to room temperature. Upon cooling, a purple solid precipitated. The precipitate was filtered, washed with pentane and dried under vacuum. Yield: 196 mg, 79%. Elemental anal. calcd (%) for $(C_{34}H_{30}B_2N_2O_4)_n$: C 73.95 H 5.48 N 5.07. Found: C 74.25 H 5.47 N 5.16. Crystals were obtained by slow diffusion of pentane into a solution of **20** in chloroform.

Polymer 21:
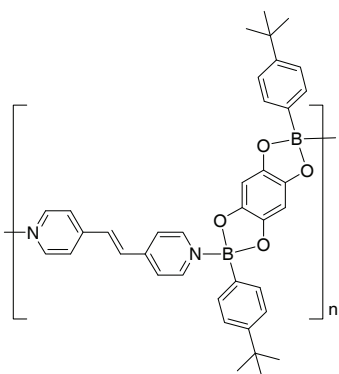
A suspension of 4-*tert*-butylphenylboronic acid (160 mg, 0.90 mmol), 1,2,4,5-tetrahydroxybenzene (64 mg, 0.45 mmol) and 1,2-di(4-pyridyl)ethylene (82 mg, 0.45 mmol) in distilled benzene (90 mL) was heated under reflux using a Dean Stark trap. After 8 h, the suspension was filtered hot and the filtrate was allowed to cool to room temperature. Upon cooling, a purple solid precipitated. The precipitate was filtered, washed with pentane and dried under vacuum. Yield: 222 mg, 81%. Elemental anal. calcd (%) for $(C_{38}H_{38}B_2N_2O_4)_n$: C 75.02 H 6.30 N 4.60. Found: C 75.18 H 6.39 N 4.39.

Boronate Ester 22:
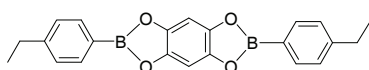
A suspension of 4-ethylphenylboronic acid (135 mg, 0.90 mmol) and 1,2,4,5-tetrahydroxybenzene (64 mg, 0.45 mmol) in distilled benzene (90 mL) was heated under reflux using a Dean Stark trap. After 8 h, the suspension was filtered hot and the filtrate was allowed to cool to room temperature. Upon cooling, white crystals formed. The crystals were filtered, washed with pentane and dried under vacuum. Yield: 93 mg, 58%. ^{1}H NMR (400 MHz, CDCl$_3$):

δ 1.29 (t, ^3J = 7 Hz, 6 H, CH$_3$), 2.73 (q, ^3J = 8 Hz, 4 H, CH$_2$), 7.31 (s, 2 H, phenyl), 7.34 (d, ^3J = 8 Hz, 4 H, phenyl), 8.00 (d, ^3J = 8 Hz, 4 H, phenyl). ^{13}C NMR (101 MHz, CDCl$_3$): δ 15.45, 29.36, 98.36, 128.08, 135.15, 143.95, 149.18. ^{11}B NMR (128 MHz, CDCl$_3$): δ 34.6 ($h_{1/2}$ = 870 Hz). Elemental anal. calcd (%) for C$_{22}$H$_{20}$B$_2$O$_4$: C 71.41 H 5.45. Found C: 71.25 H 5.57.

Polymer 23:
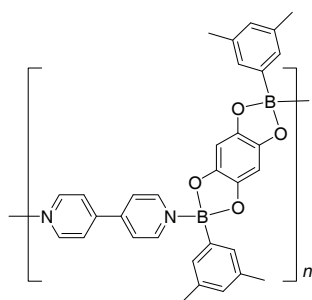
A suspension of 3,5-dimethylphenylboronic acid (135 mg, 0.90 mmol), 1,2,4,5-tetrahydroxybenzene (64 mg, 0.45 mmol) and 4,4'-bipyridyl (70 mg, 0.45 mmol) in distilled benzene (90 mL) was heated under reflux using a Dean Stark trap. After 1 h, the suspension was filtered hot and the filtrate was allowed to cool to room temperature. Upon cooling, a purple solid precipitated. The precipitate was filtered, washed with pentane and dried under vacuum. Yield: 176 mg, 74%. Elemental anal. calcd (%) for (C$_{32}$H$_{28}$B$_2$N$_2$O$_4$)$_n$: C 73.04 H 5.36 N 5.32. Found: C 72.62 H 5.43 N 5.45. Crystals were obtained by slow diffusion of pentane into a solution of **23** in chloroform.

Polymer 24:
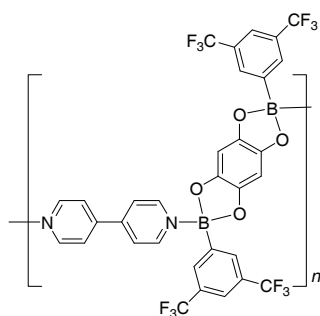
A suspension of ,5-bis(trifluoromethyl)benzeneboronic acid (129.0 mg, 0.50 mmol), 1,2,4,5-tetrahydroxybenzene (35.5 mg, 0.25 mmol) and 4,4'-bipyridyl (39.0 mg, 0.25 mmol) in distilled benzene (90 mL) was heated under reflux using a Dean Stark trap. After 2 h, the suspension was filtered hot and the filtrate was allowed to cool to room temperature. Upon cooling, a red-purple solid precipitated. The precipitate was filtered, washed with pentane and dried under vacuum. Yield: 61.1 mg, 32%. Elemental anal. calcd (%) for (C$_{32}$H$_{16}$B$_2$F$_{12}$N$_2$O$_4$•0.4C$_6$H$_6$)$_n$: C 53.43 H 2.40 N 3.62. Found: C 53.53 H 2.68 N 3.61. Crystals were obtained by slow diffusion of pentane into a solution of **24** in benzene.

Adduct 25:
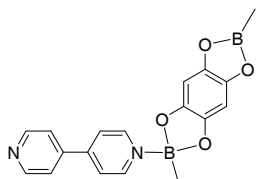
A suspension of methylboronic acid (54 mg, 0.90 mmol), 1,2,4,5-tetrahydroxybenzene (64 mg, 0.45 mmol) and 4,4'-bipyridyl (70 mg, 0.45 mmol) in distilled benzene (90 mL) was heated under reflux using a Dean Stark trap. After 1 h, the suspension was filtered hot and the filtrate was allowed to cool to room temperature. Upon cooling, a purple solid precipitated. The precipitate was filtered, washed with pentane and dried under vacuum. Yield: 110 mg, 71%. Elemental anal. calcd (%) for $C_{18}H_{16}B_2N_2O_4$: C 62.49 H 4.66 N 8.10. Found: C 62.03 H 4.46 N 7.82.

Boronate Ester 26:
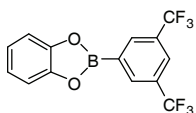
A suspension of 3,5-bis(trifluoromethyl)benzeneboronic acid (103.2 mg, 40 μmol) and catechol (44.0 mg, 40 μmol) in toluene (60 mL) was heated under reflux using a Dean-Stark trap. After 1 h, 50 mL of solvent was distilled. After cooling to room temperature, the solvent was removed under vacuum and the white residue was sublimated under vacuum, producing X-ray quality crystals of the boronic ester. Yield: 81.9 mg, 62%. ^{1}H NMR (400 MHz, CDCl$_3$) : δ 7.20 (dd, ^3J = 6 Hz, ^4J = 3 Hz, 2 H, catechol), 7.37 (dd, ^3J = 6 Hz, ^4J = 3 Hz, 2 H, catechol), 8.07 (s, 1 H, phenyl), 8.53 (s, 2 H, phenyl); ^{13}C NMR (101 MHz, CDCl$_3$) : δ 113.08, 122.63, 123.42 (q, $^1J_{CF}$ = 273 Hz), 125.94 (sept, $^3J_{CF}$ = 4 Hz), 131.81 (q, $^2J_{CF}$ = 34 Hz), 134.91 (bd, $^3J_{CF}$ = 3 Hz), 148.26; ^{11}B NMR (128 MHz, CDCl$_3$) : δ 31.9; ^{19}F NMR (188 MHz, CDCl$_3$) : δ -63.40. Elemental anal. calcd. for $C_{14}H_7BF_6O_2$: C 50.65 H 2.13. Found: C 51.27 H 2.11.

Diboronate Ester 27:
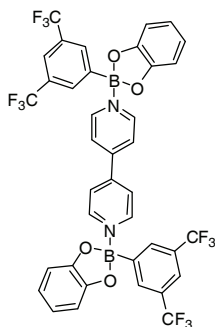
A suspension of 3,5-bis(trifluoromethyl)benzeneboronic acid (103.2 mg, 0.4 mmol), catechol (44.0 mg, 0.4 mmol) and 4,4'-bipyridyl (31.2 mg, 0.2 mmol) in toluene (60 mL) was heated under reflux using a Dean-Stark trap. After 1h, 50 mL of solvent was distilled. The orange solution was allowed to cool to room temperature and then stored in the freezer for the night. This treatment results in the formation of an

orange precipitate which was filtered, washed with pentane and dried under vacuum. Yield: 62.3 mg, 35%. ^{1}H NMR (400 MHz, CDCl$_3$) : δ 6.96 (dd, ^3J = 6 Hz, ^4J = 3 Hz, 4 H, catechol), 7.12 (dd, ^3J = 6 Hz, ^4J = 3 Hz, 4 H, catechol), 7.73 (d, ^3J = 7 Hz, 4 H, pyridyl), 7.91 (s, 2 H, phenyl), 8.26 (s, 4 H, phenyl), 8.91 (d, ^3J = 7 Hz, 4 H, pyridyl); ^{13}C NMR (101 MHz, CDCl$_3$) : δ 111.90, 121.87, 122.99, 123.72 (q, $^1J_{CF}$ = 273 Hz), 123.80 (bt, $^3J_{CF}$ = 4 Hz), 131.33 (q, $^2J_{CF}$ = 33 Hz), 133.19 (b), 147.52, 147.79, 149.62; ^{11}B NMR (128 MHz, CDCl$_3$) : δ 20.3; ^{19}F NMR (188 MHz, CDCl$_3$) : δ -63.18. Elemental anal. calcd. for C$_{38}$H$_{22}$B$_2$F$_{12}$N$_2$O$_4$•0.67C$_7$H$_8$: C 58.13 H 3.12 N 3.18. Found: C 58.35 H 3.05 N 3.43.

Diboronate Ester 28:
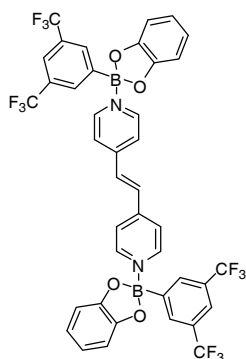
A suspension of 3,5-bis(trifluoromethyl)benzeneboronic acid (103.2 mg, 0.4 mmol), catechol (44.0 mg, 0.4 mmol) and 1,2-bis(4-pyridyl)ethylene (36.4 mg, 0.2 mmol) in toluene (60 mL) was heated under reflux using a Dean-Stark trap. After 1h, 50 mL of solvent was distilled. The orange solution was allowed to cool to room temperature and then stored in the freezer for the night. This treatment results in the formation of a yellow-orange precipitate which was filtered, washed with pentane and dried under vacuum. Yield: 94.1 mg, 55%. ^{1}H NMR (400 MHz, CDCl$_3$) : δ 6.85 (dd, ^3J = 6 Hz, ^4J = 3 Hz, 4 H, catechol), 7.00 (dd, ^3J = 6 Hz, ^4J = 3 Hz, 4 H, catechol), 7.35 (s, 2 H, ethylene), 7.67 (d, ^3J = 7 Hz, 4 H, pyridyl), 7.83 (s, 2 H, phenyl), 8.12 (s, 4 H, phenyl), 8.79 (d, ^3J = 7 Hz, 4 H, pyridyl); ^{13}C NMR (101 MHz, CDCl$_3$) : δ 111.28, 120.97, 123.24, 122.74 (bt, $^3J_{CF}$ = 4 Hz), 123.83 (q, $^1J_{CF}$ = 273 Hz), 131.02 (q, $^2J_{CF}$ = 33 Hz), 132.30, 132.40 (b), 145.85, 147.11, 150.26; ^{11}B NMR (128 MHz, CDCl$_3$) : δ 15.6; ^{19}F NMR (188 MHz, CDCl$_3$) : δ -63.09. Elemental anal. calcd. for C$_{40}$H$_{24}$B$_2$F$_{12}$N$_2$O$_4$: C 56.77 H 2.86 N 3.31. Found: C 56.87 H 2.68 N 3.41. Crystals were obtained by slow diffusion of pentane into a solution of **28** in toluene.

Rotaxane 29:
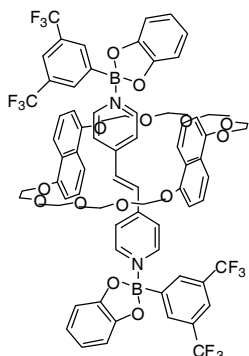
A suspension of 3,5-bis(trifluoromethyl)benzeneboronic acid (5.2 mg, 20 μmol,), catechol (2.2 mg, 20 μmol), 1,2-di(4-pyridyl)ethylene (1.8 mg, 10 μmol) and 1,5-dinaphto-38-crown-10 (6.4 mg, 10 μmol) in toluene (30 mL) was heated under reflux using a Dean-Stark trap. After 1 h, 25 mL of solvent was distilled. After cooling to room temperature, the volume of the solvent was further reduced to 2 mL. This resulted in the precipitation of an orange solid, which was filtered, washed with pentane, and dried under vacuum. Yield: 10.2 mg, 67%. ^{1}H NMR (400 MHz, CDCl$_3$) : δ 3.76 (b, 16 H, CE), 3.81 (b, 16 H, CE), 6.17 (b, 4 H, CE), 6.85 (dd, ^3J = 6 Hz, ^4J = 3 Hz, 4 H, catechol), 6.95-7.02 (m, 8 H, CE+catechol), 7.32 (m, 4 H, CE), 7.59 (d, ^3J = 7 Hz, 4 H, pyridyl), 7.84 (s, 2 H, phenyl), 8.16 (s, 4 H, phenyl), 8.70 (d, ^3J = 7 Hz, 4 H, pyridyl); ^{13}C NMR (101 MHz, CDCl$_3$) : δ 67.75, 69.90, 71.12, 71.18, 105.23, 111.08, 114.37, 120.73, 122.42 (b), 123.35, 123.92 (q, $^1J_{CF}$ = 273 Hz), 125.05, 126.50, 130.93 (q, $^2J_{CF}$ = 33 Hz), 132.26 (b), 145.08 (b), 146.92, 150.58, 154.10; ^{11}B NMR (128 MHz, CDCl$_3$) : δ 14.5; ^{19}F NMR (188 MHz, CDCl$_3$) : δ –63.01. Elemental anal. calcd. for C$_{76}$H$_{68}$B$_2$F$_{12}$N$_2$O$_{14}$•0.5 C$_7$H$_8$: C 62.45 H 4.75 N 1.83. Found: C 62.76 H 4.95 N 1.87. Crystals were obtained by slow evaporation of a solution of **29** in chloroform.

Rotaxane 30:
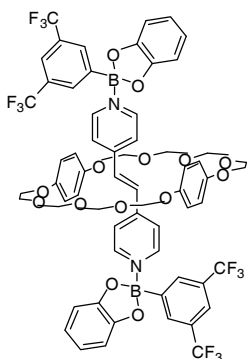
A suspension of 3,5-bis(trifluoromethyl)benzeneboronic acid (12.9 mg, 50 μmol), catechol (5.5 mg, 50 μmol), 1,2-di(4-pyridyl)ethylene (4.6 mg, 25 μmol) and bis-*p*-phenylene-34-crown-10 (13.4 mg, 25 μmol) in benzene (30 mL) was heated under reflux using a Dean-Stark trap. After 1 h, 25 mL of solvent was distilled. After cooling to room temperature, the yellow solution was placed in a fridge for 1 h. This resulted in the formation of a yellow precipitate, which was isolated, washed with pentane, and dried under vacuum. Yield: 21.9 mg, 63%. ^{1}H NMR (400 MHz, CDCl$_3$) : δ 3.65-3.74 (m, 16 H, CE), 3.80-3.87 (m, 8 H, CE), 3.93-4.01 (m, 8 H, CE), 6.73 (s, 8 H, CE), 6.87 (dd, ^3J = 6 Hz, ^4J = 3 Hz, 4 H, catechol), 7.01 (dd, ^3J = 6 Hz, ^4J = 3 Hz, 4 H, catechol), 7.32 (s, 2 H, ethylene), 7.65 (d, ^3J = 7 Hz, 4 H, pyridyl), 7.84 (s, 2 H, phenyl), 8.14 (s, 4 H, phenyl), 8.78 (d, ^3J

= 7 Hz, 4 H, pyridyl); ^{13}C NMR (101 MHz, CDCl$_3$) : δ 68.29, 69.94, 70.89, 71.03, 111.32, 115.64, 121.04, 122.83 (bt, $^3J_{CF}$ = 4 Hz), 123.20, 123.82 (q, $^1J_{CF}$ = 273 Hz), 131.03 (q, $^2J_{CF}$ = 33 Hz), 132.47 (b), 133.22, 145.93, 147.03, 150.22, 153.21; ^{11}B NMR (128 MHz, CDCl$_3$) : δ 16.1; ^{19}F NMR (188 MHz, CDCl$_3$) : δ –63.09. Elemental anal. calcd. for C$_{68}$H$_{64}$B$_2$F$_{12}$N$_2$O$_{14}$: C 59.06 H 4.66 N 2.03. Found: C 58.85 H 4.81 N 1.90. Crystals were obtained by slow diffusion of pentane into a solution of **30** in toluene.

Host-Guest Complex 31:
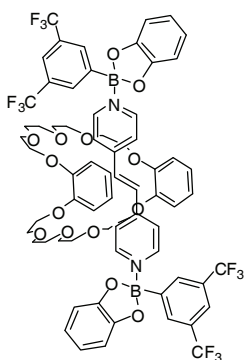

A suspension of 3,5-bis(trifluoromethyl)benzeneboronic acid (31.0 mg, 120 μmol), catechol (13.3 mg, 120 μmol), 1,2-bis(4-pyridyl)ethylene (10.9 mg, 60 μmol) and dibenzo-30-crown-10 (32.2 mg, 60 μmol) in toluene (30 mL) was heated under reflux using a Dean-Stark trap. After 1h, 28 mL of solvent was distilled. After cooling to room temperature, the yellow solution was stored in the freezer overnight. This treatment results in the formation of a yellow precipitate which was isolated, washed with pentane and dried under vacuum. Yield: 64.9 mg, 76%. ^{1}H NMR (400 MHz, CDCl$_3$) : δ 3.65-3.70 (m, 8 H, CE), 3.74-3.79 (m, 8 H, CE), 3.84-3.89 (m, 8 H, CE), 4.10-4.14 (m, 8 H, CE), 6.83-6.91 (m, 12 H, catechol + CE), 7.00 (dd, ^3J = 6 Hz, ^4J = 3 Hz, 4 H, catechol), 7.34 (s, 2 H, ethylene), 7.66 (d, ^3J = 7 Hz, 4 H, pyridyl), 7.83 (s, 2 H, phenyl), 8.12 (s, 4 H, phenyl), 8.78 (d, ^3J = 7 Hz, 4 H, pyridyl); ^{13}C NMR (101 MHz, CDCl$_3$) : δ 69.26, 69.95, 70.89, 71.06, 111.27, 114.64, 120.96, 121.66, 122.72 (bt, $^3J_{CF}$ = 4 Hz), 123.27, 123.83 (q, $^1J_{CF}$ = 273 Hz), 131.01 (q, $^2J_{CF}$ = 33 Hz), 132.29, 132.36 (b), 145.81, 147.12, 149.15, 150.28; ^{11}B NMR (128 MHz, CDCl$_3$) : δ 16.0; ^{19}F NMR (188 MHz, CDCl$_3$) : δ -63.08. Elemental anal. calcd. for C$_{68}$H$_{64}$B$_2$F$_{12}$N$_2$O$_{14}$•0.5C$_7$H$_8$: C 60.10 H 4.80 N 1.96. Found: C 60.26 H 4.75 N 2.23.
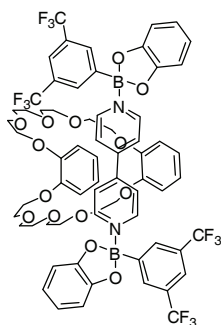
Host-Guest Complex 32:

A suspension of 3,5-bis(trifluoromethyl)benzeneboronic acid (20.6 mg, 80 μmol), catechol (8.8 mg, 80 μmol), 4,4'-dipyridyl (6.2 mg, 40 μmol) and dibenzo-30-crown-10 (21.5 mg, 40 μmol) in toluene (30 mL) was heated under reflux using a Dean-Stark trap. After 1 h, 25 mL of solvent was distilled. After cooling to room temperature, the volume of solvent was further reduced to 2 mL and the yellow solution was placed in a freezer for 12 h. This resulted in the formation of X-ray quality crystals, which were isolated, washed with pentane and dried under vacuum. Yield: 35.5 mg, 60%. ^{1}H NMR (400 MHz, CDCl$_3$) : δ 3.65-3.70 (m, 8 H, CE), 3.73-3.79 (m, 8 H, CE), 3.86 (t, ^3J = 5 Hz, 8 H, CE), 4.11 (t, ^3J = 5 Hz, 8 H, CE), 6.82-6.91 (m, 8 H, CE), 6.96 (dd, ^3J = 6 Hz, ^4J = 3 Hz, 4 H, catechol), 7.11 (dd, ^3J = 6 Hz, ^4J = 3 Hz, 4 H, catechol), 7.70-7.76 (m, 4 H, pyridyl), 7.91 (s, 2 H, phenyl), 8.26 (s, 4 H, phenyl), 8.87-8.92 (m, 4 H, pyridyl); ^{13}C NMR (101 MHz, CDCl$_3$) : δ 69.23, 69.94, 70.87, 71.04, 111.83, 114.62, 121.66, 121.76, 123.10, 123.68 (bt, $^3J_{CF}$ = 4 Hz), 123.70 (q, $^1J_{CF}$ = 273 Hz), 131.26 (q, $^2J_{CF}$ = 33 Hz), 133.10 (b), 147.56 (overlap), 149.12, 149.65; ^{11}B NMR (128 MHz, CDCl$_3$) : δ 20.4; ^{19}F NMR (188 MHz, CDCl$_3$) : δ –63.15. Elemental anal. calcd. for C$_{66}$H$_{62}$B$_2$F$_{12}$N$_2$O$_{14}$•1.2C$_7$H$_8$: C 60.90 H 4.92 N 1.91. Found: C 61.36 H 4.95 N 2.23.

Macrocycle 33:
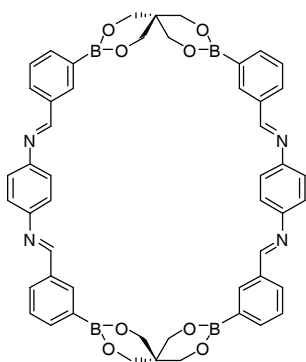
A suspension of 3-formylphenylboronic acid (30.0 mg, 0.20 mmol), pentaerythritol (13.6 mg, 0.10 mmol) and 1,4-diaminobenzene (10.8 mg, 0.10 mmol) in a 1:2 mixture of THF/toluene (90 mL) was heated under reflux using a Dean-Stark trap. After 7 h, the THF had been completely eliminated and the suspension was filtered hot to remove an orange precipitate. The volume of the filtrate was then reduced to 10 mL, which resulted in precipitation of a white solid. The precipitate was isolated, recrystallized from CHCl$_3$/hexane and dried under vacuum. Yield: 19.3 mg, 44%. ^{1}H NMR (CDCl$_3$, 400 MHz): δ 4.10 (s, 16 H, CH$_2$), 7.29 (s, 8 H, phenyl), 7.49 (t, ^3J = 7 Hz, 4 H, phenyl), 7.85 (d, ^3J = 7 Hz, 4 H, phenyl), 8.04 (d, ^3J = 8 Hz, 4 H, phenyl), 8.38 (s, 4 H, phenyl), 8.56 (s, 4 H, imine). ^{13}C NMR (CDCl$_3$, 101

MHz): δ 37.31, 64.95, 121.99, 128.38, 130.88, 135.61, 135.77, 136.64, 150.26, 160.21. ^{11}B NMR (CDCl$_3$, 128 MHz) δ 31.0. Elemental anal. calcd. for C$_{50}$H$_{44}$B$_4$N$_4$O$_8 \bullet$0.1CHCl$_3$: C 68.06 H 5.03 N 6.34. Found: C 68.15 H 5.15 N 5.84. Crystals were obtained by slow diffusion of pentane into a solution of **33** in chloroform.

Macrocycle 34:
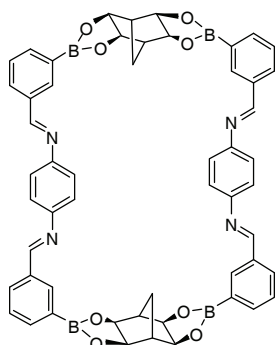
A suspension of 3-formylphenylboronic acid (30.0 mg, 0.20 mmol), *all-exo*-bicyclo[2.2.1]heptane-2,3,5,6-tetraol (16.0 mg, 0.10 mmol) and 1,4-diaminobenzene (10.8 mg, 0.10 mmol) in a 1:2 mixture of THF/toluene (90 mL) was heated under reflux using a Dean-Stark trap. After 4 h, the THF had been completely eliminated and the suspension was filtered hot to remove an orange precipitate. The volume of the filtrate was then reduced to 10 mL, which resulted in precipitation of a pale yellow solid. The precipitate was isolated, washed with pentane and dried under vacuum. Yield: 13.1 mg, 28%. ^{1}H NMR (CDCl$_3$, 400 MHz): δ 1.75 (b, 4 H, CH$_2$), 2.76 (b, 4 H, CH), 4.53 (b, 8 H, CH), 7.30 (s, 8 H, phenyl), 7.52 (t, [3]J = 7 Hz, 4 H, phenyl), 7.93 (d, [3]J = 7 Hz, 4 H, phenyl), 8.09 (d, [3]J = 8 Hz, 4 H, phenyl), 8.33 (s, 4 H, phenyl), 8.56 (s, 4 H, imine). ^{13}C NMR (CDCl$_3$, 101 MHz): δ 21.62, 47.01, 80.32, 122.02, 122.55, 127.48, 128.59, 131.81, 135.98, 150.05, 159.55. ^{11}B NMR (CDCl$_3$, 128 MHz) δ 30.8. Elemental anal. calcd. for C$_{54}$H$_{44}$B$_4$N$_4$O$_8$: C 70.48 H 4.82 N 6.09. Found: C 67.22 H 4.97 N 5.84.

Macrocycle 35:
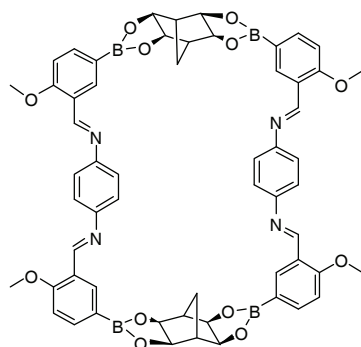
A suspension of 3-formyl-4-methoxyphenylboronic acid (36.0 mg, 0.20 mmol), *all-exo*-bicyclo[2.2.1]heptane-2,3,5,6-tetraol (16.0 mg, 0.10 mmol) and 1,4-diaminobenzene (10.8 mg, 0.10 mmol) in a 1:2 mixture of THF/toluene (90 mL) was heated under reflux using a Dean-Stark trap. After 6 h, the THF had been completely eliminated and the suspension was filtered hot to remove an orange precipitate. The volume of the filtrate was then reduced to 5 mL, which resulted in precipitation of a pale yellow solid. The precipitate was isolated, washed

with pentane and dried under vacuum. Yield: 12.7 mg, 24%. ^{1}H NMR (CDCl$_3$, 400 MHz): δ 1.70 (b, 4 H, CH$_2$), 2.70 (b, 4 H, CH), 3.94 (s, 12H, CH$_3$O), 4.47 (b, 8 H, CH), 6.97 (d, ^3J = 8 Hz, 4 H, phenyl), 7.28 (s, 8 H, phenyl), 7.97 (d, ^3J = 7 Hz, 4 H, phenyl), 8.61 (s, 4 H, phenyl or imine), 8.96 (s, 4 H, phenyl or imine). ^{13}C NMR (CDCl$_3$, 101 MHz): δ. 24.57, 47.14, 55.72, 80.21, 110.72, 122.08, 124.68, 135.05, 139.66, 150.85, 155.44, 162.18. ^{11}B NMR (CDCl$_3$, 128 MHz) δ 30.4. Elemental anal. calcd. for C$_{58}$H$_{52}$B$_4$N$_4$O$_{12}$: C 66.96 H 5.04 N 5.39. Found: C 67.07 H 5.48 N 5.34. Crystals were obtained by slow diffusion of pentane into a solution of **35** in 1,2-dichloroethane.

Macrocycle 36:
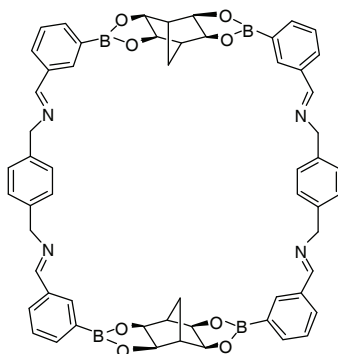
A suspension of 3-formylphenylboronic acid (30.0 mg; 0.2 mmol), all-exo-bicyclo[2.2.1]heptane-2,3,5,6-tetraol (16.0 mg; 0.1 mmol) and p-xylylenediamine (13.6 mg; 0.1 mmol) in a 1:2 mixture of THF/toluene (90 mL) was heated under reflux using a Dean-Stark trap. After 1h30, the suspension was filtered hot. The volume of the filtrate was then reduced to 10 mL, which resulted in precipitation of a white solid. The product was isolated, dissolved in 1,2-dichloroethane and crystallized by diffusion of pentane. Yield: <1%. ^{1}H-NMR (CDCl$_3$, 400 MHz): δ 1.64 (b, 4H, CH$_2$), 2.66 (b, 4H, CH), 4.46 (b, 8H, CH), 4.81 (s, 8H, CH$_2$), 7.29 (s, 8H, phenyl), 7.43 (t, ^3J = 7 Hz, 4H, phenyl), 7.83 (d, ^3J = 7 Hz, 4H, phenyl), 7.91 (d, ^3J = 8 Hz, 8H, phenyl), 8.16 (s, 4H, phenyl), 8.38 (s, 4H, imine) ^{13}C-NMR: no data. ^{11}B NMR: no data. MALDI-MS (m/z): 977.43 [**36**+H]$^+$, 999.41 [**36**+Na]$^+$. Elemental anal. no data. Crystals were obtained by slow diffusion of pentane into a solution of **36** in 1,2-dichloroethane.

Macrocycle 37:
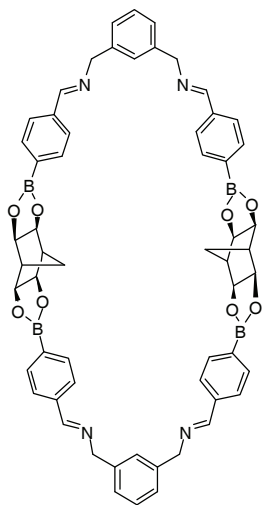
A suspension of 4-formylphenylboronic acid (30.0 mg; 0.2 mmol), all-exo-bicyclo[2.2.1]heptane-2,3,5,6-tetraol (16.0 mg; 0.1 mmol) and m-xylylenediamine (13.6 mg; 0.1 mmol) in a 1:2 mixture of THF/toluene (90 mL) was heated under reflux using a Dean-Stark trap. After 1h30, the suspension was filtered hot. The volume of the filtrate was then reduced to 10 mL, which resulted in precipitation of a white solid. The product was isolated by filtration and dried under vacuum. Yield: 6.0 mg, 12%. ^{1}H NMR (CDCl$_3$, 400 MHz): δ 2.35 (s, 4H, CH$_2$), 2.71 (s, 4H, CH), 4.49 (s, 8H, CH), 4.83 (s, 8H, CH$_2$), 7.17 (d, ^3J = 7 Hz, 4H, phenyl), 7.33 (t, ^3J = 7 Hz, 2H, phenyl), 7.39 (s, 2H, phenyl), 7.69 (d, ^3J = 7 Hz, 8H, phenyl), 7.79 (d, ^3J = 7 Hz, 8H, phenyl), 8.34 (s, 4H, imine) ^{13}C NMR (CDCl$_3$, 101 MHz): δ 49.9, 67.8, 80.2, 83.1, 128.3, 130.0, 130.5, 130.8, 131.2, 131.5, 132.0, 138.2, 141.9, 142.4, 164.6. ^{11}B NMR: no data. MALDI-MS (m/z): 976.45 [37][+]. Elemental anal. calcd. for C$_{58}$H$_{52}$B$_4$N$_4$O$_8$: C 71.35 H 5.37 N 5.74. Found: C 71.51 H 5.48 N 5.62. Crystals were obtained by slow diffusion of pentane into a solution of 37 in 1,2-dichloroethane.

Cage 38:
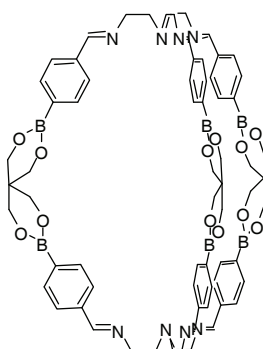
A solution of 4-formylphenylboronic acid (90.0 mg, 0.60 mmol), pentaerythritol (40.8 mg, 0.30 mmol) and tris(2-aminoethyl)amine (29.2 mg, 0.20 mmol) in ethanol (80 mL) was heated under reflux using a Dean-Stark trap. After a few minutes, a white solid precipitated. The suspension was refluxed for another 2 h during which 60 mL of the solvent was removed. After cooling, the resulting solid was filtered, washed with pentane and dried under vacuum. Yield: 110.5 mg, 82%. ^{1}H NMR (CDCl$_3$, 400 MHz): δ 2.80 (b, 12 H, CH$_2$N), 3.55 (b, 12 H, CH$_2$N), 4.16 (s, 24 H, CH$_2$O), 6.90 (d, ^3J = 8 Hz, 12 H, phenyl), 7.66 (s, 6 H, imine), 7.70 (d, ^3J = 8 Hz, 12 H, phenyl). ^{13}C NMR (CDCl$_3$, 101 MHz): δ 36.81, 56.36, 60.02, 65.11, 127.32, 134.38, 138.66, 162.19. ^{11}B NMR (CDCl$_3$, 128 MHz) δ 33.8. ESI-MS (m/z): 639.32 [38][2+]. Elemental anal. calcd. for C$_{69}$H$_{78}$B$_6$N$_8$O$_{12}$•1.5C$_2$H$_5$OH: C 64.28 H 6.52 N 8.33. Found: C 63.92 H 6.95 N 8.76. Crystals were obtained by slow diffusion of pentane into a solution of 38 in chloroform.

Cage 39:
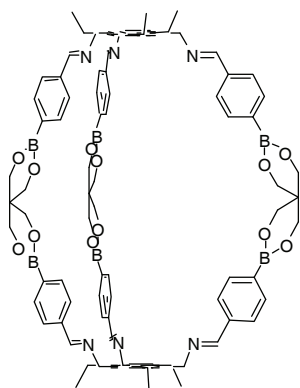
A solution of 4-formylphenylboronic acid (30.0 mg, 0.20 mmol), pentaerythritol (13.6 mg, 0.10 mmol) and 1,3,5-trisaminomethyl-2,4,6-triethylbenzene (16.3 mg, 0.07 mmol) in ethanol (90 mL) was heated under reflux using a Dean-Stark trap. The solution was refluxed for 2 h during which 70 mL of the solvent was removed. Upon cooling, a white solid precipitated. The precipitate was filtered, washed with pentane and dried under vacuum. Yield: 27.5 mg, 53%. ^{1}H NMR (CDCl$_3$, 400 MHz): δ 1.28 (t, ^3J = 7 Hz, 18 H, CH$_3$), 2.69 (q, ^3J = 7 Hz, 12 H, CH$_2$), 4.05 (s, 24 H, CH$_2$O), 4.97 (s, 12 H, CH$_2$N), 7.68 (d, ^3J = 8 Hz, 12 H, phenyl), 7.79 (d, ^3J = 8 Hz, 12 H, phenyl), 8.18 (s, 6 H, imine). ^{13}C NMR (CDCl$_3$, 101 MHz): δ 15.89, 23.20, 36.74, 57.16, 64.99, 127.44, 132.38, 133.79, 134.28, 138.76, 143.86, 160.52. ^{11}B NMR (CDCl$_3$, 128 MHz) δ 25.0. ESI-MS (m/z): 742.39 [**39**]$^{2+}$. Elemental anal. calcd. for C$_{87}$H$_{96}$B$_6$N$_6$O$_{12}$•0.75C$_2$H$_4$Cl$_2$: C 68.28 H 6.41 N 5.40. Found: C 68.14 H 6.70 N 5.67. Crystals were obtained by slow diffusion of pentane into a solution of **39** in 1,2-dichloroethane.

Macrocycle 40:
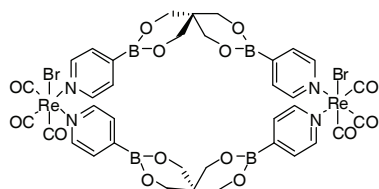
A suspension of Re(CO)$_5$Br (40.6 mg, 0.1 mmol), 4-pyridineboronic acid (24.6 mg, 0.2 mmol) and pentaerythritol (13.6 mg, 0.1 mmol) in a 1:2 mixture of THF/toluene (90 mL) was heated under reflux using a Dean-Stark trap. After 2h, 60 mL of solvent had been eliminated and a yellow solid had precipitate. After cooling, the solid was filtered, washed with pentane and dried under vacuum. Yield: 52.7 mg, 80%. ^{1}H NMR (CDCl$_3$, 400 MHz) δ 4.12 (s, 16 H, CH$_2$), 7.58 (d, ^3J = 6 Hz, 8 H, pyridyl), 8.64 (d, ^3J = 6 Hz, 8 H, pyridyl). ^{13}C NMR (CDCl$_3$, 101 MHz) δ 37.39, 65.14, 130.22, 153.74 (the two peaks for the CO ligands were not detected). ^{11}B NMR (CDCl$_3$, 128 MHz) δ 31.6. IR (υ_{CO}, cm^{-1}) 2021, 1918, 1885. Elemental anal. calcd. for C$_{36}$H$_{32}$B$_4$Br$_2$N$_4$O$_{14}$Re$_2$: C 32.75 H 2.44 N 4.24. Found: C 32.72 H 2.69 N 3.84. Crystals were obtained by slow diffusion of pentane into a solution of **40** in 1,2-dichloroethane.

Macrocycle 41:
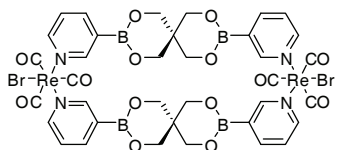
A suspension of Re(CO)$_5$Br (40.6 mg, 0.1 mmol), 3-pyridineboronic acid (24.6 mg, 0.2 mmol) and pentaerythritol (13.6 mg, 0.1 mmol) in a 1:2 mixture of THF/toluene (90 mL) was heated under reflux using a Dean-Stark trap. After 2h, 60 mL of solvent had been eliminated and a yellow solid had precipitate. After cooling, the solid was filtered, washed with pentane and dried under vacuum. Yield: 49.6 mg, 71%. ^{1}H NMR (CDCl$_3$, 400 MHz) δ 3.97 (d, ^2J = 12 Hz, 4 H, CH$_2$), 4.00 (s, 8 H, CH$_2$), 4.05 (d, ^2J = 12 Hz, 4 H, CH$_2$), 7.32-7.37 (m, 4H, pyridyl), 8.20 (d, ^3J = 7 Hz, 4 H, pyridyl), 8.80 (d, ^3J = 10 Hz, 4 H, pyridyl), 8.93 (dd, ^3J = 8 Hz, ^3J = 5 Hz, 4 H, pyridyl). ^{13}C NMR (CDCl$_3$, 101 MHz) δ 36.97, 65.00, 125.23, 143.77, 156.61, 159.33, 192.15, 195.33. ^{11}B NMR (CDCl$_3$, 128 MHz) δ 31.9. IR (υ$_{CO}$, cm^{-1}) 2020, 1879 (shoulder). Elemental anal. calcd. for C$_{36}$H$_{32}$B$_4$Br$_2$N$_4$O$_{14}$Re$_2$•C$_6$H$_6$: C 36.08 H 2.74 N 4.01. Found: C 36.14 H 3.13 N 4.46. Crystals were obtained by slow diffusion of pentane into a solution of **41** in 1,2-dichloroethane.

## Macrocycle 42:
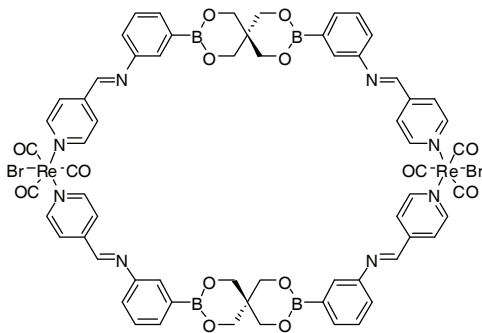
A suspension of Re(CO)$_5$Br (40.6 mg, 0.10 mmol), 3-aminophenylboronic acid monohydrate (31.0 mg, 0.20 mmol), 4-formylpyridine (21.4 mg, 0.20 mmol) and pentaerythritol (13.6 mg, 0.10 mmol) in a 1:2 mixture of THF/benzene (60 mL) was heated under reflux using a Dean-Stark trap. After 1 h (20 mL of solvent eliminated), the yellow suspension was filtered hot. After cooling, 20 mL of pentane were added to the filtrate, allowing the precipitation of a yellow solid. The precipitate was filtered, washed with pentane and dried under vacuum. Yield: 25.3 mg, 29%. The crude yield was ~ 70-80 % as estimated by ^{1}H-NMR spectroscopy. ^{1}H NMR (CDCl$_3$, 400 MHz) δ 4.09 (s, 16 H, CH$_2$), 7.36-7.49 (m, 8 H, phenyl), 7.67 (s, 4 H, phenyl), 7.73-7.80 (m, 12 H, phenyl + pyridyl), 8.52 (s, 4 H, imine), 8.93 (d, ^3J = 6 Hz, 8 H, pyridyl). ^{13}C NMR (CDCl$_3$, 101 MHz) δ 36.89, 65.12, 124.18, 124.86, 124.97, 125.88, 129.03, 133.76, 145.03, 149.52, 155.19, 195.03 (one peak for a CO ligand was not detected). ^{11}B NMR (CDCl$_3$, 128 MHz) δ 30.8. IR (υ$_{CO}$, cm^{-1}) 2021, 1917, 1879.

Elemental anal. calcd. for $C_{64}H_{52}B_4Br_2N_8O_{14}Re_2 \bullet 0.25\ C_6H_6$: C 44.90 H 3.08 N 6.40. Found: C 45.15 H 3.45 N 6.07.

Macrocycle 43:
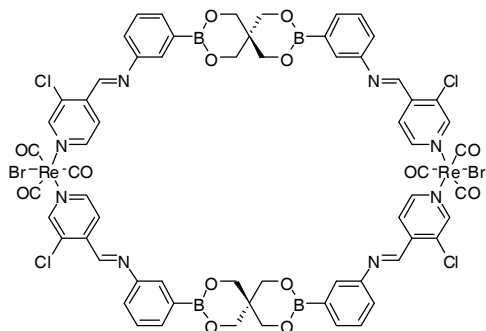
A suspension of Re(CO)$_5$Br (40.6 mg, 0.10 mmol), 3-aminophenylboronic acid monohydrate (31.0 mg, 0.20 mmol), 3-chloro-4-formylpyridine (28.3 mg, 0.20 mmol) and pentaerythritol (13.6 mg, 0.10 mmol) in a 2:1 mixture of THF/benzene (90 mL) was heated under reflux using a Dean-Stark trap. The suspension was refluxed for 6 h during which 60 mL of the solvent was removed. The yellow solution was allowed to cool and its volume was reduced to 10 mL. Upon addition of 10 mL of hexane a yellow precipitate formed. The precipitate was isolated, recrystallized from CHCl$_3$/hexane and dried under vacuum. Yield: 54.8 mg, 58%. ^{1}H NMR (CDCl$_3$, 400 MHz) δ 4.10 (s, 16 H, CH$_2$), 7.36-7.49 (m, 8 H, phenyl), 7.70 (s, 4 H, phenyl), 7.77 (d, ^3J = 7 Hz, 4 H, phenyl), 8.13 (d, ^3J = 6 Hz, 4 H, pyridyl) 8.73 (d, ^3J = 6 Hz, 4 H, pyridyl), 8.88 (s, 4 H, imine or pyridyl), 9.02 (s, 4 H, imine or pyridyl). ^{13}C NMR (CDCl$_3$, 101 MHz) δ 36.90, 65.14, 123.46, 124.93, 126.44, 129.08, 134.04, 134.23, 142.48, 149.39, 151.91, 152.52, 155.13, 194.36 (one peak for a CO ligand was not detected). ^{11}B NMR (CDCl$_3$, 128 MHz) δ 31.1. IR (υ_{CO}, cm^{-1}) 2024, 1922, 1881. Elemental anal. calcd. for $C_{64}H_{48}B_4Br_2Cl_4N_8O_{14}Re_2 \bullet 0.25\ C_6H_6$: C 41.63 H 2.64 N 5.93. Found: C 41.64 H 2.89 N 5.72. Crystals were obtained by slow diffusion of pentane into a solution of **43** in 1,2-dichloroethane.

**Complex 44:**
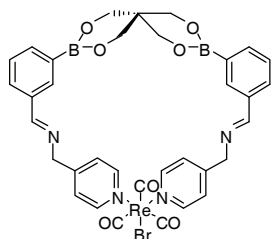
A suspension of Re(CO)$_5$Br (40.6 mg, 0.1 mmol), 3-formylphenylboronic acid (30.0 mg, 0.2 mmol), 4-(aminomethyl)pyridine (21.6 mg, 0.2 mmol) and pentaerythritol (13.6 mg, 0.1 mmol) in a 2:1 mixture of THF/benzene (90 mL) was heated under reflux using a Dean-Stark trap. After 6h, 35 mL of solvent was distilled. The solution was allowed to cool to room temperature and its volume was reduced to 10 mL. Upon addition of 20 mL of hexane a white precipitate formed which was filtered, washed with hexane and dried under vacuum. Yield: 59.8 mg, 67%. ^{1}H NMR (CDCl$_3$, 400 MHz) δ 4.06 (s, 16 H, CH$_2$O), 4.82 (s, 8 H, CH$_2$N), 7.36 (d, ^3J = 6 Hz, 8 H, pyridyl), 7.45 (t, ^3J = 7 Hz, 4 H, phenyl), 7.58 (d, ^3J = 8 Hz, 4 H, phenyl), 7.83 (d, ^3J = 7 Hz, 4 H, phenyl), 8.47 (s, 4 H, imine or phenyl), 8.53 (s, 4 H, imine or phenyl), 8.77 (d, ^3J = 6 Hz, 8 H, pyridyl). ^{13}C NMR (CDCl$_3$, 101 MHz) δ 37.30, 63.26, 64.86, 125.02, 128.13, 132.00, 133.55, 134.77, 136.63, 151.85, 154.38, 164.41, 192.19, 195.43. ^{11}B NMR (CDCl$_3$, 128 MHz) δ .29.1. IR (υ$_{CO}$, cm^{-1}) 2019, 1912, 1885. Elemental anal. calcd. for C$_{34}$H$_{30}$B$_2$BrN$_4$O$_7$Re$_2$•0.75CHCl$_3$: C 42.42 H 3.15 N 5.69. Found: C 42.10 H 3.27 N 5.66. Crystals were obtained by slow diffusion of pentane into a solution of **44** in chloroform.

Complex 45:
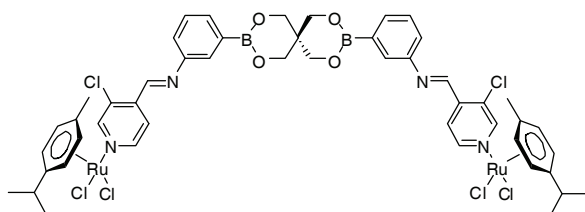
A suspension of [(p-Pr^{i}C$_6$H$_4$Me)RuCl$_2$]$_2$ (61.2 mg, 0.1 mmol), 3-aminophenylboronic acid monohydrate (31.0 mg, 0.2 mmol), 3-chloro-4-formylpyridine (28.3 mg, 0.2 mmol) and pentaerythritol (13.6 mg, 0.1 mmol) in a 1:2 mixture of methanol/benzene (90 mL) was heated under reflux using a Dean-Stark trap. The solution was refluxed for 2 h during which 70 mL of the solvent was removed. Upon cooling, an orange-brown solid precipitated. After cooling, the precipitate was filtered, washed with pentane and dried under vacuum. Yield: 86.3 mg, 72%. ^{1}H NMR (CDCl$_3$, 400 MHz): δ 1.33 (d, 12 H, ^3J = 7 Hz, CH$_3$), 2.14 (s, 6 H, CH(CH$_3$)$_2$), 3.00 (sept, ^3J = 7 Hz, 2 H, CH(CH$_3$)$_2$), 4.11 (s, 8 H, CH$_2$), 5.27 (d, 4 H, ^3J = 6 Hz, p-Pr^{i}C$_6$H$_4$Me), 5.49 (d, 4 H, ^3J = 6 Hz, p-Pr^{i}C$_6$H$_4$Me), 7.36-7.49 (m, 4 H phenyl), 7.71 (s, 2 H, phenyl), 7.77 (d, ^3J = 7 Hz, 2 H, phenyl), 8.07

(d, ^3J = 6 Hz, 2 H, pyridine), 8.87 (s, 2 H, pyridine or imine), 9.04 (d, ^3J = 6 Hz, 2 H, pyridine), 9.16 (s, 2 H, pyridine or imine). ^{13}C NMR (CDCl$_3$, 400 MHz): δ 18.46, 22.42, 30.84, 36.87, 65.06, 82.36, 83.24, 97.71, 103.87, 121.81, 124.98, 126.17, 128.98, 132.29, 133.91, 141.57, 149.57, 152.54, 153.39, 155.09. ^{11}B NMR (CDCl$_3$, 400 MHz): δ 28.5. Elemental anal. calcd. for C$_{49}$H$_{52}$B$_2$Cl$_6$N$_4$O$_4$Ru$_2$: C 49.15 H 4.38 N 4.68. Found: C 49.13 H 4.58 N 4.46.

Complex 46:
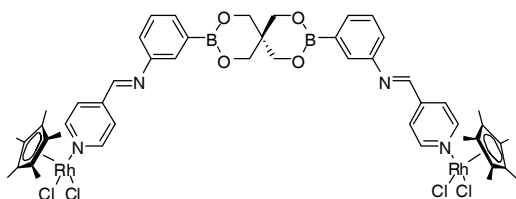
A suspension of [(C$_5$Me$_5$)RhCl$_2$]$_2$ (74.2 mg, 0.12 mmol), 3-aminophenylboronic acid monohydrate (37.2 mg, 0.24 mmol), pyridine-4-formylpyridine (25.7 mg, 0.24 mmol) and pentaerythritol (16.3 mg, 0.12 mmol) in a 1:2 mixture of methanol/benzene (90 mL) was heated under reflux using a Dean-Stark trap. The solution was refluxed for 1 h during which 50 mL of the solvent was removed. Upon cooling, an orange solid precipitated. After cooling, the precipitate was filtered, washed with pentane and dried under vacuum. Yield: 100.8 mg, 74%. ^{1}H NMR (CDCl$_3$, 400 MHz): δ 1.59 (s, 30 H, CH$_3$), 4.09 (s, 8 H, CH$_2$), 7.35-7.46 (m, 4 H phenyl), 7.67 (s, 2 H, phenyl), 7.73 (d, ^3J = 7 Hz, 2 H, phenyl), 7.83 (d, ^3J = 6 Hz, 4 H, pyridine), 8.52 (s, 2 H, imine), 9.12 (b, 4 H, pyridine). ^{13}C NMR (CDCl$_3$, 400 MHz): δ 9.03, 36.92, 65.09, 94.33, 94.40, 123.69, 124.92, 125.77, 128.94, 133.44, 144.59, 149.76, 154.24, 155.92. ^{11}B NMR (CDCl$_3$, 400 MHz): δ 28.4. Elemental anal. calcd. for C$_{49}$H$_{56}$B$_2$Cl$_4$N$_4$O$_4$Rh$_2$: C 51.89 H 4.98 N 4.94. Found: C 49.14 H 4.97 N 4.05.

8.3 Measurements

Scrambling experiments: $CDCl_3$ stock solutions of macrocycles **5** and **6** (8.3 mM) were prepared. 0.3 mL of each of the solutions were mixed in an NMR tube. A ^{1}H NMR spectrum was recorded 15 minutes after mixing. Spectra recorded more than 1h after mixing showed decomposition of the sample. A similar experiment was performed with tetrameric macrocycles **1** and **2** but no decomposition was observed after 24h.

Amine exchange on 16: A $CDCl_3$ solution (8.3 mM) of complex **16** was prepared and 8 equivalents of *p*-methoxyaniline were added. Three ^{1}H NMR spectra of the solution were recorded after 15 minutes (Figure 3.4b), 3 and 24 h. An analogous experiment (c(**16**) = 4.5 mM) was performed with benzylamine instead of *p*-methoxyaniline.

NMR titration of 26: $CDCl_3$ stock solutions of ester **26** (100 mM), 4,4'-dipyridyl (50 mM) and 1,2-di(4-pyridyl)ethylene (50 mM) were prepared. 50 μl of the stock solution of **26** were placed in an NMR tube and various amounts of ligand were added. The volume was then adjusted to 0.5 ml with $CDCl_3$ so that the final concentration of **26** was 10 mM. Thirteen ^{1}H NMR spectra were recorded corresponding to ligand concentrations of 0, 0.5, 1.0, 2.5, 5.0, 6.0, 7.5, 10.0, 15.0, 20.0, 25.0, 30.0 and 40.0 mM. The chemical shift values of the signal for the H^2 and H^6 atoms of the boronic ester phenyl ring were plotted versus the ligand concentration. The data was fitted with the non-linear least square curve-fitting program WinEQNMR[236] using a 2:1 binding model. An analogous experiment was performed using 4,4'-dipyridyl instead of 1,2-di(4-pyridyl)ethylene. Selected ^{1}H NMR spectra and the resulting binding curves are shown in the Figures 8.1 – 8.4.
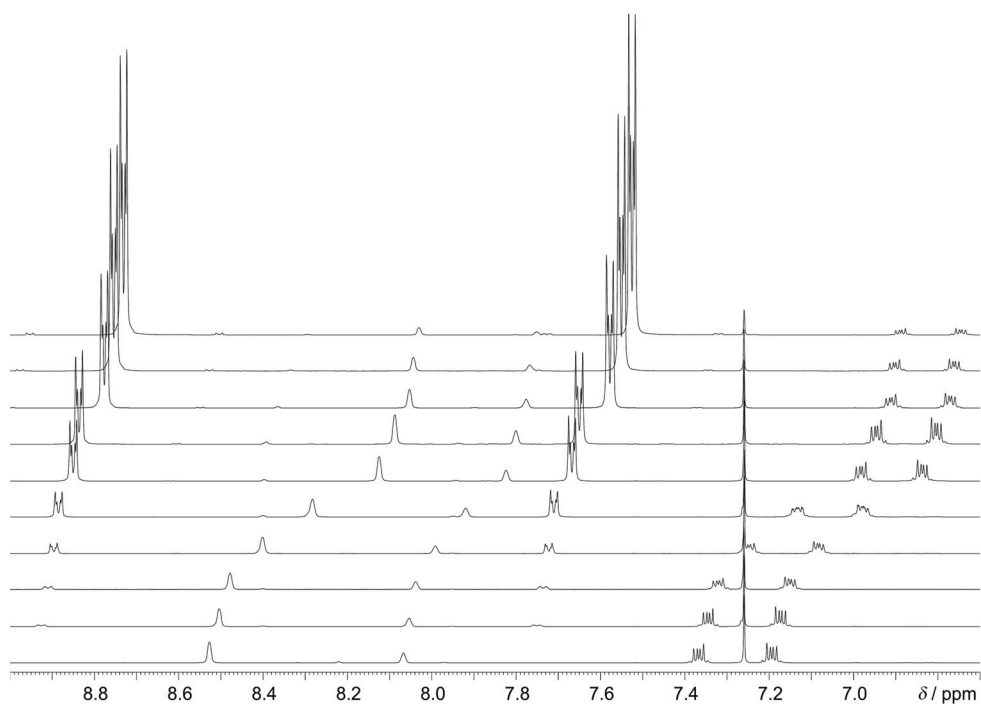
Figure 8.1: Selected ^{1}H NMR spectra in the aromatic region for the titration of **26** with 4,4'-dipyridyl (the amount of 4,4'-dipyridyl increases from the bottom to the top).
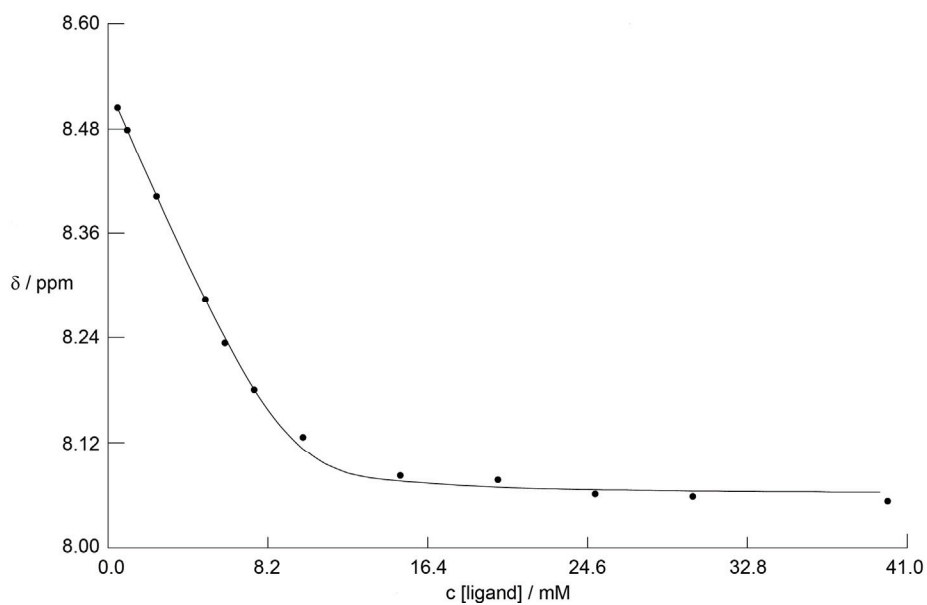
Figure 8.2: Experimental points and fitting curve for the titration of **26** with 4,4'-dipyridyl.
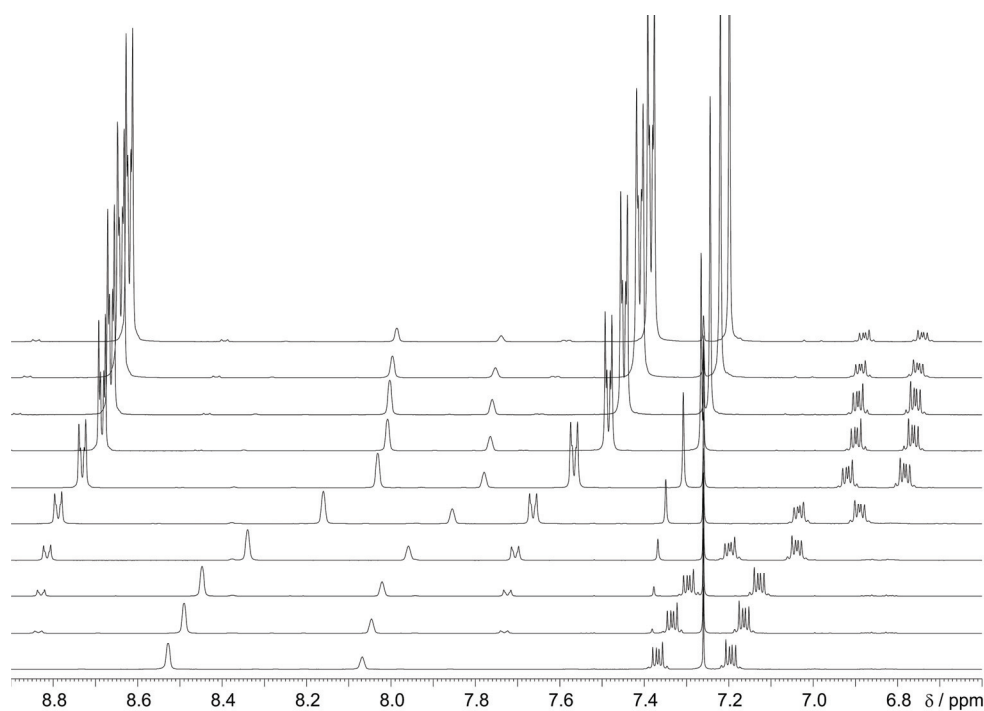
Figure 8.3: Selected ^{1}H NMR spectra in the aromatic and olefinic region for the titration of **26** with 1,2-di(4-pyridyl)ethylene (the amount of 1,2-bis(4-pyridyl)ethylene increases from the bottom to the top).
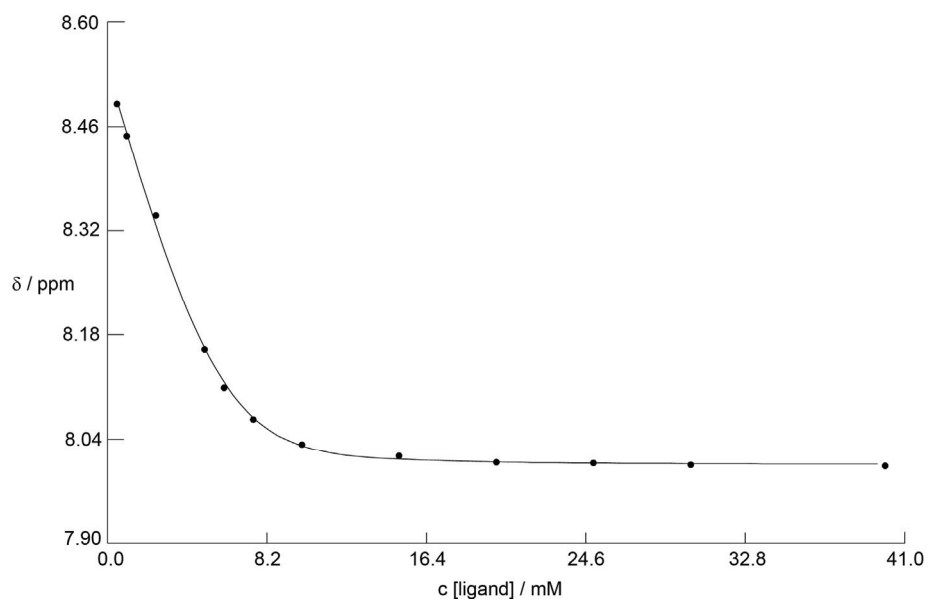
Figure 8.4: Experimental points and fitting curve for the titration of **26** with 1,2-bis(4-pyridyl)ethylene.

Chapter 9

Appendix

Table 9.1: Crystallographic data for tetramers **1** and **2**:

	Compound **1**	Compound **2** • 2 C_6H_6 • 0.5 C_5H_{12}
Empirical formula	$C_{44}H_{32}B_4N_4O_8$	$C_{78.5}H_{86}B_4N_8O_{12}$
Formula weight	787.98	1376.79
Temperature / K	140(2)	140(2)
Wavelength / Å	0.71073	0.71070
Crystal system	Tetragonal	Orthorhombic
Space group	$I4_1/a$	$Iba2$
a / Å	16.7128(8)	26.3143(18)
b / Å	16.7128(8)	28.029(2)
c / Å	13.9916(11)	20.2248(11)
α / °	90	90
β / °	90	90
γ / °	90	90
Volume / Å^3	3908.1(4)	14917.2(17)
Z	4	8
Density (calculated) / g cm^{-3}	1.339	1.226
Absorption coefficient / mm^{-1}	0.091	0.082
F(000)	1632	5832
Crystal size / mm^3	0.17 x 0.17 x 0.14	0.28 x 0.26 x 0.20
Θ range / °	3.09 to 25.02	2.91 to 25.03
Index ranges	-19 → h → 19 -18 → k → 19 -16 → l → 16	-31 → h → 31 -33 → k → 33 -22 → l → 22
Reflections collected	11750	44532
Independent reflections	1729 [R(int) = 0.0384]	12697 [R(int) = 0.0756]
Completeness to Θ / %	99.9	98.1
Absorption correction	Semi-empirical from equivalents (MULABS)	Semi-empirical from equivalents (MULABS)
Max. and min. transmission	0.863 and 0.555	1.0157 and 0.9438
Refinement method	Full-matrix least-squares on F^2	Full-matrix least-squares on F^2
Data / restraints / parameters	1729 / 0 / 137	12697 / 77 / 998
Goodness-of-fit on F^2	1.079	0.959
Final R indices [I>2sigma(I)]	R1 = 0.0347, wR2 = 0.0874	R1 = 0.0625, wR2 = 0.1348
R indices (all data)	R1 = 0.0499, wR2 = 0.0943	R1 = 0.0998, wR2 = 0.1498
Largest diff. peak and hole / e.Å^{-3}	0.350 and -0.177	0.442 and -0.208

Table 9.2: Crystallographic data for tetramer **3** and pentamer **4**:

	Compound **3** • 2 C_6H_6	Compound **4**
Empirical formula	$C_{56}H_{32}B_4F_{12}N_4O_8$	$C_{60}H_{50}B_5N_5O_{10}$
Formula weight	1160.10	1055.10
Temperature / K	140(2)	140(2)
Wavelength / Å	0.71073	0.71073
Crystal system	Triclinic	Triclinic
Space group	$P\bar{1}$	$P\bar{1}$
a / Å	13.538(4)	14.8647(16)
b / Å	13.595(10)	15.086(3)
c / Å	13.813(12)	15.349(3)
α / °	80.64(7)	100.494(15)
β / °	85.41(4)	98.176(11)
γ / °	80.58(4)	111.896(13)
Volume / $Å^3$	2471(3)	3055.9(8)
Z	2	2
Density (calculated) / g cm^{-3}	1.559	1.147
Absorption coefficient / mm^{-1}	0.133	0.077
F(000)	1176	1100
Crystal size / mm^3	0.14 x 0.14 x 0.14	0.15 x 0.14 x 0.13
Θ range / °	2.99 to 25.02	2.76 to 22.99
Index ranges	$-14 \rightarrow h \rightarrow 15$ $-16 \rightarrow k \rightarrow 16$ $-16 \rightarrow l \rightarrow 16$	$-16 \rightarrow h \rightarrow 16$ $-16 \rightarrow k \rightarrow 16$ $-16 \rightarrow l \rightarrow 16$
Reflections collected	16104	15522
Independent reflections	8192 [R(int) = 0.1172]	7644 [R(int) = 0.1056]
Completeness to Θ / %	93.8	89.9
Absorption correction	Semi-empirical from equivalents (MULABS)	None
Max. and min. transmission	1.2427 and 0.8806	
Refinement method	Full-matrix least-squares on F^2	Full-matrix least-squares on F^2
Data / restraints / parameters	8192 / 8 / 798	7644 / 245 / 726
Goodness-of-fit on F^2	0.814	0.765
Final R indices [I>2sigma(I)]	R1 = 0.0774, wR2 = 0.1810	R1 = 0.0802, wR2 = 0.1725
R indices (all data)	R1 = 0.2037, wR2 = 0.2432	R1 = 0.2455, wR2 = 0.2234
Largest diff. peak and hole / e.$Å^{-3}$	0.333 and -0.283	0.366 and -0.276

Table 9.3: Crystallographic data for pentamers **6** and **7**:

	Compound **6** • 3 C_6H_6	Compound **7** • 0.5 C_6H_6 • 0.25 C_5H_{12}
Empirical formula	$C_{73}H_{53}B_5F_5N_5O_{10}$	$C_{49.25}H_{66}B_5N_5O_{10}$
Formula weight	1309.25	942.12
Temperature / K	140(2)	100(2)
Wavelength / Å	0.71073	0.71073
Crystal system	Triclinic	Monoclinic
Space group	$P\bar{1}$	$P2_1/c$
a / Å	13.2245(19)	24.050(5)
b / Å	14.709(2)	25.720(3)
c / Å	17.609(3)	16.369(4)
α / °	71.844(15)	90
β / °	81.373(13)	90.566(14)
γ / °	83.910(13)	90
Volume / Å^3	3211.5(9)	10125(3)
Z	2	8
Density (calculated) / g cm^{-3}	1.354	1.236
Absorption coefficient / mm^{-1}	0.099	0.084
F(000)	1352	4012
Crystal size / mm^3	0.18 x 0.15 x 0.13	0.26 x 0.24 x 0.16
Θ range / °	3.04 to 25.03	2.92 to 25.03
Index ranges	$-15 \rightarrow h \rightarrow 13$ $-17 \rightarrow k \rightarrow 17$ $-20 \rightarrow l \rightarrow 20$	$-28 \rightarrow h \rightarrow 28$ $-30 \rightarrow k \rightarrow 30$ $-18 \rightarrow l \rightarrow 19$
Reflections collected	19323	55412
Independent reflections	9958 [R(int) = 0.1271]	17505 [R(int) = 0.0667]
Completeness to Θ / %	87.7	97.8
Absorption correction	Semi-empirical from equivalents (MULABS)	None
Max. and min. transmission	1.3826 and 0.8351	
Refinement method	Full-matrix least-squares on F^2	Full-matrix least-squares on F^2
Data / restraints / parameters	9958 / 290 / 868	17505 / 6 / 1279
Goodness-of-fit on F^2	0.861	1.026
Final R indices [I>2sigma(I)]	$R1$ = 0.0858, w$R2$ = 0.2085	$R1$ = 0.0962, w$R2$ = 0.2435
R indices (all data)	$R1$ = 0.2529, w$R2$ = 0.2743	$R1$ = 0.1386, w$R2$ = 0.2910
Largest diff. peak and hole / e.Å^{-3}	1.045 and -0.458	1.121 and -0.401

Table 9.4: Crystallographic data for pentamer **10** and diboroxine **18**:

	Compound **10** • 2 $CHCl_3$ • 0.5 C_5H_{12}	Compound **18** • 2 C_7H_8
Empirical formula	$C_{94.50}H_{73}B_5Cl_6N_{10}O_{10}$	$C_{74}H_{44}B_6F_{36}N_2O_6$
Formula weight	1775.38	1805.97
Temperature / K	100(2)	140(2)
Wavelength / Å	0.71073	0.71073
Crystal system	Triclinic	Triclinic
Space group	$P\bar{1}$	$P\bar{1}$
a / Å	15.9647(19)	10.2549(4)
b / Å	16.2747(18)	13.2535(5)
c / Å	19.192(2)	14.9049(6)
α / °	112.104(8)	87.613(3)
β / °	101.901(9)	81.358(3)
γ / °	94.520(9)	70.462(4)
Volume / Å^3	4452.9(9)	1887.37(13)
Z	2	1
Density (calculated) / g cm^{-3}	1.324	1.589
Absorption coefficient / mm^{-1}	0.258	0.159
F(000)	1834	904
Crystal size / mm^3	0.64 x 0.47 x 0.24	0.29 x 0.26 x 0.20
Θ range / °	1.18 to 22.99	2.70 to 26.02
Index ranges	$-17 \rightarrow h \rightarrow 17$ $-17 \rightarrow k \rightarrow 17$ $-21 \rightarrow l \rightarrow 21$	$-12 \rightarrow h \rightarrow 12$ $-15 \rightarrow k \rightarrow 16$ $-18 \rightarrow l \rightarrow 16$
Reflections collected	51049	15165
Independent reflections	12101 [R(int) = 0.0651]	7374 [R(int) = 0.0324]
Completeness to Θ / %	97.9	99.2
Absorption correction	Semi-empirical from equivalents (SADABS)	Semi-empirical from equivalents
Max. and min. transmission	1.0000 and 0.7178	1.00000 and 0.91900
Refinement method	Full-matrix least-squares on F^2	Full-matrix least-squares on F^2
Data / restraints / parameters	12101 / 6 / 1142	7374 / 198 / 722
Goodness-of-fit on F^2	1.556	0.893
Final R indices [I>2sigma(I)]	$R1$ = 0.1268, w$R2$ = 0.3497	$R1$ = 0.0475, w$R2$ = 0.1046
R indices (all data)	$R1$ = 0.1972, w$R2$ = 0.4102	$R1$ = 0.1157, w$R2$ = 0.1240
Largest diff. peak and hole / e.Å^{-3}	1.783 and -1.163	0.270 and -0.214

Table 9.5: Crystallographic data for polymers **20** and **23**:

	Compound **20** • CHCl$_3$	Compound **23**
Empirical formula	C$_{35}$H$_{31}$B$_2$Cl$_3$N$_2$O$_4$	C$_{16}$H$_{14}$BNO$_2$
Formula weight	671.59	263.09
Temperature / K	100(2)	100(2)
Wavelength / Å	0.71073	0.71073
Crystal system	Triclinic	Monoclinic
Space group	$P\bar{1}$	$P2_1/n$
a / Å	9.989(2)	8.104(5)
b / Å	12.797(4)	11.507(7)
c / Å	13.452(4)	14.356(8)
α / °	100.01(3)	90
β / °	91.234(17)	95.82(6)
γ / °	102.769(19)	90
Volume / Å^3	1648.3(8)	1331.8(14)
Z	2	4
Density (calculated) / g cm^{-3}	1.353	1.312
Absorption coefficient / mm^{-1}	0.320	0.085
F(000)	696	552
Crystal size / mm^3	0.59 x 0.29 x 0.16	0.52 x 0.15 x 0.10
Θ range / °	3.32 to 25.02	3.36 to 25.00
Index ranges	-11 → h → 11 -15 → k → 15 -16 → l → 16	-9 → h → 9 -13 → k → 13 -17 → l → 17
Reflections collected	28027	16398
Independent reflections	5765 [R(int) = 0.0729]	2338 [R(int) = 0.1178]
Completeness to Θ / %	99.3	99.7
Absorption correction	Semi-empirical from equivalents	Semi-empirical from equivalents
Max. and min. transmission	1.0000 and 0.8119	1.0000 and 0.4708
Refinement method	Full-matrix least-squares on F^2	Full-matrix least-squares on F^2
Data / restraints / parameters	5765 / 0 / 452	2338 / 0 / 181
Goodness-of-fit on F^2	1.127	1.118
Final R indices [I>2sigma(I)]	R1 = 0.0564, wR2 = 0.0860	R1 = 0.0678, wR2 = 0.1207
R indices (all data)	R1 = 0.1081, wR2 = 0.1025	R1 = 0.1249, wR2 = 0.1408
Largest diff. peak and hole / e.Å^{-3}	0.307 and -0.279	0.264 and -0.233

Table 9.6: Crystallographic data for polymer **24** and boronic ester **26**:

	Compound **24** • C_6H_6	Compound **26**
Empirical formula	$C_{22}H_{14}BF_6NO_2$	$C_{14}H_7BF_6O_2$
Formula weight	449.15	332.01
Temperature / K	100(2)	140(2)
Wavelength / Å	0.71073	0.71073
Crystal system	Triclinic	Orthorhombic
Space group	$P\bar{1}$	*Pnma*
a / Å	8.8253(18)	15.8438(13)
b / Å	10.773(2)	15.0455(10)
c / Å	10.991(2)	5.6520(4)
α / °	104.22(3)	90
β / °	97.76(3)	90
γ / °	93.71(3)	90
Volume / Å^3	998.4(4)	1347.31(17)
Z	2	4
Density (calculated) / g cm^{-3}	1.494	1.637
Absorption coefficient / mm^{-1}	0.133	0.162
F(000)	456	664
Crystal size / mm^3	0.74 x 0.33 x 0.20	0.30 x 0.20 x 0.12
Θ range / °	3.56 to 25.03	2.57 to 26.37
Index ranges	$-10 \rightarrow h \rightarrow 10$ $-12 \rightarrow k \rightarrow 12$ $-13 \rightarrow l \rightarrow 13$	$-19 \rightarrow h \rightarrow 19$ $-18 \rightarrow k \rightarrow 18$ $-7 \rightarrow l \rightarrow 7$
Reflections collected	14048	11379
Independent reflections	3464 [R(int) = 0.0771]	1422 [R(int) = 0.0511]
Completeness to Θ / %	98.2	99.8
Absorption correction	Semi-empirical from equivalents	Semi-empirical from equivalents
Max. and min. transmission	1.0000 and 0.5098	1.00000 and 0.63614
Refinement method	Full-matrix least-squares on F^2	Full-matrix least-squares on F^2
Data / restraints / parameters	3464 / 0 / 290	1422 / 0 / 109
Goodness-of-fit on F^2	1.087	1.042
Final R indices [I>2sigma(I)]	$R1 = 0.0671$, w$R2 = 0.1326$	$R1 = 0.0515$, w$R2 = 0.1372$
R indices (all data)	$R1 = 0.1051$, w$R2 = 0.1511$	$R1 = 0.0766$, w$R2 = 0.1512$
Largest diff. peak and hole / e.Å^{-3}	0.438 and -0.415	0.350 and -0.370

Table 9.7: Crystallographic data for complex **28** and rotaxane **29**:

	Compound **28**	Compound **29**
Empirical formula	$C_{40}H_{24}B_2F_{12}N_2O_4$	$C_{76}H_{68}B_2F_{12}N_2O_{14}$
Formula weight	846.23	1482.94
Temperature / K	140(2)	100(2)
Wavelength / Å	0.71073	0.71073
Crystal system	Monoclinic	Monoclinic
Space group	$P2_1/n$	$P2_1/c$
a / Å	9.3538(3)	11.7382(12)
b / Å	15.8385(5)	16.517(3)
c / Å	12.5323(4)	17.832(4)
α / °	90	90
β / °	93.371(3)	98.670(13)
γ / °	90	90
Volume / Å^3	1853.45(10)	3417.7(10)
Z	2	2
Density (calculated) / g cm^{-3}	1.516	1.441
Absorption coefficient / mm^{-1}	0.138	0.119
F(000)	856	1536
Crystal size / mm^3	0.32 x 0.25 x 0.19	0.46 x 0.36 x 0.31
Θ range / °	2.80 to 26.37	3.33 to 25.01
Index ranges	$-11 \rightarrow h \rightarrow 11$ $-19 \rightarrow k \rightarrow 19$ $-15 \rightarrow l \rightarrow 15$	$-13 \rightarrow h \rightarrow 13$ $-19 \rightarrow k \rightarrow 19$ $-21 \rightarrow l \rightarrow 21$
Reflections collected	15445	40239
Independent reflections	3763 [R(int) = 0.0154]	5990 [R(int) = 0.0786]
Completeness to Θ / %	99.2	98.7
Absorption correction	Semi-empirical from equivalents	Semi-empirical from equivalents
Max. and min. transmission	1.00000 and 0.90625	1.0000 and 0.8159
Refinement method	Full-matrix least-squares on F^2	Full-matrix least-squares on F^2
Data / restraints / parameters	3763 / 0 / 272	5990 / 10 / 498
Goodness-of-fit on F^2	1.037	2.105
Final R indices [I>2sigma(I)]	$R1$ = 0.0368, w$R2$ = 0.0907	$R1$ = 0.1633, w$R2$ = 0.4567
R indices (all data)	$R1$ = 0.0476, w$R2$ = 0.0991	$R1$ = 0.2110, w$R2$ = 0.5002
Largest diff. peak and hole / e.Å^{-3}	0.491 and -0.454	0.720 and -0.642

Table 9.8: Crystallographic data for rotaxane **30** and complex **32**:

	Compound **30** • 3 C_7H_8	Compound **32** • C_7H_8
Empirical formula	$C_{89}H_{88}B_2F_{12}N_2O_{14}$	$C_{73}H_{70}B_2F_{12}N_2O_{14}$
Formula weight	1659.23	1448.93
Temperature / K	140(2)	140(2)
Wavelength / Å	0.71073	0.71073
Crystal system	Triclinic	Monoclinic
Space group	$P\bar{1}$	$P2_1/c$
a / Å	13.4013(9)	14.0418(4)
b / Å	14.5562(10)	22.0219(6)
c / Å	22.3107(17)	22.2997(6)
α / °	96.487(6)	90
β / °	107.062(6)	96.386(3)
γ / °	92.798(6)	90
Volume / Å^3	4118.6(5)	6852.9(3)
Z	2	4
Density (calculated) / g cm^{-3}	1.338	1.404
Absorption coefficient / mm^{-1}	0.107	0.117
F(000)	1732	3008
Crystal size / mm^3	0.11 x 0.08 x 0.07	0.42 x 0.28 x 0.17
Θ range / °	2.60 to 22.98	2.61 to 25.03
Index ranges	$-14 \rightarrow h \rightarrow 14$ $-15 \rightarrow k \rightarrow 15$ $-24 \rightarrow l \rightarrow 24$	$-16 \rightarrow h \rightarrow 16$ $-26 \rightarrow k \rightarrow 26$ $-26 \rightarrow l \rightarrow 26$
Reflections collected	26573	45866
Independent reflections	11389 [R(int) = 0.1597]	12085 [R(int) = 0.0413]
Completeness to Θ / %	99.5	99.9
Absorption correction	Semi-empirical from equivalents	Semi-empirical from equivalents
Max. and min. transmission	1.00000 and 0.80453	1.00000 and 0.88194
Refinement method	Full-matrix least-squares on F^2	Full-matrix least-squares on F^2
Data / restraints / parameters	11389 / 804 / 1141	12085 / 0 / 947
Goodness-of-fit on F^2	1.038	1.042
Final R indices [I>2sigma(I)]	$R1$ = 0.1543, w$R2$ = 0.3282	$R1$ = 0.0696, w$R2$ = 0.1601
R indices (all data)	$R1$ = 0.3203, w$R2$ = 0.4318	$R1$ = 0.1260, w$R2$ = 0.2075
Largest diff. peak and hole / e.Å^{-3}	0.933 and -0.382	1.074 and -0.758

Table 9.9: Crystallographic data for macrocycles **33** and **35**:

	Compound **33** • 2 CHCl$_3$	Compound **35** • 6 C$_2$H$_4$Cl$_2$
Empirical formula	C$_{52}$H$_{46}$B$_4$Cl$_6$N$_4$O$_8$	C$_{70}$H$_{76}$B$_4$Cl$_{12}$N$_4$O$_{12}$
Formula weight	1110.87	1633.99
Temperature / K	100(2)	100(2)
Wavelength / Å	0.71073	0.71073
Crystal system	Monoclinic	Triclinic
Space group	$P2_1/n$	$P\bar{1}$
a / Å	6.475(3)	10.1065(18)
b / Å	19.32(2)	12.1629(17)
c / Å	21.19(2)	18.220(3)
α / °	90	100.056(12)
β / °	94.73(6)	101.974(14)
γ / °	90	101.579(14)
Volume / Å^3	2641(4)	2091.0(6)
Z	2	1
Density (calculated) / g cm^{-3}	1.397	1.298
Absorption coefficient / mm^{-1}	0.383	0.454
F(000)	1144	844
Crystal size / mm^3	0.62 x 0.09 x 0.08	0.18 x 0.12 x 0.10
Θ range / °	3.31 to 22.99	2.59 to 25.03
Index ranges	-7 → h → 7 -21 → k → 21 -23 → l → 23	-12 → h → 11 -14 → k → 14 -20 → l → 21
Reflections collected	25326	15271
Independent reflections	3606 [R(int) = 0.2049]	7300 [R(int) = 0.1377]
Completeness to Θ / %	98.5	98.9
Absorption correction	None	Semi-empirical from equivalents
Max. and min. transmission		1.00000 and 0.57029
Refinement method	Full-matrix least-squares on F^2	Full-matrix least-squares on F^2
Data / restraints / parameters	3606 / 0 / 362	7300 / 34 / 457
Goodness-of-fit on F^2	1.094	0.855
Final R indices [I>2sigma(I)]	R1 = 0.1103, wR2 = 0.2098	R1 = 0.1403, wR2 = 0.3430
R indices (all data)	R1 = 0.2097, wR2 = 0.2643	R1 = 0.3268, wR2 = 0.4014
Largest diff. peak and hole / e.Å^{-3}	0.384 and -0.284	0.756 and -0.631

Table 9.10: Crystallographic data for macrocycles **36** and **37**:

	Compound **36**	Compound **37** • 3 $C_2H_4Cl_2$
Empirical formula	$C_{58}H_{52}B_4N_4O_8$	$C_{64}H_{64}B_4Cl_6N_4O_8$
Formula weight	976.28	1273.13
Temperature / K	100(2)	100(2)
Wavelength / Å	0.71073	0.71073
Crystal system	Triclinic	Triclinic
Space group	$P\bar{1}$	$P\bar{1}$
a / Å	6.2923(13)	6.2306(12)
b / Å	15.464(3)	13.846(3)
c / Å	16.056(3)	18.880(4)
α / °	103.15(3)	77.29(3)
β / °	95.55(3)	87.94(3)
γ / °	101.18(3)	88.75(3)
Volume / Å^3	1476.2(5)	1587.7(5)
Z	1	1
Density (calculated) / g cm^{-3}	1.098	1.332
Absorption coefficient / mm^{-1}	0.072	0.328
F(000)	512	662
Crystal size / mm^3	0.88 x 0.21 x 0.09	0.54 x 0.14 x 0.06
Θ range / °	3.31 to 23.25	3.32 to 23.26
Index ranges	-6 → h → 6 -17 → k → 17 -27 → l → 27	-6 → h → 6 -15 → k → 15 -20 → l → 20
Reflections collected	15397	11757
Independent reflections	4146 [R(int) = 0.0892]	4368 [R(int) = 0.1432]
Completeness to Θ / %	98.2	96.1
Absorption correction	Semi-empirical from equivalents	Semi-empirical from equivalents
Max. and min. transmission	1.0000 and 0.6687	1.0000 and 0.7271
Refinement method	Full-matrix least-squares on F^2	Full-matrix least-squares on F^2
Data / restraints / parameters	4146 / 0 / 334	4368 / 325 / 465
Goodness-of-fit on F^2	1.035	1.068
Final R indices [I>2sigma(I)]	$R1$ = 0.0931, w$R2$ = 0.2168	$R1$ = 0.1165, w$R2$ = 0.1567
R indices (all data)	$R1$ = 0.1499, w$R2$ = 0.2438	$R1$ = 0.2929, w$R2$ = 0.2115
Largest diff. peak and hole / e.Å^{-3}	0.460 and -0.307	0.435 and -0.478

Table 9.11: Crystallographic data for cages **38** and **39**:

	Compound **38** • 4 $CHCl_3$	Compound **39** • 8 $C_2H_4Cl_2$
Empirical formula	$C_{73}H_{82}B_6Cl_{12}N_8O_{12}$	$C_{103}H_{128}B_6Cl_{16}N_6O_{12}$
Formula weight	1753.73	2274.17
Temperature / K	100(2)	100(2)
Wavelength / Å	0.71073	0.71073
Crystal system	Rhombohedral	Orthorhombic
Space group	$R\bar{3}c$	$P2_12_12_1$
a / Å	18.110(3)	15.021(3)
b / Å	18.110(3)	15.613(2)
c / Å	50.971(10)	49.722(9)
α / °	90	90
β / °	90	90
γ / °	120	90
Volume / Å^3	14477(4)	11661(3)
Z	6	4
Density (calculated) / g cm^{-3}	1.207	1.295
Absorption coefficient / mm^{-1}	0.398	0.434
F(000)	5436	4744
Crystal size / mm^3	0.33 x 0.33 x 0.21	0.58 x 0.18 x 0.14
Θ range / °	3.45 to 20.06	3.32 to 20.60
Index ranges	$-17 \rightarrow h \rightarrow 17$ $-17 \rightarrow k \rightarrow 17$ $-48 \rightarrow l \rightarrow 48$	$-14 \rightarrow h \rightarrow 14$ $-15 \rightarrow k \rightarrow 14$ $-49 \rightarrow l \rightarrow 49$
Reflections collected	36623	70710
Independent reflections	1514 [R(int) = 0.1511]	11693 [R(int) = 0.0640]
Completeness to Θ / %	99.3	99.2
Absorption correction	Semi-empirical from equivalents	Semi-empirical from equivalents
Max. and min. transmission	1.0000 and 0.5621	1.0000 and 0.6897
Refinement method	Full-matrix least-squares on F^2	Full-matrix least-squares on F^2
Data / restraints / parameters	1514 / 60 / 217	11693 / 888 / 1302
Goodness-of-fit on F^2	1.106	1.102
Final R indices [I>2sigma(I)]	$R1$ = 0.1298, w$R2$ = 0.3160	$R1$ = 0.0739, w$R2$ = 0.1833
R indices (all data)	$R1$ = 0.1578, w$R2$ = 0.3347	$R1$ = 0.0968, w$R2$ = 0.2010
Largest diff. peak and hole / e.Å^{-3}	0.496 and -0.318	0.977 and -0.551

Table 9.12: Crystallographic data for macrocycles **40** and **41**:

	Compound **40**	Compound **41** • 4 $C_2H_4Cl_2$
Empirical formula	$C_{36}H_{32}B_4Br_2N_4O_{14}Re_2$	$C_{44}H_{48}B_4Br_2Cl_8N_4O_{14}Re_2$
Formula weight	1320.12	1715.92
Temperature / K	100(2)	100(2)
Wavelength / Å	0.71073	0.71073
Crystal system	Monoclinic	Monoclinic
Space group	$P2_1$	$P2_1/n$
a / Å	14.666(5)	14.292(3)
b / Å	11.014(3)	13.3488(12)
c / Å	19.728(9)	16.141(2)
α / °	90	90
β / °	102.85(3)	100.100(13)
γ / °	90	90
Volume / Å^3	3106.7(19)	3031.8(7)
Z	2	2
Density (calculated) / g cm^{-3}	1.411	1.880
Absorption coefficient / mm^{-1}	5.227	5.721
F(000)	1256	1656
Crystal size / mm^3	0.31 x 0.30 x 0.11	0.35 x 0.28 x 0.16
Θ range / °	3.36 to 25.03	3.32 to 27.53
Index ranges	$-17 \rightarrow h \rightarrow 17$ $-13 \rightarrow k \rightarrow 13$ $-23 \rightarrow l \rightarrow 22$	$-18 \rightarrow h \rightarrow 18$ $-17 \rightarrow k \rightarrow 17$ $-20 \rightarrow l \rightarrow 20$
Reflections collected	38074	65757
Independent reflections	10602 [R(int) = 0.1087]	6952 [R(int) = 0.0486]
Completeness to Θ / %	99.5	99.6
Absorption correction	Semi-empirical from equivalents	Semi-empirical from equivalents
Max. and min. transmission	1.0000 and 0.4597	1.0000 and 0.6324
Refinement method	Full-matrix least-squares on F^2	Full-matrix least-squares on F^2
Data / restraints / parameters	10602 / 235 / 601	6952 / 0 / 399
Goodness-of-fit on F^2	1.054	1.214
Final R indices [I>2sigma(I)]	$R1 = 0.0784$, w$R2 = 0.1960$	$R1 = 0.0310$, w$R2 = 0.0620$
R indices (all data)	$R1 = 0.0912$, w$R2 = 0.2070$	$R1 = 0.0421$, w$R2 = 0.0663$
Largest diff. peak and hole / e.Å^{-3}	3.952 and -1.624	1.127 and -1.005

Table 9.13: Crystallographic data for macrocycles **43** and **44**:

	Compound **43** • 3 $C_2H_4Cl_2$	Compound **44** • $CHCl_3$
Empirical formula	$C_{70}H_{60}B_4Br_2Cl_{10}N_8O_{14}Re_2$	$C_{35}H_{31}B_2BrCl_3N_4O_7Re$
Formula weight	2167.22	1013.72
Temperature / K	100(2)	100(2)
Wavelength / Å	0.71073	0.71073
Crystal system	Triclinic	Monoclinic
Space group	$P\bar{1}$	$P2_1/n$
a / Å	15.23(2)	16.332(3)
b / Å	16.991(12)	12.2860(9)
c / Å	20.60(2)	20.1121(16)
α / °	97.48(7)	90
β / °	107.74(9)	98.686(9)
γ / °	101.23(8)	90
Volume / Å^3	4876(9)	3989.3(8)
Z	2	4
Density (calculated) / g cm^{-3}	1.476	1.688
Absorption coefficient / mm^{-1}	3.628	4.299
F(000)	2116	1984
Crystal size / mm^3	0.61 x 0.33 x 0.14	0.59 x 0.23 x 0.21
Θ range / °	3.31 to 22.99	3.31 to 27.51
Index ranges	-16 → h → 16 -18 → k → 18 -22 → l → 22	-21 → h → 21 -15 → k → 15 -26 → l → 26
Reflections collected	55052	81882
Independent reflections	13133 [R(int) = 0.1471]	9112 [R(int) = 0.0846]
Completeness to Θ / %	97.0	99.3
Absorption correction	Numerical	Semi-empirical from equivalents
Max. and min. transmission	1.0000 and 0.3567	1.0000 and 0.3816
Refinement method	Full-matrix least-squares on F^2	Full-matrix least-squares on F^2
Data / restraints / parameters	13133 / 56 / 1068	9112 / 0 / 531
Goodness-of-fit on F^2	1.053	1.190
Final R indices [I>2sigma(I)]	$R1$ = 0.1079, w$R2$ = 0.2492	$R1$ = 0.0488, w$R2$ = 0.0826
R indices (all data)	$R1$ = 0.1787, w$R2$ = 0.3088	$R1$ = 0.0804, w$R2$ = 0.0936
Largest diff. peak and hole / e.Å^{-3}	3.842 and -3.067	1.092 and -0.964

Chapter 10

Bibliography

[1] B. Dietrich, P. Viout, J.-M. Lehn, *Macrocyclic Chemistry: Aspects of Organic and Inorganic Supramolecules*, Wiley-VCH, Weinheim **1993**.

[2] Z. R. Laughrey, B. C. Gibb, *Top. Curr. Chem.* **2005**, *249*, 67-125.

[3] F. Diederich, P. J. Stang, *Templated Organic Synthesis*, Wiley-VCH, Weinheim **2000**.

]4] J.-M. Lehn, *Supramolecular Chemistry: Concepts and Perspectives*, Wiley-VCH, Weinheim, **1995**.

[5] J. W. Steed, J. L. Atwood, *Supramolecular Chemistry*, Wiley-VCH, Weinheim, **2000**.

[6] P. T. Corbett, J. Leclaire, L. Vial, K. R. West, J.-L. Wietor, J. K. M. Sanders, S. Otto, *Chem. Rev.* **2006**, *106*, 3652-3711.

[7] S. J. Rowan, S. J. Cantrill, G. R. L. Cousins, J. K. M. Sanders, J. F. Stoddart, *Angew. Chem. Int. Ed.* **2002**, *41*, 898-952.

[8] D. Philp, J. F. Stoddart, *Angew. Chem. Int. Ed. Engl.* **1996**, *35*, 1154-1196.

[9] P. J. Stang, B. Olenyuk, *Acc. Chem. Res.* **1997**, *30*, 502-518.

[10] S. Leininger, B. Olenyuk, P. J. Stang, *Chem. Rev.* **2000**, *100*, 853-908.

[11] B. J. Holliday, C. A. Mirkin, *Angew. Chem. Int. Ed.* **2001**, *40*, 2022-2043.

[12] N. E. Borisova, M. D. Reshetova, Y. A. Ustynyuk, *Chem. Rev.* **2007**, *107*, 46-79.

[13] P. A. Vigato, S. Tamburini, *Coord. Chem. Rev.* **2004**, *248*, 1717-2128.

[14] P. A. Vigato, S. Tamburini, L. Bertolo, *Coord. Chem. Rev.* **2007**, *251*, 1311-1492.

[15] H. Höpfl, *Struct. Bonding* **2002**, *103*, 1-56.

[16] S. R. Seidel, P. J. Stang, *Acc. Chem. Res.* **2002**, *35*, 972-983.

[17] L. R. MacGillivray, J. L. Atwood, *Angew. Chem. Int. Ed.* **1999**, *38*, 1018-1033.

[18] M. Ruben, J. Rojo, F. J. Romero-Salguero, L. H. Uppadine, J.-M. Lehn, *Angew. Chem. Int. Ed.* **2004**, *43*, 3644-3662.

[19] M. Albrecht, *Chem. Rev.* **2001**, *101*, 3457-3497.

[20] D. R. Turner, A. Pastor, M. Alajarin, J. W. Steed, *Struct. Bond.* **2004**, *108*, 97-168.

[21] G. F. Swiegers, T. J. Malefetse, *Chem. Rev.* **2000**, *100*, 3483-3537.

[22] P. M. Stricklen, E. J. Volcko, J. G. Verkade, *J. Am. Chem. Soc.* **1983**, *105*, 2494-2495.

[23] M. Fujita, J. Yazaki, K. Ogura, *J. Am. Chem. Soc.* **1990**, *112*, 5645-5647.

[24] M. Fujita, M. Tominaga, A. Hori, B. Therrien, *Acc. Chem. Res.* **2005**, *38*, 371-380.

[25] A. Sautter, D. G. Schmid, G. Jung, F. Würthner, *J. Am. Chem. Soc.* **2001**, *123*, 5424-5430.

[26] M. Schweiger, S. R. Seidel, A. M. Arif, P. J. Stang, *Inorg. Chem.* **2002**, *41*, 2556-2559.

[27] B. Olenyuk, A. Fechtenkötter, P. J. Stang, *J. Chem. Soc., Dalton Trans.* **1998**, 1707-1728.

[28] M. Fujita, K. Umemoto, M. Yoshizawa, N. Fujita, T. Kusukawa, K. Biradha, *Chem. Commmun.* **2001**, 509-517.

[29] M. Fujita, D. Oguro, M. Miyazawa, H. Oka, K. Yamaguchi, K. Ogura, *Nature* **1995**, *378*, 469-471.

[30] M. Kawano, Y. Kobayashi, T. Ozeki, M. Fujita, *J. Am. Chem. Soc.* **2006**, *128*, 6558-6559.

[31 S. Tashiro, M. Tominaga, M. Kawano, B. Therrien, T. Ozeki, M. Fujita, *J. Am. Chem. Soc.* **2005**, *127*, 4546-4547.

[32] M. Yoshizawa, T. Kusukawa, M. Fujita, K. Yamaguchi, *J. Am. Chem. Soc.* **2000**, *122*, 6311-6312.

[33] M. Yoshizawa, M. Tamura, M. Fujita, *Science* **2006**, *312*, 251-254.

[34] A. W. Maverick, F. E. Klavetter, *Inorg. Chem.* **1984**, *23*, 4129-4130.

[35] A. W. Maverick, S. C. Buckingham, Q. Yao, J. R. Bradbury, G. G. Stanley, *J. Am. Chem. Soc.* **1986**, *108*, 7430-7431.

[36] R. W. Saalfrank, A. Stark, M. Bremer, H.-U. Hummel, *Angew. Chem. Int. Ed. Engl.* **1990**, *29*, 311-314.

[37] R. W. Saalfrank, E. Uller, B. Demleitner, I. Bernt, *Struct. Bonding* **2000**, *96*, 149-175.

[38] P. N. W. Baxter, J.-M. Lehn, A. DeCian, J. Fischer, *Angew. Chem. Int. Ed. Engl.* **1993**, 69-72.

[39] P. N. W. Baxter, J.-M. Lehn, G. Baum, D. Fenske, *Chem. Eur. J.* **1999**, *5*, 102-112.

[40] P. N. W. Baxter, J.-M. Lehn, B. Kneisel, G. Baum, D. Fenske, *Chem. Eur. J.* **1999**, *5*, 113-120.

[41] C. Brückner, R. E. Powers, K. N. Raymond, *Angew. Chem. Int. Ed.* **1998**, *37*, 1837-1839.

[42] D. L. Caulder, C. Brückner, R. E. Powers, S. König, T. N. Parac, J. A. Leary, K. N. Raymond, *J. Am. Chem. Soc.* **2001**, *123*, 8923-8938.

[43] D. L. Caulder, K. N. Raymond, *Acc. Chem. Res.* **1999**, *32*, 975-982.

[44] D. L. Caulder, K. N. Raymond, *J. Chem. Soc., Dalton Trans.* **1999**, 1185-1200.

[45] D. H. Leung, D. Fiedler, R. G. Bergman, K. N. Raymond, *Angew. Chem. Int. Ed.* **2004**, *43*, 963-966.

[46] D. Fiedler, R. G. Bergman, K. N. Raymond, *Angew. Chem. Int. Ed.* **2004**, *43*, 6748-6751.

[47] M. D. Pluth, R. G. Bergman, K. N. Raymond, *Science* **2007**, *316*, 85-88.

[48] M. D. Pluth, R. G. Bergman, K. N. Raymond, *Angew. Chem. Int. Ed.* **2007**, *46*, 8587-8589.

[49] J. R. Farrell, C. A. Mirkin, I. A. Guzei, L. M. Liable-Sands, A. L. Rheingold, *Angew. Chem. Int. Ed.* **1998**, *37*, 465-467.

[50] J. R. Farrell, C. A. Mirkin, *J. Am. Chem. Soc.* **1998**, *120*, 11834-11835.

[51] N. C. Gianneschi, M. S. Masar III, C. A. Mirkin, *Acc. Chem. Res.* **2005**, *38*, 825-837.

[52] N. C. Gianneschi, P. A. Bertin, S. T. Nguyen, C. A. Mirkin, L. N. Zakharov, A. L. Rheingold, *J. Am. Chem. Soc.* **2003**, *125*, 10508-10509.

[53] N. C. Gianneschi, S. T. Nguyen, C. A. Mirkin, *J. Am. Chem. Soc.* **2005**, *127*, 1644-1645.

[54] H. J. Yoon, J. Heo, C. A. Mirkin, *J. Am. Chem. Soc.* **2007**, *129*, 14182-14183.

[55] B. Olenyuk, J. A. Whiteford, A. Fechtenkötter, P. J. Stang, *Nature* **1999**, *398*, 796-799.

[56] S.-S. Sun, A. J. Lees, *J. Am. Chem. Soc.* **2000**, *122*, 8956-8967.

[57] D. Dragancea, V. B. Arion, S. Shova, E. Rentschler, N. V. Gerbeleu, *Angew. Chem. Int. Ed.* **2005**, *44*, 7938-7942.

[58] C. Pariya, C. R. Sparrow, C.-K. Back, G. Sandí, F. R. Fronczek, A. W. Maverick, *Angew. Chem. Int. Ed.* **2007**, *46*, 6305-6308.

[59] C.-Y. Su, Y.-P. Cai, C.-L. Chen, M. D. Smith, W. Kaim, H.-C. zur Loye, *J. Am. Chem. Soc.* **2003**, *125*, 8595-8613.

[60] R. Lin, J. H. K. Yip, K. Zhang, L. L. Koh, K.-W. Wong, K. P. Ho, *J. Am. Chem. Soc.* **2004**, *126*, 15852-15869.

[61] G. Li, W. Yu, J. Ni, T. Liu, Y. Liu, E. Sheng, Y. Cui, *Angew. Chem. Int. Ed.* **2008**, *47*, 1245-1249.

[62] B. Hasenknopf, J.-M. Lehn, N. Boumediene, A. Dupont-Gervais, A. Van Dorsselaer, B. Kneisel, D. Fenske, *J. Am. Chem. Soc.* **1997**, *119*, 10956-10962.

[63] K. Severin, *Chem. Commun.* **2006**, 3859-3867.

[64] I. M. Müller, D. Möller, C. A. Schalley, *Angew. Chem. Int. Ed.* **2005**, *44*, 480-484.

[65] M. A. Pitt, D. W. Johnson, *Chem. Soc. Rev.* **2007**, *36*, 1441-1453.

[66] J.-C. G. Bünzli, C. Piguet, *Chem. Rev.* **2002**, *102*, 1897-1928.

[67] J. L. Kiplinger, J. A. Pool, E. J. Schelter, J. D. Thompson, B. L. Scott, D. E. Morris, *Angew. Chem. Int. Ed.* **2006**, *45*, 2036-2041.

[68] P. J. Steel, *Molecules* **2004**, *9*, 440-448.

[69] P. J. Steel, *Acc. Chem. Res.* **2005**, *38*, 243-250.

[70] M. Albrecht, I. Janser, R. Fröhlich, *Chem. Commun.* **2005**, 157-165.

[71] F. A. Cotton, C. Lin, C. A. Murillo, *Acc. Chem. Res.* **2001**, *34*, 759-771.

[72] P. Thanasekaran, R.-T. Liao, Y.-H. Liu, T. Rajendra, S. Rajagopal, K.-L. Lu, *Coord. Chem. Rev.* **2005**, *249*, 1085-1110.

[73] H. Schiff, *Justus Liebigs Ann. Chem.* **1864**, *131*, 118-119.

[74] L. A. Wessjohann, D. G. Rivera, F. León, *Org. Lett.* **2007**, *9*, 4733-4736.

[75] J. Gawronski, H. Kolbon, M. Kwit, A. Katrusiak, *J. Org. Chem.* **2000**, *65*, 5768-5773.

[76] N. Kuhnert, A. Lopez-Periago, G. M. Rossignolo, *Org. Biomol. Chem.* **2005**, *3*, 524-537.

[77] M. Kwit, A. Plutecka, U. Rychlewska, J. Gawronski, A. F. Khlebnikov, S. I. Kozhushkov, K. Rauch, A. de Meijere, *Chem. Eur. J.* **2007**, *13*, 8688-8695.

[78] J.-M. Lehn, *Acc. Chem. Res.* **1978**, *11*, 49-57.

[79] O. D. Fox, T. D. Rolls, M. G. B. Drew, P. D. Beer, *Chem. Commun.* **2001**, 1632-1633.

[80] S. Schmidt, W. Bauer, F. W. Heinemann, H. Laning, A. Grohmann, *Angew. Chem. Int. Ed.* **2000**, *39*, 913-916.

[81] M. L. C. Quan, D. J. Cram, *J. Am. Chem. Soc.* **1991**, *113*, 2754-2755.

[82] S. Ro, S. J. Rowan, A. R. Pease, D. J. Cram, J. F. Stoddart, *Org. Lett.* **2000**, *2*, 2411-2414.

[83] X. Liu, Y. Liu, G. Li, R. Warmuth, *Angew. Chem. Int. Ed.* **2006**, *45*, 901-904.

[84] X. Liu, R. Warmuth, *J. Am. Chem. Soc.* **2006**, *128*, 14120-14127.

[85] Y. Liu, X. Liu, R. Warmuth, *Chem. Eur. J.* **2007**, *13*, 8953-8959.

[86] P. T. Glink, A. I. Oliva, J. F. Stoddart, A. J. P. White, D. J. Williams, *Angew. Chem. Int. Ed.* **2001**, *40*, 1870-1875.

[87] F. Aricó, T. Chang, S. J. Cantrill, S. I. Khan, J. F. Stoddart, *Chem. Eur. J.* **2005**, *11*, 4655-4666.

[88] A. R. Williams, B. H. Northrop, T. Chang, J. F. Stoddart, A. J. P. White, D. J. Williams, *Angew. Chem. Int. Ed.* **2006**, *45*, 6665-6669.

[89] G. A. Melson, D. H. Busch, *J. Am. Chem. Soc.* **1964**, *86*, 4834-4837.

[90] A. González-Álvarez, I. Alfonso, F. López-Ortiz, Á. Aguirre, S. García-Granda, V. Gotor, *Eur. J. Org. Chem.* **2004**, 1117-1127.

[91] J. R. Nitschke, *Acc. Chem. Res.* **2007**, *40*, 103-112.

[92] J. R. Nitschke, *Angew. Chem. Int. Ed.* **2004**, *43*, 3073-3075.

[93] M. Hutin, C. A. Schalley, G. Bernardinelli, J. R. Nitschke, *Chem. Eur. J.* **2006**, *12*, 4069-4079.

[94] D. A. Leigh, P. J. Lusby, S. J. Teat, A. J. Wilson, J. K. Y. Wong, *Angew. Chem. Int. Ed.* **2001**, *40*, 1538-1543.

[95] C. D. Meyer, C. S. Joiner, J. F. Stoddart, *Chem. Soc. Rev.* **2007**, *36*, 1705-1723.

[96] K. S. Chichak, S. J. Cantrill, A. R. Pease, S.-H. Chiu, G. W. V. Cave, J. L. Atwood, J. F. Stoddart, *Science* **2004**, *304*, 1308-1312.

[97] S. J. Cantrill, K. S. Chichak, A. J. Peters, J. F. Stoddart, *Acc. Chem. Res.* **2005**, *38*, 1-9.

[98] C. D. Pentecost, K. S. Chichak, A. J. Peters, G. W. V. Cave, S. J. Cantrill, J. F. Stoddart, *Angew. Chem. Int. Ed.* **2007**, *46*, 218-222.

[99] D. G. Hall, *Boronic Acids*, Wiley-VCH, Weinheim, **2005**.

[100] E. Frankland, B. F. Duppa, *Justus Liebigs Ann. Chem.* **1860**, *115,* 319.

[101] N. Miyaura, K. Yamada, A. Suzuki, *Tetrahedron Lett.* **1979**, *36*, 3437-3440.

[102] N. Miyaura, A. Suzuki, *Chem. Rev.* **1995**, *95*, 2457-2483.

[103] E. Khotinsky, M. Melamed, *Ber. Dtsch. Chem. Ges.* **1909**, *42*, 3090.

[104] J. P. Lorand, J. O. Edwards, *J. Org. Chem.* **1959**, *24*, 769-774.

[105] L. I. Bosch, T. M. Fyles, T. D. James, *Tetrahedron* **2004**, *60,* 11175-11190.

[106] L. Babcock, R. Pizer, *Inorg. Chem.* **1980**, *19*, 56–61.

[107] F. C. Fisher, E. Havinga, *Recl. Trav. Chim. Pays-Bas* **1974**, *93*, 21–24.

[108] S. Geller, *J. Chem. Phys.* **1960**, *32*, 1569-1570

[109] M. A. Dvorak, R. S. Ford, R. D. Suenram, F. J. Lovas, K. R. Leopold, *J. Am. Chem. Soc.* **1992**, *114*, 108-115.

[110] H. C. Brown, H. Bartholomay, M. D. Taylor, *J. Am. Chem. Soc.* **1944**, *66*, 435-442.

[111] S. Toyota, M. Oki, *Bull. Chem. Soc. Jpn.* **1992**, *65,* 1832-1840

[112] H. Höpfl, *J. Organomet. Chem.* **1999**, *581*, 129-149.

[113] S. L. Wiskur, J. J. Lavigne, H. Ait-Haddou, V. Lynch, Y. H. Chiu, J. W. Canary, E. V. Anslyn, *Org. Lett.* **2001**, *3*, 1311-1314.

[114] L. Zhu, S. H. Shabbir, M. Gray, V. M. Lynch, S. Sorey, E. V. Anslyn, *J. Am. Chem. Soc.* **2006**, *128*, 1222-1232.

[115] Y. Tokunaga, Y. Shimomura, T. Seo, *Heterocycles* **2002**, *57*, 787-790.

[116] P. W. Fowler, E. Steiner, *J. Phys. Chem. A* **1997**, *101*, 1409-1413.

[117] H. R. Snyder, M. S. Konecky, W. J. Lennarz, *J. Am. Chem. Soc.* **1958**, *80,* 3611-3615.

[118] J. Beckmann, D. Dakternieks, A. Duthie, A. E. K. Lim, E. R. T. Tiekink, *J. Organomet. Chem.* **2001**, *633*, 149-156.

[119] Q. G. Wu, G. Wu, L. Brancaleon, S. Wang, *Organometallics* **1999**, *18*, 2553-2556.

[120] H. G. Kuivila, A. H. Keough, E. J. Soboczenski, *J. Org. Chem.* **1954**, *19*, 780-783.

[121] R. A. Bowie, O. C. Musgrave, *J. Chem. Soc., Chem. Commun.* **1963**, 3945-3949.

[122] C. D. Roy, H. C. Brown, *J. Organomet. Chem.* **2007**, *692*, 784-790.

[123] T. D. James, K. R. A. S. Sandanayake, S. Shinkai, *Angew. Chem. Int. Ed. Engl.* **1996**, *35*, 1910-1922.

[124] H. Höpfl, N. Farfán, *J. Organomet. Chem.* **1997**, *547*, 71-77.

[125] G. Vargas, N. Farfán, R. Santillan, A. Gutiérrez, E. Gómez, V. Barba, *Inorganica Chimica Acta* **2005**, *358*, 2996-3002.

[126] H. Höpfl, M. Sánchez, V. Barba, N. Farfán, S. Rojas, R. Santillan, *Inorg. Chem.* **1998**, *37*, 1679-1692.

[127] M. Sánchez, H. Höpfl, M. E. Ochoa, N. Farfán, R. Santillan, S. Rojas-Lima, *Chem. Eur. J.* **2002**, *8*, 612-621.

[128] V. Barba, E. Gallegos, R. Santillan, N. Farfán, *J. Organomet. Chem.* **2001**, *622*, 259-264.

[129] V. Barba, H. Höpfl, N. Farfán, R. Santillan, H. I. Beltran, L. S. Zamudio-Rivera, *Chem. Commun.* **2004**, 2834-2835.

[130] V. Barba, R. Villamil, R. Luna, C. Godoy-Alcántar, H. Höpfl, H. I. Beltran, L. S. Zamudio-Rivera, R. Santillan, N. Farfán, *Inorg. Chem.* **2006**, *6*, 2553-2561.

[131] V. Barba, I. Betanzos, *J. Organomet. Chem.* **2007**, *692*, 4903-4908.

[132] L. D. Sarson, K. Ueda, M. Takeuchi, S. Shinkai, *Chem. Commun.* **1996**, 619-620.

[133] R. Dreos, G. Nardin, L. Randaccio, G. Tauzher, S. Vuano, *Inorg. Chem.* **1997**, *36*, 2463-2464.

[134] R. Dreos, G. Nardin, L. Randaccio, P. Siega, G. Tauzher, V. Vrdoljak, *Inorg. Chem.* **2001**, *40*, 5536-5540.

[135] R. Dreos, G. Nardin, L. Randaccio, P. Siega, G. Tauzher, *Eur. J. Inorg. Chem.* **2002**, 2885-2890.

[136] J. K. Day, C. Bresner, I. A. Fallis, L.-L. Ooi, D. J. Watkin, S. J. Coles, L. Male, M. B. Hursthouse, S. Aldridge, *Dalton Trans.* **2007**, 3486-3488.

[137] N. Iwasawa, H. Takahagi, *J. Am. Chem. Soc.* **2007**, *129*, 7754-7755.

[138] K. Kataoka, T. D. James, Y. Kubo, *J. Am. Chem. Soc.* **2007**, *129*, 15126-15127.

[139] M. Hutin, G. Bernardinelli, J. R. Nitschke, *Chem. Eur. J.* **2008**, *14*, 4585-4593.

[140] Y. Pérez-Fuertes, A. M. Kelly, A. L. Johnson, S. Arimori, S. D. Bull, T. D. James, *Org. Lett.* **2006**, *8*, 609-612.

[141] A. M. Kelly, Y. Pérez-Fuertes, S. Arimori, S. D. Bull, T. D. James, *Org. Lett.* **2006**, *8*, 1971-1974.

[142] M. Mikami, S. Shinkai, *J. Chem. Soc., Chem. Commun.* **1995**, 153-154.

[143] M. Mikami, S. Shinkai, *Chem. Lett.* **1995**, 603-604.

[144] I. Nakazawa, S. Suda, M. Masuda, M. Asai, T. Shimizu, *Chem. Commun.* **2000**, 881-882.

[145] W. Niu, C. O'Sullivan, B. M. Rambo, M. D. Smith, J. J. Lavigne, *Chem. Commun.* **2005**, 4342-4344.

[146] W. Niu, M. D. Smith, J. J. Lavigne, *J. Am. Chem. Soc.* **2006**, *128*, 16466-16467.

[147] B. M. Rambo, J. J. Lavigne, *Chem. Mater.* **2007**, *19*, 3732-3739.

[148] Y. Li, J. Ding, M. Day, Y. Tao, J. Lu, M. D'iorio, *Chem. Mater.* **2003**, *15*, 4936-4942.

[149] A. P. Côté, A. J. Benin, N. W. Ockwig, M. O'Keeffe, A. J. Matzger, O. M. Yaghi, *Science* **2005**, *310*, 1166-1170.

[150] R. W. Tilford, W. R. Gemmill, H.-C. zur Loye, J. J. Lavigne, *Chem. Mater.* **2006**, 5296-5301.

[151] A. P. Côté, H. M. El-Kaderi, H. Furukawa, J. R. Hunt, O. M. Yaghi, *J. Am. Chem. Soc.* **2007**, *129*, 12914-12915.

[152] H. M. El-Kaderi, J. R. Hunt, J. L. Mendoza-Cortés, A. P. Côté, R. E. Taylor, M. O'Keeffe, O. M. Yaghi, *Science* **2007**, *316*, 268-272.

[153] J.-H. Fournier, T. Maris, J. D. Wuest, W. Guo, E. Galoppini, *J. Am. Chem. Soc.* **2003**, *125*, 1002-1006.

[154] V. R. Pedireddi, N. SeethaLekshmi, *Tetrahedron Lett.* **2004**, *45*, 1903-1906.

[155] A. Weiss, H. Pritzkow, W. Siebert, *Angew. Chem. Int. Ed.* **2000**, *39*, 547-549.

[156] A. Weiss, V. Barba, H. Pritzkow, W. Siebert, *J. Organomet. Chem.* **2003**, *680*, 294-300.

[157] Y. Sugihara, R. Miyatake, K. Takakura, S. Yano, *J. Chem. Soc., Chem. Commun.* **1994**, 1925-1926.

[158] S. Wakabayashi, S. Imamura, Y. Sugihara, M. Shimizu, T. Kitagawa, Y. Ohki, K. Tatsumi, *J. Org. Chem.* **2008**, *73*, 81-87.

[159] T. Murafuji, R. Mouri, Y. Sugihara, *Tetrahedron* **1996**, *52*, 13933-13938.

[160] M. Fontani, F. Peters, W. Scherer, W. Wachter, M. Wagner, P. Zanello, *Eur. J. Inorg. Chem.* **1998**, 1453-1465.

[161] M. Grosche, E. Herdtwerck, F. Peters, M. Wagner, *Organometallics* **1999**, *18*, 4669-4672.

[162] R. E. Dinnebier, L. Ding, K. Ma, M. A. Neumann, N. Tanpipat, F. J. J. Leusen, P. W. Stephens, M. Wagner, *Organometallics* **2001**, *20*, 5642-5647.

[163] B. F. Abrahams, D. J. Price, R. Robson, *Angew. Chem. Int. Ed.* **2006**, *45*, 806-810.

[164] H. Katagiri, T. Miyagawa, Y. Furusho, E. Yashima, *Angew. Chem. Int. Ed.* **2006**, *45*, 1741-1744.

[165] C. Ikeda, T. Nabeshima, *Chem. Commun.* **2008**, 721-723.

[166] E. Barnea, T. Andrea, M. Kapon, M. S. Eisen, *J. Am. Chem. Soc.* **2004**, *126*, 5066-5067.

[167] K. Severin, *Coord. Chem. Rev.* **2003**, *245*, 3-10.

[168] G. Mezei, C. M. Zaleski, V. L. Pecoraro, *Chem. Rev.* **2007**, *107*, 4933-5003.

[169] H. Piotrowski, K. Polborn, G. Hilt, K. Severin, *J. Am. Chem. Soc.* **2001**, *123*, 2699-2700.

[170] H. Piotrowski, G. Hilt, A. Schulz, P. Mayer, K. Polborn, K. Severin, *Chem. Eur. J.* **2001**, *7*, 3196-3208.

[171] Z. Grote, M.-L. Lehaire, R. Scopelliti, K. Severin, *J. Am. Chem. Soc.* **2003**, *125*, 13638-13639.

[172] Z. Grote, R. Scopelliti, K. Severin, *J. Am. Chem. Soc.* **2004**, *126*, 16959-16972.

[173] Z. Grote, R. Scopelliti, K. Severin, *Angew. Chem. Int. Ed.* **2003**, *42*, 3821-3825.

[174] I. Saur, K. Severin, *Chem. Commun.* **2005**, 1471-1473.

[175] Z. Grote, S. Bonazzi, R. Scopelliti, K. Severin, *J. Am. Chem. Soc.* **2006**, *128*, 10382-10383.

[176] C. Olivier, Z. Grote, E. Solari, R. Scopelliti, K. Severin, *Chem. Commun.* **2007**, 4000-4002.

[177] C. Olivier, E. Solari, R. Scopelliti, K. Severin, *Inorg. Chem.* **2008**, *47*, 4454-4456.

[178] M.-L. Lehaire, R. Scopelliti, L. Herdeis, K. Polborn, P. Mayer, K. Severin, *Inorg. Chem.* **2004**, *43*, 1609-1617.

[179] T. Habereder, M. Warchhold, H. Nöth, K. Severin, *Angew. Chem. Int. Ed.* **1999**, *38*, 3225-3228.

[180] T. Brasey, R. Scopelliti, K. Severin, *Inorg. Chem.* **2005**, *44*, 160-162.

[181] T. Brasey, A. Buryak, R. Scopelliti, K. Severin, *Eur. J. Inorg. Chem.* **2004**, 964-967.

[182] H. Nöth, B. Wrackmayer, in *NMR Spectroscopy of Boron Compounds* (Ed.: P. Diehl, E. Fluck, R. Kosfeld), NMR-Basic Principles and Progress 14, Springer-Verlag, Berlin, **1974**.

[183] W. Clegg, A. J. Scott, F. E. S. Souza, T. B. Marder, *Acta Cryst.* **1999**, *C55*, 1885-1888.

[184] N. Farfán, H. Höpfl, V. Barba, M. E. Ochoa, R. Santillan, E. Gómez, A. Gutiérrez, *J. Organomet. Chem.* **1999**, *581*, 70-81.

[185] B. L. Ellis, A. K. Duhme, R. C. Hilder, M. B. Hossain, S. Rizvi, D. van des Helm, *J. Med. Chem.* **1996**, *39*, 3659-3670.

[186] R. L. N. Harris, *Aust. J. Chem.* **1976**, *29*, 1329-1334.

[187] G. R. Newkome, C. N. Moorefield, F. Vögtle, *Dendrimers and Dendrons: Concepts, Syntheses, Applications*, Wiley-VCH, Weinheim **2001**.

[188] C. Hawker, J. M. J. Fréchet, *J. Chem. Soc., Chem. Commun.* **1990**, 1010-1013.

[189] S. M. Grayson, J. M. J. Fréchet, *Chem. Rev.* **2001**, *101*, 3819-3867.

[190] J. M. J. Fréchet, *Proc. Natl. Acad. Sci. U.S.A.* **2002**, *99*, 4782-4787.

[191] D. K. Smith, A. R. Hirst, C. S. Love, J. G. Hardy, S. V. Brignell, B. Huang, *Prog. Polym. Sci.* **2005**, *30*, 220-293.

[192] S. C. Zimmerman, F. W. Zeng, D. E. C. Reichert, *Science* **1996**, *271*, 1095-1098.

[193] A. Franz, W. Bauer, A. Hirsch, *Angew. Chem. Int. Ed.* **2005**, *44*, 1564-1567.

[194] G. R. Newkome, C. N. Moorefield, *Chem. Rev.* **1999**, *99*, 1689-1746.

[195] M. Kawa, J. M. J. Fréchet, *Chem. Mater.* **1998**, *10*, 286-296.

[196] H.-B. Yang, N. Das, F. Huang, A. M. Hawkridge, D. C. Muddiman, P. J. Stang, *J. Am. Chem. Soc.* **2006**, *128*, 10014-10015.

[197] H.-B. Yang, A. M. Hawkridge, S. D. Huang, N. Das, S. D. Bunge, D. C. Muddiman, P. J. Stang, *J. Am. Chem. Soc.* **2007**, *129*, 2120-2129.

[198] F. Vögtle, M. Plevoets, G. Nachtsheim, U. Wörsdörfer, *J. prakt. Chem.* **1998**, *340*, 112-121.

[199] D. Schultz, J. R. Nitschke, *J. Am. Chem. Soc.* **2006**, *128*, 9887-9892.

[200] J.-M. Lehn, *Prog. Polym. Sci.* **2005**, *30*, 814-831.

[201] L. Brunsveld, B. J. B. Folmer, E. W. Meijer, R. P. Sijbesma, *Chem. Rev.* **2001**, *101*, 4071-4097.

[202] H. Hofmeier, U. S. Schubert, *Chem. Commmun.* **2005**, 2423-2432.

[203] N. Giuseppone, J.-M. Lehn, *J. Am. Chem. Soc.* **2004**, *126*, 11448-11449.

[204] N. Giuseppone, G. Fuks, J.-M. Lehn, *Chem. Eur. J.* **2006**, *12*, 1723-1735.

[205] Y. Qin, C. Cui, F. Jäkle, *Macromolecules* **2007**, *40*, 1413-1420.

[206] F. Jäkle, *Coord. Chem. Rev.* **2006**, *250*, 1107-1121.

[207] W. Niu, M. D. Smith, J. J. Lavigne, *Crystal Growth & Design* **2006**, *6*, 1274-1277.

[208] O. Christiansen, H. Koch, P. Jørgensen, *Chem. Phys. Lett.* **1995**, *243*, 409-418.

[209] Y. Qin, I. Kiburu, S. Shah, F. Jäkle, *Org. Lett.* **2006**, *8*, 5227-5230.

[210] Y. Cui, Q.-D. Liu, D.-R. Bai, W.-L. Jia, Y. Tao, S. Wang, *Inorg. Chem.* **2005**, *44*, 601-609.

[211] E. Wasserman, *J. Am. Chem. Soc.* **1960**, *82*, 4433-4434.

[212] D. B. Amabilino, J. F. Stoddart, *Chem. Rev.* **1995**, *95*, 2725-2828.

[213] F. Aricó, J. D. Badjic, S. J. Cantrill, A. H. Flood, K. C.-F. Leung, J. F. Stoddart, *Top. Curr. Chem.* **2005**, *249*, 203-259.

[214] B. Champin, P. Mobian, J.-P. Sauvage, *Chem. Soc. Rev.* **2007**, *36*, 358-366.

[215] M. D. Lankshear, P. D. Beer, *Acc. Chem. Res.* **2007**, *40*, 657-668.

[216] S. J. Cantrill, S. J. Rowan, J. F. Stoddart, *Org. Lett.* **1999**, *1*, 1363-1366.

[217] M. Horn, J. Ihringer, P. T. Glink, J. F. Stoddart, *Chem. Eur. J.* **2003**, *9*, 4046-4054.

[218] S. J. Rowan, J. F. Stoddart, *Org. Lett.* **1999**, *1*, 1913-1916.

[219] J. Wu, K. C.-F. Leung, J. F. Stoddart, *Proc. Natl. Acad. Sci. USA* **2007**, *104*, 17266-17271.

[220] Y. Furusho, T. Oku, T. Hasegawa, A. Tsuboi, N. Kihara, T. Takata, *Chem. Eur. J.* **2003**, *9*, 2895-2903.

[221] A. F. M. Kilbinger, S. J. Cantrill, A. W. Waltman, M. W. Day, R. H. Grubbs, *Angew. Chem. Int. Ed.* **2003**, *42*, 2381-3285.

[222] A. G. Cheetham, T. D. W. Claridge, H. L. Anderson, *Org. Biomol. Chem.* **2007**, *5*, 457-462.

[223] M. J. Gunter, N. Bampos, K. D. Johnstone, J. K. M. Sanders, *New. J. Chem.* **2001**, *25*, 166-173.

[224] K.-S. Jeong, J. S. Choi, S.-Y. Chang, H.-Y. Chang, *Angew. Chem. Int. Ed.* **2000**, *39*, 1692-1695.

[225] C. A. Hunter, C. M. R. Low, M. J. Packer, S. E. Spey, J. G. Vinter, M. O. Vysotsky, C. Zonta, *Angew. Chem. Int. Ed.* **2001**, *40*, 2678-2682.

[226] E. Lee, J. Heo, K. Kim, *Angew. Chem. Int. Ed.* **2000**, *39*, 2699-2671.

[227] E. Lee, J. Kim, J. Heo, D. Whang, K. Kim, *Angew. Chem. Int. Ed.* **2001**, *40*, 399-402.

[228] K.-M. Park, D. Whang, E. Lee, J. Heo, K. Kim, *Chem. Eur. J.* **2002**, *8*, 498-508.

[229] G. J. E. Davidson, S. J. Loeb, *Angew. Chem. Int. Ed.* **2003**, *42*, 74-77.

[230] D. J. Hoffart, S. J. Loeb, *Angew. Chem. Int. Ed.* **2005**, *44*, 901-904.

[231] P. R. Ashton, D. Philp, N. Spencer, J. F. Stoddart, *J. Chem. Soc., Chem. Commun.* **1992**, 1124-1128.

[232] P. L. Anelli, P. R. Ashton, R. Ballardini, V. Balzani, M. Delgado, M. T. Gandolfi, T. T. Goodnow, A. E. Kaifer, D. Philp, M. Pietraszkiewicz, L. Prodi, M. V. Reddington, A. M. Z. Slawin, N. Spencer, J. F. Stoddart, C. Vicent, D. J. Williams, *J. Am. Chem. Soc.* **1992**, *114*, 193-218.

[233] B. L. Allwood, H. Shahriari-Zavareh, J. F. Stoddart, D. J. Williams, *J. Chem. Soc., Chem. Commun.* **1987**, 1058-1061.

[234] B. L. Allwood, N. Spencer, H. Shahriari-Zavareh, J. F. Stoddart, D. J. Williams, **1987**, 1064-1066.

[235] P. R. Ashton, A. M. Z. Slawin, N. Spencer, J. F. Stoddart, D. J. Williams, *J. Chem. Soc., Chem. Commun.* **1987**, 1066-1069.

[236] M. J. Hynes, J. Chem. Soc., Dalton Trans. **1993**, 311-312.

[237] H. M. Colquhoun, J. F. Stoddart, D. J. Williams, J. B. Wolstenholme, R. Zarzycki, *Angew. Chem. Int. Ed.* **1981**, *20*, 1051-1053.

[238] H. M. Colquhoun, E. P. Goodings, J. M. Maud, J. F. Stoddart, J. B. Wolstenholme, D. J. Williams, *J. Chem. Soc., Perkin Trans. II* **1985**, 607-624.

[239] B. L. Allwood, H. M. Colquhoun, S. M. Doughty, F. H. Kohnke, A. M. Z. Slawin, J. F. Stoddart, D. J. Williams, R. Zarzycki, *J. Chem. Soc., Chem. Commun.* **1987**, 1054-1058.

[240] G. M. Culver, *Biopolymers* **2003**, *68*, 234-249.

[241] M. Yoshizawa, M. Nagao, K. Kumazawa, M. Fujita, *J. Organomet. Chem.* **2005**, *690*, 5383-5388.

[242] Z. Grote, R. Scopelliti, K. Severin, *Eur. J. Inorg. Chem.* **2007**, 694-700.

[243] J. Zhang, P. W. Miller, M. Nieuwenhuyzen, S. L. James, *Chem. Eur. J* **2006**, *12*, 2448-2453.

[244] P. N. W. Baxter, J.-M. Lehn, G. Baum, D. Fenske, *Chem. Eur. J.* **1999**, *5*, 102-112.

[245] M. Schmittel, V. Kalsani, D. Fenske, A. Wiegrefe, *Chem. Commun.* **2004**, 490-491.

[246] M. Schmittel, V. Kalsani, R. S. K. Kishore, H. Cölfen, J. W. Bats, *J. Am. Chem. Soc.* **2005**, *127*, 11544-11545.

[247] P. N. W. Baxter, G. S. Hanan, J.-M. Lehn, *Chem. Commun.* **1996**, 2019-2020.

[248] P. N. W. Baxter, J.-M. Lehn, A. DeCian, J. Fischer, *Angew. Chem. Int. Ed. Engl.* **1993**, 69-72.

[249] P. N. W. Baxter, J.-M. Lehn, B. Kneisel, G. Baum, D. Fenske, *Chem. Eur. J.* **1999**, *5*, 113-120.

[250] M. Schmittel, V. Kalsani, C. Michel, P. Mal, H. Ammon, F. Jäckel, J. P. Rabe, *Chem. Eur. J* **2007**, *13*, 6223-6237.

[251] R. S. K. Kishore, T. Paululat, M. Schmittel, *Chem. Eur. J* **2006**, *12*, 8136-8149.

[252] P. N. W. Baxter, H. Sleiman, J.-M. Lehn, K. Rissanen, *Angew. Chem. Int. Ed. Engl.* **1997**, *36*, 1294-1296.

[253] J. R. Nitschke, J.-M. Lehn, *Proc. Natl. Acad. Sci. USA* **2003**, *100*, 11970-11974.

[254] J. R. Nitschke, M. Hutin, G. Bernardinelli, *Angew. Chem. Int. Ed.* **2004**, *43*, 6724-6727.

[255] J. R. Nitschke, D. Schultz, G. Bernardinelli, D. Gérard, *J. Am. Chem. Soc.* **2004**, *126*, 16538-16543.

[256] M. Hutin, R. Frantz, J. R. Nitschke, *Chem. Eur. J.* **2006**, *12*, 4077-4082.

[257] M. Albrecht, M. Fiege, M. Baumert, M. de Groot, R. Fröhlich, L. Rosso, K. Rissanen, *Eur. J. Inorg. Chem.* **2007**, 609-616.

[258] M. Albrecht, S. Mirtschin, M. de Groot, I. Janser, J. Runsink, G. Raabe, M. Kogej, C. A. Schalley, R. Fröhlich, *J. Am. Chem. Soc.* **2005**, *127*, 10371-10387.

[259] S. H. Chikkali, D. Gudat, F. Lissner, M. Nieger, T. Schleid, *Dalton Trans.* **2007**, 3906-3913.

[260] S. Lüthje, C. Bornholdt, U. Lüning, *Eur. J. Org. Chem.* **2006**, 909-915.

[261] D. Chen, A. E. Martell, *Tetrahedron* **1991**, *47*, 6895-6902.

[262] M. Y. Redko, R. Huang, J. L. Dye, J. E. Jackson, *Synthesis* **2006**, 759-761.

[263] S. Brooker, J. D. Ewing, J. Nelson, *Inorg. Chim. Acta* **2001**, *317*, 53-58.

[264] C. J. Harding, Q. Lu, J. F. Malone, D. J. Marrs, N. Martin, V. McKee, J. Nelson, *J. Chem. Soc., Dalton Trans.* **1995**, 1739-1747.

[265] D. MacDowell, J. Nelson, *Tetrahedron Lett.* **1988**, *29*, 385-386.

[266] S. Brooker, J. D. Ewing, T. K. Ronson, C. J. Harding, J. Nelson, D. J. Speed, *Inorg. Chem.* **2003**, *42*, 2764-2773.

[267] Q. Lu, J.-M. Latour, C. J. Harding, N. Martin, D. J. Marrs, V. McKee, J. Nelson, *J. Chem. Soc., Dalton Trans.* **1994**, 1471-1478.

[268] K. J. Wallace, R. Hanes, E. V. Anslyn, J. Morey, K. V. Kilway, J. Siegel, *Synthesis* **2005**, 2080-2083.

[269] S.-S. Sun, A. J. Lees, *Coord. Chem. Rev.* **2002**, *230*, 171-192.

[270] F. Calderazzo, D. Vitali, *Coord. Chem. Rev.* **1975**, *16*, 13-17.

[271] R. V. Slone, J. T. Hupp, C. L. Stern, T. E. Albrecht-Schmitt, *Inorg. Chem.* **1996**, *35*, 4096-4097.

[272] T. Rajendra, B. Manimaran, R.-T. Liao, R.-J. Lin, P. Thanasekaran, G.-H. Lee, S.-M. Peng, Y.-H. Liu, I.-J. Chang, S. Rajagopal, K.-L. Lu, *Inorg. Chem.* **2003**, *42*, 6388-6394.

[273] A. Kuhl, J. A. Christopher, L. J. Farrugia, P. J. Kocienski, *Synlett* **2000**, *12*, 1765-1768.

[274] C. D. Hoff, *J. Organomet. Chem.* **1985**, *282*, 201-214.

[275] N. Christinat, R. Scopelliti, K. Severin, *Chem. Commun.* **2004**, 1158-1159.

[276] N. Christinat, R. Scopelliti, K. Severin, *J. Org. Chem.* **2007**, *72*, 2192-2200.

[277] N. Christinat, E. Croisier, R. Scopelliti, M. Cascella, U. Röthlisberger, K. Severin, *Eur. J. Inorg. Chem.* **2007**, 5177-5181.

[278] N. Christinat, R. Scopelliti, K. Severin, *Chem. Commun.* **2008**, 3660-3662.

[279] N. Christinat, R. Scopelliti, K. Severin, *Angew. Chem. Int. Ed.* **2008**, *47*, 1848-1852.

[280] N. Fujita, S. Shinkai, T. D. James, *Chem. Asian. J.* **2008**, *3*, 1076-1091.

[281] H. E. Gottlieb, V. Kotlyar, A. Nudelman, *J. Org. Chem.* **1997**, *62*, 7512-7515.

[282] G. M. Sheldrick, University of Göttingen, Göttingen, Germany, **1997**.

[283] Bruker AXS Inc., Wisconsin, 53719, USA, **1997**.

[284] M. K. Patel, R. Fox, P. D. Taylor, *Tetrahedron* **1996**, *52*, 1835-1840.

[285] P. R. Weider, L. S. Hegedus, H. Asada, S. V. D'Andreq, *J. Org. Chem.* **1985**, *50*, 4276-4281.

[286] D. B. Amabilino, P. R. Ashton, V. Balzani, S. E. Boyd, A. Credi, J. Y. Lee, S. Menzer, J. F. Stoddart, M. Venturi, D. J. Williams, *J. Am. Chem. Soc.* **1998**, *120*, 4295-4307.

[287] G. J. Kubas, *Inorg. Synth.* **1990**, *28*, 68-70.

[288] S. P. Schmidt, W. C. Trogler, F. Basolo, *Inorg. Synth.* **1985**, *23*, 160-165.

[289] M. A. Bennett, T. N. Huang, T. W. Matheson, A. K. Smith, *Inorg. Synth.* **1982**, *21*, 74-78.

[290] C. White, A. Yates, P. M. Maitlis, *Inorg. Synth.* **1992**, *29*, 228-234.

Curriculum Vitae

Nicolas Christinat

28 years old-Single-Swiss

Professional Address	Private Address
EPFL-ISIC-LCS	
BCH 3409	Av. d'Echallens 13
CH-1015 Lausanne	CH-1004 Lausanne
+41 21 693 93 12	+41 79 758 96 74
nicolas.christinat@a3.epfl.ch	

Education and Work Experience:

10/2004-09/2008: PhD in Chemistry (in progress) at the Ecole Polytechnique Fédérale de Lausanne (EPFL), Institut des Sciences et Ingénierie Chimique.
Supervisor: Prof. Kay Severin
Self-assembly of boron-based supramolecular structures

03/2004-09/2004: Civil Service at Fondation Clémence, Lausanne.

07/2001-01/2004: Graduate Degree in Chemistry, EPFL, Section de Chimie et de Génie Chimique.
Supervisor: Prof. Kay Severin
Synthesis of macrocyclic boronates

10/1998-07/2001: First Cycle in Chemistry, Université de Lausanne, Section de Chimie.

06/1998: Scientific High School Degree (Maturité fédérale) at the Gymnase de Chamblandes, Pully.

Research and Teaching Skills

Scientific Techniques:

Organometallic synthesis and catalysis, synthesis of small organic molecules.
Handling of air and moisture sensitive compounds (Schlenk and glovebox techniques).
NMR spectroscopy as well as IR and UV-vis spectroscopy.

Assistantship**:**

2006-2008: Security delegate for the laboratory
2006-2008: Research Projects for undergraduate students.
2006-2007: Practical Organic Chemistry (1st and 2nd year students).
2005-2007: Practical Inorganic Chemistry (3rd year students).

Conferences Attended:

Oral Presentation at the Fall Meeting of the Swiss Chemical Society (SCS), 2007, Lausanne.
Poster Presentation at the Summer school "Bottom-Up Approach to Nanotechnology", 2007, Villars.
Poster Presentation at the Fall Meeting of the Swiss Chemical Society (SCS), 2006, Zürich.
Poster Presentation at the Fall Meeting of the Swiss Chemical Society (SCS), 2005, Lausanne.

Awards:

2006: Proficiency prize for teaching activities.

Scientific Publications:

Boron-based rotaxanes by multicomponent self-assembly
N. Christinat, R. Scopelliti, K. Severin, *Chem. Commun.* **2008**, 3660-3662.

Multicomponent Assembly of Boronic Acid-Based Macrocycles and Cages
N. Christinat, R. Scopelliti, K. Severin, *Angew. Chem. Int. Ed.* **2008**, 47, 1848-1852.

Formation of Boronate Ester Polymers with Efficient Intrastrand Charge-Transfer Transitions by Three-Component Reactions
N. Christinat, E. Croisier. R. Scopelliti, M. Cascella, U. Röthlisberger, K. Severin, *Eur. J. Inorg. Chem.* **2007**, 33, 5177-5181.

Multicomponent Assembly of Boron-Based Dentritic Nanostructures
N. Christinat, R. Scopelliti, K. Severin, *J. Org. Chem.* **2007**, 72, 2192-2200.

A new method for the synthesis of boronates macrocycles
N. Christinat, R. Scopelliti, K. Severin, *Chem. Commun.* **2004**, 10, 1158-1159.

Languages

French: Native tongue
English: Fluent in writing and speaking
German: Basic knowledge rapidly perfectible

Personal Interests and Activities:

Sailing, Skiing, Inline-hockey.